

# J-Physics 2017



International Workshop on Multipole Physics and Related Phenomena

Sun. Sep. 24 – Thu. Sep. 28, 2017

## 24<sup>th</sup> Afternoon

16:00 – Registration

18:00 – Get-Together 12 Floor “Sky Banquet Room”

## Scientific Program

### 25<sup>th</sup> Morning Sessions

#### Opening Remark

8:30 – 8:50 Hisatomo Harima (Kobe University, Japan)

#### Session 1: Spin-Orbit Interaction I

Chair: Yoshio Kuramoto (KEK, Japan)

8:50 – 9:20 Michael R. Norman (Argonne National Laboratory, USA)

*Multipolar Order in  $Sr_2IrO_4$  and  $Cd_2Re_2O_7$*

9:20 – 9:50 Yukitoshi Motome (The University of Tokyo, Japan)

*Majorana fermions in Kitaev magnets*

9:50 – 10:10 Tong Zhang (Fudan University, China)

*STM study of surface electron-doped  $Sr_2IrO_4$*

10:10 – 10:30 Yogesh Singh (IISER Mohali, India)

*Kitaev Physics in Honeycomb Lattice Iridates*

10:30 – 11:00 *Break*

#### Session 2: Quantum Phase Transition

Chair: William Knafo (LNCMI-Toulouse, CNRS, France)

11:00 – 11:30 Manuel Brando (Technical University of Dresden, Germany)

*Quantum Multicritical Point in  $YbRh_2Si_2$*

11:30 – 12:00 Kazuhiko Deguchi (Nagoya University, Japan)

*Magnetic quasicrystal with Yb icosahedron*

12:00 – 12:20 Shinji Watanabe (Kyushu Institute of Technology, Japan)

*Quantum criticality universal to Yb-based quasicrystal and periodic crystal*

12:20 – 12:35 Shuntaro Sumita (Kyoto University, Japan)

*Superconductivity coexisting with magnetic multipole orders in Sr<sub>2</sub>IrO<sub>4</sub>*

12:35 – 14:00 *Lunch*

14:00 – 16:00 **Poster Presentation (Odd Number)**

16:00 - 16:30 *Break*

## 25<sup>th</sup> Afternoon Session

### Session 3: URu<sub>2</sub>Si<sub>2</sub>

Chair: John A. Mydosh (Leiden University, The Netherland)

16:30 – 17:00 Hiroaki Ikeda (Ritsumeikan Univeristy, Japan)

*Review of theory about URu<sub>2</sub>Si<sub>2</sub>*

17:00 – 17:30 William Knafo (LNCMI-Toulouse, CNRS, France)

*Field-induced spin-density wave in URu<sub>2</sub>Si<sub>2</sub>*

17:30 – 17:50 Shinsaku Kambe (ASRC, JAEA, Japan)

*NMR study of URu<sub>2</sub>Si<sub>2</sub>*

17:50 – 18:10 Nicholas P. Butch (NIST Center for Neutron Research, USA)

*Magnetic excitations in the hidden order and antiferromagnetic phases of URu<sub>2-x</sub>Fe<sub>x</sub>Si<sub>2</sub>*

## 26<sup>th</sup> Morning Sessions

### Session 4: Ferromagnetic Superconductor

- Chair: A. de Visser (University of Amsterdam, The Netherlands)
- 8:50 – 9:20 Georg Knebel (CEA Grenoble, France)  
*Uranium-based ferromagnetic superconductors*
- 9:20 – 9:50 Vladimir P. Mineev (CEA Grenoble, France)  
*Phase diagram of UCoGe*
- 9:50 – 10:10 Yo Tokunaga (ASRC, JAEA, Japan)  
*Reentrant superconductivity induced by quantum tricritical fluctuations in URhGe*
- 10:10 – 10:30 Yasuhiro Tada (The University of Tokyo, Japan)  
*Pairing symmetry and stripe state in ferromagnetic superconductor UCoGe*
- 10:30 - 11:00 *Break*

### Session 5: Superconductivity

- Chair: Elena Hassinger (MPI Dresden, Germany)
- 11:00 – 11:30 Michel Kenzelmann (PSI, Switzerland)  
*Possible magnetic quantum critical point in superconducting Nd-doped CeCoIn<sub>5</sub>*
- 11:30 – 11:50 Yusei Shimizu (Tohoku University, Japan)  
*Superconductivity and Non-Fermi-Liquid Behaviors in UBe<sub>13</sub> and Related compounds*
- 11:50 – 12:10 Takuya Nomoto (RIKEN, Japan)  
*Pairing symmetry and nodal structure in multi-orbital superconductors*
- 12:10 – 12:25 Ilya Sheikin (LNCMI-EMFL, CNRS, France)  
*Quantum criticality, superconductivity and Fermi surface dimensionality - comparison of CeIn<sub>3</sub>, CeRhIn<sub>5</sub>, and CePt<sub>2</sub>In<sub>7</sub>*
- 12:25 – 12:40 Kosmas Prassides (WPI-AIMR, Tohoku University, Japan)  
*Intermediate valency in hybrid f-/p-electron molecular materials*
- 12:40 – 13:00 **Group Photo**
- 13:00 – 14:20 *Lunch*
- 14:20 – 18:00 **Excursion** *Bus Tour for Yakebashiri Lava Flow*
- 18:30 – 21:00 **Banquet** *2 Floor “Dining Room Shiki”*

## 27<sup>th</sup> Morning Sessions

### Session 6: Parity Violation

Chair: Michael R. Norman (Argonne National Laboratory, USA)

- 8:50 – 9:20 Youichi Yanase (Kyoto University, Japan)  
*Exotic phases in artificial two-dimensional superconductors*
- 9:20 – 9:40 Tsutomu Nojima (Tohoku University, Japan))  
*Critical magnetic fields enhanced by spin-orbit coupling in electric-field-induced superconductors*
- 9:40 – 10:00 Jun-ichi Yamaura (Tokyo Institute of Technology, Japan)  
*Noncentrosymmetric parent phase in iron-based superconductor*
- 10:00 – 10:20 Srinivasan Ramakrishnan (Tata Institute of Fundamental Research, India)  
*Superconductivity at extremely low carrier density: Bismuth*
- 10:20 – 10:35 Robert Peters (Kyoto University, Japan)  
*Strong enhancement of the magnetoelectric effect in heavy-fermion system*
- 10:35 - 11:00 *Break*

### Session7: Multipole

Chair: Manuel Brando (Technical University of Dresden, Germany)

- 11:00 – 11:30 Hiroaki Kusunose (Meiji University, Japan)  
*Magnetoelectric responses induced by generalized multipole orders*
- 11:30 – 11:50 Satoru Hayami (Hokkaido University, Japan)  
*Emergent odd-parity multipoles by spontaneous parity breaking*
- 11:50 - 12:10 Florian Thöle (ETH Zürich, Switzerland)  
*First-principles calculations for magnetoelectric multipoles*
- 12:10 – 12:30 Takahiro Tomita (The University of Tokyo, Japan)  
*Recent Large anomalous Hall and Nernst effects at room temperature in antiferromagnet  $Mn_3Sn$*
- 12:30 – 12:50 Michi-To Suzuki (RIKEN, Japan)  
*Cluster multipole theory for macroscopic magnetization of antiferromagnetism: Application to anomalous Hall effect and recent progress*
- 12:50 – 14:00 *Lunch*
- 14:00 – 16:00 **Poster Presentation (Even Number)**

16:00 - 16:30      *Break*

## 27<sup>th</sup> Afternoon Session

### Session 8: New Compounds

Chair: Sergey L. Bud'ko (Iowa State University, USA)

- 16:30 – 16:50      Anne de Visser                      (University of Amsterdam, The Netherland)  
*Superconductivity in topological half-Heusler compounds*
- 16:50 – 17:10      Yoshichika Ōnuki                      (University of the Ryukyus, Japan)  
*Unique Electronic States in Ullmannite-type Chiral Compounds*
- 17:10 – 17:30      Kenya Ohgushi                      (Tohoku University, Japan)  
*Superconductivity in Fe-based ladder materials*
- 17:30 – 17:45      Shota Nakamura                      (The University of Tokyo, Japan)  
*Investigation of the Wing-Structure Phase Diagram of the Ising Ferromagnet URhGe  
by Angle-Resolved Magnetization Measurements*
- 17:45 – 18:00      Hidekazu Mukuda                      (Osaka University, Japan)  
*Charge Kondo Effect and Superconductivity in  $Pb_{1-x}Tl_xTe$  probed by  $^{125}Te$ -NMR*

## 28<sup>th</sup> Morning Sessions

### Session 9: 1-2-20 system

Chair: Michael Kenzelmann (PSI, Switzerland)

- 8:50 – 9:20 Sergey L. Bud'ko (Iowa State University, USA)  
*Six closely related  $\text{YbT}_2\text{Zn}_{20}$  ( $T = \text{Fe, Co, Ru, Rh, Os, Ir}$ ) heavy fermion compounds: large local moment degeneracy and tuning of physical properties*
- 9:20 – 9:50 Koichi Izawa (Tokyo Institute of Technology, Japan)  
*Transport properties of the Pr 1-2-20 system (Tentative)*
- 9:50 – 10:10 Takahiro Onimaru (Hiroshima University, Japan)  
*Emergence of quadrupole-driven phenomena in non-Kramers Pr 1-2-20 systems*
- 10:10 – 10:30 Yosuke Matsumoto (Max-Planck Institute Stuttgart, Germany)  
*Strong hybridization effect and heavy fermion superconductivity in non-magnetic quadrupolar systems  $\text{PrT}_2\text{Al}_{20}$  ( $T = \text{Ti, V}$ )*
- 10:30 – 11:00 *Break*

### Session 10: Spin-Orbit Interaction II

Chair: Georg Knebel (CEA Grenoble, France)

- 11:00 – 11:30 Elena Hassinger (MPI Dresden, Germany)  
*Fermi surface topology in Weyl semimetals*
- 11:30 – 11:50 Yoshikazu Mizuguchi (Tokyo Metropolitan University, Japan)  
*Superconductivity of layered  $\text{BiS}_2$ -based systems*
- 11:50 – 12:05 Yoshihiko Okamoto (Nagoya University, Japan)  
*Phase Transition in  $\beta$ -Pyrochlore Oxide  $\text{CsW}_2\text{O}_6$*
- 12:05 – 12:20 Toru Sakai (University of Hyogo, Japan)  
*Spin-Nematic and Spin-Liquid Phases in Low-Dimensional Quantum Antiferromagnets*
- 12:20 – 12:35 Ai Nakamura (Tohoku University, Japan)  
*Single Crystal Growth and Highly-Anisotropic Magnetic Properties of Ferromagnetic Heavy Fermion Compound  $\text{YbNiSn}$*

### Closing Remark

- 12:35 – 12:55 Kenji Ishida (Kyoto University, Japan)

## List of Poster Session

Posters must fit within a rectangle 86 cm wide and 176 cm height. All authors are requested to set up their posters before the 1st Poster Session on Sep. 25th, and display them until the end of the 2nd Poster Session on Sep. 27th. The necessary mounting material will be provided. Presentations are scheduled as follows:

25<sup>th</sup> 14:00 - 16:00, Odd Number

27<sup>th</sup> 14:00 - 16:00, Even Number

- P-01 **Masahiro Manago** Department of Physics, Kyoto University  
*NMR study of magnetic fluctuations and superconductivity of UCoGe under pressure*
- P-02 **Hideki Tou** Kobe University  
*Cu-NMR studies of heavy fermion CeCu<sub>6</sub>*
- P-03 **Satoru Nakatsuji** ISSP, The University of Tokyo  
*Anomalous Metallic State due to Quadrupolar Fluctuations in PrV<sub>2</sub>Al<sub>20</sub>*
- P-04 **Jun Ishizuka** Kyoto University  
*Electronic state and odd-parity multipole fluctuation in non-symmorphic crystalline*
- P-05 **Shunsaku Kitagawa** Kyoto University  
*NMR/NQR study on heavy-fermion superconductor CeCu<sub>2</sub>Si<sub>2</sub>*
- P-06 **Hikaru Watanabe** Department of Physics, Graduate School of Science, Kyoto University  
*Magnetic Hexadecapole Order in BaMn<sub>2</sub>As<sub>2</sub>*
- P-07 **Ryousuke Shiina** Department of Physics and Earth Sciences, University of the Ryukyus  
*A theory of valence fluctuation and field-insensitive heavy fermion in Sm compounds*
- P-08 **Motoi Kimata** IMR, Tohoku University  
*High Magnetic Field Study on URu<sub>2</sub>Si<sub>2</sub> and related compounds*
- P-09 **Akihisa Koga** Tokyo Institute of Technology  
*Role of the spin-orbit coupling in the Kugel-Khomskii model on the honeycomb lattice*
- P-10 **Takanori Taniguchi** ISSP, The University of Tokyo  
*The observation of the field induced transition in PrTi<sub>2</sub>Al<sub>20</sub>*
- P-11 **Kazunori Umeo** N-BARD, Hiroshima University  
*Pressure effects on the antiferroquadrupolar and superconducting transitions in PrIr<sub>2</sub>Zn<sub>20</sub>*
- P-12 **Taisuke Hattori** Advanced Science Research Center, Japan Atomic Energy Agency  
*Strong uniaxial spin anisotropy in the Hidden order state of URu<sub>2</sub>Si<sub>2</sub>*
- P-13 **Eiichi Matsuoka** Kobe University  
*Si-substitution effects on the physical properties and the magnetic anisotropy of a ferromagnetic Kondo-lattice compound CeRh<sub>6</sub>Ge<sub>4</sub>*
- P-14 **Haruki Matsuno** Kobe University  
*Investigation of UBe<sub>13</sub> Probed by <sup>9</sup>Be-NMR*
- P-15 **Taisuke Aoyama** Kobe University  
*NMR studies on anisotropy of antiferro spin fluctuations in UPt<sub>3</sub>*
- P-16 **Tatsuya Yanagisawa** Hokkaido University  
*Elastic Response of the Vortices-type Magnetic Order in UNi<sub>4</sub>B*
- P-17 **Akihiro Mitsuda** Department of Physics, Kyushu University  
*A new valence-ordered phase and collapse of antiferromagnetism in EuPtP induced by pressure*
- P-18 **Yo Machida** Tokyo Institute of Technology  
*Pressure effect on electrical transport properties of U<sub>1-x</sub>Th<sub>x</sub>Be<sub>13</sub>*
- P-19 **Mikito Koga** Shizuoka University  
*Antisymmetric spin-orbit coupling effect on a triangular-triple-quantum-dot Kondo system*
- P-20 **Yoshiki Sato** Graduate School of Engineering, Tohoku University  
*Single crystal growth and physical properties in Ce<sub>5</sub>Si<sub>4</sub> and La<sub>5</sub>Si<sub>4</sub> with chiral structure*
- P-21 **Yuki Yanagi** Department of Physics, Meiji University  
*Theoretical study on magnetoelectric response in the honeycomb antiferromagnet Co<sub>4</sub>Nb<sub>2</sub>O<sub>9</sub>*

- P-22 **Kazutaka Kudo** Research Institute for Interdisciplinary Science, Okayama University  
*Atomic imaging around Pr atoms in  $Ca_{1-x}Pr_xFe_2As_2$  by x-ray fluorescence holography*
- P-23 **Junpei Ogawa** Department of Physics, Tokyo Institute of Technology  
*Hall Resistivity of Non-Kramers System  $PrT_2Zn_{20}$  ( $T = Ir, Rh$ )*
- P-24 **Hironori Nakao** High Energy Accelerator Research Organization  
*Resonant x-ray scattering study on hybridized orbital states in f-electron system*
- P-25 **Shogo Sakuraba** Hirosaki University  
*Field-induced topological phase of the s-wave superconductor in a mono-layered checkerboard triangle lattice*
- P-26 **Yutaka Tobita** Hirosaki University  
*Topological Feedback on Superconductor*
- P-27 **Naoki Nakamura** Tokyo Metropolitan University  
*de Hass-van Alphen effect of the itinerant weak ferromagnetic filled skutterudite  $LaFe_4As_{12}$*
- P-28 **Dai Aoki** IMR, Tohoku University  
*Field tuned ferromagnetic instabilities in the ferromagnetic superconductor  $URhGe$  and related materials*
- P-29 **Kazutoshi Emi** Tohoku University  
*Development of Scanning Hall Probe Microscopy toward Observation of Novel Magnetic Domains*
- P-30 **Hiroyuki Hidaka** Hokkaido University  
*Systematic Study of the 4f Electronic State and Low-Energy Phonon in the Light-Rare-Earth  $RBe_{13}$*
- P-31 **Shigeki Miyasaka** Department of Physics, Osaka University  
*Study of angle resolved photoemission spectroscopy in Dirac fermion system  $NiTe_2$*
- P-32 **Hiroshi Shinaoka** Saitama University  
*Multi-orbital aspects of heavy fermion behavior in  $LiV_2O_4$*
- P-33 **Junya Otsuki** Tohoku University  
*DFT+DMFT approach to multipolar ordering in f-electron materials*
- P-34 **Norimasa Sasabe** Osaka Prefecture University  
*Spectral Change in 3d-4f Resonant Inelastic X-ray scattering of Ce intermetallics*
- P-35 **Kohei Suzuki** Tokyo Metropolitan University  
*Ground-state phase diagram of the  $S = 1$  one-dimensional Kondo lattice model with a uniaxial anisotropy under transverse field*
- P-36 **Yuichiro Noma** Kobe university  
 *$^{73}Ge$ -NQR studies on ferromagnetic superconductor  $UGe_2$  under pressure*
- P-37 **Kazumasa Hattori** Tokyo Metropolitan University  
*Magnetic-field induced interactions in  $PrTi_2Al_{20}$*
- P-38 **Atsushi Tsuruta** Department of Material Engineering Science, Osaka University  
*Theoretical study of the antiferro quadrupole and superconducting ordered state in Pr 1-2-20 systems*
- P-39 **Yasuaki Totoki** Department of physics, Kobe University  
*Structural stability and electronic structure of Rhombohedral As, Sb and Bi*
- P-40 **Kohei Oyama** Department of physics, Kyushu University  
*Magnetic structure analysis of valence ordering compound,  $YbPd$*
- P-41 **Kousuke Tanabe** Department of Physics Kyushu University  
*Transport property of  $EuT_2P_2$  ( $T = Ni, Co$ ) in magnetic field*
- P-42 **Hiroki Funashima** Department of Physics, Kobe University  
*Electronic and spin structures in ullmannite-type  $PdBiSe$  and  $NiSbS$*
- P-43 **Kohei Fukuchi** Department of Physics, Tokyo Institute of Technology  
*Unusual Normal and Superconducting States in  $U_{1-x}Th_xBe_{13}$  Probed by Thermal Transport Coefficients*
- P-44 **Kazuhei Wakiya** Yokohama National University  
*Effect of Sn substitution on the structural and magnetic properties of  $PrRu_2Zn_{20}$*
- P-45 **Yoshiki Koike** The University of Tokyo  
*Magnetotransport of  $CaMn_2Bi_2$  in pulsed high magnetic field*

- P-46 **Megumi Yatsushiro** Graduate School of Science, Hokkaido University  
*Magnetic ordering in the d-p model with spin-orbit couplings on a zigzag chain*
- P-47 **Fuminori Honda** IMR, Tohoku University  
*Single crystal growth and peculiar magnetic properties of  $U\text{IrSi}_3$*
- P-48 **Yasuki Kishimoto** Department of physics, Graduate school of Science, Kobe University  
*Ferromagnetic quantum criticality on  $\text{YbNi}_4\text{P}_2$  probed by P-NMR*
- P-49 **Genki Nakamine** Department of Physics, Kyoto University  
*Magnetic fluctuations at the interface region in the artificially engineered heavy-fermion superlattices*
- P-50 **Michiyasu Mori** Japan Atomic Energy Agency  
*Thermal Hall effect and multipole*
- P-51 **Yuina Kanai** Graduate School of Engineering Science, Osaka University  
*Observation of the linear dichroism in core-level photoemission reflecting 4f ground-state symmetry of strongly correlated cubic Ce compounds*
- P-52 **Arvind Maurya** IMR, Tohoku University, Japan  
*Crystal growth and dHvA effect studies of  $\text{U}_3\text{Ni}_3\text{Sn}_4$*
- P-53 **Akira Yamada** Tokyo Metropolitan University  
*Field-insensitive Kondo behavior in  $\text{SmT}_2\text{Al}_{20}$  and Superconducting properties in cage-structure compound  $\text{LaT}_2\text{X}_{20}$*
- P-54 **Hisashi Kotegawa** Kobe University  
*Exotic phase transitions in zig-zag structure: superconductivity in CrAs and metal-insulator transition in RuAs*
- P-55 **Joe Kajitani** Tokyo Metropolitan University  
*Observation of superlattice reflections in  $\text{BiS}_2$  layered superconductor  $\text{LaO}_{0.5}\text{F}_{0.5}\text{BiS}_2$*
- P-56 **Ryosuke Yamamura** Tokyo Metropolitan University  
*Mean-field phase diagram for multipole ordering in  $f^2$ -electron systems on the basis of a j-j coupling scheme*
- P-57 **Mamoru Yogi** University of the Ryukyus  
*NQR study on Ullmannite-type compounds*
- P-58 **Chihiro Tabata** IMSS-KEK  
*Magnetic order and coupled charge-density waves in noncentrosymmetric intermetallic  $\text{TbNiC}_2$*
- P-59 **Shin-ya Ayukawa** Research Institute for Interdisciplinary Science, Okayama University  
*The magnetic field angular dependence of flux-flow resistance in  $\text{FeSe}_{1-x}\text{Te}_x$*
- P-60 **Nonoka Higa** Graduate School of Engineering and Science, University of the Ryukyus  
*NMR studies of the incommensurate helical antiferromagnet Eu compounds*
- P-61 **Hiroki Morita** Department of Physics, Hokkaido University  
*Spectral function and density of state in superconducting state for the cuprate superconductors incorporating the strongly correlated effects*
- P-62 **Akito Sakai** ISSP, The University of Tokyo  
*Heavy fermion superconductivity and non-Fermi liquid in the quadrupole Kondo lattice  $\text{PrTr}_2\text{Al}_{20}$  ( $\text{Tr} = \text{Ti}, \text{V}$ )*
- P-63 **Yu Yamane** Hiroshima University  
*Single-site non-Fermi liquid state in a dilute Pr system  $\text{Y}_{1-x}\text{Pr}_x\text{Ir}_2\text{Zn}_{20}$*
- P-64 **Takashi Matsui** Kobe University  
*NMR study of tetrahedrite  $\text{Cu}_{12}\text{Sb}_4\text{S}_{13}$*
- P-65 **Takeshi Mito** University of Hyogo  
*Local structural anomaly in  $\text{URu}_2\text{Si}_2$  detected by NMR studies*
- P-66 **Tatsuma D. Matsuda** Tokyo Metropolitan University  
*Magnetic properties of a new compounds  $\text{RPd}_3\text{Ga}_8$  with kagome lattice (R: rare earth)*
- P-67 **Yoshiki Nakanishi** Graduate School of Science and Engineering Iwate university  
*Elastic properties of Eu-based compounds  $\text{EuX}_4$  (X: Ge, Al) probed by ultrasonic measurements*
- P-68 **Yasuhiro Nagaoka** ISSP, The University of Tokyo  
*Synthesis and thermal expansion measurement of quadrupole Kondo lattice  $\text{PrV}_2\text{Al}_{20}$*

- P-69 **Klára Uhlířová** Charles University, Faculty of Mathematics and Physics  
*Magnetism and superconductivity in the  $Ce_nPd_mIn_{3n+2m}$  and  $Ce_nPt_mIn_{3n+2m}$  homologous series*
- P-70 **Tang Nan** ISSP, The University of Tokyo  
*Low Temperature Thermal Expansion and Magnetostriction Measurements of Quantum Spin Ice system*
- P-71 **Masaya Taniguchi** Graduate School of Science and Engineering Iwate university  
*Successive phase transition in the cage compound  $PrV_2Al_{20}$  probed by ultrasonic measurements*
- P-72 **Masahiro Nakamura** Graduate School of Science and Engineering Iwate university  
*Elastic properties of the caged compound  $NdV_2Al_{20}$  probed by ultrasound measurements*
- P-73 **David Schroeter** TU Braunschweig  
*MnSi-nanostructures obtained from thin films: magnetotransport and Hall effect*
- P-74 **Michal Vališka** Department of Condensed Matter Physics, Charles University  
*Uranium ferromagnet with negligible magnetocrystalline anisotropy –  $U_4Ru_7Ge_6$*
- P-75 **Takumi Ohtsuki** ISSP, The University of Tokyo  
*Electronic and magnetotransport properties of pyrochlore  $Pr_2Ir_2O_7$  epitaxial thin films*
- P-76 **Shigeo Ohara** Nagoya Institute of Technology  
*Synthesis, structure and magnetism in honeycomb magnets of  $RNi_3Al_9$ ,  $RNi_3Ga_9$ ,  $R_2Pt_6Ga_{15}$ , and  $R_2Rh_3Ga_9$  (R: rare earth elements)*
- P-77 **Dominik M. Juraschek** ETH Zurich  
*Dynamical Multiferroicity*
- P-78 **Kazumasa Horigane** Research Institute for Interdisciplinary Science, Okayama University  
*Magnetic phase diagram in  $Sr_{2-x}La_xIrO_4$  synthesized by mechanical alloying method*
- P-79 **Kaya Kobayashi** Okayama University  
*Intercalated Bismuth Selenide superconductor: Resilient superconductivity over structural transition*
- P-80 **Muhammad Ikhlas** ISSP, The University of Tokyo  
*Doping dependence of the Anomalous Transport Properties of  $Mn_3Sn$*
- P-81 **Alix McCollam** High Field Magnet Laboratory, Radboud University  
*Relation of quasiparticle mass enhancement to antiferroquadrupolar order in  $PrOs_4Sb_{12}$*
- P-82 **Yusuke Kousaka** Okayama University  
*Homo-chiral crystallization and Mono-chiral helimagnetism in inorganic chiral magnetic compounds*
- P-83 **Yuji Muro** Toyama Prefectural University  
*Single crystal study for a ferromagnetic Kondo compound  $\alpha$ - $CeNiSb_3$*
- P-84 **Akira Sekiyama** Graduate School of Engineering Science, Osaka University  
*Linear dichroism in angle-resolved core-level photoemission spectra reflecting anisotropic strongly correlated outer-orbital charge distributions*
- P-85 **Naoyuki Katayama** Nagoya University  
*Phase transitions in vanadium chalcogenides with a two dimensional triangular lattice*
- P-86 **Satoru Hamamoto** Graduate school of engineering science, Osaka University  
*Linear dichroism in angle-resolved core level photoemission reflecting 4f ground state symmetry of strongly correlated cubic Pr compounds*
- P-87 **Matthias Raba** CNRS, Grenoble, France  
*Electronic and magnetic properties of  $CePt_2In_7$*
- P-88 **Nobuyuki Abe** The University of Tokyo  
*Magnetic structure and magnetoelectric effect in buckled honeycomb lattice antiferromagnet  $Co_4Ta_2O_9$*
- P-89 **Ryuji Higashinaka** Tokyo Metropolitan University  
*Magnetic and structural properties of  $BiS_2$ -based layered superconductors  $LnO_{1-x}F_xBiS_2$*
- P-90 **Tsuyoshi Omi** The University of Tokyo  
*Observation of a nonreciprocal signal in ferromagnetic resonance in multiferroic  $GaFeO_3$*
- P-91 **Hiraku Saito** Graduate School of Science, Hokkaido University  
*Current-Induced Magnetization on  $UNi_4B$  and  $CeRh_2Si_2$*
- P-92 **Jo Imai** Graduate School of Engineering, Iwate University  
*Ultrasonic measurement of Fe-based superconducting  $SrFe_2(As_{1-x}P_x)_2$*

## Access to the Workshop venue

[Access from Narita airport to Morioka station](#)

[Access from Haneda airport to Morioka station](#)

[Access from Morioka station to Hachimantai Royal Hotel](#)

① Free Shuttle Bus (**Reservation required** : Workshop secretary will contact you in advance.)

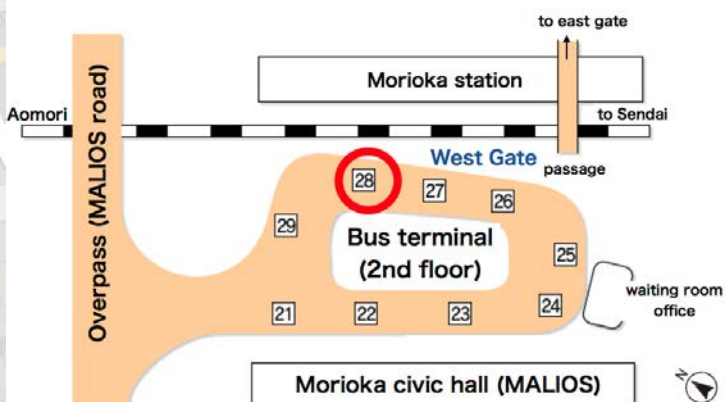
**1st Bus**            Time    : September 24 (Sunday) **13:00**  
                          Place    : [Iwate University Library](#)  
                          Bus     : Hachimantai Royal Hotel Shuttle Bus (J-Physics2017 dedicated)  
                          Capacity : 50 persons

**2nd Bus**            Time    : September 24 (Sunday) **14:00**  
                          Place    : around [Bus Stop No. 28, Morioka Station West Gate](#)  
                          Bus     : Hachimantai Spa Free Shuttle Bus  
                          Capacity : unlimited

**3rd Bus**            Time    : September 24 (Sunday) **16:00**  
                          Place    : around [Bus Stop No. 28, Morioka Station West Gate](#)  
                          Bus     : Hachimantai Royal Hotel Shuttle Bus (J-Physics2017 dedicated)  
                          Capacity : 50 persons



[Iwate University Library](#)  
[Temporary Bus Stop](#)



[Bus Stop No. 28, Morioka Station](#)  
[West Gate](#)

② Local Bus

Place : [Bus Stop No. 3, Morioka Station East Gate](#)

Bus : Northern Iwate Transportation Inc. (Iwate Kenhoku Bus)

Route and Fare :

②- 1 Destination Matsukawa Onsen (JPY 1,020)

Morioka St. No.3	→	Hachimantai Royal Hotel (Bus Stop)
6:54	→	8:33
12:12	→	13:44
13:42	→	15:12

②- 2 Hachimantai Shizen Sansaku Bus (JPY 1,020)

Morioka St. No.3	→	Hachimantai Royal Hotel (Bus Stop)
9:10	→	10:16

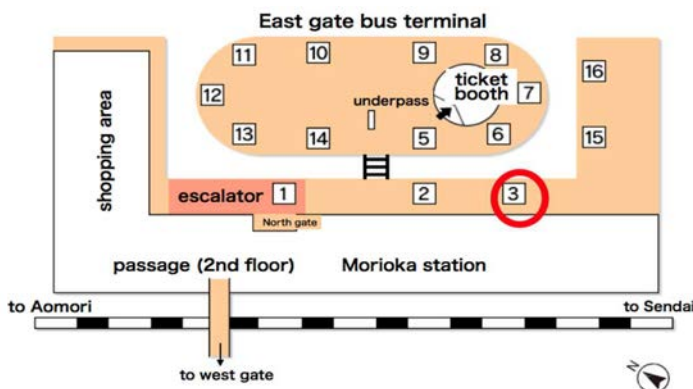
②- 3 Destination: Hachimantai Resort Hotel (JPY 1,110 or 1,020)

Morioka St. → **Hachimantai**  
**Onsenkyo**

8:02	→	9:36
9:02	→	10:40
10:42	→	12:12
11:42	→	13:20
12:42	→	14:20
14:42	→	16:23

Morioka St. → **Hachimantai**  
**Onsenkyo**

15:42	→	17:10
16:42	→	18:10
18:04	→	19:45
18:57	→	20:20
19:52	→	21:15



[Bus Stop No.3, Morioka Station East Exit](#)

[from Hachimantai Onsenkyo to Hachimantai Royal hotel \(distance: 600m\)](#)

## O-1

Multipolar Order in  $\text{Sr}_2\text{IrO}_4$  and  $\text{Cd}_2\text{Re}_2\text{O}_7$ M. R. Norman<sup>1</sup>, S. Di Matteo<sup>2</sup><sup>1</sup>Materials Science Division, Argonne National Laboratory, Argonne, IL 60439, USA<sup>2</sup>Institut de Physique de Rennes, Universite de Rennes 1, F-35042 Rennes Cedex, France

Two recent second harmonic generation (SHG) experiments have revealed the possibility of exotic order, possibly due to orbital currents, in  $\text{Sr}_2\text{IrO}_4$  [1] and  $\text{Cd}_2\text{Re}_2\text{O}_7$  [2]. Here, we analyze these data to determine whether alternate possibilities exist.

For the layered iridate  $\text{Sr}_2\text{IrO}_4$  [3], we find that two possible magnetic ground states, the magnetoelectric  $-++$  state and the non-magnetoelectric  $++++$  state, allow for an SHG signal (here,  $-/+$  refers to the sign of the net ferromagnetic moment for each of the four  $\text{IrO}_2$  layers of the unit cell). The former magnetic state is characterized by a toroidal dipole and a magnetic quadrupole, the latter by a magnetic dipole and a magnetic octupole. The observed magnetic ground state for  $\text{Sr}_2\text{IrO}_4$ , though, is the  $-++$  state, which does not have an SHG signal. Possible reasons for this discrepancy are discussed, as well as RXS experiments that could be performed to test various scenarios.

For the metallic pyrochlore  $\text{Cd}_2\text{Re}_2\text{O}_7$ , the SHG signal can be characterized by an axial toroidal quadrupole [4], but this is now known to be a secondary order parameter [2]. Instead, we find that two possible magnetic space groups could be responsible for the observed primary order parameter, each of which is characterized by a magnetic quadrupole and a magnetic octupole, and one of which is similar to the magnetic ground state that has been observed in  $\text{Cd}_2\text{Os}_2\text{O}_7$ . But NMR data do not indicate magnetic order in  $\text{Cd}_2\text{Re}_2\text{O}_7$ , and moreover the SHG data do not seem to reflect the non-zero incidence angle of the experiment. Again, possible reasons for these discrepancies are discussed, as well as RXS experiments that could be performed to test various scenarios.

We conclude by emphasizing that second harmonic generation is a wonderful method to identify hidden order associated with novel electronic states and magnetic configurations characterized by higher order, parity-odd, multipoles (e.g., magnetic quadrupoles). But we remark that such multipoles are not necessarily associated with orbital currents.

Work supported by the Materials Sciences and Engineering Division, Basic Energy Sciences, Office of Science, US DOE.

[1] L. Zhao *et al.*, *Evidence of an odd-parity hidden order in a spin-orbit coupled correlated iridate*, Nature Physics 12, 32 (2016).

[2] J. W. Harter *et al.*, *A parity-breaking electronic nematic phase transition in the spin-orbit coupled metal  $\text{Cd}_2\text{Re}_2\text{O}_7$* , Science 356, 295 (2017).

[3] S. Di Matteo and M. R. Norman, *Magnetic ground state of  $\text{Sr}_2\text{IrO}_4$  and implications for second-harmonic generation*, Phys. Rev. B 94, 075148 (2016).

[4] S. Di Matteo and M. R. Norman, *The nature of the tensor order in  $\text{Cd}_2\text{Re}_2\text{O}_7$* , arXiv:1707.03807

## O-2

## Majorana fermions in Kitaev magnets

Y. Motome

University of Tokyo, Tokyo 113-8656, Japan

The quantum spin liquid is an enigmatic quantum state of insulating magnets, in which any conventional magnetic ordering is prevented by quantum fluctuations even at zero temperature. The most prominent feature is fractionalization of quantum spins into exotic quasiparticles. We here give an overview on our recent theoretical studies on the Kitaev model which provides an exact quantum spin liquid with fractionalization into two types of Majorana fermions. We show how the fractionalized Majorana fermions manifest themselves in the temperature and energy dependence of experimental observables, such as the specific heat, entropy, magnetic susceptibility, spin-spin correlations, NMR relaxation rate, dynamical spin structure factor, magnetic Raman scattering, and thermal conductivity [1-7]. We discuss our results in comparison with the experiments for candidate materials in layered iridates and ruthenates.

This work has been done in collaboration with J. Nasu, M. Udagawa, J. Yoshitake, Y. Kato, Y. Kamiya, J. Knolle, D. L. Kovrizhin, and R. Moessner. This research was supported by Grants-in-Aid for Scientific Research under Grants No. JP15K13533, No. JP16K17747, No. JP16H02206, and No. JP16H00987. Parts of the numerical calculations were performed in the supercomputing systems in ISSP, the University of Tokyo.

- [1] J. Nasu, M. Udagawa, and Y. Motome, *Phys. Rev. B* **92**, 115122 (2015).
- [2] J. Nasu, J. Knolle, D. L. Kovrizhin, Y. Motome, and R. Moessner, *Nature Phys.* **12**, 912 (2016).
- [3] J. Yoshitake, J. Nasu, and Y. Motome, *Phys. Rev. Lett.* **11**, 157203 (2016).
- [4] J. Yoshitake, J. Nasu, Y. Kato, and Y. Motome, *Phys. Rev. B* **96**, 024438 (2017).
- [5] J. Yoshitake, J. Nasu, and Y. Motome, *Phys. Rev. B* **96**, 064433 (2017).
- [6] S.-H. Do, S.-Y. Park, J. Yoshitake, J. Nasu, Y. Motome, Y. S. Kwon, D. T. Adroja, D. J. Voneshen, K. Kim, T.-H. Jang, J.-H. Park, K.-Y. Choi, and S. Ji, preprint (arXiv:1703.01081), to appear in *Nature Phys.*
- [7] J. Nasu, J. Yoshitake and Y. Motome, preprint (arXiv:1703.10395), to appear in *Phys. Rev. Lett.*

# O-3

## STM study of surface electron-doped $\text{Sr}_2\text{IrO}_4$

Tong Zhang<sup>1,2</sup>

<sup>1</sup>State Key Laboratory of Surface Physics, Department of Physics, and Advanced Materials Laboratory,  
Fudan University, Shanghai 200433, China

<sup>2</sup>Collaborative Innovation Center of Advanced Microstructures,  
Fudan University, Shanghai 200433, China

$\text{Sr}_2\text{IrO}_4$  was predicted to be a high-temperature superconductor upon electron doping since it highly resembles the cuprates in crystal structure, electronic structure, and magnetic coupling constants. Here, we report a scanning tunneling microscopy/spectroscopy (STM/STS) study of  $\text{Sr}_2\text{IrO}_4$  with surface electron doping by depositing potassium (K) atoms. We find that as the electron doping increases, the system gradually evolves from an insulating state to a normal metallic state, via a pseudogap-like phase, and a phase with a sharp, V-shaped low-energy gap with about 95% loss of density of state (DOS) at EF. At certain K coverage (0.5–0.6 monolayer), the magnitude of the low-energy gap is 25–30 meV, and it closes at around 50 K. Our observations show that the electron-doped  $\text{Sr}_2\text{IrO}_4$  remarkably resembles hole-doped cuprate superconductors [1].

This work is supported by the National Science Foundation of China and National Basic Research Program of China.

[1] Y. J. Yan *et al.*, PHYSICAL REVIEW X 5, 041018 (2015)

## O-4

## Honeycomb Lattice Iridates as Avenues for Exploring Kitaev Physics

Yogesh Singh<sup>1</sup><sup>1</sup> Department of Physical Sciences, Indian Institute of Science Education and Research Mohali, Sector 81, S. A. S. Nagar, Manauli PO 140306, India

Kitaev's model for spins  $S = \frac{1}{2}$  on a honeycomb lattice is a rare example of an exactly solvable model of interacting spins. The ground state of the model is a quantum spin liquid (gapless or gapped depending on whether the model is isotropic or not) with Majorana Fermion excitations [1, 2]. Jackeli and Khaliullin proposed that Kitaev like magnetic interactions could be designed in honeycomb lattice Mott insulators with strong spin-orbit coupling, specifically  $A_2\text{IrO}_3$  [2, 3]. It was however, realized that in addition to pure Kitaev interactions, additional interactions might be present. The QSL phase was found to stay robust close to the strong Kitaev limit [3]. Rapid experimental progress in the study of the proposed materials was made possible by the growth of single crystals of  $\text{Na}_2\text{IrO}_3$  [4] and high quality polycrystalline  $\text{Li}_2\text{IrO}_3$  [5]. Both  $A_2\text{IrO}_3$  materials were found to have magnetically ordered ground states [4,5] and the magnetic order [6, 7] could not be understood within the nearest neighbour Kitaev-Heisenberg model of Ref [3]. There is however growing evidence, from first principles calculations [8-10] and from experiments [11-14], that large Kitaev-like interactions are present in both materials. This gives hope that one may be able to tune these materials proximate to Kitaev's QSL state. In this talk I will review the current status of work on these materials with emphasis on experimental studies.

- [1] A. Kitaev, *Ann. Phys.* **321**, 2 (2006).
- [2] G. Jackeli and G. Khaliullin, *Phys. Rev. Lett.* **102**, 017205 (2009).
- [3] J. Chaloupka, G. Jackeli, and G. Khaliullin, *Phys. Rev. Lett.* **105**, 027204 (2010).
- [4] Yogesh Singh and P. Gegenwart, *Phys. Rev. B* **82**, 064412 (2010).
- [5] Yogesh Singh, S. Manni, J. Reuther, T. Berlijn, R. Thomale, W. Ku, S. Trebst, and P. Gegenwart, *Phys. Rev. Lett.* **108**, 127203 (2012).
- [6] S. K. Choi, R. Coldea, A. N. Kolmogorov, T. Lancaster, I. I. Mazin, S. J. Blundell, P. G. Radaelli, Yogesh Singh, P. Gegenwart, K. R. Choi, S-W Cheong, P. J. Baker, C. Stock, J. Taylor
- [7] F. Ye, S. Chi, H. Cao, B. C. Chakoumakos, J. A. Fernandez-Baca, R. Custelcean, T. Qi, O. B. Korneta, and G. Cao, *Phys. Rev. B* **85**, 180403(R) (2012).
- [8] K. Foyevtsova, H. O. Jeschke, I. I. Mazin, D. I. Khomskii, and R. Valenti, *Phys. Rev. B* **88**, 035107 (2013).
- [9] V. M. Katukuri, S. Nishimoto, V. Yushankhai, A. Stoyanova, H. Kandpal, S. Choi, R. Coldea, I. Rousochatzakis, L. Hozoi, and J. van den Brink, *New J. Phys.* **16**, 013056 (2014).
- [10] Y. Yamaji, Y. Nomura, M. Kurita, R. Arita, and M. Imada, *Phys. Rev. Lett.* **113**, 107201 (2014).
- [11] S. H. Chun, J.-W. Kim, J. Kim, H. Zheng, C. C. Stoumpos, C. D. Malliakas, J. F. Mitchell, K. Mehlawat, Y. Singh, Y. Choi, T. Gog, A. Al-Zein, M. Moretti Sala, M. Krisch, J. Chaloupka, G. Jackeli, G. Khaliullin, and B. J. Kim, *Nat. Phys.* **11**, 462 (2015).
- [12] S. N. Gupta, P. V. Sriluckshmy, K. Mehlawat, A. Balochi, D. K. Mishra, S. R. Hassan, T. V. Ramakrishnan, D. V. S. Muthu, Y. Singh, and A. K. Sood, *Euro. Phys. Lett.* **114**, 47004 (2016).
- [13] Zh. Alpichshev, F. Mahmood, G. Cao, and N. Gedik, *Phys. Rev. Lett.* **114**, 017203 (2015).
- [14] Kavita Mehlawat, A. Thamizhavel, and Yogesh Singh, *Phys. Rev. B* **95**, 144406, (2017).

## O-5

Quantum Multicritical Point in  $\text{YbRh}_2\text{Si}_2$ 

M. Brando<sup>1</sup>, S. Hamann<sup>1</sup>, J. Zhang<sup>1,2</sup>, D. Jang<sup>1</sup>, A. Hannaske<sup>1</sup>, L. Steinke<sup>1,3</sup>, S. Lausberg<sup>1</sup>, L. Pedrero<sup>1</sup>, C. Klingner<sup>1</sup>, F. Steglich<sup>1,2</sup>, C. Geibel<sup>1</sup>, C. Krellner<sup>4</sup>

<sup>1</sup>Max Planck Institute for Chemical Physics of Solids, D-01187 Dresden, Germany

<sup>2</sup>Center of Correlated Matter, Zhejiang University, CHN-310058 Hangzhou, China

<sup>3</sup>Condensed Matter Physics and Materials Science Department, Brookhaven National Laboratory, Upton, New York 11973, USA

<sup>4</sup>Institute of Physics, Goethe University Frankfurt, D-60438 Frankfurt am Main, Germany

During the last few decades, the existence of quantum critical points (QCPs) has been verified in low-temperature antiferromagnets like  $\text{YbRh}_2\text{Si}_2$  which has a transition temperature of 70 mK. In this material the QCP can be induced by a small magnetic field ( $\mathbf{B}$ ) applied both along the crystallographic  $c$ -axis ( $\mathbf{B} \parallel c$ ) or within the  $ab$ -plane ( $\mathbf{B} \perp c$ ). The nature of this QCP is undoubtedly not conventional and still under strong debate. Investigations on the Co-substituted  $\text{YbRh}_2\text{Si}_2$  provide solid basis of evidence that the nature of the QCP in  $\text{YbRh}_2\text{Si}_2$  with  $\mathbf{B} \parallel c$  is different from that with  $\mathbf{B} \perp c$ . In fact, with  $\mathbf{B} \parallel c$ , the QCP is the endpoint of a first order transition line and it is therefore a quantum multicritical point. Such a situation has never been observed in any material before and it is in excellent agreement with the theory proposed by Misawa *et al.*, (T. Misawa, Y. Yamaji, and M. Imada, JPSJ **77**, 093712 (2008)).

## O-6

## Magnetic quasicrystal with Yb icosahedron

K. Deguchi<sup>1</sup>, K. Namba<sup>1</sup>, S. Matsukawa<sup>1</sup>, S. Hirokawa<sup>1</sup>, Y. Yoneyama<sup>1</sup>, S. Yokota<sup>1</sup>, K. Imura<sup>1</sup>,  
T. Ishimasa<sup>2,3</sup>, and N. K. Sato<sup>1</sup>

<sup>1</sup>Department of Physics, Graduate School of Science, Nagoya University, Nagoya 464-8602, Japan

<sup>2</sup>Division of Applied Physics, Graduate School of Engineering, Hokkaido University, Sapporo 060-8628, Japan

<sup>3</sup>Toyota Physical and Chemical Research Institute, Nagakute, Aichi 480-1192, Japan

Heavy fermion intermetallic compounds have attracted much interest to study unconventional superconductivity and non-Fermi-liquid states, related to quantum criticality. Until very recently, quantum criticality has been intensively studied in only crystalline materials. Quasicrystals possess long-range, quasi-periodic structures with diffraction symmetries forbidden to crystals. Recently, a new type of icosahedral Yb quasicrystal and approximant was discovered. The Au-Al-Yb quasicrystal with Tsai-type cluster exhibits novel quantum critical behavior as observed in Yb-based heavy fermion materials with intermediate Yb valence, while the Au-Al-Yb approximant shows heavy Fermi liquid behavior [1]. Furthermore, quantum critical phenomenon of the Au-Al-Yb quasicrystal is remarkably robust against hydrostatic pressure, related to the critical state unique to the quasicrystal. By contrast, the Au-Al-Yb approximant shows heavy fermion behavior, very sensitive to hydrostatic pressure and quantum criticality of the approximant is induced by pressure [2]. Therefore, the quantum critical state of the Au-Al-Yb quasicrystal might correspond to an electronic state unique to the quasicrystals. Furthermore, we have found superconductivity of Au-Ge-Yb approximants with Tsai-type cluster for the first time [3]. Although strongly correlated electrons have been intensively studied in crystalline materials, the icosahedral Yb quasicrystals and approximants shed a new light on strongly correlated electrons in quasicrystals. Interestingly, quantum criticality of the Au-Al-Yb quasicrystal seems to be closely related to heavy fermion crystalline compound. Studying the magnetism of icosahedral Yb quasicrystals and approximants by substitution of Yb ligands, we have found that the Au-Al-Yb system is actually located near the border of the valence change [4]. We will discuss the substitution effect in the Au-Al-Yb quasicrystal, supporting that the valence fluctuation plays a crucial role in the unconventional quantum criticality.

[1] K. Deguchi *et al.*, *Nature Materials* **11**, 1013 (2012).

[2] S. Matsukawa *et al.*, *J. Phys. Soc. Jpn.* **85**, 063706 (2016)

[3] K. Deguchi *et al.*, *J. Phys. Soc. Jpn.* **8**, 023705 (2015).

[4] M. Hayashi *et al.*, *J. Phys. Soc. Jpn.* **86**, 043702 (2017).

# O-7 Quantum criticality universal to Yb-based quasicrystal and periodic crystal

Shinji WATANABE

<sup>1</sup>*Department of Basic Sciences, Kyushu Institute of Technology, Kitakyushu, Japan*

Recently, it has been discovered that heavy-electron quasicrystal (QC)  $\text{Yb}_{15}\text{Al}_{34}\text{Au}_{51}$  shows unconventional quantum criticality [1]. This criticality is common to those observed in heavy-electron crystals  $\text{YbRh}_2\text{Si}_2$  and  $\beta\text{-YbAlB}_4$ , which is well explained by critical Yb-valence fluctuations (CVF) [2]. The CVF theory based on the minimal model for the QC and the approximant crystal (AC)  $\text{Yb}_{14}\text{Al}_{35}\text{Au}_{51}$ , which consist of concentric shell structures with Yb and Au-Al cluster (Tsai-type cluster), has shown (1) robustness of the quantum criticality in the QC under pressure, (2) emergence of the same criticality even in the AC when applied pressure is tuned, and (3) wider quantum critical region in the  $T$ - $P$  phase diagram of the QC than that of the AC [3,4]. These (1)-(3) have actually been observed by recent experiments [1,5].

To get insight into the mechanism of the emergence of the unconventional quantum criticality observed in the pressurized AC as well as the QC, the AC is analyzed theoretically [6]. By constructing the periodic Anderson model on the AC, which has the periodic arrangement of the bcc structure of the Yb-Au-Al cluster, the heavy quasiparticle band is shown to be formed near the Fermi level because of strong correlation of 4f electrons at Yb. This is the first clarification of the electronic state of the Yb-based AC with intermediate valence of Yb, since the band-structure calculation has not been performed because of too-many number of atoms per unit cell. We find that charge-transfer mode between 4f electron at Yb on the 3rd shell and 3p electron at Al on the 4th shell in the Yb-Au-Al cluster is considerably enhanced with almost flat momentum dependence. Then, we applied the mode-mode coupling theory of the CVF under a magnetic field developed recently [7] to the charge-transfer mode in the AC. The result shows that magnetic as well as valence susceptibility exhibits  $\chi \sim T^{-0.5}$  for the zero-field limit and is expressed as a single scaling function of the ratio of temperature to magnetic field  $T/B$  over four decades even in the AC when some condition is satisfied by varying parameters, e.g., by applying pressure [6]. The  $T/B$  scaling, which is essentially the same as that observed in  $\beta\text{-YbAlB}_4$  [8], has also been detected recently in the pressurized AC [5] and the QC [9]. The key origin is clarified to be due to strong locality of the CVF and small Brillouin zone reflecting the large unit cell, giving rise to the extremely-small characteristic energy scale of the CVF. This also gives a natural explanation for the quantum criticality in the QC [1] corresponding to the infinite limit of the unit-cell size of the AC.

In the presentation, we discuss these newly-clarified aspects of quantum critical phenomena and the key origin of the unconventional criticality commonly observed in Yb-based periodic-crystal and quasicrystal systems [10]. This presentation is based on the work done in collaboration with K. Miyake.

- [1] K. Deguchi *et al.*, Nature Mat. **11**, 1013 (2012).
- [2] S. Watanabe and K. Miyake, Phys. Rev. Lett. **105**, 186403 (2010).
- [3] S. Watanabe and K. Miyake, J. Phys. Soc. Jpn. **82**, 083704 (2013).
- [4] S. Watanabe and K. Miyake, J. Phys.: Conf. Ser. **592**, 012087 (2015).
- [5] S. Matsukawa *et al.*, J. Phys. Soc. Jpn. **85**, 063706 (2016).
- [6] S. Watanabe and K. Miyake, J. Phys. Soc. Jpn. **85**, 063703 (2016).
- [7] S. Watanabe and K. Miyake, J. Phys. Soc. Jpn. **83**, 103708 (2014).
- [8] Y. Matsumoto *et al.*, Science **331**, 316 (2011).
- [9] K. Deguchi, invited talk at SCES2016 conference, Th-S18-2.
- [10] S. Watanabe and K. Miyake, Jpn. J. Appl. Phys. **56**, 05FA01 (2017).

Superconductivity coexisting with magnetic multipole orders in  $\text{Sr}_2\text{IrO}_4$ 

Shuntaro Sumita<sup>1</sup>, Takuya Nomoto<sup>2</sup>, and Youichi Yanase<sup>1</sup>  
<sup>1</sup>Department of Physics Kyoto University, Kyoto 606-8502, Japan  
<sup>2</sup>RIKEN, Wako, Saitama 351-0198, Japan

Recently, a layered perovskite  $5d$  transition metal oxide  $\text{Sr}_2\text{IrO}_4$  has attracted much attention because a lot of similarities to high-temperature cuprate superconductors have been recognized. For example, recent experiments on electron-doped  $\text{Sr}_2\text{IrO}_4$  indicate the emergence of a pseudogap [1] and at low temperatures a  $d$ -wave gap [2]. Furthermore,  $d$ -wave superconductivity in  $\text{Sr}_2\text{IrO}_4$  by carrier doping is theoretically predicted by several studies [3-4]. Distinct differences of  $\text{Sr}_2\text{IrO}_4$  from cuprates are large spin-orbit coupling and nonsymmorphic crystal structure, both of which attract interest in the modern condensed matter physics.

Below  $T_N \simeq 230$  K, an antiferromagnetic order develops in undoped  $\text{Sr}_2\text{IrO}_4$ . Large spin-orbit coupling and rotation of octahedra lead to canted magnetic moments from the  $a$  axis and induce a small ferromagnetic moment along the  $b$  axis (Fig. 1). Several magnetic structures for stacking along the  $c$  axis have been reported in response to circumstances. In the undoped compound, the ferromagnetic component shows the stacking pattern  $-++-$  [5]. On the other hand, the  $++++$  pattern is suggested as the magnetic structure of  $\text{Sr}_2\text{IrO}_4$  in a magnetic field directed in the  $ab$  plane [5] and of Rh-doped  $\text{Sr}_2\text{Ir}_{1-x}\text{Rh}_x\text{O}_4$  [6, 7]. The recent observation [8], however, advocates the  $-++-$  magnetic pattern indicating an intriguing odd-parity hidden order in  $\text{Sr}_2\text{IrO}_4$ .

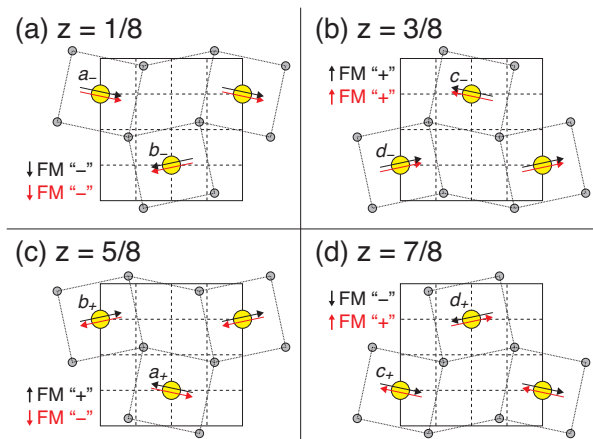


Fig. 1 Crystal and magnetic symmetries of  $\text{Sr}_2\text{IrO}_4$  in the 4  $\text{IrO}_2$  planes: (a)  $z = 1/8$ , (b)  $z = 3/8$ , (c)  $z = 5/8$ , and (d)  $z = 7/8$  [9]. The two magnetic patterns of interest,  $-++-$  (black arrows) and  $-++-$  (red arrows), are shown.

Stimulated by these backgrounds, we show that  $\text{Sr}_2\text{IrO}_4$  may be a platform realizing two unconventional superconducting states, assuming the coexistence with magnetic order,  $-++-$  and  $-++-$ . Using a group theoretical analysis, we can find that the  $-++-$  order can be regarded as a magnetic octupole order, while the  $-++-$  order is considered as an odd-parity magnetic quadrupole order. The superconducting property in each magnetic multipole state is summarized in the following. First, superconductivity with nonsymmorphic symmetry-protected gap structures is shown in the  $-++-$  state. Second, the Fulde-Ferrell-Larkin-Ovchinnikov superconductivity without macroscopic magnetization is stabilized in the  $-++-$  state.

- [1] Y. K. Kim *et al.*, *Science* **345**, 187 (2014).
- [2] Y. K. Kim *et al.*, *Nat. Phys.* **12**, 37 (2016).
- [3] F. Wang and T. Senthil, *Phys. Rev. Lett.* **106**, 136402 (2011).
- [4] H. Watanabe *et al.*, *Phys. Rev. Lett.* **110**, 027002 (2013).
- [5] B. J. Kim *et al.*, *Science* **323**, 1329 (2009).
- [6] J. P. Clancy *et al.*, *Phys. Rev. B* **89**, 054409 (2014).
- [7] F. Ye *et al.*, *Phys. Rev. B* **92**, 201112 (2015).
- [8] L. Zhao *et al.*, *Nat. Phys.* **12**, 32 (2016).
- [9] S. Di Matteo and M. R. Norman, *Phys. Rev. B* **94**, 075148 (2016).

Hidden order in URu<sub>2</sub>Si<sub>2</sub> unveiled ?

H. Ikeda

<sup>1</sup>Ritsumeikan University, Kusatsu 525-8577, Japan

The hidden order (HO) problem in URu<sub>2</sub>Si<sub>2</sub> is an unresolved issue in heavy fermion systems throughout the past 30 years since the discovery in 1984 [1]. The HO transition is characterized by a sharp specific heat jump at T<sub>HO</sub>=17.5K. In the early stage, it was considered to be a phase transition to antiferromagnetism (AFM) with the c-axis polarized moment [2]. However, the observed moment was too small to explain the large entropy loss observed at T<sub>HO</sub>. Soon afterwards, it was clarified that such small moments come from puddles of the large moment AFM [3], which appears as a long-range order under high pressure [4,5]. The transition from the HO phase to the AFM phase as a function of pressure is of the first-order type. Thus, it has been believed that the primary order parameter of the HO phase is something different from the conventional magnetic dipole order.

Theoretically, many kinds of order parameters have been proposed on the basis of the localized or the itinerant pictures; such as multipole order or density wave [6-17], chiral spin state [18], orbital AFM [19], helicity [20], dynamic symmetry breaking[21], hybridization wave [22], spin nematic [23] and hastatic order [24]. However, there are still no conclusive evidence. The complicated band structure with sizable spin-orbit coupling and the dual nature of f-electrons due to the strong electron correlation are barriers to microscopic understanding. The observed strong Ising anisotropy can be more easily described in the localized picture, while the angle resolved photoemission spectroscopy measurements partly support the itinerant picture. Under such circumstances, the recent first-principles approach provides experimentally inaccessible information and a key clue to solve the HO problem. The LDA+DMFT approach including the strong electron correlation indicates  $A_{2g}$  hexadecapole order [13], which is consistent with the localized limit analysis [15], while a weak correlation approach leads to an  $E$ -type dotriacontapole order [17]. These proposals have been supported by some recent sophisticated measurements in high-quality samples. Nematic features in the magnetic torque and cyclotron measurements [25] suggest in-plane fourfold symmetry breaking, indicative of order parameter with  $E$  representation. Raman scattering experiments [26] found a sharp low-energy excitation with  $A_{2g}$  symmetry, which is consistent with the hexadecapolar order.

In this review, we summarize the current stage in the HO problem, and discuss the consistency between these theories and experimental observations.

- [1] T. T. M. Palstra *et al.*, Phys. Rev. Lett. 55, 2727 (1985).
- [2] C. Broholm *et al.*, Phys. Rev. Lett. 58, 1467 (1987).
- [3] K. Matsuda *et al.*, Phys. Rev. Lett. 87, 087203 (2001).
- [4] H. Amitsuka *et al.*, Phys. Rev. Lett. 83, 5114 (1999).
- [5] N. P. Butch *et al.*, Phys. Rev. B 82, 060408 (2010).
- [6] P. Santini and G. Amoretti, Phys. Rev. Lett. 73, 1027 (1994); P. Santini, Phys. Rev. B 57, 5191 (1998); P. Santini *et al.*, Phys. Rev. Lett. 85, 654 (2000).
- [7] H. Ikeda and Y. Ohashi, Phys. Rev. Lett. 81, 3723 (1998).
- [8] F. J. Ohkawa and H. Shimizu, J. Phys.: Condens. Mat. 11, L519 (1999).
- [9] A. Kiss and P. Fazekas, Phys. Rev. B 71, 054415 (2005).
- [10] V. P. Mineev and M. E. Zhitomirsky, Phys. Rev. B 72, 014432 (2005).
- [11] K. Hanzawa, J. Phys.: Condens. Mat. 19, 072202 (2007).
- [12] F. Cricchio *et al.*, Phys. Rev. Lett. 103, 107202 (2009).
- [13] K. Haule and G. Kotliar, Nature Phys. 5, 796 (2009).
- [14] H. Harima, K. Miyake, and J. Flouquet, J. Phys. Soc. Jpn. 79, 033705 (2010).
- [15] H. Kusunose and H. Harima, J. Phys. Soc. Jpn. 80, 084702 (2011).
- [16] J. G. Rau and H.-Y. Kee, Phys. Rev. B 85, 245112 (2012).
- [17] H. Ikeda *et al.*, Nature Phys. 8, 528 (2012); M.-T. Suzuki and H. Ikeda, Phys. Rev. B 90, 184407 (2014).
- [18] L. P. Gor'kov and A. Sokol, Phys. Rev. Lett. 69, 2586 (1992).
- [19] P. Chandra *et al.*, Nature 417, 831 (2002).
- [20] C. M. Varma and L. Zhu, Phys. Rev. Lett. 96, 036405 (2006).
- [21] S. Elgazzar *et al.*, Nature Mater. 8, 337 (2009).
- [22] Y. Dubi and A. V. Balatsky, Phys. Rev. Lett. 106, 086401 (2011).
- [23] S. Fujimoto, Phys. Rev. Lett. 106, 196407 (2011).
- [24] P. Chandra, P. Coleman, and R. Flint, Nature 493, 621 (2013).
- [25] R. Okazaki *et al.*, Science 331, 439 (2011); S. Tonegawa *et al.*, Phys. Rev. Lett. 109, 036401 (2012).
- [26] H.-H. Kung *et al.*, Science 347, 1339 (2015); H.-H. Kung *et al.*, Phys. Rev. Lett. 117, 227601 (2016).

# O-10

## Field-induced spin-density wave in URu<sub>2</sub>Si<sub>2</sub>

William KNAFO<sup>1</sup>, Fabienne DUC<sup>1</sup>, Frédéric BOURDAROT<sup>2</sup>, Keitaro KUWAHARA<sup>3</sup>, Hiroyuki NOJIRI<sup>4</sup>, Dai AOKI<sup>2,5</sup>, Julien BILLETTE<sup>1</sup>, Paul FRINGS<sup>1</sup>, Xavier TONON<sup>6</sup>, Eddy LELIEVRE-BERNA<sup>6</sup>, Jacques FLOUQUET<sup>2</sup> & Louis-Pierre REGNAULT<sup>6</sup>

<sup>1</sup>*Laboratoire National des Champs Magnétiques Intenses, CNRS-UPS-INSA-UGA, Toulouse, France.*

<sup>2</sup>*Université Grenoble Alpes et Commissariat à l'Energie Atomique, Grenoble, France.*

<sup>3</sup>*Institute of Quantum Beam Science, Ibaraki University, Mito Japan.*

<sup>4</sup>*Institute for Materials Research, Tohoku University, Sendai, Japan*

<sup>5</sup>*Institute for Materials Research, Tohoku University, Ibaraki, Japan.*

<sup>6</sup>*Institut Laue-Langevin, Grenoble, France*

A high magnetic field applied along **c** on URu<sub>2</sub>Si<sub>2</sub> induces a cascade of first-order phase transitions in the narrow field range 35-39 T. Thanks to neutron diffraction under pulsed magnetic field, we have found that a spin-density wave is established in this high-field window [1]. After an introduction to the effects of high magnetic fields on heavy-fermion systems, our recent work on URu<sub>2</sub>Si<sub>2</sub> will be presented. Details about our new 40-T pulsed field magnet will be given. The interplay between the hidden order, the magnetic and Fermi surface properties of URu<sub>2</sub>Si<sub>2</sub> will be discussed.

[1] Knafo et al., Nature Commun. **7**, 13075 (2016).

## O-11

NMR study of URu<sub>2</sub>Si<sub>2</sub>

S. Kambe, T. Hattori, Y. Tokunaga, H. Sakai, T.D. Matsuda<sup>1</sup> and Y. Haga  
Advanced Science Research Center, Japan Atomic Energy Agency,  
Tokai-mura Ibaraki319-1195, Japan

In strongly correlated 5f-electrons systems, exotic electronic states appear due to the itinerant nature of 5f-electrons. Appearance of unconventional superconductivity under hidden ordered state in URu<sub>2</sub>Si<sub>2</sub> is typical example of it. In this study, the rotational symmetry of hidden ordered state and the superconducting gap symmetry are investigated by means of <sup>29</sup>Si-NMR. As previously reported [1-3], the strength of 2-fold rotational breaking is weak and distributed in the basal plane of hidden ordered state. Consistently, the local 4-fold symmetry is supported via 4-fold Ruderman-Kittel interaction between the nearest neighbor Si sites determined by the NMR spin echo decay in the present study. The origin of muted 2-fold symmetry will be discussed. Concerning the superconducting gap symmetry, T-dependence of Knight shift along a-axis [4] and c-axis [5] indicates that the singlet paring (i.e. d-wave) is likely for the superconducting state of URu<sub>2</sub>Si<sub>2</sub>.

This work was supported by JSPS KAKENHI Grant Number 15H05884 (J-Physics).

- [1] S. Kambe et al PRL **110** (2013) 246406.
- [2] S. Kambe et al PRB **91** (2015) 035111.
- [3] R.E. Walstedt et al PRB **93** (2016) 045122.
- [4] T. Hattori et al JPSJ **85** (2016) 073711.
- [5] T. Hattori et al in preparation.

<sup>1</sup> Present Address: Division of Physics, Tokyo Metropolitan University, Japan

## O-12

Magnetic excitations in the hidden order and antiferromagnetic phases of  $\text{URu}_{2-x}\text{Fe}_x\text{Si}_2$ N. P. Butch,<sup>1,2</sup> S. Ran,<sup>3,4</sup> I. Jeon,<sup>4,5</sup> N. Kanchanavatee,<sup>3,4</sup> K. Huang,<sup>4,5</sup> A. Breindel,<sup>3,4</sup> M. B. Maple,<sup>3,4,5</sup>R. L. Stillwell,<sup>6</sup> Y. Zhao,<sup>1,7</sup> L. Harriger,<sup>1</sup> and J. W. Lynn<sup>1</sup><sup>1</sup>NIST Center for Neutron Research, Gaithersburg, Maryland, USA<sup>2</sup>Center for Nanophysics and Advanced Materials, University of Maryland, College Park, Maryland, USA<sup>3</sup>Department of Physics, University of California San Diego, La Jolla, California, USA<sup>4</sup>Center for Advanced Nanoscience, University of California San Diego, La Jolla, California, USA<sup>5</sup>Materials Science and Engineering Program, University of California San Diego, La Jolla, California, USA<sup>6</sup>Lawrence Livermore National Laboratory, Livermore, California, USA<sup>7</sup>Department of Materials Science and Engineering, University of Maryland, College Park, Maryland, USA

The hidden order phase of  $\text{URu}_2\text{Si}_2$  is one of the best-known examples of correlated electron physics, but there is still no broad agreement regarding the underlying order parameter. I will discuss neutron scattering measurements on Fe-substituted samples, in which the hidden order phase changes to antiferromagnetism. I will describe how hybridization between uranium f-electrons and itinerant electrons leads to a correlated electron state in both phases, and what this might mean for the identity of the order parameter.

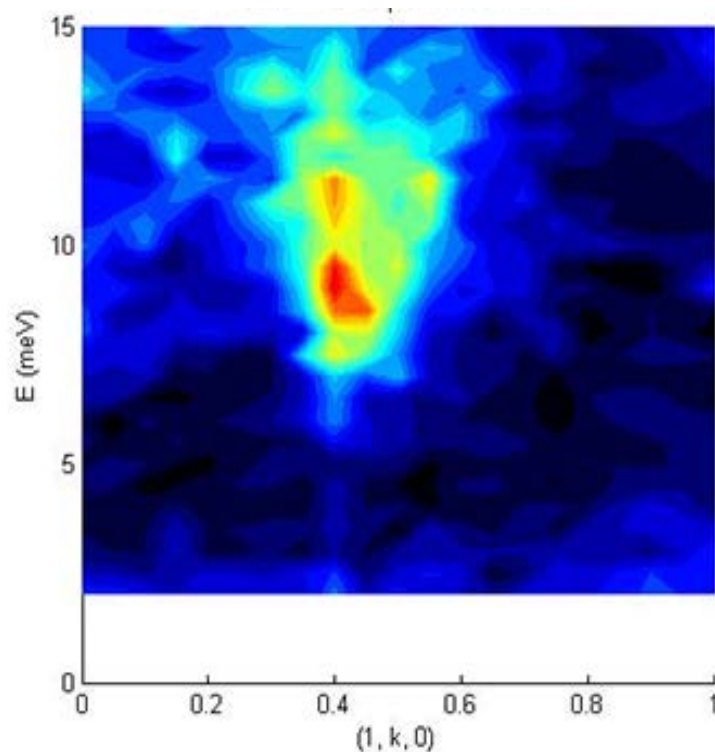


**Fig. 1** Magnetic excitations in  $\text{URu}_{1.8}\text{Fe}_{0.2}\text{Si}_2$  in the basal plane in the antiferromagnetic phase. The dominant intensity is at the incommensurate point  $(1, 0.4, 0)$ , while there is relatively little intensity at the commensurate  $(1, 0, 0)$  point.

[1] NPB, et al., Physical Review B 94, 201102(R) (2016).

## O-13

## Ferromagnetic superconductors

G. Knebel<sup>1</sup>, A. Pourret<sup>1</sup>, D. Aoki<sup>1,2</sup>, G. Bastien<sup>1</sup>, A. Gourgout<sup>1</sup>, D. Braithwaite<sup>1</sup>, J.-P. Brison<sup>1</sup>, A. Nakamura<sup>2</sup>,  
G. Seyfarth<sup>3</sup>, I. Sheikin<sup>3</sup>, and J. Flouquet<sup>1</sup>

<sup>1</sup>Univ. Grenoble Alpes, CEA, INAC-Pheliqs, 38000 Grenoble, France

<sup>2</sup>IMR, Tohoku University, Oarai, Ibaraki 311-1313, Japan

<sup>3</sup>CNRS, Laboratoire National des Champs Magnétiques Intenses LNCMI (UGA, UPS, INSA), UPR 3228, F-38042 Grenoble Cedex 9, France

We review recent studies on the ferromagnetic superconductors UCoGe and URhGe. In the first part of the presentation the high phase diagram of the ferromagnetic superconductor UCoGe will be discussed [1]. We find that superconductivity appear on a wide pressure range up to 4 GPa with the maximum of  $T_c$  at 1 GPa. The resistivity varies linearly with temperature around  $T_c$  and evolves continuously with pressure to a  $T^2$  Fermi-liquid behavior for  $p \geq 5$  GPa. Fermi surface properties of UCoGe will be discussed and we show that a cascade of Fermi surface reconstructions appear for field applied along the easy magnetization axis  $c$  [2]. In the second part the magnetic phase diagram of URhGe will be discussed and we will show that a Fermi surface instability occurs at the spin-reorientation at  $H_R$  [3], where the field induced superconducting state has its maximum. Finally we will compare the evolution of the magnetic phase diagram under pressure and under uniaxial stress applied along the  $c$  axis.

We acknowledge support from ERC grant NewHeavyFermion, French ANR Princess and the J-Physics project.

[1] G. Bastien, D. Braithwaite, D. Aoki, G. Knebel, J. Flouquet, Phys. Rev. B **93** .125110 (2016).

[2] G. Bastien, A. Gourgout, D. Aoki, A. Pourret, I. Sheikin, G. Seyfarth, J. Flouquet, G. Knebel, Phys. Rev. Lett. **116** .206401 (2016).

[3] A. Gourgout, A. Pourret, G. Knebel, D. Aoki, G. Seyfarth, J. Flouquet, Phys. Rev. Lett. **116** .046401 (2016).

# O-14

## Phase diagram of UCoGe

V.P.Mineev

Univ. Grenoble Alpes, CEA, INAC-Pheliqs, 38000 Grenoble, France

The temperature-pressure phase diagram of ferromagnetic superconductor UCoGe includes four phase transitions. They are between the paramagnetic and the ferromagnetic states with the subsequent transition in the superconducting ferromagnetic state and between the normal and the superconducting states after which the transition to the superconducting ferromagnetic state has to occur. I have developed the Landau theory description of the phase diagram and established the specific ordering arising at each type of transition.

The phase transitions to the ferromagnetic superconducting state are inevitably accompanied by the emergence of screening currents. The corresponding magnetostatics considerations allow for establishing the significant difference between the transition from the ferromagnetic to the ferromagnetic superconducting state and the transition from the superconducting to the ferromagnetic superconducting state.

## O-15

## Reentrant superconductivity induced by quantum tricritical fluctuations in URhGe

Y. Tokunaga<sup>1</sup>, D. Aoki<sup>2,3</sup>, H. Mayaffre<sup>4</sup>, S. Krämer<sup>4</sup>, M.-H. Julien<sup>4</sup>,  
C. Berthier<sup>4</sup>, M. Horvatic<sup>4</sup>, H. Sakai<sup>1</sup>, T. Hattori<sup>1</sup>, S. Kambe<sup>1</sup> and S. Araki<sup>2,5</sup>

<sup>1</sup>ASRC, Japan Atomic Energy Agency Tokai, Ibaraki 319-1195, Japan

<sup>2</sup>INAC/SPSMS, CEA-Grenoble/UJF, 38054 Grenoble, France

<sup>3</sup>IMR, Tohoku University, Ibaraki 311-1313, Japan

<sup>4</sup>LNCMI-CNRS (UPR 3228), EMFL, UGA, UPS, INSA, 38042 Grenoble, France

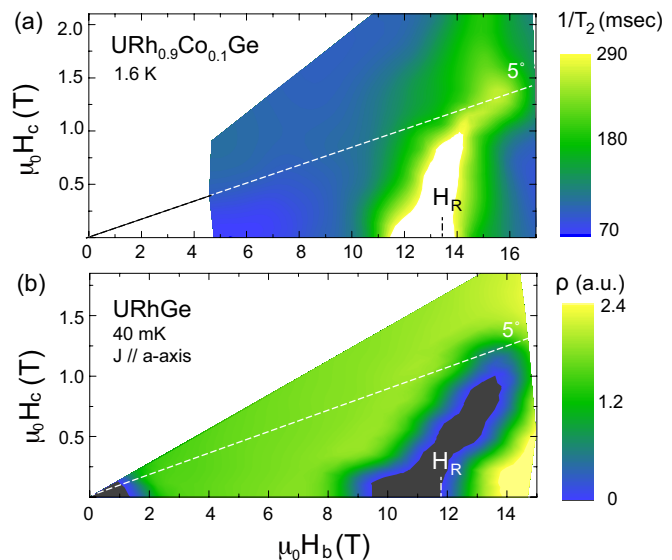
<sup>5</sup>Department of Physics, Okayama University, Okayama 700-8530, Japan

In conventional superconductors, the attractive interaction responsible for the Cooper pairs is mediated by the exchange of phonons, which do not couple with magnetic fields. The pairing interaction in the superconducting (SC) state is thus assumed to be field-independent. However, in the ferromagnetic (FM) superconductors, the pairing interaction is most likely mediated by the exchange of FM fluctuations [1,2], whose fluctuation spectrum can be strongly affected by magnetic field, as proved by recent NMR experiments [3-7]. The field dependence of the pairing strength influences their macroscopic properties like the superconducting upper critical field [3,8-10], and even provides field-induced reentrant superconductivity (RSC) in the case of the uranium-based FM superconductor URhGe [11].

The RSC highlights the close interplay between SC and magnetism in the strongly correlated electron systems. In URhGe, applied magnetic fields along the b-crystal axis ( $H_b$ ) first suppresses the lower field SC around 2 T, but then induces the RSC between 8 and 14 T. At a similar field of  $H_b = 12$  T, the FM moments are forced to be aligned along the field direction ( $\parallel b$ ). The transition is thus reminiscent of the textbook example of a quantum phase transition in a transverse Ising chain, however, the observation of first-order-like behaviors implies that the transition is not an ordinary quantum critical point, but involves a tricritical point (TCP) [5, 12-14].

In order to elucidate the nature of quantum fluctuations driving the RSC, we have performed <sup>59</sup>Co NMR in a 10% Co-doped URhGe single crystal [6,7]. Our measurements reveal a divergence of electronic spin fluctuations in the vicinity of the TCP. We mapped out the strength of spin fluctuations in the ( $H_b, H_c$ ) plane of magnetic field components, and show that critical fluctuations indeed develop in the same limited region near the field  $H_R$  as that where RSC is observed [Figure]. This strongly suggests these quantum fluctuations as the pairing glue responsible for the RSC. The fluctuations observed are characteristic of TCP, followed by a phase bifurcation toward quantum critical end points and involve a strong component perpendicular to the Ising axis ( $H \parallel b$ ). Such tricritical nature of the fluctuations should be fully involved in understanding the mechanism of the RSC [6,13,15].

Figure: (a) The contour plot of the  $1/T_2$  values at 1.6 K in URh<sub>0.9</sub>Co<sub>0.1</sub>Ge. The fluctuations diverge in the region shown by white color around  $H_R$ . (b) The contour plot of the measured resistance at 40 mK in URhGe. The black areas are regions where the sample has zero resistance. The field axes are scaled to the  $H_R$  values of each compound.



A part of this work was supported by JSPS KAKENHI Grant Number 26400375, 15K05884 (J-Physics), 26400375, 15H05745 and 15KK0174, ERC starting grant (NewHeavyFermion), ICC-IMR, and the JAEA REIMEI Research Program.

[1] V. Mineev, Phys. Rev. B **83**, 064515 (2011). [2] K. Hattori, and H. Tsunetsugu, Phys. Rev. B **87** 064501 (2013). [3] T. Hattori, *et al.* Phys. Rev. Lett. **108**, 066403 (2012). [4] T. Hattori, *et al.* J. Phys. Soc. Jpn. **83** 073708 (2014). [5] H. Kotegawa, *et al.* J. Phys. Soc. Jpn. **84**, 054710 (2015). [6] Y. Tokunaga, *et al.* Phys. Rev. Lett. **114**, 216401 (2015). [7] Y. Tokunaga, *et al.* Phys. Rev. B **93**, 201112(R) (2016). [8] Y. Tada, *et al.*, J. Phys. Soc. Jpn. **80**, SA006 (2011). [9] Y. Tada, Phys. Rev. B **93**, 174512 (2016). [10] B. Wu *et al.*, Nature commu. **8**, 14480 (2017). [11] F. Levy, *et al.*, Science **309**, 1343 (2005). [12] D. Aoki, *et al.*, J. Phys. Soc. Jpn. **83**, 094719 (2014). [13] A. Huxley, *et al.*, J. Phys. Soc. Jpn. **76**, 051011 (2007). [14] A. Gourgout, *et al.*, Phys. Rev. Lett. **117**, 046401 (2016). [15] V. P. Mineev, Phys. Rev. B **91**, 014506 (2015).

## O-16

## Pairing symmetry and stripe state in ferromagnetic superconductor UCoGe

Yasuhiro Tada<sup>1</sup><sup>1</sup>Institute for Solid State Physics, University of Tokyo, Kashiwanoha 277-8581, Japan

The ferromagnetic superconductor UCoGe is an ideal system to study interplay between ferromagnetism (FM) and superconductivity (SC) [1]. It exhibits FM below  $T_C \sim 2.6\text{K}$  and SC  $T_{sc} \sim 0.6\text{K}$  at ambient pressure, and the former is suppressed by pressure while the latter is stable over a wide range of pressure. Such a phase diagram is consistent with the previously known theoretical phase diagram of Ising magnetic fluctuations mediated superconductivity. Indeed, strong Ising anisotropy of FM and its fluctuations are found in several experiments in UCoGe.

In this study, we theoretically examine superconducting pairing symmetry and possible stripe state in UCoGe based on the scenario that the SC is mediated by Ising fluctuations. We firstly show that experimentally observed characteristic behaviors of the upper critical fields  $H_{c2}$  can be well explained theoretically for the so-called A-state by appropriately taking the Ising fluctuations into account [2, 3, 4]. The good agreement with the experiments suggests that the pairing symmetry of the SC coexisting with FM in UCoGe is the A-state which is a Weyl superconducting state with broken time reversal symmetry. Although this pairing symmetry is analogous to that of  $^3\text{He}$ -A phase, UCoGe is a charged superconductor and has the FM degrees of freedom in contrast to the neutral paramagnetic  $^3\text{He}$ . Based on these results, in the second part, we investigate the interplay between the charged Weyl SC and FM. Within a mean field approximation, it is shown that a Fulde-Ferrell-like stripe state becomes stable in the presence of FM domains in thin film geometry [5].

- [1] N. T. Huy *et al.*, Phys. Rev. Lett. 99 (2007) 067006.
- [2] T. Hattori *et al.*, Phys. Rev. Lett. 108 (2012) 066403.
- [3] Y. Tada *et al.*, J. Phys.:Conf. Ser.449 (2013) 012029.
- [4] Y. Tada, S. Takayoshi, and S. Fujimoto, Phys. Rev. B 93 (2016) 174512.
- [5] Y. Tada, *in preparation*.

Possible quantum critical point in superconducting Nd-doped CeCoIn<sub>5</sub>M. Kenzelmann<sup>1</sup><sup>1</sup>Paul Scherrer Institut, CH-5232 Villigen, Switzerland

The application of magnetic fields, chemical or hydrostatic pressure to strongly-correlated electron materials can stabilize electronic phases with different organizational principles. We study a Pauli-limited superconductor where novel superconducting and magnetic phases are expected close to the upper critical field  $H_{c2}$  [1]. It was shown a few years ago that in Ce<sub>0.95</sub>Nd<sub>0.05</sub>CoIn<sub>5</sub> a spin-density wave (SDW) exists within the superconducting state at zero field [2]. We study the field dependence of this spin-density wave using neutron diffraction, and find two different phases as a function of magnetic field [3]. At low fields, the magnetic structure appears to be stabilized by the local magnetism originating from the Nd<sup>3+</sup> ions, whereas at high fields a magnetic phase is found that may be generic to Pauli-limited superconductors at high magnetic fields.

The two magnetic structures are both spin-density waves with identical magnetic symmetry and are separated by a critical field around  $H^* = 8$  T [3]. The field-temperature (HT) phase diagram suggests the presence of a field-induced quantum phase transition at  $H^*$  (see Figure). The high-field phase shares many properties with the Q-phase in CeCoIn<sub>5</sub> [3,4], such as a first-order collapse at the upper critical field and the lower-field phase boundaries.

The identical magnetic symmetry in the two phases suggests that the instability at  $H^*$  is not magnetically driven. We propose that it is instead driven by a modification of superconducting condensate at  $H^*$ . Consistent with our earlier results on the pure CeCoIn<sub>5</sub> [4], we propose that a superconducting Cooper pair density wave condenses into the ground state and leads to coexisting singlet d-wave and triplet p-wave superconductivity

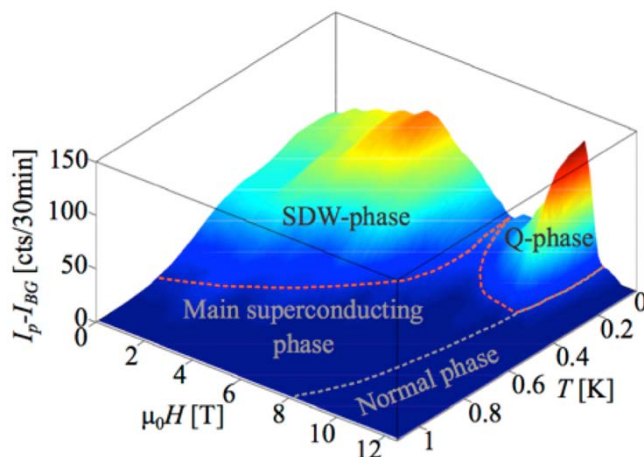


Figure: Neutron diffraction intensity as a function of temperature and magnetic field along a nodal direction of the  $d_{x^2-y^2}$  superconducting order parameter. There are two magnetic phase, termed the low-field SDW phase and the high-field Q-phase that are separated by a possible quantum critical field at  $H^*$ .

We acknowledge funding from the Swiss National Science Foundation (grant nos. 200021\_147071 and 200021\_138018), the Swiss State Secretariat for Education, Research, and Innovation through a Collaboration Research Group grant, from the European Community's Seventh Framework Programme (FP7/2007-2013) under grant agreement no. 290605 (PSI-FELLOW/COFUND), and the Danish neutron society community Danscatt.

- [1] M. Kenzelmann, *Exotic magnetic states in Pauli-limited superconductors* (invited review article), Rep. Prog. Phys. **80**, 034501 (2017).
- [2] S. Raymond, S.M. Ramos, D. Aoki, G. Knebel, V.P. Mineev and G. Lapertot, *Magnetic order in Ce<sub>0.95</sub>Nd<sub>0.05</sub>CoIn<sub>5</sub>: The Q-phase at zero magnetic field*, J. Phys. Soc. Jpn. **83**, 013707 (2014).
- [2] D.G. Mazzone, S. Raymond, J.L. Gavilano, E. Ressouche, C. Niedermayer, J.O. Birk, B. Ouladdiaf, G. Bastien, G. Knebel, D. Aoki, G. Lapertot, M. Kenzelmann, *Field-induced magnetic instability within a superconducting condensate*, Sci. Adv. **3**, e1602055 (2017).
- [3] M. Kenzelmann, Th. Strässle, C. Niedermayer, M. Sigrist, B. Padmanabhan, M. Zolliker, A. D. Bianchi, R. Movshovich, E. D. Bauer, J. L. Sarrao, and J. D. Thompson, *Coupled Superconducting and Magnetic Order in CeCoIn<sub>5</sub>*, Science **321**, 1652 (2008).
- [4] S. Gerber, M. Bartkowiak, J.L. Gavilano, E. Ressouche, N. Egetenmeyer, C. Niedermayer, A.D. Bianchi, R. Movshovich, E.D. Bauer, J.D. Thompson and M. Kenzelmann, *Switching of magnetic domains reveals evidence for spatially inhomogeneous superconductivity*, Nature Physics **10**, 126 (2014).

Superconductivity and Non-Fermi-Liquid Behaviors in  $\text{UBe}_{13}$  and Related Compounds

Yusei Shimizu

<sup>1</sup> Institute for Materials and Chemical Process, National Institute of Advanced Industrial Science and Technology, 1-1-1 Higashi, Tsukuba, Ibaraki 305-8565, Japan

Uranium-based strongly correlated 5f-electron systems show quite interesting ground-state properties, such as unconventional superconductivity, non-Fermi-liquid metallic state, and novel quantum phase, all of which are mostly caused by unusual 5f-electron degrees of freedom and Fermi-surface instabilities. In particular, the pairing mechanism of the first-generation uranium heavy-fermion superconductors, i.e.,  $\text{UBe}_{13}$  [1],  $\text{UPt}_3$  [2], and  $\text{URu}_2\text{Si}_2$  [3-5] discovered in 1980s, still remain unclear although numerous experimental and theoretical studies have been done over thirty years. To unravel the unconventional pairing mechanism, it is crucial to clarify the superconducting gap symmetries and the origin of non-Fermi-liquid behaviors because they are related to the pairing interactions and quantum fluctuations for 5f heavy electrons. In the present work, we focus on  $\text{UBe}_{13}$ , which shows an unconventional superconductivity ( $T_{SC} \sim 0.85$  K) [1] and non-Fermi-liquid behaviors at low temperatures. As for its superconducting gap symmetry, it has been discussed that a nodal gap symmetry occurs in this system [6, 7]. Furthermore, it has been reported that  $\text{U}_{1-x}\text{Th}_x\text{Be}_{13}$  shows a second phase transition [8] accompanying with the spontaneous weak magnetism at  $T_{c2} \sim 0.4$  K [9] below the bulk superconducting transition temperature ( $T_{c1} \sim 0.6$  K).

In order to gain more insight into the true nature of superconducting and unusual normal states of  $\text{UBe}_{13}$ , we have performed low-temperature heat-capacity and dc magnetization measurements using single-crystalline samples. We have recently revealed from field-orientation dependence of heat-capacity ( $C_v$ ) that nodal quasiparticle excitation is absent over the Fermi surface in  $\text{UBe}_{13}$  [10], in stark contrast to previous expectations. In addition, we have observed unusual magnetic response in dc magnetization curves [11, 12] at a magnetic field  $H \sim 2-3$  T, where a remarkable enhancement of  $C_v$  occurs inside the superconducting phase [10, 13]. Moreover, we have found that the occurrence of a peculiar paramagnetic effect near the upper-critical field  $\mu_0 H_{c2}$  [12, 14]. Regarding the non-Fermi-liquid behavior of  $\text{UBe}_{13}$ , we have precisely investigated heat capacity and dc magnetization in magnetic fields up to 14 T, focusing on their anisotropies. Our results reveal that significantly anisotropic hump anomaly occurs around 9 T, in agreement with high-field anomaly as observed by thermoelectric power measurements above  $\mu_0 H_{c2}$  [15]. We will also present recent results of heat-capacity and dc magnetization measurements for single-crystalline  $\text{U}_{1-x}\text{Th}_x\text{Be}_{13}$ , which exhibits highly unusual superconducting double transitions and non-Fermi-liquid behaviors [16].

The present work has been done in collaboration with S. Kittaka, T. Sakakibara, Y. Haga, H. Amitsuka, T. Yanagisawa, K. Machida, Y. Tsutsumi, D. Aoki, Y. Ikeda, T. Wakabayashi, K. Tenya, H. Hidaka, A. Pourret, G. Knebel, A. Palacio-Morales, S. Nakamura, Y. Homma, A. Nakamura, and E. Yamamoto [10-12, 14-16]. This work is supported in part by KAKENHI (17K14328).

- [1] H. R. Ott, H. Rudigier, Z. Fisk, and J. L. Smith, Phys. Rev. Lett. **50**, 1595 (1983).
- [2] G. R. Stewart, Z. Fisk, J. O. Willis, and J. L. Smith, Phys. Rev. Lett. **52**, 679 (1984).
- [3] T. T. M. Palstra, A. A. Menovsky, J. van den Berg, A. J. Dirkmaat, P. H. Kes, G. J. Nieuwenhuys, and J. A. Mydosh, Phys. Rev. Lett. **55**, 2727 (1985).
- [4] M.B. Maple, J.W. Chen, S.E. Lambert, Z. Fisk, J.L. Smith, H.R. Ott, J.S. Brooks, and M.J. Naughton, Phys. Rev. Lett. **5**, 477 (1985).
- [5] W. Schlabitz, J. Baumann, B. Pollit, U. Rauchschwalbe, H. M. Mayer, U. Ahlheim, and C. D. Bredl, Z. Phys. B **62**, 171 (1986).
- [6] H. R. Ott, H. Rudigier, T. M. Rice, K. Ueda, Z. Fisk, J. L. Smith, Phys. Rev. Lett. **52**, 1915 (1984).
- [7] D. E. MacLaughlin, C. Tien, W. G. Clark, M. D. Lan, Z. Fisk, J. L. Smith, H. R. Ott, Phys. Rev. Lett. **53**, 1833 (1984).
- [8] H. R. Ott, H. Rudigier, Z. Fisk, and J. L. Smith, Phys. Rev. B **31**, (R)1651 (1985).
- [9] R. H. Heffner, J. L. Smith, J. O. Willis, P. Birrer, C. Baines, F. N. Gygax, B. Hitti, E. Lippelt, H. R. Ott, A. Schenck, E. A. Knetsch, J. A. Mydosh, and D. E. MacLaughlin, Phys. Rev. Lett. **65**, 2816 (1990).
- [10] Y. Shimizu, S. Kittaka, T. Sakakibara, Y. Haga, E. Yamamoto, H. Amitsuka, Y. Tsutsumi, and K. Machida, Phys. Rev. Lett. **11**, 147002 (2015).
- [11] Y. Shimizu, Y. Haga, Y. Ikeda, T. Yanagisawa, and H. Amitsuka, Phys. Rev. Lett. **109**, 217001 (2012).
- [12] Y. Shimizu, Y. Haga, T. Yanagisawa, and H. Amitsuka, Phys. Rev. B **11**, 037001 (2016).
- [13] F. Kromer, R. Helfrich, M. Lang, F. Steglich, C. Langhammer, A. Bach, T. Michels, J. S. Kim, and G. R. Stewart, Phys. Rev. Lett. **81**, 4476 (1998).
- [14] Y. Shimizu, Y. Ikeda, T. Wakabayashi, Y. Haga, K. Tenya, H. Hidaka, T. Yanagisawa, and H. Amitsuka, J. Phys. Soc. Jpn. **80**, 093701 (2011).
- [15] Y. Shimizu, A. Pourret, G. Knebel, A. Palacio-Morales, and D. Aoki, Phys. Rev. B **92**, 241101 (2015).
- [16] Y. Shimizu, S. Kittaka, S. Nakamura, T. Sakakibara, D. Aoki, Y. Homma, A. Nakamura, and K. Machida, unpublished.

## Pairing symmetry and nodal structure in multi-orbital superconductors

Takuya Nomoto

RIKEN Center for Emergent Matter Science, Hirosawa, Wako, Saitama 351-0198, Japan

Classification of superconducting gap functions in single-orbital systems, such as summarized in Ref. [1], is indispensable for an analysis of nodal structure in various unconventional superconductors. However, the presence of unusual gap structure, which the conventional classification fails to predict, has been gradually recognized. A remarkable example is an exotic multi-gap structure in a heavy-fermion superconductor  $\text{UPt}_3$ , which we found from a gap analysis based on the first-principles calculations [2]. The obtained  $E_{2u}$  state has in-plane twofold vertical line nodes, point and horizontal line nodes on each Fermi surface, which is completely different from previous phenomenological model, and we need an explicit consideration of the multi-orbital character. In addition, T. Micklitz and M. R. Norman demonstrated in their pioneering work that new types of symmetry-protected nodes can appear at the Brillouin zone boundary in non-symmorphic systems [3]. These facts imply importance of revisiting the classification of gap structure in symmorphic/non-symmorphic space groups by explicitly considering the multi-orbital character.

In the present study, we provide the group-theoretical classification of gap functions in the multi-orbital superconductors with spin-orbit interactions [4]. We perform the gap classification by introducing generalized Cooper pairs, which possess spin-orbital coupled (multipole) degrees of freedom, instead of the conventional spin singlet/triplet in the single-orbital systems. From the classification, we obtain the following consequences: (a) A gap function with  $\Gamma^9 \otimes \Gamma^9$  in  $D_6$  possesses nontrivial momentum dependence, which is different from the usual spin 1/2 classification. This is related to the  $E_{2u}$  state in  $\text{UPt}_3$ . (b) Unconventional gap structure can be realized in the BCS approximation for a purely local interaction. We discuss the emergence of such new class of superconductivity, especially focusing on non-Kramers  $f^2$  states in cubic symmetry. (c) Reflecting symmetry of orbital basis functions there appear not symmetry protected but inevitable line nodes/gap minima, and thus, anisotropic  $d$ -wave superconductivity can be naturally explained even in the absence of competing fluctuations.

[1] M. Sgrist and K. Ueda, *Rev. Mod. Phys.* **63**, 239 (1991).

[2] T. Nomoto and H. Ikeda, *Phys. Rev. Lett.* **111**, 217002 (2016).

[3] T. Micklitz and M. R. Norman, *Phys. Rev. B* **80**, 100506(R) (2009).

[4] T. Nomoto, K. Hattori, and H. Ikeda, *Phys. Rev. B* **94**, 174513 (2016).

## O-20

Quantum criticality, superconductivity and Fermi surface dimensionality - comparison of  
CeIn<sub>3</sub>, CeRhIn<sub>5</sub>, and CePt<sub>2</sub>In<sub>7</sub>

M. Raba<sup>1</sup>; Y. Krupko<sup>1</sup>, A. Demuer<sup>1</sup>, S. Ota<sup>2</sup>, Y. Hirose<sup>2</sup>, R. Settai<sup>2</sup>, K. Götze<sup>3</sup>, J. Klotz<sup>3</sup>, T. Förster<sup>3</sup>, J.A.N. Bruin<sup>4</sup>,  
A. McCollam<sup>4</sup>, H. Harima<sup>5</sup>, D. Aoki<sup>6</sup>, I. Sheikin<sup>1</sup>

<sup>1</sup>LNCMI, CNRS, UGA, Grenoble, France

<sup>2</sup>Department of Physics, Niigata University, Niigata, Japan

<sup>3</sup>HLD, HZDR, Dresden, Germany

<sup>4</sup>HFML, Radboud University, Nijmegen, The Netherlands

<sup>5</sup>Graduate School of Science, Kobe University, Kobe, Japan

<sup>6</sup>IMR, Tohoku University, Oarai, Japan

CePt<sub>2</sub>In<sub>7</sub> is a recently discovered heavy fermion antiferromagnet with a Néel temperature  $T_N = 5.5$  K. It belongs to the same family of CeT<sub>n</sub>In<sub>2n+3</sub> ( $T$ : transition metal) systems as the well-studied CeIn<sub>3</sub> and CeRhIn<sub>5</sub>. The crystal structure of these materials consists of a sequence of CeIn<sub>3</sub> layers intercalated by  $n$  TIn<sub>2</sub> layers along the  $c$  axis. All three compounds, antiferromagnets under normal conditions, can be tuned to a quantum critical point by either pressure or magnetic field. Although their Néel temperatures differ considerably, the critical values of the tuning parameters are similar,  $P_c \sim 2.5 - 3.5$  GPa and  $H_c \sim 50 - 60$  T. Furthermore, an unconventional superconductivity emerges in the vicinity of a pressure-induced quantum critical point in all three materials.

In heavy-fermion compounds, the Fermi surface dimensionality is expected to influence both the superconducting critical temperature and the type of quantum criticality, although this issue is still somewhat controversial. While the Fermi surface is almost spherical in the anisotropic CeIn<sub>3</sub>, that of CePt<sub>2</sub>In<sub>7</sub> is almost ideally two-dimensional, with CeRhIn<sub>5</sub> located somewhat in between. I will compare the Fermi surfaces in all three materials and discuss their superconducting properties and Fermi surface reconstructions associated with quantum criticalities from this perspective.

## O-21

## Intermediate valency in hybrid f-/p-electron molecular materials

K. Prassides<sup>1</sup>, Y. Takabayashi<sup>1</sup>, T. Nakagawa<sup>1</sup>, M. Vrankic<sup>1</sup>, and J. Arvanitidis<sup>2</sup><sup>1</sup>WPI-AIMR, Tohoku University, Sendai 980-8577, Japan<sup>2</sup>Department of Physics, Aristotle University of Thessaloniki, Thessaloniki, Greece

The electronic properties of the rare earth elements are typically dominated by the +3 oxidation state. Well-established exceptions include Ce, Sm, Eu, Tm, and Yb compounds, in which the +4 or +2 oxidation states can be also stabilized. Of particular interest in such circumstances are selected rare earth systems (Kondo insulators, heavy fermions) for which the 4*f* levels lie close to the Fermi level,  $E_F$  and may exhibit mixed valence phenomena. Unambiguous signatures of electronically-driven valence changes with changes in external stimuli (temperature, pressure) are found for instance in the variation of the elastic, electronic, and magnetic properties of such mixed valence solids.

In this contribution, we will focus on our recent work on the structures and physical properties of selected mixed valence rare-earth fullerene-based architectures with stoichiometry  $RE_{2.75}C_{60}$  (Fig. 1). These materials constitute an intriguing, essentially unique class of strongly correlated electron systems because, in addition to the highly correlated cation (rare-earth) sublattice [1], they also accommodate the electronically active anion ( $C_{60}$ ) sublattice [2]. The occurrence of temperature- and pressure-driven valence transitions and giant negative thermal expansion effects and the systematic tuning of the electronic response by both isovalent and aliovalent metal substitution are being systematically mapped out by a combination of structural (synchrotron X-ray diffraction) and spectroscopic (Raman spectroscopy, synchrotron X-ray absorption spectroscopy, resonant inelastic X-ray scattering) techniques at both ambient and elevated pressures.

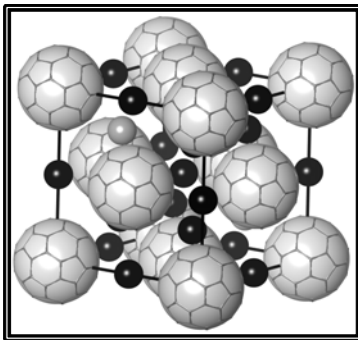


Fig. 1. Crystal structure of mixed valence rare earth fulleride  $Sm_{2.75}C_{60}$ .

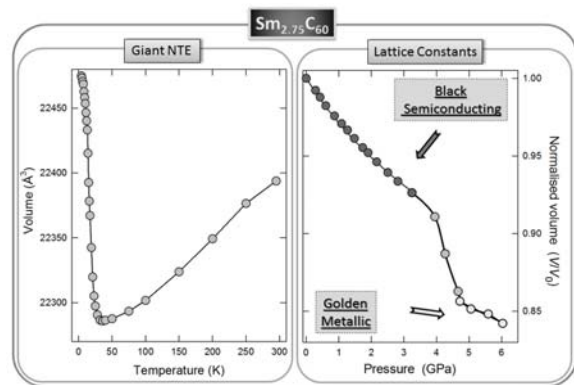


Fig. 2. Temperature and pressure response of the lattice metrics in  $Sm_{2.75}C_{60}$  in response to the valence transition.

We acknowledge financial support by JSPS under the Scientific Research on Innovative Areas ‘J-Physics’ Project (No. 15H05882).

- [1] J. Arvanitidis, K. Papagelis, S. Margadonna, K. Prassides, and A. N. Fitch, *Nature* **425**, 599-602 (2003).
- [2] R. H. Zadik, Y. Takabayashi, G. Klupp, R. H. Colman, A. Y. Ganin, A. Potočnik, P. Jeglič, D. Arčon, P. Matus, K. Kamarás, Y. Kasahara, Y. Iwasa, A. N. Fitch, Y. Ohishi, G. Garbarino, K. Kato, M. J. Rosseinsky, and K. Prassides, *Science Advances* **1**, e1500059 (2015).

## Exotic phases in artificial two-dimensional superconductors

Y. Yanase<sup>1</sup>, A. Daido<sup>1</sup>, Tsuneya Yoshida<sup>1</sup>, N. Kawakami<sup>1</sup>, Y. Nakamura<sup>2</sup>, and Tomohiro Yoshida<sup>2</sup><sup>1</sup>Kyoto University, Kyoto 606-8502, Japan<sup>2</sup>Niigata University, Niigata 950-2181, Japan

We propose exotic superconductivity by spin-orbit coupling in artificial two-dimensional superconductors.

First, we propose odd-parity superconductivity in bilayer transition metal dichalcogenides such as MoS<sub>2</sub> and WS<sub>2</sub>[1]. The superconductivity is robust against magnetic field because of the local inversion symmetry breaking, and therefore, the upper critical field exceeds the Pauli limit. Then, the odd-parity superconductivity emerges from local s-wave pairing interaction. This phase would be a new class of odd-parity superconductivity.

Second, we clarify topologically nontrivial superconducting phases realized by unconventional Cooper pairs with non-s-wave symmetry. We find several topological superconducting states controlled by spin-orbit coupling and electron correlation in two-dimensional heterostructures.

(1) Topological superconductivity designed by nodal superconductors [2,3]

Search of gapped strong topological superconductivity has been one of the central subjects in the modern condensed matter physics. We design the topological superconductivity and Weyl superconductivity based on familiar nodal spin-singlet superconductors, such as high-T<sub>c</sub> cuprates and heavy fermions, CeCoIn<sub>5</sub>, CeRhSi<sub>3</sub>, and CeIrSi<sub>3</sub> [2]. Nonequilibrium topological superconductivity induced by circularly polarized laser-light is also proposed [3].

(2) Reduction of topological classification by electron correlation [4]

Recently, it was shown that the heavy fermion superlattice CeCoIn<sub>5</sub>/YbCoIn<sub>5</sub> [5] is a platform of topological crystalline superconductivity protected by mirror symmetry [6]. In this talk, we show the breakdown of topological superconductivity by electron correlation, which can be experimentally verified by tuning the superlattice structure.

[1] Y. Nakamura and Y. Yanase, Phys. Rev. B 96, 054501 (2017).

[2] A. Daido and Y. Yanase, Phys. Rev. B 94, 054519 (2016); Phys. Rev. B 95, 134507 (2017).

[3] K. Takasan, A. Daido, N. Kawakami, and Y. Yanase, Phys. Rev. B 95, 134508 (2017).

[4] Tsuneya Yoshida, A. Daido, Y. Yanase, and N. Kawakami, Phys. Rev. Lett. 118, 147001 (2017).

[5] Y. Mizukami *et al.* Nat. Phys. 7, 849 (2011).

[6] Tomohiro Yoshida, M. Sigrist, and Y. Yanase, Phys. Rev. Lett. 115, 027001 (2015).

## Critical magnetic fields enhanced by spin-orbit coupling in electric-field-induced superconductors

T. Nojima<sup>1</sup>, T. Ouchi<sup>1</sup>, Y. Saito<sup>2</sup>, S. Shimizu<sup>3</sup> and Y. Iwasa<sup>2,3</sup>

<sup>1</sup>Institute for Materials Research, Tohoku University, Sendai 980-8577, Japan

<sup>2</sup>QPEC and Department of Applied Physics, The University of Tokyo, Tokyo 113-8656, Japan

<sup>3</sup>RIKEN Center for Emergent Matter Science, Wako 351-0198, Japan

Recently, the exotic superconducting properties have been intensively investigated in highly crystalline two-dimensional (2D) systems [1], which became available with the technological advances in thin film growth, exfoliation, and ionic gating. Among them, the 2D electron system induced by electric field gating is an ideal platform for non-centrosymmetric superconductivity with strong antisymmetric spin-orbit coupling (SOC). In this presentation, we discuss our recent experiments on electric-field-induced superconductivity in SrTiO<sub>3</sub> [2] and MoS<sub>2</sub> [3] electric double layer transistors (EDLTs) with the superconducting transition temperatures  $T_c$  of 0.4 K and 6.5 K, respectively, both of which show the remarkable enhancement of in-plane critical magnetic fields  $H_{c2//}$  far beyond the usual Pauli-Clogston-Chandrasekhar limit of  $1.86T_c$ .

The EDLT devices were fabricated at the atomically flat (001) surfaces of single crystals SrTiO<sub>3</sub> and MoS<sub>2</sub>, which were originally insulators before gating, by using an ionic liquid DEME-TSFI. These devices induced superconducting layers with the effective thicknesses of  $\sim 10$  nm for SrTiO<sub>3</sub> and  $\sim 1.8$  nm for MoS<sub>2</sub>, respectively. In SrTiO<sub>3</sub> EDLT, we succeeded to obtain the further enhancement of  $H_{c2//}$  as compared with the previous study [2] by applying a higher gate voltage, resulting in  $H_{c2//}(T \rightarrow 0)$  exceeding  $6T_c$  ( $= 2.4$  T), which is very close to the theoretical prediction [4]. We also observed that the temperature  $T$  dependence of  $H_{c2//}$  deviates upward from 2D-GL (orbital limit) formula at low  $T$ . In MoS<sub>2</sub> EDLT, in addition to the similar enhancement of  $H_{c2//}$  exceeding  $8T_c$  ( $= 52$  T) and deviation from the 2D-GL formula, we found that the angular dependence of  $H_{c2}$ , showing the cusp-like peak behavior at  $T \leq T_c$ , changes into the dome-like one at lower  $T$ . All of the above results indicate the spin-momentum and spin-valley locking phenomena caused by the enhanced Rashba-type SOC with 3d orbital mixing in SrTiO<sub>3</sub> EDLT [5] and the intrinsic Zeeman-type SOC in MoS<sub>2</sub> EDLT [3], respectively, directly affect the pair breaking mechanisms, resulting in the protection of superconductivity against the external magnetic field.

[1] Y. Saito, T. Nojima, Y. Iwasa, Nat. Rev. Mater. **2**, 16094 (2017).

[2] K. Ueno *et al.*, Phys. Rev. B **89**, 020508(R) (2014).

[3] Y. Saito *et al.*, Nature Phys. **12**, 144 (2016).

[4] Y. Nakamura and Y. Yanase, J. Phys. Soc. Jpn. **8**, 024714 (2015).

[5] Y. Nakamura and Y. Yanase, J. Phys. Soc. Jpn. **82**, 083705 (2013).

## Noncentrosymmetric parent phase in iron-based superconductor

Jun-ichi Yamaura

Materials Research Center for Element Strategy, Tokyo Institute of Technology, Japan

A new class of high- $T_c$  superconductor iron-based materials has been widely studied since the discovery in 2008. In the first obtained iron-based superconductor, ZrCuSiAs-type LaFeAsO, the superconductivity emerges via doping the carrier in place of the non-doped parent phase with the magnetic order and the structural transition. An advanced doping method using a hydrogen anion instead of fluorine in LaFeAsO surpassed the doping limit of fluorine, and uncovered the second superconducting phase (SC2) ( $T_{c,max} = 36$  K at  $x \sim 0.35$ ), following to the first dome (SC1) ( $T_{c,max} = 26$  K at  $x \sim 0.1$ ) [1]. From multi-probe studies using x-ray diffraction, neutron diffraction, and muon spin rotation measurements, we found an antiferromagnetic (AF) ordering reappears over  $x > 0.45$ , eventually the AF ordering exhibits at  $T_{N2} = 89$  K with a tetragonal-orthorhombic structural transition at  $T_{S2} \sim 95$  K for  $x = 0.51$ , ascribed to a second parent phase (PP2). The PP2 has a non-centrosymmetric structure in contrast to a centrosymmetric structure of a conventional parent phase (PP1) at  $x \sim 0$ . The magnetic moment  $1.21 \mu_B$  in PP2 is twice as large as  $0.63 \mu_B$  in PP1, implying that the strong electron correlation exists, albeit heavily electron-doped [2]. Various materials with non-centrosymmetric structures frequently exhibit the superconductivity; however, in case of the present compound, the superconductivity in SC2 with the centrosymmetric structure is induced by "hole-doping" from the non-centrosymmetric PP2. We investigated the structural fluctuation derived from PP2 by means of the extended x-ray absorption fine structure experiment. We observed the structural fluctuation below the temperature  $T^*$  far above  $T_{S2}$  for  $x = 0.51$ . With decreasing  $x$ ,  $T^*$  diminishes but we can observe it even around  $x \sim 0.35$ . The findings suggest the existence of close relationship between the superconductivity in SC2 and the structural fluctuation from PP2. Additionally, we identified that PP2 is suppressed by pressure as low as  $\sim 1.5$  GPa, contrary to the sluggish reaction to pressure in PP1 [3]. The distinguishable response to pressure also implies that PP1 and PP2 are originating from the different mechanisms for their orderings..

- [1] S. Iimura, S. Matsuishi, H. Sato, T. Hanna, Y. Muraba, S. W. Kim, J.E. Kim, M. Takata, and H. Hosono, *Nature Commun.* **3**, 943 (2012).
- [2] M. Hiraishi, S. Iimura, K.M. Kojima, J. Yamaura, H. Hiraka, K. Ikeda, P. Miao, Y. Ishikawa, S. Torii, M. Miyazaki, I. Yamauchi, A. Koda, K. Ishii, M. Yoshida, J. Mizuki, R. Kadono, R. Kumai, T. Kamiyama, T. Otomo, Y. Murakami, S. Matsuishi, and H. Hosono, *Nat. Phys.* **10**, 300 (2014).
- [3] Kensuke Kobayashi, Jun-ichi Yamaura, Soshi Iimura, Sachiko Maki, Hajime Sagayama, Reiji Kumai, Youichi Murakami, Hiroki Takahashi, Satoru Matsuishi, and Hideo Hosono, *Sci. Rep.* **6**, 39646 (2016).

## O-25

**Discovery of superconductivity of very pure single crystal of Bismuth***S. Ramakrishnan**Department of Condensed Matter Physics and Materials Science  
Tata Institute of Fundamental Research, Mumbai-400005, India*

Bismuth(Bi) has played a very important role in uncovering many interesting physical properties in condensed matter research, and still continues to draw enormous scientific interests due to its anomalous electronic properties. Many important phenomena such as Seebeck effect, Nernst effect, Shubnikov-de Haas effect, de Haas-van Alphen (dHvA) effect etc. were first discovered in Bi. Determination of the Fermi surface (FS) in Bi using dHvA measurements provided the basis to determine the Fermi surface of other elements\compounds. The layered structure of Bi plays a crucial role in observing many quantum phenomena rather easily. Some of the key properties of Bi are: a small density of states (DOS;  $2 \times 10^{-6}$  states/eV atom) at the Fermi level, very small Fermi surface (FS;  $10^{-5}$  of the Brillouin zone, consisting of small electron and hole pockets), low Fermi energy ( $E_F = 25$  meV), low carrier density ( $n_e = 3 \times 10^{17}/\text{cm}^3$  at 4.2 K) and small effective mass for charge carrier ( $m_{\text{eff}} \sim 10^{-3} m_e$ ). However, bulk rhombohedral Bi at ambient pressure is a semimetal and it remains in the normal state down to 10 mK. The superconductivity (SC) in bulk Bi is thought to be very unlikely due to extremely low carrier density. The question of SC in Bi has remained unsolved both theoretically and experimentally even today. In this talk, I will describe the first-ever observation of bulk SC in highly pure Bi single crystals (99.9999%) below **530  $\mu\text{K}$**  under ambient pressure with an estimated critical magnetic field of **5.2  $\mu\text{T}$  at 0 K**<sup>1</sup>. **These measurements are carried out using the Copper nuclear refrigerator built at TIFR.** The conventional Bardeen-Cooper-Schrieffer (BCS) theory cannot explain the observed SC in Bi, since the adiabatic approximation used in the BCS theory,  $\omega_b/E_F \ll 1$ , does not hold true for Bi. Bi has a multi-valley type electronic band structure and SC in Bi could be brought about by the inter-valley electron-phonon coupling. Such a scenario calls for new theoretical ideas to understand SC in such low carrier systems with unusual band structure in the non-adiabatic limit,  $\omega_b/E_F \geq 1$ . Further, this observation of SC in Bi makes it the lowest carrier density superconductor surpassing the record held by doped SrTiO<sub>3</sub> for nearly 50 years.

1. Om Prakash, Anil Kumar, A. Thamizhavel and S. Ramakrishnan, Science Vol. 355, Issue 6320, pp. 52-55 (2017).

# O-26

## Strong enhancement of the magnetoelectric effect in heavy-fermion system

R. Peters and Y. Yanase  
Kyoto University, Kyoto 606-8502, Japan

The magnetoelectric effect occurring in systems with broken inversion symmetry generates a spin polarization when an electric field is applied, which is most advantageous in spintronics applications. Unfortunately, it became apparent that the magnetoelectric effect in semiconductors is very small. We here demonstrate that the magnetoelectric effect can be strongly enhanced in f-electron systems and exhibits a maximum at the crossover temperature between localized and itinerant f-electrons. We furthermore show that this enhancement can be explained by a coupling between the conduction electrons and the still localized f-electrons.

## Magnetolectric responses induced by generalized multipole orders

H. Kusunose<sup>1</sup><sup>1</sup>Department of Physics, Meiji University, Kawasaki 214-8571, Japan

Microscopic magnetic dipole is a source of magnetism, and an electric charge and quadrupole are responsible for charge and orbital orderings, respectively. Such fundamental degrees of freedoms, described by multipoles in general, play important roles in the study of condensed matter physics, since they generate spontaneous symmetry breaking and corresponding responses under external fields. So far, multipoles are mainly discussed in terms of the atomic degrees of freedom in the presence of spatial inversion symmetry [1].

Recently, we generalize a concept of microscopic multipoles in two ways: (i) a cluster multipole in sublattice systems with or without spatial inversion symmetry [2,3], where a particular alignment of magnetic/electric dipoles in a cluster can be regarded as an inter-atomic multipole, and (ii) an inter-orbital multipole in the mixed orbital systems, in which electric/magnetic toroidal type of multipoles appear, in addition to ordinary electric/magnetic multipoles (see, Table I) [4]. I will talk about the concept of the generalized multipoles, and peculiar electromagnetic responses under spontaneous ordering of the generalized multipoles [2,3,4,5,6].

A series of works has been done in collaboration with S. Hayami, Y. Motome, Y. Yanagi, M.-T. Suzuki, R. Arita, T. Nomoto. These works were supported by JSPJ KAKENHI Grants Numbers 15K05176, 15H05885 (J-Physics), and 16H06590.

**Table I.** Active multipoles in the mixed orbital systems. E, M, ET, and MT represent electric, magnetic, electric toroidal, magnetic toroidal multipoles, respectively. In the even(odd)-parity systems, the true tensors (E/MT) appear in the even(odd) rank, while the pseudo tensors (M/ET) appear in the odd(even) rank.

basis	parity	#	$l = 0(1)$	$l = 1(3)$	$l = 2(5)$	$l = 3(7)$	$l = 4(9)$	$l = 5(11)$	$l = 6(13)$
$s-s$	even	1	E	—	—	—	—	—	—
$p-p$		9	E	M	E	—	—	—	—
$d-d$		25	E	M	E	M	E	—	—
$f-f$		49	E	M	E	M	E	M	E
$s-d$	even	10	—	—	E/MT	—	—	—	—
$p-f$		42	—	—	E/MT	M/ET	E/MT	—	—
$s-p$	odd	6	—	E/MT	—	—	—	—	—
$s-f$		14	—	—	—	E/MT	—	—	—
$p-d$		30	—	E/MT	M/ET	E/MT	—	—	—
$d-f$		70	—	E/MT	M/ET	E/MT	M/ET	E/MT	—

[1] Y. Kuramoto, H. Kusunose, and A. Kiss, J. Phys. Soc. Jpn. **78**, 072001 (2009).

[2] S. Hayami, H. Kusunose, and Y. Motome, J. Phys.: Condens. Matter **28**, 395601 (2016), and references therein.

[3] M.-T. Suzuki, H. Kusunose, *et al.*, in preparation.

[4] S. Hayami and H. Kusunose, in preparation.

[5] S. Hayami, H. Kusunose, and Y. Motome, J. Phys. Soc. Jpn. **85**, 053705 (2016).

[6] Y. Yanagi and H. Kusunose, J. Phys. Soc. Jpn. **86**, 083703 (2017).

*Emergent odd-parity multipoles by spontaneous parity breaking*

S. Hayami

Hokkaido University, Sapporo 060-0810, Japan

The effect of the relativistic spin-orbit coupling (SOC) in solids has drawn considerable attention in condensed matter physics. Especially, the SOC without spatial inversion symmetry, which is called the antisymmetric spin-orbit coupling (ASOC), has extensively studied, since it is essential for various intriguing phenomena, such as noncentrosymmetric superconductivity and multiferroics. By contrast, even in the centrosymmetric systems, a different type of ASOC can exist when the spatial inversion center is missing at each lattice site. In this case, the ASOC shows a sublattice dependence, while net component of the ASOC vanishes. A two-dimensional honeycomb and three-dimensional diamond structures are typical examples to possess this type of the ASOC. This ASOC will offer more intriguing situation once spatial inversion symmetry is spontaneously broken by electronic orderings caused by electron correlations. These orderings accompany cluster-type multipoles with an odd parity, such as magnetic quadrupole and magnetic toroidal moments [1,2], which bring about a peculiar modulation of the electronic structures and unconventional off-diagonal responses including the magnetoelectric effect [3,4] and asymmetric modulation of collective spin-wave excitations [5]. However, the analysis of such systems with local asymmetry has not been fully carried out. It will be interesting to study the competition between multiple degrees of freedom, such as charge, spin, and orbital. To clarify these issues, calculations for a fundamental model are needed.

In the present study, we investigate a spontaneous inversion symmetry breaking by electronic orders in a two-orbital Hubbard model with the atomic SOC on honeycomb and diamond structures [6,7]. These models include the interorbital hopping, atomic SOC, and spontaneous bipartite electronic orders to capture the ASOC physics. First, we present the analysis of all possible parity-broken states in charge, spin, and orbital channels from the symmetry point of view. We also discuss emergent odd-parity multipoles associated with bipartite electronic orders. Next, we show an effective ASOC induced by the emergence of charge, spin, and orbital orderings, which give rise to fascinating properties, such as the spin/valley Hall effect, spin/valley splitting in the band structure in Fig. 1, and peculiar off-diagonal responses including the magnetoelectric effects [8]. Finally, we discuss how our fundamental theory is applicable to realistic situations by taking  $5d$  transition metal oxides,  $A\text{OsO}_4$  ( $A = \text{K, Rb, and Cs}$ ), as an example. This work has been collaborated with Prof. Hiroaki Kusunose at Meiji University and Prof. Yukitoshi Motome at University of Tokyo.

This work was supported by JSPS KAKENHI Grant Numbers 24340076, 15K05176, 16H06590, and 15H05885 (J-Physics).

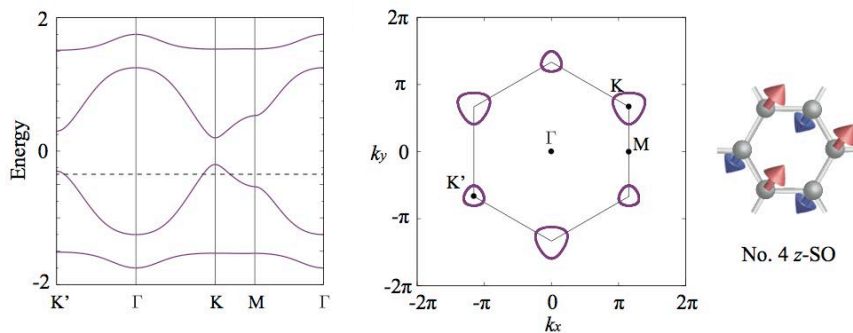


**Fig. 1: Valley splitting in the band structure for the staggered antiferromagnetic ordering**

- [1] B. Volkov, A. Gorbatshev, Y. V. Kopaev, and V. Tugushev, *Zh. Eksp. Thor. Fiz.* 81, 742 (1981).
- [2] N. A. Spaldin, M. Fiebig, and M. Mostovoy, *J. Phys.: Condens. Matter* 20, 434203 (2008).
- [3] Y. Yanase, *J. Phys. Soc. Jpn.* 83, 014703 (2014).
- [4] S. Hayami, H. Kusunose, and Y. Motome, *Phys. Rev. B* 90, 024432 (2014).
- [5] S. Hayami, H. Kusunose, and Y. Motome, *J. Phys. Soc. Jpn.* 85, 053705 (2016).
- [6] S. Hayami, H. Kusunose, and Y. Motome, *Phys. Rev. B* 90, 081115(R) (2014).
- [7] S. Hayami, H. Kusunose, and Y. Motome, *J. Phys.: Conf. Ser.* 592, 012131 (2015).
- [8] S. Hayami, H. Kusunose, and Y. Motome, *J. Phys.: Condens. Matter* 28, 395601 (2016).

## O-29

## First-principles calculations for magnetoelectric multipoles

F. Thöle<sup>1</sup>, Nicola A. Spaldin<sup>1</sup><sup>1</sup>Materials Theory, ETH Zurich, Switzerland

The magnetoelectric multipoles form the second-order term in the interaction energy of the magnetization density  $\mu(\mathbf{r})$  with an inhomogeneous magnetic field  $\mathbf{H}(\mathbf{r})$ . [1] They are often represented as three irreducible components, the magnetoelectric monopole, the toroidal moment or anapole, and the magnetic quadrupole and occur in materials with broken time-reversal and space-inversion symmetries.

In this talk, we will present the formalism to calculate magnetoelectric multipoles from first principles within the density functional theory framework. At a microscopic level, multipoles are calculated from a decomposition of the on-site density matrix into irreducible spherical tensor moments [1]. At a macroscopic level, we use a formalism similar to the Berry phase theory for the ferroelectric polarization [2].

We apply these methods to the prototypical magnetoelectric material  $\text{Cr}_2\text{O}_3$  and novel materials such as metal surfaces. Furthermore, we compare calculations for magnetoelectric multipoles and the estimated size of the magnetoelectric response.

[1] N. A. Spaldin, M. Fechner, E. Bousquet, A. Balatsky, and L. Nordström, *Phys. Rev. B* **88**, 94429 (2013)

[2] F. Thöle, M. Fechner, and N.A. Spaldin, *Phys. Rev. B* **93**, 195167 (2016)

## O-30

Large anomalous Hall and Nernst effects at room temperature in antiferromagnet  $Mn_3Sn$ 

T. Tomita<sup>1</sup>, M. Ikhlas<sup>1</sup>, T. Koretsune<sup>2</sup>, M.-T Suzuki<sup>2</sup>, D. Nishio-Hamane<sup>1</sup>, R. Arita<sup>2,4</sup>, Y. Otani<sup>1,2,4</sup>,  
and S. Nakatsuji<sup>1,3,4</sup>

<sup>1</sup>Institute for Solid State Physics, University of Tokyo, Kashiwa 277-8581, Japan.

<sup>2</sup>RIKEN-CEMS, 2-1 Hirosawa, Wako 351-0198, Japan.

<sup>3</sup>PRESTO, Japan Science and Technology Agency (JST), 4-1-8 Honcho Kawaguchi, Saitama 332-0012, Japan.

<sup>4</sup>CREST, Japan Science and Technology Agency (JST), 4-1-8 Honcho Kawaguchi, Saitama 332-0012, Japan.

It has been recently found that  $Mn_3Sn$  exhibits a large anomalous Hall effect (AHE) as the first case in antiferromagnet. [1] Ordinarily this AHE is known to be proportional to the magnetization and thus observed only in ferromagnets. The spontaneous Hall resistivity in the antiferromagnet with vanishingly small magnetization indicates the large fictitious field of a few hundred T must exist. [1, 2] From recent theoretical works, an antiferromagnetic Weyl semimetal state is predicted by a band calculation in  $Mn_3Sn$ . [3-5] The large fictitious field estimated from AHE may well come from a significantly enhanced Berry curvature associated with the formation of Weyl points nearby the Fermi energy  $E_F$ .

Here, it is expected that the anomalous Nernst effect, which is the thermoelectric counterpart of the anomalous Hall effect, could be large in the material. In the results of  $Mn_3Sn$ , we found a large spontaneous anomalous Nernst effect showing  $0.35 \mu V/K$  at room temperature and  $0.6 \mu V/K$  at low temperature. These Nernst signals are also found to be enhanced by the Berry curvature associated with the Weyl points near  $E_F$ . [6] In our talk, we also propose that the large anomalous Hall and Nernst effects are useful for memory and thermopile devices, respectively.

[1] S. Nakatsuji, N. Kiyohara, and T. Higo, *Nature* **52**, 212 (2015).

[2] N. Kiyohara, T. Tomita, and S. Nakatsuji, *Phys. Rev. Applied* **5**, 064009 (2016).

[3] J. Kübler and C. Felser, *Europhys. Lett.* **108**, 67001 (2014).

[4] H. Yang, Y. Sun, Y. Zhang, W.-J. Shi, S. S. P. Parkin, and B. Yan, *New Journal of Physics* **19** (1), 015008 (2017).

[5] X. Wan, A. M. Turner, A. Vishwanath, and S. Y. Savrasov, *Phys. Rev.* **83**, 205101 (2011).

[6] M. Ikhlas, T. Tomita, T. Koretsune, M. -T. Suzuki, D. Nishio-Hamane, R. Arita, Y. Otani, and S. Nakatsuji. *Nature Physics*. (10.1038/NPHYS4181) (2017).

## Cluster multipole theory for macroscopic magnetization of antiferromagnetism: Application to anomalous Hall effect and recent progress

M.-T. Suzuki<sup>1</sup>

<sup>1</sup>RIKEN-Center for Emergent Matter Science (CEMS), Wako, Saitama 351-0198, Japan

We introduce a theoretical framework with a novel concept, cluster multipole (CMP), which provides macroscopic order parameters corresponding to the magnetization of antiferromagnetism as well as dipole magnetization of ferromagnetism. The CMP characterizes the magnetic degree of freedom which induces the macroscopic physical property in magnetic materials. We describe the recent application of the CMP theory for the anomalous Hall effect (AHE) in the antiferromagnetic (AFM) states without net magnetization [1] and discuss the further applications of the CMP theory.

The modern formalism of the intrinsic anomalous Hall conductivity (AHC) provides profound insight into the AHE being closely related to the topology of one-electron energy bands [2,3]. Whereas the AHE is usually observed in ferromagnets and explained as an outcome of the macroscopic dipole magnetization, the AHE has been studied also for certain noncollinear AFM states by first-principles calculations [4,5]. Furthermore, a large AHC was recently discovered for the AFM states in  $Mn_3Z$  ( $Z=Sn, Ge$ ), whose magnetic configuration only has tiny uniform magnetization [6-8]. The CMP theory revealed the AHE in the noncollinear AFM states of  $Mn_3Z$  ( $Z=Sn, Ge$ ) is associated with the magnetic octupole moments which belong to the same symmetry as the magnetic dipole moments. The theory can thus deal with the AHE in antiferromagnets on an equal footing with that of simple ferromagnets. We compare the AHE in  $Mn_3Z$  and bcc-Fe based on first-principles calculations and find out their similarity with respect to the CMP (Fig. 1).

We recently generalize the CMP theory to produce an orthonormal basis set of magnetic structures in crystal systems, classified according to the CMP moments and these ranks [9]. The multipole expansion of a magnetic structure by using the symmetrized CMP basis set easily identifies the presence of macroscopic properties in the magnetic state, such as AHE and electromagnetic effect, and the magnetic degree of freedom inducing these phenomena.

The works have been done in collaboration with T. Koretsune, M. Ochi, R. Arita, H. Kusunose, T. Nomoto, S. Hayami, Y. Yanagi and supported by JSPJ KAKENHI Grants Numbers 15K17713, 15H05883 (J-Physics) and 16H04021.

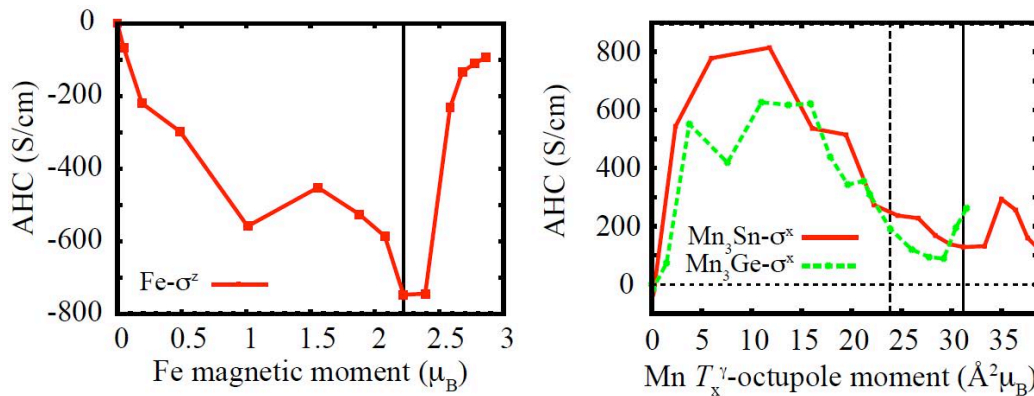


Fig. 1: AHC in ferromagnetic states of bcc-Fe and antiferromagnetic states of  $Mn_3Z$  with respect to the CMPs.

- [1] M.-T. Suzuki, T. Koretsune, M. Ochi, R. Arita, Phys. Rev. B, 95, 094406 (2017).
- [2] N. Nagaosa, J. Sinova, S. Onoda, A. MacDonald, and N. Ong, Rev. Mod. Phys., 82, 1539 (2010).
- [3] D. Xiao, M.-C. Chang, and Q. Niu, Rev. Mod. Phys., 82, 1959 (2010).
- [4] H. Chen, Q. Niu, and A. H. MacDonald, Phys. Rev. Lett., 112, 017205 (2014).
- [5] J. Kübler and C. Felser, Europhys. Lett., 112, 017205 (2014).
- [6] S. Nakatsuji, N. Kiyohara, and T. Higo, Nature, 527, 212 (2015).
- [7] N. Kiyohara, T. Tomita, and S. Nakatsuji, Phys. Rev. Appl., 5, 064009 (2016).
- [8] A. K. Nayak et al., Sci. Adv., 2, e1501870 (2016).
- [9] M.-T. Suzuki, H. Kusunose, T. Nomoto, S. Hayami, Y. Yanagi, R. Arita, in preparation.

## Superconductivity in topological half-Heusler compounds

A.M. Nikitin<sup>1</sup>, Y. Pan<sup>1</sup>, T.V. Bay<sup>1</sup>, Y.K. Huang<sup>1</sup>, C. Paulsen<sup>2</sup>, B.H. Yan<sup>3</sup> and A. de Visser<sup>1</sup><sup>1</sup>University of Amsterdam, The Netherlands,<sup>2</sup>Institute Néel, CNRS, France<sup>3</sup>Max Planck Institute, Dresden, Germany

Half-Heusler compounds crystallize in a cubic structure with 1:1:1 composition. They attract ample attention because of their flexible electronic structure. By playing with the chemical composition a wide range of materials properties, ground states and functionalities can be realized. New in this respect is the topological zero-gap semiconducting ground state in selected half-Heusler compounds with strong spin-orbit coupling. Here non-trivial metallic states protected by topology are predicted to exist at the surface. Yet another interesting aspect is that a number of topological half-Heusler compounds, such as LaPtBi, YPtBi, LuPtBi, and LuPdBi, superconducts (for a survey see [1]). Moreover, in the rare earth palladium bismuthides, such as ErPdBi [2] and HoPdBi [3], superconductivity sets in close to antiferromagnetic ordering of the  $4f$  local-moments. Since  $T_c \sim T_N$ , the interaction of superconductivity and magnetism is expected to give rise to a complex ground state. Electronic structure calculations show these materials have a non-trivial band inversion and thus may serve as a new platform to study the interplay of topological states, superconductivity and magnetic order. This presentation reviews the intriguing electronic properties of this interesting family of materials.

[1] B. H. Yan and A. de Visser, MRS Bulletin **39**, 859 (2014).

[2] Y. Pan *et al.*, Europhysics Letters **104**, 27001 (2013).

[3] A.M. Nikitin *et al.*, J. Phys. Cond. Matter **27**, 275701 (2015).

## Unique Electronic States in Ullmannite-type Chiral Compounds

Y. Ōnuki<sup>1</sup>, Masashi Kakihana<sup>2</sup>, K. Nishimura<sup>2</sup>, Y. Ashitomi<sup>2</sup>, D. Aoki<sup>3</sup>, A. Nakamura<sup>3</sup>, F. Honda<sup>3</sup>,  
M. Nakashima<sup>4</sup>, Y. Amako<sup>4</sup>, Y. Uwatoko<sup>5</sup>, T. Sakakibara<sup>5</sup>, S. Nakamura<sup>5</sup>, T. Takeuchi<sup>6</sup>, Y. Haga<sup>7</sup>, H. Harima<sup>8</sup>,  
M. Hedo<sup>1</sup> and T. Nakama<sup>1</sup>

<sup>1</sup>Faculty of Science, University of the Ryukyus, Nishihara, Okinawa 903-0213, Japan

<sup>2</sup>Graduate School of Engineering and Science, University of the Ryukyus, Nishihara, Okinawa 903-0213, Japan

<sup>3</sup>Institute for Materials Research, Tohoku University, Oarai, Ibaraki 311-1313, Japan

<sup>4</sup>Department of Physics, Faculty of Science, Shinsyu University, Matumoto, Nagano 390-8621, Japan

<sup>5</sup>Institute for Solid State Physics, University of Tokyo, Kashiwa, Chiba 277-8581, Japan

<sup>6</sup>Low Temperature Center, Osaka University, Toyonaka, Osaka 560-0043, Japan

<sup>7</sup>Advanced Science Research Center, Japan Atomic Energy Agency, Tokai, Ibaraki 319-1195, Japan

<sup>8</sup>Graduate School of Science, Kobe University, Kobe, Hyogo 657-8501, Japan

We succeeded in growing single crystals of the NiSbS, PdBiSe and EuPtSi with cubic chiral structure ( $P2_13$ , No. 198) [1, 2, 3]. Reflecting the non-centrosymmetric structure, a Fermi surface splits into two kinds of Fermi surfaces, depending on the spin states. The magnitudes of splitting energies in NiSbS and PdBiSe are discussed from a viewpoint of the spin-orbit coupling and mass correction based on the relativistic effect. In EuPtSi, we observed the first-order like antiferromagnetic transition at 4.0 K, which is small in magnitude, reflecting the frustration of divalent Eu-spins in the chiral structure. We also found a new magnetic phase, which reminds us a so-called A-phase in MnSi [4]. Note that EuPtSi and MnSi belong to the same space group in the crystal structure.

## References

- [1] M. Kakihana, A. Nakamura, A. Teruya, H. Harima, Y. Haga, M. Hedo, T. Nakama, and Y. Ōnuki, *J. Phys. Soc. Jpn.* **84** (2015) 033701.
- [2] M. Kakihana, A. Teruya, K. Nishimura, A. Nakamura, T. Takeuchi, Y. Haga, H. Harima, M. Hedo, T. Nakama, and Y. Ōnuki, *J. Phys. Soc. Jpn.* **84** (2015) 094711.
- [3] M. Kakihana, K. Nishimura, Y. Ashitomi, T. Yara, D. Aoki, A. Nakamura, F. Honda, M. Nakashima, Y. Amako, Y. Uwatoko, T. Sakakibara, S. Nakamura, T. Takeuchi, Y. Haga, E. Yamamoto, H. Harima, M. Hedo, T. Nakama, and Y. Ōnuki, *J. Electron. Mater.* **46** (2017) 3572.
- [4] S. Mühlbauer, B. Binz, F. Jonietz, C. Pfleiderer, A. Rosch, A. Neubauer, R. Georgii, and P. Böni, *Science* **323** (2009) 915.

## Superconductivity in Fe-based ladder materials

Kenya Ohgushi<sup>1</sup>, Yasuyuki Hirata<sup>2</sup>, Touru Yamauchi<sup>2</sup>, Fei Du<sup>3</sup>, Yutaka Ueda<sup>4</sup>, Yusuke Nambu<sup>5</sup>, Maxim Avdeev<sup>6</sup>, Taku J. Sato<sup>7</sup>, Akira Sugimoto<sup>8</sup>, Chizuru Kawashima<sup>8</sup>, Hideto Soeda<sup>8</sup>, and Hiroki Takahashi<sup>8</sup>

<sup>1</sup>Department of Physics, Tohoku University, Japan

<sup>2</sup>Institute for Solid State Physics, University of Tokyo, Japan

<sup>3</sup>College of Physics, Jilin University, China

<sup>4</sup>Toyota Physical and Chemical Research Institute, Japan

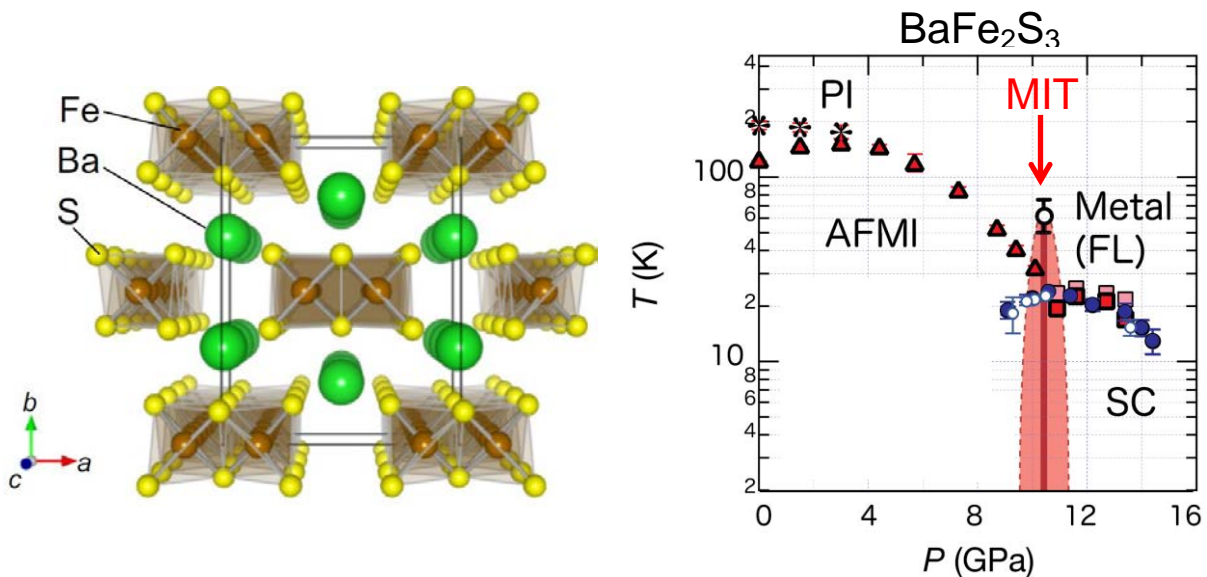
<sup>5</sup>Institute for Materials Research, Tohoku University, Japan

<sup>6</sup>Bragg Institute, Australian Nuclear Science and Technology Organisation, Australia

<sup>7</sup>Institute of Multidisciplinary Research for Advanced Materials, Tohoku University, Japan

<sup>8</sup>College of Humanities & Sciences, Nihon University, Japan

All the iron-based superconductors identified so far share a square lattice composed of iron atoms as a common feature. In copper-based high- $T_c$  materials, the superconducting phase emerges not only in square-lattice structures but also in ladder structures, which give nice hints for elucidating the microscopic mechanism of the superconductivity. Here, we report the discovery of pressure-induced superconductivity in the iron-based ladder material  $\text{BaFe}_2\text{S}_3$ , a Mott insulator with striped-type magnetic ordering below 120 K [1-10]. On the application of pressure, this compound exhibits a metal-insulator transition at about 11 GPa, followed by the appearance of superconductivity below  $T_c = 24$  K. Our findings indicate that square lattice is not the necessary ingredients of the superconductivity and that not only the spin and orbital fluctuations but also the charge fluctuations could play a key role in the emergence of the superconductivity in iron-based superconductors.



- [1] Y. Nambu, *et al.*, Phys. Rev. B **85**, 064413 (2012).  
 [2] F. Du, *et al.*, Phys. Rev. B **85**, 214436 (2012).  
 [3] F. Du, *et al.*, Phys. Rev. B **90**, 085143 (2014).  
 [4] D. Ootsuki, *et al.*, Phys. Rev. B **91**, 014505 (2015).  
 [5] T. Hawaii, *et al.*, Phys. Rev. B **91**, 184416 (2015).  
 [6] H. Takahashi, *et al.*, Nat. Mater. **14**, 1008 (2015).  
 [7] Y. Hirata, *et al.*, Phys. Rev. B **92**, 205109 (2015).  
 [8] T. Yamauchi, *et al.*, Phys. Rev. Lett. **115**, 246402 (2015).  
 [9] Songxue Chi, *et al.*, Phys. Rev. Lett. **117**, 047003 (2016).  
 [10] Kou Takubo, *et al.*, arXiv:1704.04864.

## Investigation of the Wing-Structure Phase Diagram of the Ising Ferromagnet URhGe by Angle-Resolved Magnetization Measurements

Shota NAKAMURA<sup>1</sup>, Toshiro SAKAKIBARA<sup>1</sup>, Yusei SHIMIZU<sup>2</sup>, Yohei KONO<sup>1</sup>, Shunichiro KITTAKE<sup>1</sup>,  
Yoshinori HAGA<sup>3</sup>, Jiří POSPÍŠIL<sup>3,4</sup>, and Etsuji YAMAMOTO<sup>3</sup>

<sup>1</sup>Institute for Solid State Physics, The University of Tokyo, Kashiwa 277-8581, Japan

<sup>2</sup>Institute for Materials Research, Tohoku University, Oarai 311-1313, Japan

<sup>3</sup>Japan Atomic Energy Agency, Tokai 319-1106, Japan

<sup>4</sup>Charles University in Prague, Faculty of Mathematics and Physics, DCMP, Ke Karlovu 5, 121 16 Prague 2, Czech Republic

Recently, a ferromagnetic (FM) quantum phase transition in clean metals has attracted much interest because a first-order quantum phase transition is commonly observed at low temperatures below a tricritical point (TCP) [1]. Below the TCP, a FM first-order plane (wings) is expected in the three-dimensional phase diagram. This type of “ $T-H$  phase diagram” has been studied in itinerant FM compounds, such as UGe<sub>2</sub>, URhAl, UCoGa, and ZrZn<sub>2</sub> with pressure as a tuning parameter [2-5]. Whereas much theoretical work has been reported, the “wings” have been studied experimentally to a much less extent because a high-pressure environment is usually required in the observation of the “wings”. By contrast, as a magnetic field  $H$  parallel to the magnetic hard axis being the tuning parameter, URhGe provides a good opportunity to investigate the “wing” in the whole FM phase diagram [6, 7]. In this system, the location of TCP is under debate [8, 9], regarding the origin of reentrant superconductivity (RSC) that is possibly be induced by ferromagnetic fluctuations [7].

In the present study, high-precision angle-resolved dc magnetization and magnetic torque measurements were performed on a single-crystalline sample of URhGe in order to investigate the wings in a field near the magnetic hard axis. For this purpose, we develop a two-axis piezo-stepper-driven goniometer that is installed in a capacitively-detected Faraday magnetometer [10], and have achieved an in-situ orientation of the sample within an accuracy of 0.1 deg. We have obtained the magnetization curves at several temperatures ( $0.25 \text{ K} \leq T \leq 6 \text{ K}$ ) and angles ( $0 \text{ deg.} \leq \theta \leq 5.64 \text{ deg.}$ ;  $\theta$  is an angle from the  $a$  towards the  $c$  axes). The magnetization curve at 0.25 K in the field along the  $a$  axis ( $H_b$ ) shows metamagnetic jump at  $\mu_0 H_R \sim 11.2 \text{ T}$  with a small hysteresis, indicating the first-order transition occurs. Figure 1 shows the contour plot of the amplitude of  $\partial M / \partial H$  at  $H_R$ , projected on  $T-H_c$  plane, where  $H_c$  is the  $c$ -axis component of the field. The plot gives an imaging of the wings, viewed from the  $H$  axis. Open squares show the data points from which the plot is constructed. In this figure, the amplitude of  $\partial M / \partial H$  is still high at 6 K in a narrow range of  $|\mu_0 H_c| < 0.1 \text{ T}$  ( $|\theta| < 0.5 \text{ deg.}$ ), suggesting that the TCP is above 4 K. The two wing edges, the second-order transition lines, are found to meet tangentially at TCP, as suggested by the recent phenomenological theory [11]. We have succeeded, for the first time, in directly determining the detail profiles of the “wings” and the position of the TCP in the three-dimensional  $T-H-H_c$  phase diagram of URhGe.

The present work was supported in part by a Grant-in-Aid for Scientific Research on Innovative Areas “J-Physics” (15H05883) and KAKENHI (15H03682) from MEXT.

- [1] M. Brando *et al* Rev. Mod. Phys. **88**, 025006 (2016).
- [2] C. Pfleiderer *et al* PRL **89**, 147005 (2002).
- [3] M. Uhlarz *et al* PRL **93**, 256404 (2004).
- [4] Y. Shimizu *et al* PRB **91**, 125115 (2015).
- [5] M. Míšek *et al* AIP Advances **8**, 055712 (2017).
- [6] F. Lévy *et al* Science **309**, 1343 (2005).
- [7] Y. Tokunaga *et al* PRL **111**, 216401 (2015).
- [8] A. Gourgout *et al* PRL **111**, 046401 (2016).
- [9] H. Kotegawa *et al* JPSJ **8**, 054710 (2015).
- [10] T. Sakakibara *et al* JPSJ **33**, 5067 (1994).
- [11] V. Taufour *et al*, PRB **9**, 060410 (2016).

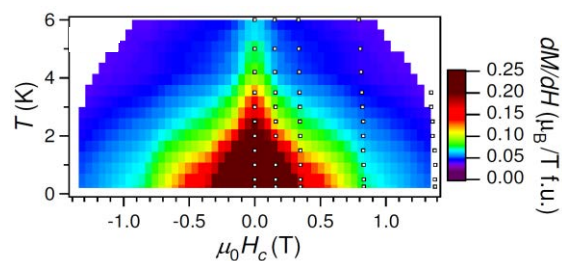


Fig. 1: The contour plot of the amplitude of  $\partial M / \partial H$  on  $H_R$ , projected on  $T-H_c$  plane. The plot gives an imaging of wings, viewed from the  $H$  axis. Open squares show the data points.

Charge Kondo Effect and Superconductivity in  $\text{Pb}_{1-x}\text{Tl}_x\text{Te}$  probed by  $^{125}\text{Te}$ -NMR

H. Mukuda<sup>1</sup>, T. Matsumura<sup>1</sup>, S. Maki<sup>1</sup>, M. Yashima<sup>1</sup>, Y. Kitaoka<sup>1</sup>, K. Miyake<sup>2</sup>  
 H. Murakami<sup>3</sup>, P. Giraldo-Gallo<sup>4</sup>, T. H. Geballe<sup>4</sup>, and I. R. Fisher<sup>4</sup>

<sup>1</sup> Graduate School of Engineering Science, Osaka University, Osaka 560-8531, Japan

<sup>2</sup> Toyota Physical and Chemical Research Institute, Nagakute, Aichi 480-1192, Japan

<sup>3</sup> Institute of Laser Engineering, Osaka University, Osaka 565-0871, Japan

<sup>4</sup> Department of Physics, Stanford University, Stanford, California 94305-4045, USA

A narrow-gap semiconductor PbTe exhibits superconductivity by a small amount of substitution of Tl for Pb, when  $x$  exceeds  $x_c \sim 0.3$  % in  $\text{Pb}_{1-x}\text{Tl}_x\text{Te}$ [1]. The dopant (Tl) is known to take either  $\text{Tl}^{1+}(6s^2)$  or  $\text{Tl}^{3+}(6s^0)$ , but to skip an intermediate valence  $\text{Tl}^{2+}(6s^1)$  due to the stability of a filled shell electron configuration. In  $\text{Pb}_{1-x}\text{Tl}_x\text{Te}$ , the hole density  $p$ , that is evaluated by Hall-coefficient measurement, exhibits a linear increase up to  $x \leq x_c$ , which is corroborated by the formal-valence substitution of  $\text{Tl}^{1+}$  for  $\text{Pb}^{2+}$ . As  $x$  increases further, however, the increase in  $p$  is gradually saturated for  $x > x_c$ , implying that the additional carriers seem to be compensated due to the possible degenerate states of  $\text{Tl}^{1+}$ (hole-doping) and  $\text{Tl}^{3+}$ (electron-doping)[1-3]. As a matter of fact, some degenerate state of  $\text{Tl}^{1+}$  and  $\text{Tl}^{3+}$  was corroborated by an observation of a logarithmic upturn in resistivity at low temperature for  $x > x_c$  that reminds us of the “spin” Kondo effect[1]. This is because two degenerate charge states of  $2e^-(\text{Tl}^{1+})$  and  $0e^-(\text{Tl}^{3+})$  is possible to form a resonating valence state, which has been theoretically accounted for by “charge” Kondo effect in analogy with two degenerate spin states in “spin” Kondo effect. The fact that the “charge” Kondo effect is observed only in the SC samples for  $x > x_c$  have attracted theoretical interests on an unconventional superconducting pairing mechanism in terms of “negative-U” model that introduces seemingly an attractive on-site interaction [3-6]. These experiments and theoretical works have motivated us to investigate local electronic states around valence skipping Tl dopants from microscopic points of view by means of  $^{125}\text{Te}$ -NMR [7].

Here we present  $^{125}\text{Te}$ -NMR study on  $\text{Pb}_{1-x}\text{Tl}_x\text{Te}$  ( $x=0, 0.35, 1.0$  %), which reveals that possible two nearly degenerate valence states of the Tl dopant, i.e. valence skipping nature between  $\text{Tl}^{1+}(6s^2)$  and  $\text{Tl}^{3+}(6s^0)$ , result in a resonating valence state upon cooling below 10 K. In the superconducting sample at  $x=1.0$  %,  $^{125}\text{Te}$  nuclear spin relaxation rate ( $1/T_1T$ ) in the vicinity of the Tl dopants is unexpectedly enhanced below 10 K, which coincides with the temperature below which the resistivity experiences an upturn. By contrast, such the anomalies were not detected in the non-superconducting sample at  $x=0.35$  %. These microscopic experimental evidences below 10 K are consistent with a model of “charge” Kondo effect that is theoretically proposed. In this context, we suggest that the coherent hopping of  $6s$ -electron pair may develop the Cooper-pairing formation to cause the superconductivity below  $T_c \sim 1$  K, which is called the negative-U scenario for the onset of superconductivity.

[1] Y. Matsushita *et al.*, Phys. Rev. Lett. **94**, 157002 (2005).

[2] H. Murakami *et al.*, Physica C(Amsterdam) **269**, 83 (1996).

[3] T. A. Costi and V. Zlatic, Phys. Rev. Lett. **108**, 036402 (2012).

[4] A. Taraphder and P. Coleman, Phys. Rev. Lett. **66**, 2814 (1991).

[5] M. Dzero and J. Schmalian, Phys. Rev. Lett. **94**, 157003 (2005).

[6] H. Matsuura and K. Miyake, J. Phys. Soc. Jpn **81**, 113705 (2012).

[7] H. Mukuda *et al.*, arXiv 1705.00747.

## O-37

Six closely related  $\text{YbT}_2\text{Zn}_{20}$  ( $T = \text{Fe, Co, Ru, Rh, Os, Ir}$ ) heavy fermion compounds: large local moment degeneracy and tuning of physical properties.

Sergey L. Bud'ko

Ames Laboratory, US DOE and Department of Physics and Astronomy, Iowa State University, Ames, IA 50011, USA

Dilute, rare earth (R) bearing, intermetallic compounds offer the possibility of investigating the interaction between conduction electrons and 4f electrons in fully ordered compounds for relatively low concentrations of rare earths. For the case of  $R = \text{Yb}$  or  $\text{Ce}$ , these materials offer the possibility of preserving low temperature, coherent effects while more closely approximating the single ion Kondo impurity limit. A very promising example of such compounds is derived from the family of  $\text{RT}_2\text{Zn}_{20}$  ( $T = \text{transition metal}$ ) [1], which has recently been shown to allow for the tuning of the nonmagnetic  $R = \text{Y}$  and  $\text{Lu}$  members to exceedingly close to the Stoner limit as well as allowing for the study of the effects of such a highly polarizable background on local moment magnetic ordering for  $R = \text{Gd}$  [2]. A brief overview of the discovery and physical properties of six closely related Yb-based heavy fermion compounds,  $\text{YbT}_2\text{Zn}_{20}$  ( $T = \text{Fe, Co, Ru, Rh, Os, Ir}$ ), will be presented [3]. Given these compounds' dilute nature, systematic changes in  $T$  only weakly perturb the Yb site and allow for insight into the effects of degeneracy on the thermodynamic and transport properties of these model correlated electron systems. The data show that, whereas there is relatively little variation in the low temperature thermodynamic properties, or Wilson ratio, associated with the  $T = \text{Fe, Ru, Rh, Os, Ir}$  compounds, there is an order of magnitude variation in the value of the coefficient of the  $T^2$  resistivity. This observation can be rationalized using the idea of a generalized Kadowaki – Woods ratio [4] that can vary by over an order of magnitude, depending upon the value of the degeneracy of the Yb ion when it hybridizes. The  $\text{YbT}_2\text{Zn}_{20}$  data indicate that for  $T = \text{Fe, Ru}$  the Yb ion has a significantly larger degeneracy upon entering the Kondo-screened state than it does for the  $T = \text{Rh, Os, Ir}$  compounds.  $\text{YbCo}_2\text{Zn}_{20}$  appears to be different from the other members of this family It has a substantially lower Kondo temperature, and may be closer to a quantum critical point than the other,  $T = \text{Fe, Ru, Rh, Os, Ir}$  members of the family [2].

We will also review the evolution of the Kondo effect in the series of  $\text{Yb}(\text{Fe}_{1-x}\text{Co}_x)_2\text{Zn}_{20}$  ( $0 \leq x \leq 1$ ), compounds, studied by means of temperature-dependent electric resistivity and specific heat [5]. With Co substitution, the Kondo coherence temperature of  $\text{YbFe}_2\text{Zn}_{20}$  decreases gradually with emerging features in specific heat that can be associated with CEF effect. On the  $\text{YbCo}_2\text{Zn}_{20}$  side, the coherence temperature is also suppressed at the beginning of Fe substitution. For  $0.4 \leq x \leq 0.9$  the CEF features can be observed in both resistivity and specific heat data while showing no clear feature of coherence down to 500 mK. The data suggest that the CEF splitting stays roughly unchanged across the series. The ground state evolves from an  $N = 8$  coherent state for  $\text{YbFe}_2\text{Zn}_{20}$  to an  $N = 2$  coherent state in  $\text{YbCo}_2\text{Zn}_{20}$  [5].

Finally we will discuss a search for pressure-induced quantum criticality in  $\text{YbFe}_2\text{Zn}_{20}$  [6] via electrical resistivity measurements under pressures up to  $\sim 8.2$  GPa and down to temperatures of nearly 0.3 K. The pressure dependence of the low-temperature Fermi-liquid state was evaluated by fitting the temperature dependent resistivity as  $\rho(T) = \rho_0 + AT^n$  at low temperatures. Power-law analysis of the low-temperature resistivities indicates  $n = 2$  over a broad temperature range for  $P \lesssim 5$  GPa. However, at higher pressures, the fits show a wider range of  $n < 2$  power-law behavior in the low-temperature resistivities. As pressure is increased, the Fermi-liquid temperature diminished from  $\sim 11$  K at ambient pressure to  $\sim 0.6$  K at 8.2 GPa. Over the same pressure range, the  $A$  parameter increased dramatically with a functional form of  $A \propto 1/(P-P_c)^2$  with  $P_c \approx 9.8$  GPa being the critical pressure for a possible quantum critical point. We will compare these results with the available pressure data for other  $\text{YbT}_2\text{Zn}_{20}$  compounds and discuss the possibilities for the magnetic ground state for  $\text{YbFe}_2\text{Zn}_{20}$  under pressure.

This work was supported by the U.S. Department of Energy, Office of Science, Basic Energy Sciences, Materials Science and Engineering Division. The research was performed at the Ames Laboratory, which is operated for the U.S. DOE by Iowa State University under Contract No. DE-AC02-07CH11358.

- [1] T. Nasch, W. Jeitschko, and U. C. Rodewald, *Z. Naturforsch.* **52**, 1023 (1997).
- [2] S. Jia, S. L. Bud'ko, G. D. Samolyuk, and P. C. Canfield, *Nat. Phys.* **3**, 334 (2007).
- [3] M. S. Torikachvili, S. Jia, E. D. Mun, S. T. Hannahs, R. C. Black, W. K. Neils, D. Martien, S. L. Bud'ko, and P. C. Canfield, *Proc. Natl. Acad. Sci. USA* **10**, 9960 (2007).
- [4] N. Tsujii, H. Kontani, and K. Yoshimura, *Phys. Rev. Lett.* **9**, 057201 (2005).
- [5] Tai Kong, Valentin Taufour, Sergey L. Bud'ko, and Paul C. Canfield, *Phys. Rev. B* **95**, 155103 (2017).
- [3] S. K. Kim, M. S. Torikachvili, S. L. Bud'ko, and P. C. Canfield, *Phys. Rev. B* **88**, 045116 (2013).

## Novel electronic states and phase diagram of non-Kramers doublet systems

Taichi YOSHIDA<sup>1</sup>, Yo MACHIDA<sup>1</sup>, Yuki SHIMADA<sup>2</sup>, Naohiro NAGASAWA<sup>2</sup>,  
 Takahiro ONIMARU<sup>2</sup>, Toshiro TAKABATAKE<sup>2</sup>, Adrien GOURGOUT<sup>3</sup>, Alexandre POURRET<sup>3</sup>,  
 Georg KNEBEL<sup>3</sup>, Jean-Pascal BRISON<sup>3</sup>, Koichi IZAWA<sup>1</sup>

<sup>1</sup> Department of Physics, Tokyo Institute of Technology, Tokyo, Japan

<sup>2</sup> Graduate School of Advanced Sciences of Matter, Hiroshima University Hiroshima, Japan

<sup>3</sup> Université Grenoble Alpes, CEA, INAC-PHELIQS, Grenoble, France

Strongly correlated electron systems with  $f$ -electrons display a rich variety of intriguing phenomena, such as magnetic order, multipole order, heavy-fermion, metamagnetic transition, non-Fermi liquid behavior near a magnetic quantum critical point, and unconventional superconductivity. These phenomena are characterized in terms of the itinerant-localized duality of  $f$ -electrons derived from atomic  $f$ -orbitals via the hybridization between conduction and  $f$ -electrons. The vast majority of these phenomena are governed by spin degrees of freedom and have been explained in terms of the interplay between Kondo effect and magnetic RKKY interactions, i.e. the Doniach picture. On the other hand, electronic properties of systems in the presence of the hybridization between multipoles and conduction electrons remains unclear because of the lack of suitable systems to study this issue. Praseodymium-based compounds  $\text{PrT}_2\text{Zn}_{20}$  ( $T=\text{Ir, Rh}$ ) provide a rare opportunity to elucidate the nature of electronic states inherent in multipole degrees of freedom; they have a  $\Gamma_3$  non-Kramers doublet ground state possessing only quadrupole and octapole degeneracies [1,2].

Here we present the low temperature transport properties of  $\text{PrT}_2\text{Zn}_{20}$  ( $T=\text{Ir, Rh}$ ) under magnetic fields. Our measurements reveal that the  $B$ - $T$  phase diagram involves four intriguing states, i.e. an “unusual” non-Fermi liquid (NFL) state, a novel heavy-fermion (HF) states, a field-induced singlet (FIS) state as well as a long range antiferroquadrupole (AFQ) ordered state, regardless of the orientation of the magnetic field while the energy scale of these states shows a remarkable anisotropy with respect to the field orientation. In the NFL state, for instance, the resistivity showing a convex curve can be expressed by a scaling function based on a quadrupole Kondo lattice model [3] with a characteristic temperature scale  $T_0$  regardless of the field orientation, but the field dependence of  $T_0$  is obviously anisotropic. Interestingly, we found that the anisotropy of the energy scales of four states including  $T_0$  can be described in terms of the field-induced energy splitting of the  $\Gamma_3$  non-Kramers doublet  $\delta(\mathbf{B})$  [4]; the transport properties inherent in itinerant electrons are intimately governed by the localized character of the  $f$ -electrons. This clearly shows itinerant-localized duality of  $f$ -electrons in this quadrupolar system. On the basis of these results, we discuss a universal phase diagram for the non-Kramers system with respect to the energy splitting of non-Kramers doublet  $\delta(\mathbf{B})$ . We also discuss the orbital-selective quadrupolar Kondo effect, i.e. the composite order [5] as a possible origin of the HF state.

[1] T. Onimaru, *et al.*, Phys. Rev. Lett., **106**, 177001 (2011).

[2] A. Sakai *et al.*, J. Phys. Soc. Jpn. **81**, 083702 (2012).

[3] A. Tsuruta and K. Miyake, J. Phys. Soc. Jpn. **84**, 114714 (2015).

[4] T. Yoshida *et al.*, J. Phys. Soc. Jpn. **86**, 044711 (2017).

[5] S. Hoshino and Y. Kuramoto, Phys. Rev. Lett. **112**, 167204 (2014).

## Emergence of quadrupole-driven phenomena in non-Kramers Pr 1-2-20 systems

T. Onimaru<sup>1</sup>, Y. Yamane<sup>1</sup>, R. J. Yamada<sup>1</sup>, K. Umeo<sup>2</sup>, A. S. Wörl<sup>3</sup>, Y. Tokiwa<sup>3</sup>, P. Gegenwart<sup>3</sup>,  
and T. Takabatake<sup>1</sup>

<sup>1</sup>Graduate School of Advanced Sciences of Matter, Hiroshima University, Higashi-Hiroshima 739-8530, Japan

<sup>2</sup>N-BARD, Hiroshima University, Higashi-Hiroshima 739-8526, Japan

<sup>3</sup>Center for Electronic Correlations and Magnetism, University of Augsburg, Augsburg 86159, Germany.

A variety of exotic phenomena arising from active quadrupoles in non-Kramers doublet of  $4f^2$  systems,  $\text{PrT}_2\text{X}_{20}$  ( $T$ : transition metal,  $X$ : Al, Zn, and Cd), are presented [1].  $\text{PrT}_2\text{X}_{20}$  crystallizes in the cubic  $\text{CeCr}_2\text{Al}_{20}$ -type structure, where the  $\text{Pr}^{3+}$  ion is encapsulated in a symmetric cage formed by sixteen  $X$  atoms [2]. The cubic point group of  $T_d$  at the Pr site may bring about a degenerated  $4f^2$  crystalline electric field (CEF) ground state. Furthermore, the  $s$ - $p$  orbitals of cage atoms would hybridize with the  $4f^2$  state. In fact, the CEF ground states of  $\text{Pr}^{3+}$  in  $\text{PrT}_2\text{X}_{20}$  were revealed to be the non-Kramers  $\Gamma_3$  doublet by inelastic neutron scattering experiments [3,4], although that of  $\text{PrRh}_2\text{Zn}_{20}$  is the  $\Gamma_{23}$  doublet for the cubic point group of  $T$  due to the symmetry lowering of the Pr sites by a possible structural transition [4,5]. Since both of the non-Kramers doublets have no magnetic dipole but quadrupolar degrees of freedom, the transport, thermodynamic and magnetic properties could be governed by the active quadrupoles of the doublet in a low temperature range below a few K, being lower than a few tens K of the CEF splitting energy. At the low temperature range, the quadrupoles play a key role in the phenomena such as long-range quadrupole order, superconductivity, non-Fermi liquid (NFL) behavior, and magnetic-field induced Fermi liquid state [6-9].

Among the Pr 1-2-20 systems,  $\text{PrIr}_2\text{Zn}_{20}$  has been intensively studied. It exhibits an antiferroquadrupolar (AFQ) order at  $T_Q = 0.11$  K, below which a superconducting transition sets in at  $T_c = 0.05$  K [6,7]. Although the entropy release of  $R\ln 2$  is expected from an order of the  $\Gamma_3$  doublet, the entropy at  $T_Q$  estimated from the specific heat is only 20% of  $R\ln 2$ , suggesting a possible interplay between the quadrupole fluctuations and the superconducting Cooper-pair formation. In the moderately wide temperature range at  $T > T_Q$ , the NFL behavior was clearly observed in the electrical resistivity  $\rho$  and the  $4f$  contribution to the specific heat  $C_{4f}$  [9]. In magnetic fields of  $B < 6$  T applied along the [100] direction,  $\chi$  can be well scaled with characteristic temperatures, suggesting existence of low-energy excitations by the quadrupolar degrees of freedom. A promising candidate is the formation of the quadrupole Kondo lattice due to the hybridization between the quadrupoles and the conduction electrons [9,10]. Furthermore,  $\rho$  and  $C_{4f}$  exhibit anomalies at  $T^* = 0.13$  K in the vicinity of 5 T, around which the AFQ order collapses by applying the magnetic field. The coefficient  $A$  for  $\rho = \rho_0 + AT^2$ ,  $C_{4f}/T$ , and the Seebeck coefficient divided by temperature,  $S/T$ , have significant enhancement as a function of  $B$ . The concomitant increase in  $dM/dB$  indicates formation of a magnetic-field-induced Fermi-liquid ground state to remove the residual entropy in the quadrupole Kondo lattice. We also present experimental results of the thermal expansion and magnetostriction measurements and discuss possible interplay between the quadrupole order parameters and the lattice distortion.

This work was financially supported by Grants-in-Aid from MEXT/JSPS of Japan, Nos. JP15KK0169, JP15H05886, and JP16H01076 (J-Physics).

- [1] T. Onimaru and H. Kusunose, *J. Phys. Soc. Jpn.* **85**, 082002 (2016).
- [2] T. Nasch *et al.*, *Z. Naturforsch. B* **52**, 1023 (1997).
- [3] T. J. Sato *et al.*, *Phys. Rev. B* **86**, 184419 (2012).
- [4] K. Iwasa *et al.*, *J. Phys. Soc. Jpn.* **82**, 043707 (2013).
- [5] T. Onimaru *et al.*, *Phys. Rev. B* **86**, 184426 (2012).
- [6] T. Onimaru *et al.*, *J. Phys. Soc. Jpn.* **79**, 033704 (2010).
- [7] T. Onimaru *et al.*, *Phys. Rev. Lett.* **106**, 177001 (2011).
- [8] A. Sakai and S. Nakatsuji, *J. Phys. Soc. Jpn.* **80**, 063701 (2011).
- [9] T. Onimaru *et al.*, *Phys. Rev. B* **94**, 075134 (2016).
- [10] A. Tsuruta and K. Miyake, *J. Phys. Soc. Jpn.* **84**, 114714 (2015).

## Strong hybridization effect and heavy fermion superconductivity in non-magnetic quadrupolar systems $\text{PrT}_2\text{Al}_{20}$ ( $T = \text{Ti, V}$ )

Yosuke Matsumoto\*

Institute for Solid State Physics, University of Tokyo, Kashiwa, Chiba, 277-8581, Japan

$f$  electrons' orbital degrees of freedom could be a source of novel metallic states when they strongly hybridized with conduction electrons. This possibility has been extensively studied. In particular, quadrupole Kondo effect, originally suggested as a single ion effect in the nonmagnetic cubic  $\Gamma_3$  crystal electric field doublet [1], has attracted a lot of attention because of its non-Fermi liquid ground state. On the other hand, the even highly non-trivial problems are what happens in the lattice systems and what types of ground state emerges in the vicinity of a quantum critical point (QCP) of orbital orderings under the influence of strong hybridization. In order to answer these questions, we need to study clean materials with strong hybridization.

Recent studies have revealed that  $\text{PrT}_2\text{Al}_{20}$  ( $T = \text{Ti, V}$ ) provide ideal systems for such studies. Both systems have the nonmagnetic cubic  $\Gamma_3$  crystal electric field doublet [2, 3]. In addition, the hybridization is strong as is evident in many physical properties. We found that both exhibit heavy fermion superconductivity inside the multipole ordering phases [4-6]. Especially, in the case of  $\text{PrV}_2\text{Al}_{20}$ , the effective mass is highly enhanced ( $m^*/m_0 \sim 140$ ) even at ambient pressure, revealing even stronger hybridization in  $\text{PrV}_2\text{Al}_{20}$  [6]. Surprisingly, the transition temperatures of these superconductivities are strongly enhanced under pressure. In the case of  $\text{PrTi}_2\text{Al}_{20}$ , it is enhanced up to 1.1 K at  $P = 8.7$  GPa, where ferro-quadrupole ordering temperature exhibits considerable decrease [5]. These observations indicate the realization of the novel superconductivity arising from the orbital fluctuation of the  $f$  electrons in the vicinity of an orbital QCP.

While  $\text{PrTi}_2\text{Al}_{20}$  exhibits a ferro-quadrupole ordering at 2.0 K,  $\text{PrV}_2\text{Al}_{20}$  exhibits double multipolar orderings at  $T = 0.65$  and 0.75 K [6, 7]. The specific heat exhibits the  $T^4$  power law behavior below 0.5 K indicating the formation of the gapless mode due to strong orbital fluctuation. In the magnetic fields, these systems exhibit complicated phase diagrams depending on the field direction. In this talk, I will review these observations. Possible quadrupolar quantum criticality [8] and quadrupole Kondo effect will be also discussed.

This talk is based on the research in collaboration with S. Nakatsuji, A. Sakai, Y. Shimura, M. Tsujimoto, T. Tomita, K. Matsubayashi, Y. Uwatoko, T. Sakakibara, T. Sato, D. Okuyama, Y. Nakanishi, M. Yoshizawa, M. Takigawa, and T. Taniguchi.

\*Present affiliation: Max Planck Institute for Solid State Research, 70569 Stuttgart, Germany.

- [1] D. L. Cox, PRL **59**, 1240 (1987).
- [2] A. Sakai, and S. Nakatsuji, JPSJ **80**, 063701 (2011). *References therein*.
- [3] T. J. Sato, S. Ibuka, Y. Nambu, T. Yamazaki, T. Hong, A. Sakai, and S. Nakatsuji, PRB **86**, 184419 (2012).
- [4] A. Sakai, K. Kuga, S. Nakatsuji, JPSJ **81**, 083702 (2012).
- [5] K. Matsubayashi, T. Tanaka, A. Sakai, S. Nakatsuji, Y. Kubo, and Y. Uwatoko, PRL **109**, 187004 (2012).
- [6] M. Tsujimoto, Y. Matsumoto, T. Tomita, A. Sakai, and S. Nakatsuji, PRL **113**, 267001 (2014). *References therein*.
- [7] K. Araki, Y. Shimura, N. Kase, T. Sakakibara, A. Sakai, S. Nakatsuji, JPS Conf. Proc. **3**, 011093 (2014).
- [8] Y. Shimura, M. Tsujimoto, B. Zeng, L. Balicas, A. Sakai, and S. Nakatsuji, PRB **91**, 241102(R) (2015).

## O-41

## Fermi Surface Topology of Weyl Semimetals

E. Hassinger<sup>1,2</sup>, F. Arnold<sup>1</sup>, M. Naumann<sup>1</sup>, R. Dos Reis, M. Nicklas, S.C. Wu<sup>1</sup>, Y. Sun<sup>1</sup>, B. Yan<sup>1</sup>, M. Schmidt<sup>1</sup>, H. Borrmann<sup>1</sup>, and C. Felser<sup>1</sup>

<sup>1</sup>Max Planck Institute for Chemical Physics of Solids, Dresden, Germany

<sup>2</sup>TU Munich, Germany

Weyl Fermions are the solution of the massless Dirac equations and have been long sought after in high energy physics [1]. Weyl semimetals host quasiparticles that can be described as Weyl electrons. Recently the non-centrosymmetric mono-pnictides (Ta,Nb)(P,As) were predicted to be Weyl semimetals by ab initio DFT calculations [2]. The presence of Weyl nodes and Fermi arc surface states in these materials was later confirmed by ARPES [3]. Here, we present the precise Fermi surface topography of our TaP and TaAs single crystals as determined by quantum oscillation measurements and ab initio bandstructure calculations. It will be shown that chirality in TaP is ill-defined due to a large energy separation of the Fermi energy from the Weyl points [4]. In TaAs, on the other hand, well-defined Weyl pockets of opposite chirality exist [5]. Thus quantum phenomena due to chirality are only expected in TaAs. As a second point, we also show evidence that experimental results of the longitudinal magnetoresistance in these compounds can easily be dominated by effects of a field-induced resistance anisotropy. In that case, current inhomogeneities [6] can lead to an apparent “negative magnetoresistance” as expected for the chiral anomaly [7].

We acknowledge financial support from the MPRG “Physics of Unconventional Metals and Superconductors” and the ANR/DFG project “Fermi-surface topology and emergence of novel electronic states in strongly correlated electron systems”.

- [1] H. Weyl, *Zeitschrift f. Physik* 56, 330 (1929)
- [2] H. Weng et al., *Phys. Rev. X* 5, 011029 (2015)
- [3] B. Q. Lv et al., *Phys. Rev. X* 5, 031013 (2015), S.-Y. Xu et al. *Science* 349, 613 (2015)
- [4] F. Arnold et al., *Nat. Comm.* 7, 11615 (2016)
- [5] F. Arnold et al., *Phys. Rev. Lett.* 117, 146401 (2016)
- [6] K. Yoshida, *JPSJ* 41, 574 (1975)
- [7] R. Dos Reis et al., *NJP* 18, 085006 (2016)

Superconductivity of layered BiS<sub>2</sub>-based systemsY. Mizuguchi<sup>1</sup><sup>1</sup>Tokyo Metropolitan University, Hachioji 192-0397, Japan

Since the discovery of superconductivity in BiS<sub>2</sub>-based layered compounds, Bi<sub>4</sub>O<sub>4</sub>S<sub>3</sub> [1] and LaO<sub>1-x</sub>F<sub>x</sub>BiS<sub>2</sub> [2], BiS<sub>2</sub>-based systems studies have drawn much attention as a new class of layered superconductors. The crystal structure composed of alternate stacks of the conducting BiS<sub>2</sub> layer and the insulating (blocking) layer resembles to that of the cuprate or the Fe-based superconductors; hence, many superconductors have been discovered by replacing the blocking and/or conducting layers. Typically the parent phase of the BiS<sub>2</sub>-based superconductor is a semiconductor with a band gap. Electron doping by element substitution at the blocking layer induces superconductivity [3].

On the other hand, LaO<sub>1-x</sub>F<sub>x</sub>BiS<sub>2</sub>, which is an electron-doped system, does not show bulk superconductivity without external pressure effects, such as strain effects by high-pressure annealing or pressuring using a pressure cell. The high-pressure phase of LaO<sub>0.5</sub>F<sub>0.5</sub>BiS<sub>2</sub> shows superconductivity with a  $T_c$  of ~11 K [1,4]. Chemical pressure effect, which can be applied by substitution by an isovalent element with a different ionic radius, also enhances superconductivity, and bulk superconductivity has been observed in chemical-pressure systems, REO<sub>1-x</sub>F<sub>x</sub>BiS<sub>2</sub> (RE: La, Ce, Pr, Nd, Sm) [5,6]. In addition, similar chemical pressure effect has been observed in Se-substituted system, LaO<sub>0.5</sub>F<sub>0.5</sub>BiS<sub>2-x</sub>Se<sub>x</sub> [7]. Recently, we have revealed that the effects of chemical pressure in the BiS<sub>2</sub> systems can be explained by in-plane chemical pressure (or misfit strain), and the suppression of in-plane disorder, which is essential for the emergence of bulk superconductivity in the BiS<sub>2</sub> systems [6,8].

Based on these experimental investigations, we found that the LaO<sub>1-x</sub>F<sub>x</sub>Bi(S,Se)<sub>2</sub> system with enough Se concentration at the in-plane chalcogen site, was the best system to investigate superconducting properties of the BiCh<sub>2</sub> (Ch: S, Se) system because in-plane disorder is fully suppressed in the system. Using LaO<sub>0.6</sub>F<sub>0.4</sub>Bi(S,Se)<sub>2</sub>, we have recently investigated the isotope effect on  $T_c$ . The experimental results tested using homogeneous samples with <sup>76</sup>Se and <sup>80</sup>Se isotopes clearly indicated that the electron-phonon interaction was not essential for the superconductivity mechanisms of the BiCh<sub>2</sub> systems [9]. This is consistent with recent theoretical calculations by Morice et al. [10], and would be supporting the anisotropic superconducting gap observed in angle-resolved photoemission spectroscopy (ARPES) [11].

In this presentation, I will review the crystal structure and superconducting properties of the BiS<sub>2</sub> systems and introduce recent results on this system.

This work was partly supported by a Grant-in-Aid for Scientific Research (Nos. 15H05886, 16H04493, 17K19058, and 16K17944) and JST-CREST (No. JPMJCR16Q6), Japan.

- [1] Y. Mizuguchi et al., Phys. Rev. B 86, 220510 (2012).
- [2] Y. Mizuguchi et al., J. Phys. Soc. Jpn. 81, 114725 (2012).
- [3] Y. Mizuguchi, J. Phys. Chem. Solids, 84, 34 (2015). [Review article]
- [4] Y. Mizuguchi et al., J. Phys. Soc. Jpn. 83, 053704 (2014).
- [5] J. Kajitani et al., J. Phys. Soc. Jpn. 84, 044712 (2015).
- [6] Y. Mizuguchi et al., Sci. Rep. 5, 14968 (2015).
- [7] T. Hiroi et al., J. Phys. Soc. Jpn 84, 024723 (2015).
- [8] K. Nagasaka et al., J. Phys. Soc. Jpn. 86, 074701 (2017).
- [9] K. Hoshi, Y. Goto, Y. Mizuguchi, arXiv:1708.08252.
- [10] C. Morice et al., Phys. Rev. B 95, 180505 (2017).
- [11] Y. Ota et al., Phys. Rev. Lett. 118, 167002 (2017).

Phase Transition in  $\beta$ -Pyrochlore Oxide  $\text{CsW}_2\text{O}_6$ 

Y. Okamoto, H. Amano, K. Niki, R. Mitoka, N. Katayama, H. Sawa, Y. Nakamura, H. Kishida, and K. Takenaka  
Dept. Appl. Phys., Nagoya University, Nagoya 464-8603, Japan

Metal-insulator transitions in  $d$  electron systems with pyrochlore structure have been a longstanding issue in the field of condensed matter physics since the discovery of Verwey transition in magnetite. They are caused by various mechanisms such as a dimer formation in  $\text{CuIr}_2\text{S}_4$  and all-in-all-out type magnetic order in  $\text{Cd}_2\text{Os}_2\text{O}_7$  and  $\text{Nd}_2\text{Ir}_2\text{O}_7$ . Here we report that the  $\beta$ -pyrochlore oxide  $\text{CsW}_2\text{O}_6$ , where  $\text{W}^{5.5+}$  ions having  $5d^{0.5}$  electron configuration form a pyrochlore structure, exhibits a unique metal-insulator transition different from other pyrochlore systems.  $\text{CsW}_2\text{O}_6$  was first synthesized by Cava *et al.* in 1993 [1] and then found to show a metal-insulator transition accompanied by a decrease of magnetic susceptibility [2]. However, formation mechanism of the transition is still not fully understood, because all the previous studies were employed using polycrystalline samples.

We succeeded in preparing single crystals of  $\text{CsW}_2\text{O}_6$  by a vapour transport method. As shown in the left figure, electrical resistivity of a  $\text{CsW}_2\text{O}_6$  single crystal strongly increases at  $T_{\text{MI}} = 215$  K with decreasing temperature, indicating that the metal-insulator transition occurs at this temperature. Magnetic susceptibility also decreases at this transition, consistent with the previous results obtained by using polycrystalline samples. Single crystal X-ray diffraction experiments revealed that a structural change accompanied by the  $\text{W}_3$  trimer formation, while keeping the cubic symmetry, occurs at this transition. To our knowledge, such a trimer formation has never been observed in other pyrochlore systems, indicating that a unique metal-insulator transition is realized in  $\text{CsW}_2\text{O}_6$ .

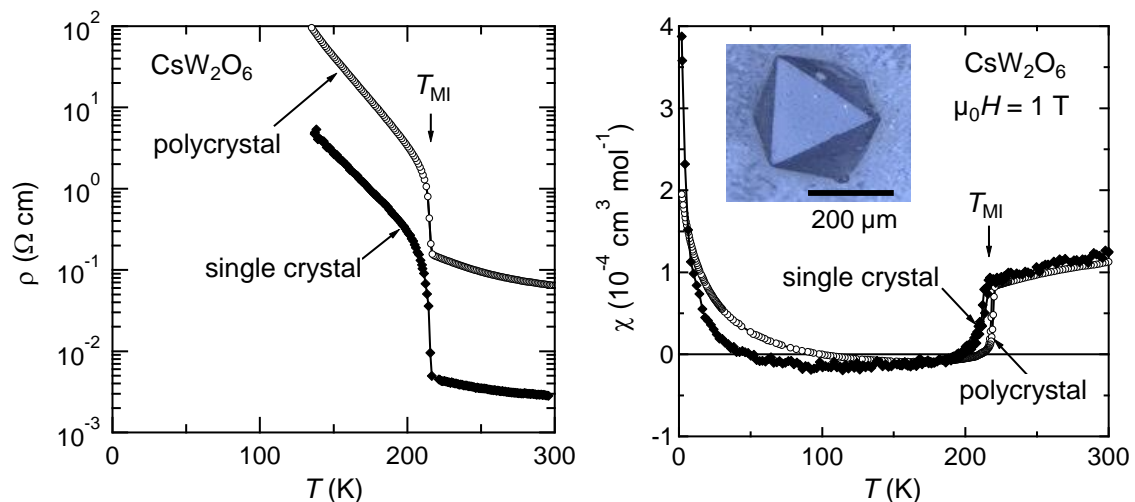


Fig. Temperature dependences of electrical resistivity (left) and magnetic susceptibility of single crystals and polycrystalline samples of  $\text{CsW}_2\text{O}_6$ . A single crystal is shown in the inset.

[1] R. J. Cava *et al.*, J. Solid State Chem. **103**, 359 (1993).

[2] D. Hirai *et al.*, Phys. Rev. Lett. **110**, 166402 (2013).

## Spin-Nematic and Spin-Liquid Phases in Low-Dimensional Antiferromagnets

T. Sakai<sup>1 2 3</sup><sup>1</sup>Graduate School of Material Science, University of Hyogo, Hyogo 678-1297, Japan<sup>2</sup>Research Center for New Functional Materials, University of Hyogo, Hyogo 678-1297, Japan<sup>3</sup>National Institutes for Quantum and Radiological Science and Technology (QST), SPring-8, Hyogo 679-5148, Japan

The spin nematic phase, which is a kind of multipole phases, has attracted a lot of interest in the field of the strongly correlated electron systems, as well as the quantum spin liquid phase. Using the numerical exact diagonalization, the density matrix renormalization group (DMRG) calculation, and the finite-size scaling analysis, it is found that some spin nematic and spin liquid phases appear in the anisotropic and/or frustrated quantum spin systems.

In our previous work, quasi-one-dimensional quantum spin systems with the easy-axis anisotropy in magnetic field are theoretically investigated using the numerical exact diagonalization, the density matrix renormalization group (DMRG) and the finite-size scaling analysis[1]. It was found that a field-induced nematic phase appears at some critical field in the anisotropic spin ladder and the mixed spin chain. The nematic phase is characterized by the power-law decay in the correlation function of the second-order spin moment. In addition at some higher critical field a quantum phase transition can occur to the conventional field-induced Tomonaga-Luttinger liquid. Several typical magnetization curves calculated by DMRG are presented. We will also propose an experiment to observe these field-induced transitions by NMR measurements. The field-induced incommensurate order observed in azurite, which is modeled by the distorted diamond chain, by the recent NMR measurement will be also discussed.

Recently the field-induced nematic phase was observed on the frustrated spin ladder system[2,3]. So we study on a frustrated spin ladder system[4], using the numerical diagonalization and DMRG. As a result, it is found that several exotic quantum phases, including the spin-nematic liquid phase. We also report some exact eigen states of the present model.

[1] T. Sakai, T. Tonegawa and K. Okamoto, *Physica Status Solidi B* 247 (2010) 583.

[2] N. Buttgen et al., *Phys. Rev B* 90, (2014) 134401.

[3] K. Nawa et al., *J. Phys. Soc. Jpn.*, 82 (2013) 094709.

[4] T. Hikihara, T. Tonegawa, K. Okamoto and T. Sakai, *J. Phys. Soc. Jpn.* 86 (2017) 054709.

## Single Crystal Growth and Highly-Anisotropic Magnetic Properties of Ferromagnetic Heavy Fermion Compound YbNiSn

A. Nakamura<sup>1</sup>, G. Knebel<sup>2,3</sup>, A. Pourret<sup>2,3</sup>, A. Gougout<sup>2,3</sup>, D. Braithwaite<sup>2,3</sup>, Y. Shimizu<sup>1</sup>, A. Maurya<sup>1</sup>, F. Honda<sup>1</sup>, Y. Homma<sup>1</sup>, D. X. Li<sup>1</sup>, J. Flouquet<sup>2,3</sup>, and D. Aoki<sup>1,2,3</sup>

<sup>1</sup>Institute for Materials Research, Tohoku University, Oarai, Ibaraki 311-1313, Japan

<sup>2</sup>University Grenoble Alpes, INAC-PHELIQS, F-38000 Grenoble, France

<sup>3</sup>CEA, INAC-PHELIQS, F-38000 Grenoble, France

The spin reorientation and the reentrant superconductivity observed in URhGe for  $H \parallel b$ -axis are quite unique phenomena among ferromagnets [1,2]. In order to understand the collapse of the Curie temperature under magnetic field, we have studied a heavy fermion ferromagnet YbNiSn with the identical crystal structure. YbNiSn crystallizes in the TiNiSi-type orthorhombic crystal structure, and is a heavy fermion compound with the Curie temperature  $T_C=5.5$  K and Sommerfeld coefficient  $\gamma=300$  mJ/(K<sup>2</sup>mol) [3-5]. We have succeeded in growing high-quality single crystals using the Bridgman method with W-crucibles. In the present work, we clarify the highly-anisotropic magnetic properties and its magnetic phase diagram by measuring the magnetoresistance, magnetization, and thermoelectric power.

Figure 1 shows the temperature dependence of the electrical resistivity  $\rho$  for the current  $J$  along the  $b$ -axis in YbNiSn. The residual resistivity  $\rho_0$  is  $1.37 \mu\Omega\cdot\text{cm}$  and the residual resistivity ratio RRR ( $=\rho_{RT}/\rho_0$ ,  $\rho_{RT}$ : resistivity at room temperature) is 55, revealing a high-quality sample. The electrical resistivity  $\rho(T)$  shows a double-peak structure around 60 K and 10 K with Kondo-lattice behavior as same as a previous study [3], and  $\rho(T)$  exhibits a drop due to the ferromagnetic transition at  $T_C = 5.68$  K. We also measured a magnetic field dependence of the electrical resistivity of YbNiSn for  $H \parallel a$ -axis. The electrical resistivity under magnetic fields show plateau in a field range from 10 to 20 kOe below 5 K, as shown in Fig. 2 due to a spin-flop. With increasing temperature, the field range of the resistive plateau becomes narrower and finally disappears above  $T_C$ . A field dependence of the magnetization  $M$  for  $H \parallel a$ -axis shows the canting process and three anomalies at the fields  $H_{c1}$ ,  $H_{c2}$ , and  $H_{c3}$ . Such phenomena come from the spin-flop behaviors for an Ising ferromagnet under magnetic fields in agreement with the previous studies [4, 5]. The values of  $H_{c1}$ ,  $H_{c2}$ , and  $H_{c3}$  decrease with increasing temperature and merge at around the Curie temperature. Finally, we summarize the magnetic phase diagram of YbNiSn for  $H \parallel a$ -axis and discuss the nature of anomalies observed from our transport and magnetization measurements.

This work was supported by JSPS KAKENHI Grant Numbers 25247055, 15H05884, 15H05882, 16H04006, and 16K17733 and start-up research costs from the Project to Promote Gender Equality and Support Female Researchers from Tohoku University.

- [1] F. Lévy et al., *Science* **309**, 1343 (2005).
- [2] F. Lévy et al., *Nat. Phys.* **3**, 460 (2007).
- [3] M. Kasaya et al., *J. Magn. Magn. Mater.* **76 & 77**, 278 (1988).
- [4] M. Kasaya et al., *J. Phys. Soc. Jpn.* **60**, 3145 (1991).
- [5] P. Bonville et al., *Physica B* **182**, 105 (1992).

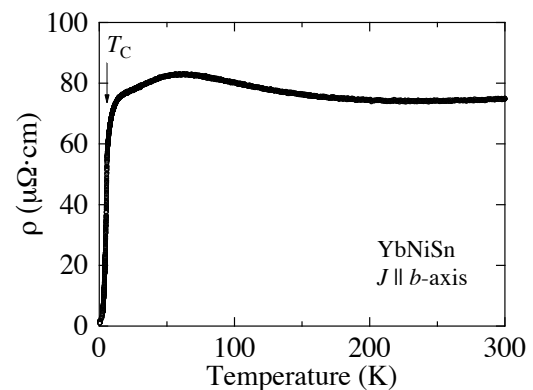


Figure 1. Temperature dependence of electrical resistivity in YbNiSn.

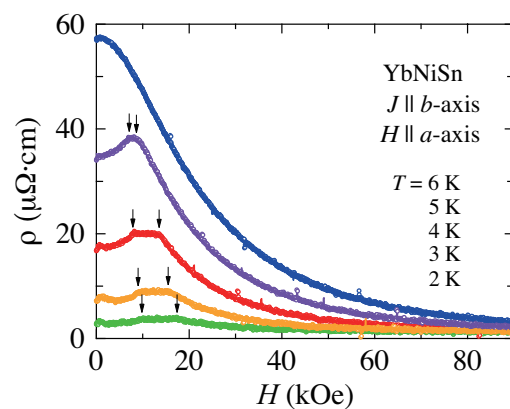


Figure 2. A magnetic field dependence of electrical resistivity of YbNiSn for  $H \parallel a$ -axis.

# P-1

## NMR study of magnetic fluctuations and superconductivity of UCoGe under pressure

M. Manago<sup>1</sup>, S. Kitagawa<sup>1</sup>, K. Ishida<sup>1</sup>, K. Deguchi<sup>2</sup>, N. K. Sato<sup>2</sup>, T. Yamamura<sup>3</sup>, and D. Aoki<sup>3,4</sup>

<sup>1</sup>Kyoto University, Kyoto 606-8502, Japan

<sup>2</sup>Nagoya University, Nagoya 464-8602, Japan

<sup>3</sup>IMR, Tohoku University, Sendai 980-8577, Japan

<sup>4</sup>INAC/SPSMS, CEA Grenoble, 38054 Grenoble, France

In uranium-based ferromagnetic superconductors, an anomalous state that superconductivity emerges inside the ferromagnetic state is realized [1]. UCoGe is one of the members of such ferromagnetic superconductors, and it was revealed that the ferromagnetic fluctuations with Ising anisotropy are essential for the realization of the superconductivity [2]. The ferromagnetic phase of UCoGe is suppressed by hydrostatic pressure, while the superconductivity survives in the paramagnetic side [3]. This phase diagram suggests that the ferromagnetic fluctuations are changed by the pressure, and it is expected that this change leads to the enhancement of the superconductivity.

We performed <sup>59</sup>Co nuclear quadrupole resonance (NQR) on UCoGe under pressure to know how the ferromagnetic fluctuations are changed. We found that nuclear spin-lattice relaxation rate  $1/T_1$  is strongly enhanced under pressure above the superconducting transition temperature  $T_{SC}$ . Because  $T_{SC}$  is also enhanced where the ferromagnetic phase is suppressed, this result is consistent with that the ferromagnetic fluctuations are pairing glue in this system, which is in agreement with previous results. The  $1/T_1$  in the superconducting state in the paramagnetic side implies the line-node (-like) gap, which is similar to that in the ferromagnetic side at ambient pressure [4].

We also performed <sup>73</sup>Ge NMR and NQR to study the contribution of Co 3d electrons to the ferromagnetism and to compare the results with other family compounds. We found that the <sup>73</sup>Ge NMR results are similar to those of <sup>59</sup>Co, which indicates that U 5f electrons play dominant roles in the ferromagnetism in UCoGe.

[1] D. Aoki and J. Flouquet, J. Phys. Soc. Jpn. **81**, 011003 (2012).

[2] T. Hattori *et al.*, Phys. Rev. Lett. **108**, 066403 (2012).

[3] E. Slooten *et al.*, Phys. Rev. Lett. **103**, 097003 (2009).

[4] T. Ohta *et al.*, J. Phys. Soc. Jpn. **79**, 023707 (2010).

Cu-NMR studies of heavy fermion CeCu<sub>6</sub>H. Tou<sup>1</sup>, K. Kuroda<sup>1</sup>, K. Morita<sup>1</sup>, H. Kotegawa<sup>1</sup>, H. Sugawara<sup>1</sup>, H. Harima<sup>1</sup>, H. Tanida<sup>2</sup> and M. Sera<sup>3</sup><sup>1</sup>Department of Physics, Kobe University, Kobe 657-8501, Japan<sup>2</sup>Department of Liberal Arts and Sciences, Faculty of Engineering, Toyama Prefectural University, Imizu 939-0398, Japan<sup>3</sup>Department of Physics, Graduate School of AdSM, Hiroshima University, Higashi-Hiroshima 657-8501, Japan

CeCu<sub>6</sub> is a well-known prototypical heavy fermion material showing the Fermi liquid behaviour at low temperatures: The electronic specific heat  $C_e$  is proportional temperature as  $C_e = \gamma T$ ; magnetic susceptibility exhibits temperature independent as  $\chi \propto N^*(E_F)$  [1,2], where  $N^*(E_F)$  is the effective electron density of states at the Fermi level [1,2]; nuclear magnetic relaxation rate  $1/T_1$  obeys the Korringa relation as  $1/T_1 T \propto \text{constant}$ . [3]. Strong electron-electron correlations attributed to Ce-4f<sup>1</sup> electrons are evidenced by the large electronic specific heat coefficient  $\gamma = 1600$  (mJ/K<sup>2</sup>mol) [1]. From the temperature dependence of Cu-NQR relaxation rate  $1/T_1$ , the coherent Kondo temperature  $T_K$  is estimated to be about 6 K [3]. Temperature independent paramagnetic susceptibility and the Korringa relation of the NQR relaxation rate divided by temperature,  $1/(T_1 T K^2) \propto \text{const.}$ , below 1 K are evidence for the disappearance of the local moment due to the coherent Kondo state [3].

In the early stage, high field specific heat and susceptibility measurements at low temperatures reported that the HF ground state of CeCu<sub>6</sub> is completely suppressed by magnetic field of 24 T. These magnetic field dependences were qualitatively explained by the resonant level model (RLM) for single impurity Kondo system [4]. The successful explanation of the magnetic field dependences by such a simple phenomenological model provides evidence that the heavy fermi liquid (HFL) state in CeCu<sub>6</sub> is originated in the magnetic Kondo effect. This behaviour invokes that the HFL state of CeCu<sub>6</sub> is broken with the change of the Fermi surfaces by applying the magnetic field. Thus, the magnetic field is an important tuning parameter. In this context, we expect that the nuclear magnetic resonance (NMR) shift and relaxation rate ( $1/T_1$ ) should be strongly suppressed by magnetic field. Unfortunately, however, temperature dependences of NMR Knight shift and  $1/T_1$  of CeCu<sub>6</sub> have not been put forth yet because of the complexity of the Cu NMR spectrum inherent in the crystal structure [5].

We have succeeded to assign the complex Cu-NMR spectra (See Figure) and we will report temperature dependences of NMR Knight shift and  $1/T_1$  for a single crystal CeCu<sub>6</sub> with the c axis parallel and perpendicular to the magnetic field. Our results clearly show that the quasiparticle susceptibility is quite anisotropic ascribed to the unique crystal electric field ground state in heavy fermion systems.

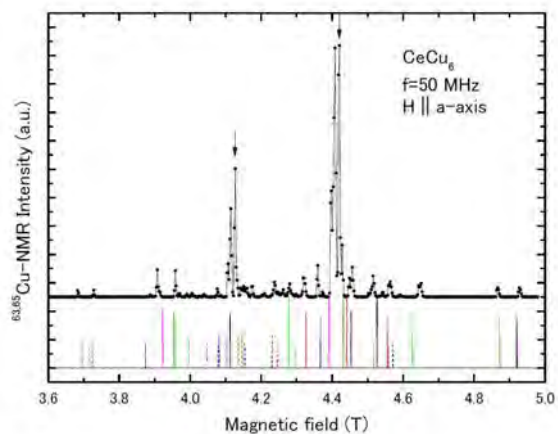


Figure 1 <sup>63,65</sup>Cu-NMR spectra of CeCu<sub>6</sub> measured at T=5K and H||a-axis. Colored lines are results of spectrum simulations

## References

- [1] Y. Onuki et al.: J. Phys. Soc. Jpn. 53, 1210 (1984).
- [2] G. R. Stewart et al.: Phys. Rev. B 30, 482 (1984).
- [3] Y. Kitaoka et al.: J. Phys. Soc. Jpn. 54, 3686 (1985).
- [4] A. S. Edelstein et al.: Physica B 163, 504 (1990).
- [5] M. L. Vrtis et al.: Physica. 136B, 489 (1986).

## P-3

Anomalous Metallic State due to Quadrupolar Fluctuations in PrV<sub>2</sub>Al<sub>20</sub>

Y. Shimura<sup>1</sup>, B. Zeng<sup>2</sup>, R. U. Schoenemann<sup>2</sup>, Q. Zhang<sup>2</sup>, D. Rhodes<sup>2</sup>, M. Tsujimoto<sup>1</sup>, Y. Matsumoto<sup>3</sup>, K. Matsubayashi<sup>4</sup>, Y. Uwatoko<sup>1</sup>, A. Sakai<sup>1</sup>, T. Sakakibara<sup>1</sup>, K. Araki<sup>5</sup>, W. Zheng<sup>2</sup>, Q. Zhou<sup>2</sup>, L. Balicas<sup>2</sup>, and S. Nakatsuji<sup>1</sup>

<sup>1</sup>*Institute for Solid State Physics, The University of Tokyo, Kashiwa, Chiba, Japan*

<sup>2</sup>*National High Magnetic Field Laboratory, Florida State University, Tallahassee, Florida, USA*

<sup>3</sup>*Department of Quantum Materials, Max Planck Institute for Solid State Research, Stuttgart, Germany*

<sup>4</sup>*Graduate School of Information Science and Technology, The University of Electro-Communications, Chohu, Tokyo, Japan*

<sup>5</sup>*Department of Applied Physics, National Defense Academy, Yokosuka, Kanagawa, Japan*

The coupling between the magnetic moments and conduction electrons has been studied for a long time. It provides various amazing phenomena such as Kondo effect, non-trivial superconductivity, and giant magnetoresistance. We have been searching for a new type of the coupling effect between the non-magnetic orbital moments and conduction electrons. The Pr-based compounds PrV<sub>2</sub>Al<sub>20</sub> is one of the best systems for this study. One reason is that the Pr ions show non-magnetic doublet ground state ( $\Gamma_3$  state) carrying only orbital (multipole) moments by the highly-symmetric cubic crystalline-electronic-field [1]. Another reason is that strong hybridization between conduction electrons and localized moments was revealed in the various bulk, transport and microscopic properties. One of the hallmark of such phenomena is the heavy fermion superconductivity observed below 0.05 K [2]. This superconductivity appears in the antiferro-electric-quadrupole (AFQ) phase realized below 0.6 - 0.7 K. Though the AFQ phase is insensitive for the magnetic field below 8 T [1,3], the magnetic phase is strongly anisotropic at higher field region. For [111] directions, the magnetic field of 11 T fully suppresses the AFQ phase, leading to the quadrupolar quantum criticality such as critical enhancement of the residual resistivity  $\rho_0$  and the sublinear temperature dependence of the resistivity [4].

In contrast, for [100] direction, another high-field phase exists above  $B_c \sim 11$ -12 T [5]. Our magnetoresistance measurements in the high DC field up to 31 T revealed emergence of the large anisotropic magnetoresistance ratio of  $\rho_{\perp} - \rho_{\parallel}$  up to 30% in this high field phase. This is due to the formation of the anisotropic band structure induced by the antiferro-quadrupole (orbital) ordering of  $O_2^2$  type quadrupole moments [6].

[1] A. Sakai and S. Nakatsuji: J. Phys. Soc. Jpn. **80**, 063701 (2011).

[2] M. Tsujimoto, Y. Matsumoto, T. Tomita, A. Sakai and S. Nakatsuji: Phys. Rev. Lett. **113**, 267001 (2015).

[3] Y. Matsumoto, M. Tsujimoto and S. Nakatsuji: unpublished

[4] Y. Shimura, M. Tsujimoto, B. Zeng, L. Balicas, A. Sakai, and S. Nakatsuji: Phys. Rev. B **91**, 241102(R) (2015).

[5] Y. Shimura, Y. Ohta T. Sakakibara, A. Sakai and S. Nakatsuji, J. Phys. Soc. Jpn. **82**, (2013) 043705.

[6] Y. Shimura, B. Zeng, R. U. Schoenemann, Q. Zhang, D. Rhodes, M. Tsujimoto, Y. Matsumoto, K. Matsubayashi, Y. Uwatoko, A. Sakai, T. Sakakibara, K. Araki, W. Zheng, Q. Zhou, L. Balicas, and S. Nakatsuji, preprint (2017).

# P-4

## Odd-parity multipole fluctuation in non-symmorphic crystalline

J. Ishizuka<sup>1</sup>, Y. Yanase<sup>1</sup>

<sup>1</sup>*Department of Physics Kyoto University, Kyoto 606-8502, Japan*

The concept of multipole moment has been established to characterize the anisotropy of electronic and magnetic charge distribution. In particular, higher-rank multipole order has been intensively investigated in many *d*- and *f*-orbital systems both theoretically and experimentally, since unconventional superconducting state is expected to be realized induced by higher-rank multipole fluctuation. For instance, the hidden order in a uranium compound URu<sub>2</sub>Si<sub>2</sub> provides one possibility into multipole-fluctuation-induced superconductivity.

The even-parity multipole order commonly appears in *f*-orbital system, and then many theoretical studies have been carried out on the basis of localized picture. These studies provide profound understanding of the even-parity multipole order. On the other hand, in locally non-centrosymmetric systems, in which local site lacks inversion symmetry, the odd-parity electromagnetic multipole order is found to be realized [1], followed by the global inversion symmetry breaking. Thus, the odd-parity multipole order drives intriguing nature, such as magnetoelectronic effect [2]. However, the superconductivity induced by the *odd-parity multipole fluctuation* has not been explicitly investigated so far. Since the odd-parity multipole fluctuation is induced by anti-symmetric spin-orbit coupling, pairing interactions derived from this fluctuation may be dissimilar to the even-parity one, resulting in a different type of superconductivity.

We investigate fundamental properties of the odd-parity fluctuation. The target material is 5*d* transition metal compound Sr<sub>2</sub>IrO<sub>4</sub>. This material shows antiferromagnetic Mott insulating state at half filling in *j*=1/2 doublet, similarity to copper oxides, and therefore, is believed to emerge superconductivity by electron doping. Moreover, several experiments have proposed several types of antiferromagnetic alignment, one of which belongs to the same symmetry of an odd-parity magnetic quadrupole moment [3]. We study the electronic structure, antiferromagnetic and quadrupole fluctuations, and superconductivity of Sr<sub>2</sub>IrO<sub>4</sub> from a microscopic model with anti-symmetric spin-orbit coupling and electronic correlation. We also calculate these properties from first-principles calculation.

[1] S. Sumita, et al., arXiv: 1702.08659 (2017).

[2] Y. Yanase, J. Phys. Soc. Jpn. 83, 014703 (2014).

[3] L. Zhao, et al., Nat. Phys. 12, 32 (2016).

## P-5

NMR/NQR study on heavy-fermion superconductor CeCu<sub>2</sub>Si<sub>2</sub>S. Kitagawa<sup>1</sup>, T. Higuchi<sup>1</sup>, M. Manago<sup>1</sup>, T. Yamanaka<sup>1</sup>, K. Ishida<sup>1</sup>, H. S. Jeevan<sup>2</sup>, C. Geibel<sup>2</sup>, F. Steglich<sup>2</sup><sup>1</sup>Department of Physics, Kyoto University, Kyoto 606-8502, Japan<sup>2</sup>Max-Planck Institute for Chemical Physics of Solids, D-01187 Dresden, Germany

The first heavy-fermion superconductor CeCu<sub>2</sub>Si<sub>2</sub> discovered in 1979[1] was considered to be a nodal unconventional superconductor, since the SC phase is located in the verge of the AFM phase, and the  $T^5$  dependence of the nuclear spin-lattice relaxation rate  $1/T_1$  together with the absence of a coherence peak[2] and  $T^2$ -like temperature dependence of the specific heat in the SC state[3] indicate a line nodal SC gap in CeCu<sub>2</sub>Si<sub>2</sub>. In addition, a clear spin excitation gap was observed in the SC state with the inelastic neutron scattering[4], suggesting the existence of AFM fluctuations as the main origin for SC pairing in CeCu<sub>2</sub>Si<sub>2</sub>. These results were considered as an evidence of a  $d$ -wave gap symmetry with line nodes in CeCu<sub>2</sub>Si<sub>2</sub>, such as  $d_{x^2-y^2}$  or  $d$  type.

However, the recent specific-heat measurements on an  $a$ -type CeCu<sub>2</sub>Si<sub>2</sub> single crystal down to 40 mK strongly suggest that CeCu<sub>2</sub>Si<sub>2</sub> possesses a full gap with a multi-band character[5]. In addition, a small  $H$ -linear coefficient of the specific heat at low temperatures and its isotropic  $H$ -angle dependence under a rotating magnetic field within the  $a$  plane are in sharp contrast to the expected behaviours in the nodal  $d$ -wave superconductivity.

We have performed <sup>63</sup>Cu-nuclear magnetic resonance (NMR)/nuclear quadrupole resonance (NQR) measurements in order to investigate the magnetic and SC properties on a "superconductivity dominant ( $a$ -type)" single-crystal CeCu<sub>2</sub>Si<sub>2</sub>.  $1/T_1$  at zero field is almost identical to that in the previous polycrystalline samples down to 130 mK and slightly deviates downward from that below 120 mK.  $1/T_1$  in the SC state can be fit with the two-gap  $s_{\pm}$ -wave rather than the two-gap  $s_{++}$ -wave model down to 90 mK as shown in Fig.. Under magnetic fields, the spin susceptibility in both directions clearly decreases below  $T_c$ , indicative of the formation of the spin singlet pairing. The residual part of spin susceptibility is well understood by the field induced residual density of states evaluated from  $1/T_1 T$ , which is ascribed to the effect of the vortex cores. In addition, the enhancement of  $1/T_1 T$  just below  $T_c$  is observed near upper critical field  $H_{c2}$ , suggesting the realization of FFLO state. No magnetic anomaly but the development of the AFM fluctuations were observed above  $H_{c2}$ , indicating that the superconductivity is realized in the strong AFM fluctuations.

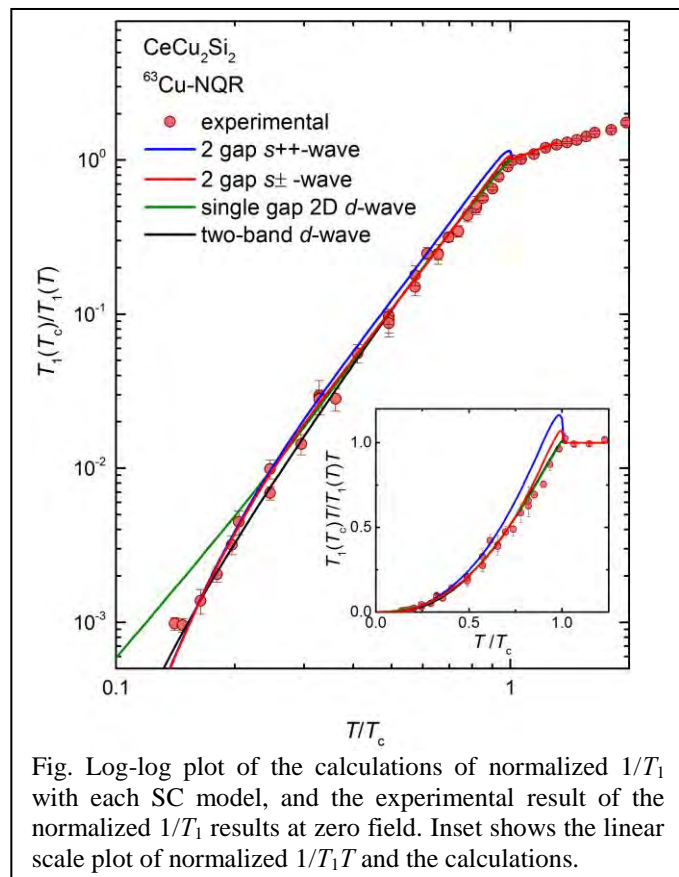


Fig. Log-log plot of the calculations of normalized  $1/T_1$  with each SC model, and the experimental result of the normalized  $1/T_1$  results at zero field. Inset shows the linear scale plot of normalized  $1/T_1 T$  and the calculations.

This work was partially supported by Kyoto Univ. LTM center, and Grant-in-Aids for Scientific Research (KAKENHI) (Grant Numbers JP15H05882, JP15H05884, JP15K21732, JP25220710, and JP15H05745).

- [1] F. Steglich et al., Phys. Rev. Lett. **3**, 1892 (1979).
- [2] K. Ishida et al., Phys. Rev. Lett. **82**, 5353 (1999).
- [3] J. Arndt et al., Phys. Rev. Lett. **106**, 246401 (2011).
- [4] O. Stockert et al., Nature Physics, **7**, 1119 (2011).
- [5] S. Kittaka et al., Phys. Rev. Lett. **112**, 067002 (2014).

## P-6

Magnetic Hexadecapole Order in BaMn<sub>2</sub>As<sub>2</sub>

Hikaru Watanabe and Youichi Yanase

Department of Physics, Graduate School of Science, Kyoto University, Kyoto 606-8502

In these decades, there are a lot investigations of multipole order in condensed matter, especially d or f electron systems [1]. The multipole order is derived from the entanglement between spin/ orbital angular momentum of localized electrons, and essentially characterized by the even-parity under the space-inversion operation. In contrast, *odd-parity multipole order* in noncentrosymmetric systems are recently reported [2]. In this exotic ordered state, various emergent phenomena such as FFLO superconductivity, magnetoelectric effect arise from the entanglement between spin, orbital, and sublattice.

The compound we focus on is BaMn<sub>2</sub>As<sub>2</sub>, a related material of the Iron-based 122 family. The Iron-based 122 family such as BaFe<sub>2</sub>As<sub>2</sub> shows a lot exotic phase such as high-T<sub>c</sub> superconductor and electronic nematic order. On the other hand, BaMn<sub>2</sub>As<sub>2</sub> shows the G-type antiferromagnetic order and semiconducting behavior below 625 K [3], and therefore this compound has been regarded as a conventional Mott-insulating system and no other exotic phases like other 122 family has not been identified.

The seemingly conventional G-type AFM transition, however, causes not only time-reversal symmetry breaking but also space-inversion symmetry breaking. Thus, odd-parity magnetic multipole ordering is implied. Moreover, this compound is driven to metallic phase by hole-doping without the AFM order quenching [4]. The itinerant electron system with odd-parity multipole order may be realized.

In this work, we identify that the *magnetic hexadecapole ordering* is realized in BaMn<sub>2</sub>As<sub>2</sub>. This conclusion is supported by group-theoretical approach based on Landau's theory of phase transitions and also by examining the electronic state in microscopic models. Furthermore, we propose the effective single d-orbital Hamiltonian in the AFM state, which is the dominant component in the valence band [5]. We discuss the electromagnetic responses in the magnetic hexadecapole state such as magnetoelectric effect, which is discussed in the field of multiferroic systems, , and interestingly *antiferromagnetic Edelstein effect* [2] and *current-induced nematicity*, which is an exotic phenomena characterizing odd-parity magnetic multipole ordering in the itinerant system, hole-doped BaMn<sub>2</sub>As<sub>2</sub>. [6]

[1] H. Kusunose, J. Phys. Soc. Japan **77**, 064710 (2008).

[2] Y. Yanase, J. Phys. Soc. Japan **83**, 14703 (2014).; S. Hayami, H. Kusunose, and Y. Motome, Phys. Rev. B **90**, 24432 (2014); S. Sumita and Y. Yanase, Phys. Rev. B **93**, 224507 (2016); T. Hitomi and Y. Yanase, J. Phys. Soc. Japan **85**, 124702 (2016).

[3] Y. Singh, M.A. Green, Q. Huang, A.Kreyssig, R. J. McQueeney, D. C. Johnston, and A. I. Goldman, Phys. Rev. B **80**, 100403 (2009); Y. Singh, A. Ellern, and D. C. Johnston, Phys. Rev. B **79**, 094519 (2009).

[4] A. Pandey, R. S. Dhaka, J. Lamsal, Y. Lee, V. K. Anand, A. Kreyssig, T. W. Heitmann, R. J. McQueeney, A. I. Goldman, B. N. Harmon, A. Kaminski, and D. C. Johnston, Phys. Rev. Lett. **108**, 087005 (2012).

[5] W.-L. Zhang, P. Richard, A. van Roekeghem, S.-M. Nie, N. Xu, P. Zhang, H. Miao, S.-F. Wu, J.-X. Yin, B. B. Fu, L.-Y. Kong, T. Qian, Z.-J. Wang, Z. Fang, A. S. Sefat, S. Biermann, and H. Ding, Phys. Rev. B **94**, 155155 (2016).

[6] H. Watanabe and Y. Yanase, arXiv:1705.10349. (submitted)

## P-7

## A theory of valence fluctuation and field-insensitive heavy fermion in Sm compounds

Ryousuke Shiina

Department of Physics, University of Ryukyus, Okinawa 903-0213, Japan

It has long been known that Sm compounds display a number of mysterious properties, such as a small-moment ferromagnetism, strong valence fluctuations, and exotic Kondo-insulator behaviors. In this presentation, we will discuss the origin of a new low-temperature phenomenon of Sm compounds, namely field-insensitive heavy-fermion (HF) states, which have been discovered in recent experimental studies.

It was reported first for the skutterudite  $\text{SmOs}_4\text{Sb}_{12}$  [1] that the Sommerfeld coefficient of electronic specific heat  $\gamma$  and the  $T^2$  coefficient of electrical resistivity  $A$  show the HF behavior with a very large effective mass. A remarkable feature is an insensitivity of the HF state to the external magnetic field; the  $\gamma$  and  $A$  values were found to be almost unchanged up to 15T of the field strength. This is apparently inconsistent with a common knowledge on the Kondo effect that the field easily suppresses such a large effective mass associated with a small Kondo temperature.

Recently, similar phenomena have been discovered for  $\text{SmTa}_2\text{Al}_{20}$  and  $\text{SmTi}_2\text{Al}_{20}$  in the so-called 1-2-20 compounds [2,3]. Both these compounds exhibit cusp singularities in specific heat below 10K, which are probably attributed to antiferromagnetic phase transitions, and the  $\gamma$  values of specific heat are significantly enhanced above the transition temperatures. In particular, it was unveiled that these features of specific heat are not influenced by the magnetic field at least up to 8T. Thus, one can naturally consider that the unusual HF behaviors found in the Sm skutterudite and 1-2-20 compounds have a common microscopic origin.

In order to understand the origin of those exotic HF states, an importance of valence fluctuation in Sm ions has recently been pointed out through an analysis of the X-ray scattering spectrum [4,5]. It was shown by analyzing a cluster model that the spectrum involves a significant contribution of the  $f^6$  valence state with  $J=0$ , which might be responsible for the insensitivity to the field. Thus, it is obviously important at this stage to clarify the nature of valence fluctuation from the  $f^6$  configuration and the possible difference of the resulting HF state from that in the conventional  $f^0$ - $f^1$  fluctuation in Ce ions.

As a first step to explore this problem, we consider in this study a two-orbital impurity Anderson model with an effective  $f^2$ - $f^1$  valence fluctuation in  $\Gamma_8$  orbitals of Sm ions; it is mapped from the realistic model with a strong crystal field (CF) potential, where the CF-split 4f states in different  $J$  multiplets are mixed. This model exhibits a quantum critical point (QCP) between the local-singlet and the Kondo-singlet states in the variation of the c-f hybridization [6]. On the basis of a previous study of the phase diagram, we study here the Fermi-liquid properties around the QCP by using the numerical renormalization-group (NRG) method.

It is shown in the model that the  $\gamma$  value of specific heat is definitely enhanced around the QCP. It is particularly remarkable that the enhancement of  $\gamma$  is associated with a significant suppression of the Wilson ratio, thus realizing a field-insensitive HF state. It is also shown that the parameter region in which the HF state appears is of intermediate valence and is enlarged as the local excitation energy in the effective  $f^2$  configuration is increased. The microscopic nature of the HF state is discussed by analyzing the flow diagram of the NRG method. The relevance of these results to the experimental results is also discussed.

- [1] S. Sanada et al., J. Phys. Soc. Jpn. **74**, 246 (2005).
- [2] R. Higashinaka et al., J. Phys. Soc. Jpn. **80**, 093703 (2011).
- [3] A. Yamada et al., J. Phys. Soc. Jpn. **82**, 123710 (2013)
- [4] S. Tsutsui et al., J. Phys. Soc. Jpn. **82**, 023707 (2013).
- [5] Y. Nanba et al., J. Phys. Soc. Jpn. **82**, 104712 (2013).
- [6] R. Shiina et al. J. Phys. Soc. Jpn. **86**, 034705 (2017).

## High Magnetic Field Neutron Diffraction and Transport Studies on U-compounds

M. Kimata<sup>1</sup>, H. Nojiri<sup>1</sup>, T. Kihara<sup>1</sup>, D. Aoki<sup>1</sup>, K. Kuwahara<sup>2</sup>,  
W. Knafo<sup>3</sup>, F. Duc<sup>3</sup>, F. Bourdarot<sup>4</sup>, L.-P. Regnault<sup>5</sup>

<sup>1</sup>IMR, Tohoku University, Sendai, 980-8577, Japan

<sup>2</sup>Institute of Quantum Beam Science, Ibaraki University, Mito 310-8512, Japan

<sup>3</sup>LNCMI, 143 Avenue de Rangueil, 31400 Toulouse, France

<sup>4</sup>Commissariat al Energie Atomique, 38054 Grenoble, France

<sup>5</sup>Institut Laue-Langevin, 38042 Grenoble, France

A high magnetic field is one of the most unique and powerful parameter to tune the states of magnetic compounds. In frustrated anti-ferromagnets, a variety of non-trivial magnetic structures tend to show up by the tuning of systems by strong magnetic fields. In strongly correlated systems, the duality of the localized and itinerant natures of electrons produces incommensurate and spin density wave orders with Fermi surface reconstructions. It is essential to combine neutron diffraction techniques with pulsed magnetic fields to explore these interesting phenomena and novel phases.

In the first part of this work, we report the overview of the recent activities examining magnetic phase diagrams of URu<sub>2</sub>Si<sub>2</sub> and related compounds. In pure and Rh doped URu<sub>2</sub>Si<sub>2</sub>, successive magnetic field induced phase transitions from the hidden order phase were observed in magnetization and transport experiments. Because these phases appear in very high magnetic fields, there had been no neutron diffraction experiments on these high field phases. We have developed a pulsed neutron diffraction system by using the compact pulsed magnet techniques. Experiments can be performed in both reactor and spallation sources.

For Rh 4 % system, we found that the high field phase is the commensurate magnetic order with the wave vector of (2/3, 0, 0). When Rh is reduced to 2 %, this commensurate order disappears. Finally, for pure URu<sub>2</sub>Si<sub>2</sub>, the spin density wave like magnetic order with the wave vector of (0.6, 0, 0) is found. It should be noted that the (0.6, 0, 0) is the incommensurate modulation.

	Rh 0%	Rh 2%	Rh 4%
Wave vector	(0.6, 0, 0)	×(2/3, 0, 0)	(2/3, 0, 0)
Normalized Magnetization	0.35(Phase II) 0.61(Phase III)	0.33(Phase II) 0.61(Phase III)	0.33(Phase II)
Ferromagnetic components	No	—	Yes

Table 1 Summary of magnetic wave vectors and the normalized magnetizations

The change of the magnetization processes with Rh-doping shows the close relation with the variation of the magnetic structures. For example, in 4 % Rh sample, the magnetization is 1/3 of the saturation for the phase II with (2/3, 0, 0) wave vector. While the magnetization is 0.35 and 0.61 for pure sample. The magnetic wave vectors and the normalized magnetization by the saturation magnetization is summarized in table 1. This result shows that the magnetic wave vector is sensitive to Rh doping. It indicates that the magnetic wave vector is closely related to the Fermi surface and its nesting. In this context, it is important to investigate if the magnetic wave vector is single or multiple. Such information needs the use of a spallation neutron source and the experiment on the pure sample is running during this conference by some of the coauthors.

In the second part, we will report recent progress of transport experiment in static high magnetic fields. Here, we are focused on the large negative magnetoresistance (MR) observed in  $\beta$ -US<sub>2</sub> as another example of exotic high magnetic field phase of U compounds. At zero magnetic field, the resistivity of this material shows semiconducting behavior with an energy gap of ~90 K, but this semiconducting behavior is strongly suppressed when the magnetic field is applied parallel to the [001]. The resultant MR change reaches to several orders of magnitude and is comparable to that of colossal MR effect in Mn oxides. However, the origin of this MR is totally different from that in Mn oxides because the ferromagnetic correlation develops at low temperatures, whereas the antiferromagnetic correlation is observed in Mn oxides. In the Mn oxides, the suppression of antiferromagnetic correlation by magnetic field is essential for the MR effect. To reveal the underlying physics of this exciting phenomenon in  $\beta$ -US<sub>2</sub>, detailed angular dependent experiment in high magnetic field is necessary because this MR effect is only observed for B||[001]. For this purpose, we have developed double axes rotational transport probe for small solenoid bore. The maximum available magnetic field is 24 T with the lowest temperature of 0.5 K. The performance of this new equipment and experimental test data will be presented.

[1] K. Kuwahara *et al.*, Phys. Rev. Lett. **110** (2013) 216406.

[2] W. Kanfo *et al.*, Nature Commun. **7** (2016) 13075.

# P-9

## Role of the spin-orbit coupling in the Kugel-Khomskii model on the honeycomb lattice

A. Koga, S. Nakauchi, and J. Nasu  
Tokyo Institute of Technology, Tokyo 152-8551, Japan

Strongly correlated electron systems with orbital degrees of freedom have attracted much interest. One of the intriguing examples is the series of the honeycomb-layered compounds,  $A_2\text{IrO}_3$  ( $A=\text{Li, Na}$ ) with 5d electrons [1] and  $\alpha\text{-RuCl}_3$  with 4d electrons [2]. In these compounds, a strong spin-orbit interaction should cause the anisotropy in the exchange coupling between spins. Then, the compounds are regarded as the candidates for realizing the Kitaev model [3]. Recently, fermionic response has been discussed in  $\alpha\text{-RuCl}_3$  at finite temperatures [4], which stimulates further theoretical and experimental investigations on the Kitaev and related models [5]. A simple question that naturally arises is whether or not the finite spin-orbit interaction yields interesting ground-state and low temperature properties characteristic of the Kitaev model.

To clarify this, we consider the spin-orbital model with the Kugel-Khomskii type superexchange interaction on the honeycomb lattice. This model should be derived from the multi-orbital Hubbard model with  $t_{2g}$  orbitals in the strong coupling limit. Using the cluster mean-field approximations [6], we treat the superexchange interaction and spin-orbit coupling on equal footing. Then, we clarify how some magnetically ordered states compete with each other. Furthermore, we discuss the stability of the spin liquid state realized in a strong spin-orbit coupling limit (Kitaev limit).

[1] Y. Singh and P. Gegenwart, Phys. Rev. B 82, 064412 (2010) ; Y. Singh, et al, Phys. Rev. Lett. 108, 127203 (2012) ; R. Comin, et al., Phys. Rev. Lett. 109, 266406 (2012).

[2] Y. Kubota, et al., Phys. Rev. B 91, 094422 (2015).

[3] A. Kitaev, Ann. Phys. 321, 2 (2006).

[4] J. Nasu, et al, Nat. Phys. 12, 912 (2016).

[5] G. Jackeli and G. Khaliullin, Phys. Rev. Lett. 102, 017205 (2009) ; J. Nasu et al, Phys. Rev. Lett. 113, 197205 (2014), Y. Yamaji et al., Phys. Rev. Lett. 113, 107201 (2014).

[6] T. Oguchi, Prog. Theor. Phys. 13, 148 (1955).

# P-10

## The observation of the field induced transition in PrTi<sub>2</sub>Al<sub>20</sub>

T. Taniguchi, H. Takeda, M. Takigawa, S. Nakamura, T. Sakakibara, M. Tsujimoto, A. Sakai and S. Nakatani  
 Institute for Solid State Physics, University of Tokyo, Kashiwa 277-8581, Japan

The cubic compound PrTi<sub>2</sub>Al<sub>20</sub> shows a phase transition near 2 K [1-3] associated with the quadrupole moments of Pr ions, for which the ground state of crystal field is non-magnetic but has non-zero matrix elements for two types of quadrupoles,  $T_{20} = (3z^2 - J^2)/2$  and  $T_{22} = \sqrt{3}(x^2 - y^2)/2$ , and one octupole  $T_{xyz} = (\sqrt{15}/6) \overline{xyz}$  [4], where the bar represents the sum over possible permutation of the indices x, y, and z [5]. A phase transition was detected by a peak in the specific heat near 2 K. A clear anomaly in ultrasonic measurement combined with the absence of an anomaly in the magnetic susceptibility indicates that this is a quadrupole transition.

In this presentation, we will discuss the *H-T* phase diagrams from <sup>27</sup>Al-NMR and magnetization measurements in a single crystal of PrTi<sub>2</sub>Al<sub>20</sub>. Figures 1, 2 show the phase diagrams associated with the quadrupole moments in the magnetic field applied along <111> and <100> directions. When a magnetic field is applied along the <111> direction above 0.5 T, certain lines of the NMR spectrum split upon entering into the ordered phase, indicating breaking of the  $O_h$  symmetry due to field induced magnetic dipole moment perpendicular to the field. This provides the first evidence for symmetry-breaking ferro-quadrupole order of  $O_{20}$  type [3]. When a magnetic field is applied along <100> direction above 3 T, the Knight shifts of all 96g Al sites increase near the transition temperature. On the other hand, the Knight shifts decrease at 1 T. This clear anomaly combined with an anomaly of the field dependence of magnetization near 2 T below 2 K indicates that this is the field induced transition associated with the quadrupole moment. To determine the symmetry of the low-field phase, we have measured the nuclear magnetic relaxation rate ( $1/T_1$ ) at all 96g Al sites in various temperature and magnetic field.

This work was supported by the Japan Society for the Promotion of Science through Grants-in-Aid for Scientific Research (KAKENHI Grant Numbers 25287083, 15H05882, and 15H05883) and the Program for Advancing Strategic International Networks to Accelerate the Circulation of Talented Researchers (No. R2604). T.T. was supported by JSPS through the Program for Leading Graduate Schools (MERIT).

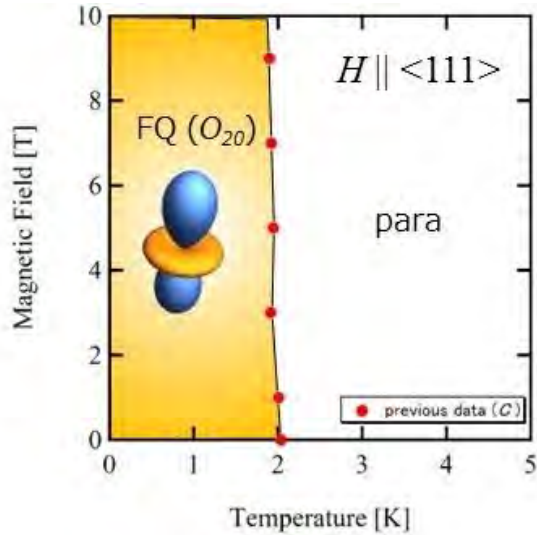


Fig. 1. the phase diagram in the magnetic field applied along <111> direction

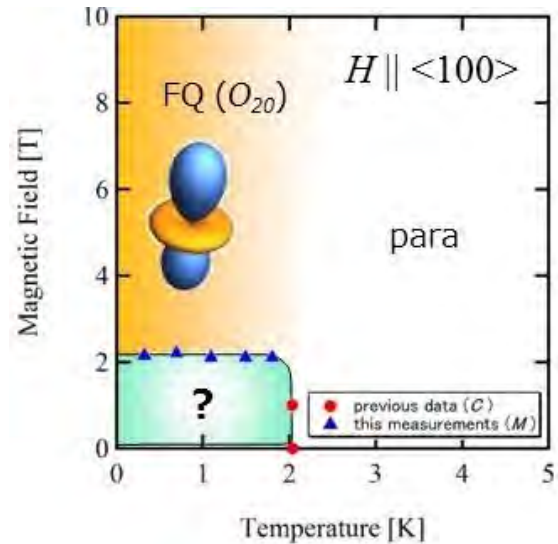


Fig. 2. the phase diagram in the magnetic field applied along <100> direction

- [1] A. Sakai, *et al.*, *J. Phys. Chem. C*, **80**, 063701 (2011).
- [2] M. Koseki, *et al.*, *J. Phys. Chem. C*, **80**, SA049 (2011).
- [3] T. Taniguchi, *et al.*, *J. Phys. Chem. C*, **85**, 113703 (2016).
- [4] T. J. Sato, *et al.*, *J. Phys. Chem. C*, **86**, 184419 (2012).
- [5] R. Shiina, *et al.*, *J. Phys. Chem. C*, **66**, 1741 (1997).

## P-11

Pressure effect on the antiferroquadrupolar and superconducting transitions in PrIr<sub>2</sub>Zn<sub>20</sub>K. Umeo<sup>1</sup>, M. Adachi<sup>2</sup>, K. T. Matsumoto<sup>3</sup>, T. Onimaru<sup>2</sup>, T. Takabatake<sup>2</sup><sup>1</sup>N-BARD, Hiroshima Univ., Higashi-Hiroshima 739-8526, Japan<sup>2</sup>AdSM, Hiroshima Univ., Higashi-Hiroshima 739-8530, Japan<sup>3</sup>Graduate School of Science and Engineering, Ehime University, Matsuyama, 790-8577, Japan

The cubic compound PrIr<sub>2</sub>Zn<sub>20</sub> consists of polyhedral cages formed by 16 zinc atoms in which the Pr<sup>3+</sup> ion is encapsulated. Under the crystalline electric field, the 4<sup>2</sup> state of the Pr<sup>3+</sup> ion falls into a ground state of nonmagnetic  $\Gamma_3$  doublet at temperatures below 30 K [1]. In this compound, an antiferroquadrupolar (AFQ) order occurs at  $T_Q = 0.11$  K and a superconducting (SC) transition sets in at  $T_c = 0.05$  K [1]. The entropy release up to  $T_Q$  is 20% of  $R\ln 2$ , which is expected for the  $\Gamma_3$  doublet with the quadrupolar degrees of freedom. This fact hints to the interplay between the AFQ and SC orders.

In order to reveal the possible interplay we have measured the electrical resistivity  $\rho$  for single crystalline samples under pressures up to 10 GPa and at temperatures down to 0.04 K. As shown in Fig. 1,  $\rho(T)$  for  $P > 1$  GPa bends at  $T^\dagger$  above the sharp drop at  $T_Q$  due to the AFQ order. With increasing pressure, two anomalies shift to higher temperatures. The pressure dependences of  $T^\dagger$ ,  $T_Q$ , and  $T_c$  plotted in Fig. 2 show that  $T_Q$  rises from 0.11 K for  $P = 0$  to 0.23 K for  $P = 10.6$  GPa, while  $T_c$  hardly changes at 0.07 K. These contrasting changes indicate a weak interplay between SC and AFQ orders for this compound, in contrast to the strong interplay suggested for PrTi<sub>2</sub>Al<sub>20</sub> [2].

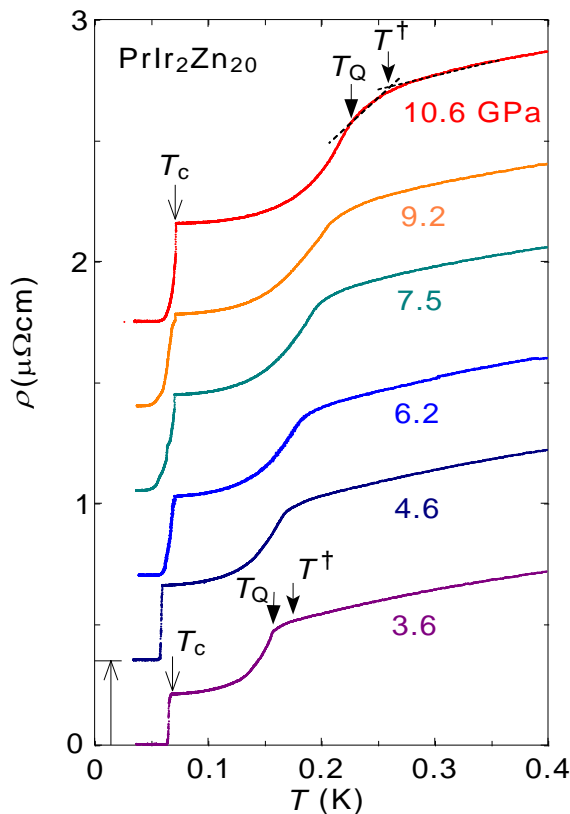
[1] T. Onimaru *et al*, Phys. Rev. Lett., **106**, 177001 (2011).[2] K. Matsubayashi *et al*, Phys. Rev. Lett., **109**, 187004 (2012).

Fig. 1 Temperature dependence of the electrical resistivity of PrIr<sub>2</sub>Zn<sub>20</sub> under various pressures.

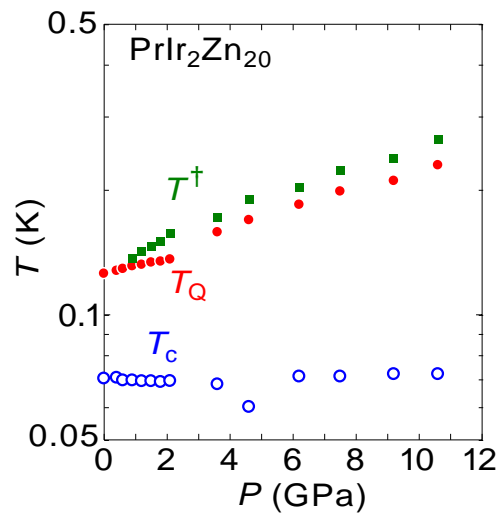


Fig. 2 Pressure dependence of  $T^\dagger$ ,  $T_Q$ , and  $T_c$ .

Strong uniaxial spin anisotropy in the Hidden order state of URu<sub>2</sub>Si<sub>2</sub>T. Hattori, H. Sakai, Y. Tokunaga, S. Kambe, T. D. Matsuda<sup>Å</sup>, and Y. Haga

Advanced Science Research Center, Japan Atomic Energy Agency, Ibaraki 319-1195, Japan

In heavy-fermion compound URu<sub>2</sub>Si<sub>2</sub>, unconventional superconductivity appears in the so-called ‘hidden order’ (HO) state with a superconducting (SC) transition temperature of  $T_{SC} \sim 1.4$  K [1]. In the HO state, long-range electronic order is well established below  $T_{HO} \sim 18$  K, but the order parameter has so far been undetectable, and hence has not yet been identified. It is an intriguing subject to clarify the mechanism of superconductivity in the HO state and the relation between both orders.

As for the SC gap symmetry in URu<sub>2</sub>Si<sub>2</sub>, the angular dependence of thermal conductivity [2, 3] and specific heat measurements [4, 5] revealed the existence of two point nodes and a horizontal line node. For the spin part, the suppression of  $H_{c2}$  in any field direction at lower temperatures [2, 6, 7] suggests the existence of Pauli paramagnetic effects characteristic for a spin-singlet pairing state. However, any change in NMR Knight shift below  $T_{SC}$ , which could be a direct evaluation of spin susceptibility, has not been detected [8].

By using the high-quality single crystalline URu<sub>2</sub>Si<sub>2</sub>, we have successfully carried out <sup>29</sup>Si NMR experiments on the SC state with highest resolution so far. However, with the external magnetic field along the magnetic hard axis of  $a$  axis, still no observable change in Knight shift was detected [9]. Recently we have succeeded to measure the temperature dependence of Knight shift under magnetic field applied along the crystalline  $c$  axis, corresponding to the magnetic easy axis. We will discuss the spin state of the SC URu<sub>2</sub>Si<sub>2</sub>.

This work was partially supported by a Grant-in-Aid for Scientific Research from the Japan Society for the Promotion of Science (JSPS), KAKENHI Grant Numbers 15K05152, 16K17757, 15KK0174, 15H05745, and 15H05884 (J-Physics).

<sup>Å</sup>Present address: Department of Physics, Tokyo Metropolitan University, Hachioji, Tokyo 192-0397, Japan

[1] See, for example, J. A. Mydosh and P. M. Oppeneer, *Rev. Mod. Phys.* **83**, 1301 (2011).

[2] Y. Kasahara *et al.*, *Phys. Rev. Lett.* **99**, 116402 (2007),

[3] Y. Kasahara *et al.*, *New J. Phys.* **11**, 055061 (2009).

[4] K. Yano *et al.*, *Phys. Rev. Lett.* **100**, 017004 (2008)

[5] S. Kittaka *et al.*, *J. Phys. Soc. Jpn.* **85**, 033704 (2016).

[6] J. Brison *et al.*, *Physica C* **250**, 128 (1995).

[7] R. Okazaki *et al.*, *Phys. Rev. Lett.* **100**, 037004 (2008).

[8] Y. Kohori, K. Matsuda and T. Kohara, *J. Phys. Soc. Jpn.* **65**, 1083 (1996)

[9] T. Hattori *et al.*, *J. Phys. Soc. Jpn.* **85**, 073711 (2016).

## Si-substitution effects on the physical properties and the magnetic anisotropy of a ferromagnetic Kondo-lattice compound $\text{CeRh}_6\text{Ge}_4$

E. Matsuoka<sup>1</sup>, C. Hondo<sup>1</sup>, T. Fujii<sup>1</sup>, Y. Iwakiri<sup>1</sup>, N. Chikuchi<sup>1</sup>, H. Sugawara<sup>1</sup>, T. Sakurai<sup>2</sup>, and H. Ohta<sup>3</sup>

<sup>1</sup>Department of Physics, Graduate School of Science, Kobe University, Kobe 657-8501, Japan

<sup>2</sup>Research Facility Center for Science and Technology, Kobe University, Kobe 657-8501, Japan

<sup>3</sup>Molecular Photoscience Research Center, Kobe University, Kobe 657-8501, Japan

$\text{CeRh}_6\text{Ge}_4$  crystallizes in the hexagonal  $\text{LiCo}_6\text{P}_4$  type structure with the non-centrosymmetric space group  $P\bar{6}m2$  [1]. Our magnetic and transport properties measurements using polycrystalline samples revealed that  $\text{CeRh}_6\text{Ge}_4$  has the trivalent Ce ions at high temperatures and exhibits a FM order at  $T_C = 2.5$  K, which is the lowest Curie temperature for Ce compounds found to date [2]. The low  $T_C$ , the small magnetic entropy released at  $T_C$  ( $0.19R\ln 2$ ), and the large electronic specific heat coefficient ( $0.25 \text{ J}\cdot\text{mol}^{-1}\cdot\text{K}^{-2}$ ) are presumably due to the proximity of a quantum critical point [2]. On the other hand, the isomorphous compound  $\text{CeRh}_6\text{Si}_4$  is a nonmagnetic compound with the Ce ions being in an intermediate-valence state [2]. In this study, we report on the magnetic and transport properties of the polycrystalline samples of Si-substituted compound  $\text{CeRh}_6(\text{Ge}_{1-x}\text{Si}_x)_4$ . In addition, the results of magnetic susceptibility and electrical resistivity measurements of single-crystalline samples of  $\text{CeRh}_6\text{Ge}_4$  are reported.

The unit cell volume  $V$  of  $\text{CeRh}_6(\text{Ge}_{1-x}\text{Si}_x)_4$  deduced by the X-ray powder diffraction experiments does not obey a simple Vegard's law. For two ranges of  $0 \leq x \leq 0.125$  and  $0.125 \leq x \leq 1$ ,  $V$  shows a linear decrease with increasing  $x$  but the slope of the former range is steeper than that of the latter one. Considering the fact that  $\text{CeRh}_6\text{Si}_4$  ( $x = 1$ ) is an intermediate-valence compound, the change in the slope would be ascribable to the valence instability of the Ce ions for compounds with  $x \geq 0.125$ .

The magnetic susceptibility and the electrical resistivity measurements of  $\text{CeRh}_6(\text{Ge}_{1-x}\text{Si}_x)_4$  revealed that  $T_C$  decreases rapidly with increasing  $x$ . As shown in the Fig. 1, a FM critical point where  $T_C$  reaches to 0 K exists at approximately  $x_C = 0.12$ . The  $x_C$  is very close to the  $x$  where the decreasing rate of  $V$  changes. The  $A$  value (a coefficient of quadratic temperature term in the resistivity) shows a maximum around  $x_C$  as shown in the Fig 1. This fact implies that the magnetic fluctuation develops near  $x_C$ . In such situation, one can expect the occurrence of superconductivity for compounds with the vicinity of  $x_C$ , but no superconductivity was observed down to 0.4 K.

Voßwinkel *et al.* have grown single-crystalline samples of  $\text{CeRh}_6\text{Ge}_4$  by a flux method using Bi as a flux [1]. We have referred to their method and obtained needle-like single crystals. A typical length and a diameter of the crystals were 1 mm and 0.075 mm, respectively. Fig. 2 shows the magnetic susceptibilities of  $\text{CeRh}_6\text{Ge}_4$  measured by applying magnetic field parallel ( $H \parallel c$ ) and perpendicular ( $H \perp c$ ) to the  $c$  axis. These susceptibilities show an upturn at 2.5 K which corresponds to the FM transition. The perpendicular susceptibility is about 100 times larger than the parallel one at 1.8 K, implying that the magnetic moments of Ce lie on the  $c$  plane.

[1] D. Voßwinkel, O. Niehaus, Ute Ch. Rodewald, and R. Pöttgen, *Z. Naturforsch.* **67b**, 1241 (2012).

[2] E. Matsuoka, C. Hondo, T. Fujii, A. Oshima, H. Sugawara, T. Sakurai, H. Ohta, F. Kneidinger, L. Salamakha, H. Michor, and E. Bauer, *J. Phys. Soc. Jpn.* **84**, 073704 (2015).

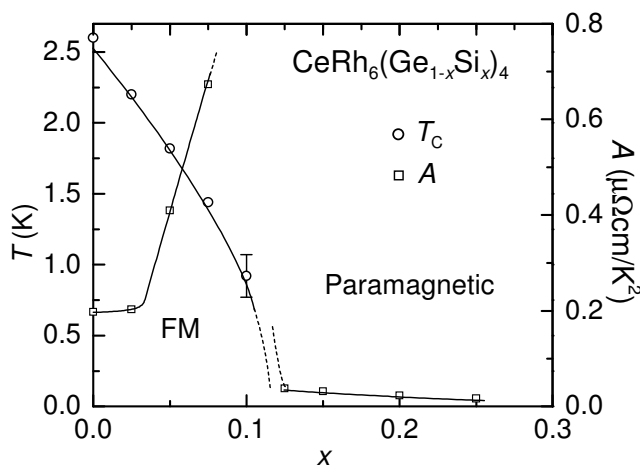


Fig. 1

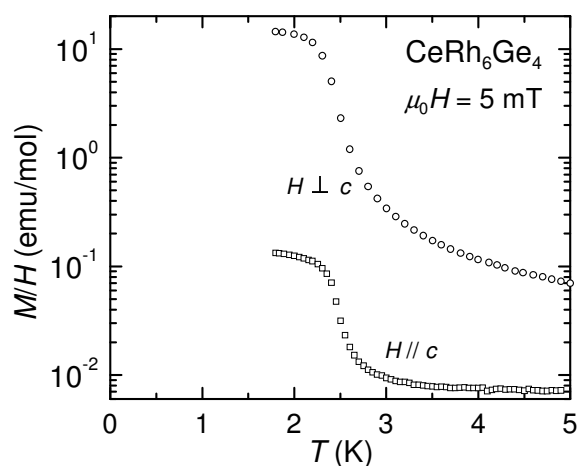


Fig. 2

Investigation of  $\text{UBe}_{13}$  Probed by  $^9\text{Be}$ -NMR

Haruki MATSUNO<sup>1</sup>, Kyohei MORITA<sup>1</sup>, Hisashi KOTEGAWA<sup>1</sup>, Hideki TOU<sup>1</sup>,  
Yoshinori HAGA<sup>2</sup>, Etsuji YAMAMOTO<sup>2</sup>, Yoshichika ONUKI<sup>3</sup>

<sup>1</sup>Kobe University, Kobe, Hyogo, 675-8501, Japan

<sup>2</sup>Japan Atomic Energy Agency, Tokai, Ibaraki, 319-1195, Japan

<sup>3</sup>University of Ryukyus, Nishihara, Okinawa, 903-0213, Japan

The heavy fermion superconductor  $\text{UBe}_{13}$  attracts much attention because of peculiar normal and superconducting (SC) properties. Although a number of studies have been carried out on unusual properties in  $\text{UBe}_{13}$  over the past three decades, many questions still remain, e.g. the symmetry of Cooper pairing, the SC properties etc. The electronic specific heat coefficient of  $\text{UBe}_{13}$  is extremely large ( $\sim 1100 \text{ mJ/mol K}^2$ ) associated with strong electronic correlations. The SC transition occurs at  $T_c = 0.86 \text{ K}$  with large specific heat jump, indicating that the heavy quasiparticles are responsible for superconductivity. The  $T$  dependence of the electric resistivity is proportional to  $-\ln T$  above 30 K, associated with the magnetic Kondo effect. On the other hand, temperature dependence of resistivity does not follow  $T^2$  in low temperature region and a non-Fermi liquid behavior can be observed under field in normal state. Also unusual behaviors are observed in SC state. The field dependence of specific heat reveals an anomaly in SC state (closed squares) [1]. This anomaly has been observed in other measurements, surface impedance (open squares) [2], magnetization (dashed line) [3]. These results are summarized in SC B-T phase diagram as shown in Fig.1.

To explicate these unusual properties, various ideas have been proposed e.g. the change of the SC order parameter, the change of the carrier density, the short range magnetic order etc. In NMR measurements, the reduction of the Knight shift of Be(II) at  $T_a$  was observed. From these results, the change of the order parameter of the superconductivity has been discussed. However, the origin of this anomaly at  $T_a$  and the parity of the superconductivity of  $\text{UBe}_{13}$  are still ambiguous.

In order to clarify the origin of anomaly in SC state, we have carried out  $^9\text{Be}$ -NMR measurements for a single crystal  $\text{UBe}_{13}$  down to 0.03 K under various magnetic fields. The  $^9\text{Be}$  Knight shift of Be(II) site stays constant in the temperature range between  $T_c$  and  $T_a$  ( $< T_c$ ), whereas the shift suddenly shows a fractional reduction below  $T_a$ . However, the reduction of the Knight shift below  $T_a$  is as small as one tenth of the spin part of Knight shift which is estimated by the electronic specific coefficient. On the other hand, the  $^9\text{Be}$  Knight shift for Be(I) site does not change at all even below  $T_a$ . The spin part of the Knight shift for the Be(I) site is as large as that for the Be(II) site. Thus, an even-parity pairing state is ruled out and the behaviors of the Knight shift are consistent with the odd-parity pairing state. In addition, the anomalies at  $T_a$  observed for Be(II) are not attributed to the change of the multiple SC order parameters like  $\text{UPt}_3$ , because the  $^9\text{Be}$  Knight shifts both for Be(I) and Be(II) sites should decrease below  $T_a$ . Hence, the anomaly observed at  $T_a$  does not relate in the superconductivity. The anomaly may originate in magnetic or electric order. In our presentation, we will discuss the pairing symmetry and the origin of the anomalies at  $T_a$  in  $\text{UBe}_{13}$ .

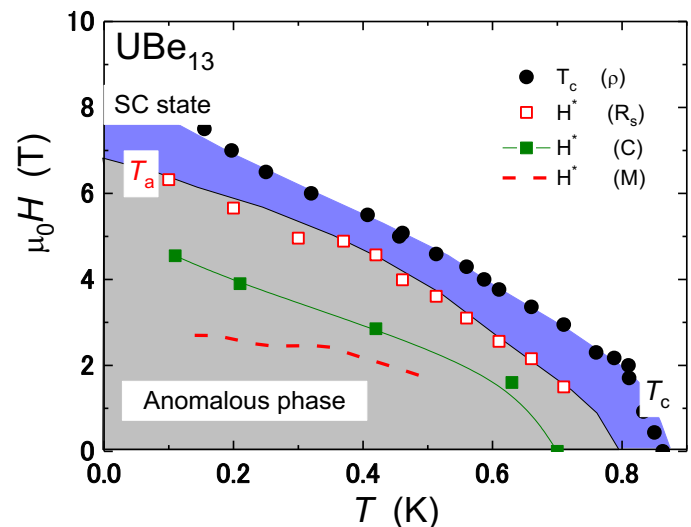


Fig.1: SC phase diagram in  $\text{UBe}_{13}$

- [1] F. Kromer *et al.*, Phys. Rev. Lett., **81**, 4476 (1998).  
 [2] H. Tou *et al.*, J. Phys. Soc. Jap., **75**, 201-203 (2006).  
 [3] Y. Shimizu *et al.*, Phys. Rev. Lett., **109**, 217001 (2012).

### NMR studies on anisotropy of antiferro spin fluctuations in UPt<sub>3</sub>

T. Aoyama<sup>1</sup>, H. Kotegawa<sup>1</sup>, H. Tou<sup>1</sup>, N. Kimura<sup>2</sup>, Y. Haga<sup>3</sup>, E. Yamamoto<sup>3</sup>, Y. Onuki<sup>4</sup>

<sup>1</sup> Department of Physics, Kobe University, Kobe 657-8501, Japan

<sup>2</sup> Department of Physics, Tohoku University, Sendai 980-8577, Japan

<sup>3</sup> Advanced Science Research Center, Japan Atomic Energy Agency, Ibaraki 319-1184, Japan

<sup>4</sup> Department of Physics and Earth Science, University of the Ryukyus, Okinawa 903-0213, Japan

UPt<sub>3</sub> is a heavy-Fermion superconductor discovered in the earliest stage of study of strong correlated electron system. This compound has multiple superconducting phases in the temperature-magnetic field plane. From temperature dependence of NMR/ $\mu$ SR-Knight shift[1,2] and field-angle dependence of thermal conductivity[3], it has been believed that the superconducting pairing is spin-triplet odd-parity state. Particularly recent field-angle resolved thermal conductivity obtained various information about gap symmetry in UPt<sub>3</sub>. However experimental and theoretical issues still remain to be clarified.

One of the issues is a test for the symmetry breaking field which lifts degenerated superconducting order parameters and brings about the characteristic superconducting multiple phases. It is expected that the AFM order detected by neutron scattering below  $\sim 5$ K [4,5] yields the symmetry breaking field. However, the AFM order cannot be detected by NMR/ $\mu$ SR-Knight shift[6,2]. Therefore, it is predicted the AFM order is a dynamical antiferromagnetic spin fluctuation with a slow frequency less than MHz. However, the details of antiferromagnetic spin fluctuation have not been elucidated yet.

In our previous studies, we performed <sup>195</sup>Pt-NMR for H $\parallel$ [11-20] and measured NMR spin-lattice relaxation time  $T_1$  and NMR spin-spin relaxation time  $T_2$  to detect the antiferromagnetic spin fluctuation below 5K. As the result, we found that the AFM correlation length develops below 6K. In the present presentation, we are planning to report about the anisotropy of AFM correlation length.

This work was supported by JPSJ KAKENHI Grant numbers 15H05745, 15H05885 (J-Physics), 15H05882 (J-Physics), and 15H03689.

- [1] H. Tou, Y. Kitaoka, K. Ishida, K. Asayama, N. Kimura, Y. Onuki, E. Yamamoto, Y. Haga, and K. Maezawa *Phys. Rev. Lett.* **80** 3129 (1998)
- [2] G. M. Luke, L. P. Le, B. J. Sternlieb, W. D. Wu, Y. J. Uemura, J. H. Brewer, R. Kadono, R. F. Kiefl, S. R. Kreitzman, T. M. Riseman, Y. Dalichaouch, B. W. Lee, M. B. Maple, C. L. Seaman, P. E. Armstrong, R. W. Ellis, Z. Fisk and J. L. Smith *Phys. Lett. A* **15** 173 (1991)
- [3] K. Izawa, Y. Machida, A. Itoh, Y. So, K. Ota, Y. Haga, E. Yamamoto, N. Kimura, Y. Onuki, Y. Tsutsumi, and K. Machida *J. Phys. Soc. Jpn.* **83** 061013 (2014)
- [4] G. Aeppli, E. Bucher, C. Broholm, J. K. Kjems, J. Baumann and J. Hufnagl *Phys. Rev. Lett.* **60** 615 (1988)
- [5] S. M. Hayden, L. Taillefer, C. Vettier and J. Flouquet *Phys. Rev. B* **6**, 8675 (1992)
- [6] H. Tou, Y. Kitaoka, K. Asayama, N. Kimura, Y. Onuki, E. Yamamoto, and K. Maezawa *Phys. Rev. Lett.* **77**. 1374 (1996)

## P-16

Elastic Response of the Vortices-type Magnetic Order in UNi<sub>4</sub>B

Tatsuya Yanagisawa, Hiroaki Matsumori, Takeaki Saito, Hiraku Saito,  
Hiroyuki Hidaka and Hiroshi Amitsuka

Graduate School of Science, Hokkaido University, Sapporo 060-0810, Japan

UNi<sub>4</sub>B crystallizes in an orthorhombic structure (Cmcm,  $D_{2h}^{17}$ , No. 63) [1]. Below  $T_N = 20.4$  K, this compound orders antiferromagnetically in a magnetic structure where the magnetic moments carried by the 2/3 of U ions ( $U_{AFM}$ ) make the vortices in each pseudo-honeycomb plane and the 1/3 of U ions ( $U_{PM(1)}$  and  $U_{PM(2)}$ ) located in the centres of magnetic vortices remain paramagnetic state as shown in Fig. 1 [2, 3]. Such exotic magnetic structure was predicted by neutron scattering experiment with assuming hexagonal crystal structure (P6/mmm,  $D_{6h}^1$ , No. 191) [4]. The detailed magnetic structure has, however, not been fully identified yet, and a contribution of electric quadrupole degrees of freedom to this non-collinear magnetic order has not been investigated and discussed. On the other hand, S. Hayami *et al.* recently pointed out that such vortices-type magnetic structure believed in UNi<sub>4</sub>B is a candidate of a “toroidal order” [5]. This theory also predicts a new magnetoelectric effect, such as magnetization induced by electric current, can occur in the ferro-toroidal ordered metals. In the present study, we measured elastic constants of single-crystalline UNi<sub>4</sub>B by means of ultrasound in order to check possible contributions of electric quadrupoles to the non-collinear magnetic order and also verify a previously proposed crystalline electric field level scheme [6]. We found that the transverse ultrasonic mode  $C_{66}$  shows Curie-type elastic softening below 30 K both in paramagnetic phase and antiferromagnetic (AFM) phase down to at least 1.2 K. This result strongly suggests that the ground state of the present compound has degeneracy for  $\Gamma_5$  electric quadrupole or some kind of degrees of freedom with  $\Gamma_2$  symmetry in  $D_{6h}$  point group, which couples to the strain or the rotation induced by elastic wave of transverse  $C_{66}$  mode. We also performed ultrasonic experiments on UNi<sub>4</sub>B under applied magnetic field up to 17 T and found that the softening of  $C_{66}$  is once reduced under low-magnetic field ( $\sim 8$  to 12 T along  $[2\bar{1}\bar{1}0]$  axis), where the AFM magnetic structure is partially broken due to spin-reorientation, but the softening is enhanced again above  $\sim 12$  T. This fact implies a possible contribution of the electric quadrupoles to the spin-reorientation phenomena. We will also report the results of ultrasonic measurements under electric current to check the magnetoelectric effect via elastic response in zero magnetic field.

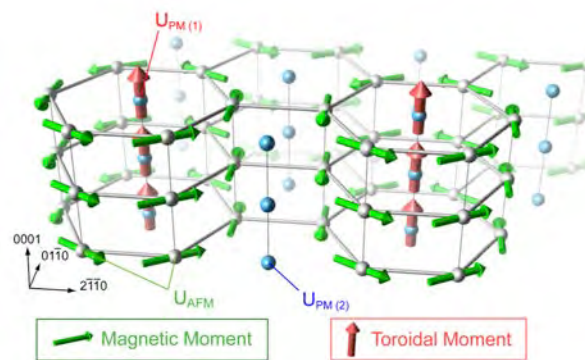


Fig.1 Schema of the Vortices-type magnetic structure and ferro-toroidal moment (the center of the vortices) of UNi<sub>4</sub>B, compiled from Refs. 1 and 5. Here, only U atoms are displayed, *i.e.*, Ni and B atoms are omitted.

The present research was supported by JSPS KAKENHI Grant Numbers JP17K05525 (C), JP15KK0146 (Fostering Joint International Research), JP15K05882 and JP15K21732 (J-Physics). The authors would like to thank Prof. H. Kusunose and Dr. S. Hayami for fruitful discussions.

- [1] Y. Haga, A. Oyamada, T. D. Matsuda, S. Ikeda, and Y. Ōnuki, *Physica B* **403**, 900-902 (2008).
- [2] S. A. M. Mentink, A. Drost, G. J. Nieuwenhuys, E. Frikkee, A. A. Menovsky, and J. A. Mydosh, *Phys. Rev. Lett.* **73**, 1031 (1994).
- [3] R. Movshovich, M. Jaime, S. Mentink, A.A. Menovsky, and J.A. Mydosh, *Phys. Rev. Lett.* **83**, 2065 (1999).
- [4] J. A. Mydosh, G. J. Nieuwenhuys, S. A. M. Mentink, and A. A. Menovsky, *Phil. Mag. B* **65**, 1343 (1992).
- [5] S. Hayami, H. Kusunose, and Y. Motome, *Phys. Rev. B* **90**, 024432 (2014).
- [6] A. Oyamada, M. Kondo, K. Fukuoka, T. Itou, S. Maegawa, D. X. Li, and Y. Haga, *J. Phys. Condens. Matter* **19**, 145246 (2007).

## P-17

## A new valence-ordered phase and collapse of antiferromagnetism in EuPtP induced by pressure

A. Mitsuda<sup>1</sup>, S. Manabe<sup>1</sup>, M. Umeda<sup>1</sup>, H. Wada<sup>1</sup>, K. Matsubayashi<sup>2</sup>, Y. Uwatoko<sup>2</sup>,  
M. Mizumaki<sup>3</sup>, N. Kawamura<sup>3</sup>, K. Nitta<sup>3</sup>, N. Hirao<sup>3</sup>, Y. Ohishi<sup>3</sup>, N. Ishimatsu

<sup>1</sup>Department of Physics, Kyushu University, Fukuoka 819-0395, Japan

<sup>2</sup>Institute for Solid State Physics, The University of Tokyo, Kashiwa 277-8581, Japan

<sup>3</sup>Japan Synchrotron Radiation Research Institute, Sayo, Hyogo 679-5198, Japan

<sup>4</sup>Department of Physics, Graduate School of Science, Hiroshima University, Higashi-Hiroshima 739-8526, Japan

EuPtP crystallizes in the layered hexagonal ZrBeGe-type (space group  $P6_3/mmc$ ) structure and consists of alternate stacking of Eu and Pt-P layers along the  $c$ -axis. This compound exhibits two valence transitions at  $T_1=235\text{K}$  and  $T_2=195\text{K}$  and an antiferromagnetic (AF) order below  $T_3=7\text{K}$ [1]. With decreasing temperature, the mean Eu valence is changed from 2.16 to 2.3 at  $T_1$  and from 2.3 to 2.4 at  $T_2$ . The phases at  $T>T_1$ ,  $T_2<T<T_1$ , and  $T<T_2$  are called  $\alpha$ -,  $\beta$ -, and  $\gamma$ -phase, respectively[2]. In the  $\beta$ - and  $\gamma$ -phases,  $\text{Eu}^{2+}$  and  $\text{Eu}^{3+}$  ions are arranged regularly, namely valence order. In both phases, the Eu valence in one Eu layer becomes either 2+ or 3+ uniformly. The  $\beta$ -phase has stacking of  $\cdots-(2+)-(2+)-(3+)-(2+)-(2+)-(3+)-\cdots$  (2+:  $\text{Eu}^{2+}$  layer, 3+:  $\text{Eu}^{3+}$  layer) along the  $c$ -axis. The  $\gamma$ -phase does stacking of  $\cdots-(2+)-(3+)-(2+)-(3+)-\cdots$ [3]. Thus, this compound also shows the valence order at  $T_1$  and its modulation at  $T_2$  accompanied by the valence transitions. Anticipating that the application of pressure to this sample would induce a valence transition, a new valence-ordered phase and a new phenomenon associated with valence fluctuation, we examined the electrical resistivity  $\rho$ , the Eu  $L_3$ -edge X-ray absorption (XA) spectroscopy, and the powder X-ray diffraction (XRD) under high pressure. We found a new valence transition from the  $\gamma$ -phase to  $\delta$ -phase at around  $P = 2.5\text{ GPa}$  and superlattice XRD peaks of  $(0\ 0\ 2/3)$ ,  $(1\ 0\ 4/3)$ , and  $(1\ 0\ 8/3)$  at  $T=8\text{ K}$  in the pressure range between 3 and 4 GPa. In the  $\delta$ -phase, a new valence-ordered structure which consists of stacking of  $\cdots-(2+)-(3+)-(3+)-(2+)-(3+)-(3+)-\cdots$  is inferred. This is the first evidence of the valence order in the  $\delta$ -phase. Upon further increases in pressure, the superlattice peaks disappear at around  $P=4\text{ GPa}$ , which means that the  $\delta$ -phase collapses. Another valence-ordered phase should be realized up to  $P = 6\text{ GPa}$  since the AF order survives at  $P=6\text{ GPa}$  in spite of the mean Eu valence close to 2.7. Finally, the AF order collapses in the pressure range between 6 GPa and 8 GPa, which is not accompanied by a valence transition. This result suggests the continuous suppression of the AF order in contrast to a sudden collapse of AF in  $\text{EuNi}_2\text{Ge}_2$  and  $\text{EuRh}_2\text{Si}_2$ , which implies that there possibly exists a quantum critical point between 6 GPa and 8 GPa.

[1] N. Lossau et al., Z. Phys. B , 227 (1989).

[2] N. Lossau et al., Z. Phys. B , 393 (1989).

[3] T. Inami et al., Phys. Rev. B 82, 195133 (2010).

Pressure Effect on Electrical Transport Properties of  $U_{1-x}Th_xBe_{13}$ 

Y. Machida<sup>1</sup>, T. Imai<sup>1</sup>, K. Fukuchi<sup>1</sup>, K. Izawa<sup>1</sup>, Y. Shimizu<sup>2</sup>, Y. Homma<sup>2</sup>, D. Aoki<sup>2</sup>, Y. Haga<sup>3</sup>, E. Yamamoto<sup>3</sup>,  
and Y. Onuki<sup>4</sup>

<sup>1</sup>Department of Physics, Tokyo Institute of Technology, Meguro, Tokyo 152-8551, Japan

<sup>2</sup>Institute for Materials Research, Tohoku University, Oarai, Ibaraki 311-1313, Japan

<sup>3</sup>Advanced Science Research Center, Japan Atomic Energy Agency, Tokai, Ibaraki 319-1195, Japan

<sup>4</sup>Faculty of Science, University of the Ryukyus, Nishihara, Okinawa 903-0213, Japan

Metallic behaviour that deviates from the Fermi liquid theory, dubbed non-Fermi liquid (NFL) behaviour, has been observed in a wide variety of materials such as heavy fermion metals, transition-metal oxides, and iron pnictides. The NFL behaviour is often associated with quantum criticality and most enhanced on the verge of magnetically ordered state due to quantum-critical fluctuations. Occasionally, unconventional superconductivity emerges out of such anomalous metallic state.

$UBe_{13}$  is the heavy fermion metal that exhibits the NFL behaviours in the normal state and undergoes a transition to the unconventional superconducting state at low temperatures. Despite the intensive studies on this material over the past decades, nature of the NFL properties and its linkage to the superconductivity remain unresolved. However, the prior experimental results reporting that the NFL behaviours become more significant toward  $x \rightarrow x_c \sim 0.03$  in the thoriated system  $U_{1-x}Th_xBe_{13}$  and the superconducting transition temperature has a local maximum around  $x_c$  imply presence of a singular point close to  $x \sim x_c$  by an analogy to a quantum critical point in the heavy fermion systems [1,2]. Since Th substitution expands the lattice, it most simply corresponds to a negative pressure, so that the thoriated system  $U_{1-x}Th_xBe_{13}$  with  $x > x_c$  can be continuously tuned to such a singular point by applying pressure.

In order to examine this possibility, we carried out the electrical transport measurements on the single crystalline  $U_{1-x}Th_xBe_{13}$  under pressure. For the parent undoped compound  $UBe_{13}$ , we found that the anomalous peaks in resistivity and Hall coefficient, which characterize the NFL properties of this system, are gradually suppressed with increasing pressure, suggesting that the system goes away from the singular point. Moreover, the peak positions concomitantly shift to higher temperature with pressure. On the other hand, for the thoriated compound  $U_{1-x}Th_xBe_{13}$  with  $x = 0.04$ , the anomalous peak is absent at ambient pressure. Interestingly, however, an application of pressure provides a remarkable increase of both resistivity and Hall coefficient at low temperatures. In the presentation, we will discuss the nature of the NFL behaviours of  $U_{1-x}Th_xBe_{13}$  and its relevance to the putative pressure-induced singular point.

[1] E. A. Knetsch, G. J. Nieuwenhuys, J. A. Mydosh, R. H. Heffner, and J. L. Smith, *Physica B* **186-188**, 251 (1993).

[2] J. L. Smith, Z. Fisk, J. O. Willis, B. Batlogg, and H. R. Ott, *J. Appl. Phys.* **55**, 1996 (1984).

## Antisymmetric spin-orbit coupling effect on a triangular-triple-quantum-dot Kondo system

M. Koga<sup>1</sup>, M. Matsumoto<sup>2</sup>, and H. Kusunose<sup>3</sup><sup>1</sup>Department of Physics, Faculty of Education, Shizuoka University, Shizuoka 422-8529, Japan<sup>2</sup>Department of Physics, Faculty of Science, Shizuoka University, Shizuoka 422-8529, Japan<sup>3</sup>Department of Physics, Meiji University, Kawasaki 214-8571, Japan

Recently, the antisymmetric spin-orbit (ASO) coupling effect has attracted numerous researchers to novel physics associated with the absence of the inversion symmetry in bulk systems, such as the spintronics in semiconductors, topological insulators, and non-centrosymmetric superconductors. On the nanoscale, an ASO coupling also arises in coupled atoms with different-parity orbitals in the absence of the inversion symmetry related to the two-dimensionality. It is expected that the ASO coupling effect plays an essential role in parity mixing of degenerate molecular orbitals in coupled magnetic atoms, which can be realized by artificial devices such as a triangular triple quantum dot (TTQD). In fact, the recent development of a fabrication technique has stimulated theoretical studies on the Kondo effect in TTQD systems with various configurations as versatile quantum devices.

We investigate the interplay between the Kondo and ASO coupling effects in the TTQD at half-filling, where the emergence of electric polarization is closely associated with the spin reconfiguration of TTQD states. Here, one of the three QDs is coupled to a metallic lead through electron tunneling, while the ASO interaction is introduced in the other coupled QDs on the opposite side of the lead (see Fig. 1). We study an extended Anderson model for this TTQD system using Wilson's numerical renormalization group method. When the ASO coupling is absent, the local electric polarization is induced by the Kondo singlet formation at the left QD with the lead in Fig. 1, and a dimerized spin-singlet state is realized in the coupled QDs on the right side of the TTQD. In the presence of a magnetic field, there is a quantum critical point (QCP) between strong and weak coupling fixed points of local Fermi liquid in the Kondo effect, which cannot be explained by a simple level crossing. At a critical magnetic field, the emergent electric polarization  $\delta n^*$  exhibits an abrupt sign reversal as a consequence of a quantum transition between different parities of the TTQD molecular orbitals. Simultaneously, the local spin is flipped at the QD coupled to the lead [1].

Although the ASO coupling effect is very weak and not easily detectable in general, it essentially causes marked spin and charge reconfigurations in the Kondo screening process [2]. We show that the abrupt sign reversal of  $\delta n^*$  is also realized by changing the local ASO coupling  $\gamma$  in the coupled QDs. This is owing to the marked change of the parity mixing of the TTQD states in the vicinity of the QCP. In Fig. 2, the overall feature of the sign reversal  $\delta n^* > 0 \leftrightarrow \delta n^* < 0$  is illustrated by the temperature  $T$  vs. magnetic field  $h$  diagram for  $\gamma = 0$  and the  $\gamma$  vs.  $h$  diagram at  $T \rightarrow 0$  [3].

This work was supported by JSPS KAKENHI Grant Numbers 16H01070 (J-Physics), 15H05885 (J-Physics), 17K05516, and 15K05176.

[1] M. Koga, M. Matsumoto, and H. Kusunose, J. Phys. Soc. Jpn. 82, 093706 (2013).

[2] M. Koga, M. Matsumoto, and H. Kusunose, J. Phys. Soc. Jpn. 86, 054703 (2017).

[3] M. Koga, M. Matsumoto, and H. Kusunose, Physica B (<http://dx.doi.org/10.1016/j.physb.2017.08.033>).

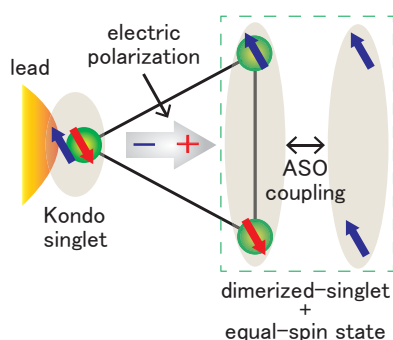


**Fig. 1.** Illustration of the TTQD Kondo system

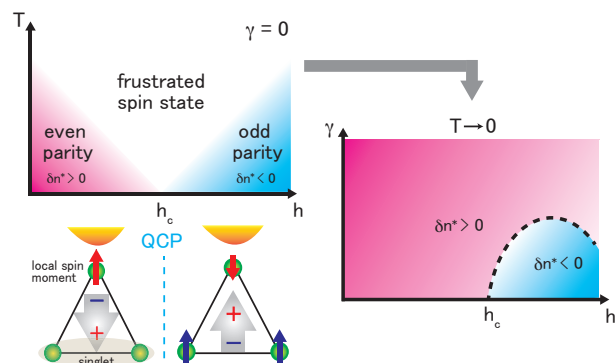


**Fig. 2.** Sign reversal of the emergent electric polarization  $\delta n^*$ :  $T$  vs.  $h$  diagram for  $\gamma = 0$  and  $\gamma$  vs.  $h$  diagram at  $T \rightarrow 0$ .

## P-20

Single crystal growth and physical properties in  $\text{Ce}_5\text{Si}_4$  and  $\text{La}_5\text{Si}_4$  with chiral structureY. Sato<sup>1,2</sup>, F. Honda<sup>2</sup>, Y. Homma<sup>2</sup>, D. X. Li,<sup>2</sup> Y. Shimizu<sup>2</sup>, A. Nakamura<sup>2</sup>, and D. Aoki<sup>2</sup><sup>1</sup>Grad. School of Eng., Tohoku University, Sendai, Miyagi 980-8577, Japan<sup>2</sup>IMR, Tohoku University, Oarai, Ibaraki 311-1313, Japan

Compounds with a chiral structure attract much attention because of their peculiar properties, such as magnetic skyrmion[1]. We present single crystal growth and physical properties in  $\text{Ce}_5\text{Si}_4$  and  $\text{La}_5\text{Si}_4$  with a chiral structure. It has been reported that  $\text{Ce}_5\text{Si}_4$  shows antiferromagnetic ordering below  $T_N = 5.6$  K [2] and  $T_N = 3.8$  K [3], as reported independently. While the former  $T_N$  has been obtained from specific heat and ac susceptibility measurements, the latter  $T_N$  value has been obtained from dc magnetization measurements. In the present work, we aim to elucidate its intrinsic magnetic ground state and its anisotropy effects in  $\text{Ce}_5\text{Si}_4$  by means of resistivity, specific heat, and dc magnetization measurements using single crystalline samples.

Both  $\text{Ce}_5\text{Si}_4$  and  $\text{La}_5\text{Si}_4$  crystallize in the tetragonal  $\text{Zr}_5\text{Si}_4$ -type structure (space group  $P4_12_12$ , #92). We have succeeded in growing single crystalline samples of  $\text{Ce}_5\text{Si}_4$  and  $\text{La}_5\text{Si}_4$  for the first time. Single crystals of these compounds were grown by the Czochralski method in a tetra-arc furnace, and were annealed at 1000 °C for 6 days under the vacuum of  $1 \times 10^{-4}$  Pa. The crystal structure was confirmed using a single crystal X-ray diffractometer and a powder X-ray diffractometer.

Figure.1 shows the temperature dependence of the specific heat in the form of  $C/T$  for  $\text{Ce}_5\text{Si}_4$ .  $C/T$  shows a clear peak corresponding to the occurrence of antiferromagnetic order ( $T_N \approx 2.7$  K). Figure.2 shows the temperature dependence of the resistivity in  $\text{Ce}_5\text{Si}_4$ . Resistivity value is clearly anisotropic between for the electrical current  $J//[001]$  and  $J//[110]$ . The resistivity  $\rho(T)$  increases at low temperature for  $J//[001]$  and  $J//[110]$  with decreasing temperature, and a kink anomaly corresponding to the magnetic phase transition is seen at  $T \approx 2.7$  K. It has also been found that a moderate negative magnetoresistance occurs in  $\text{Ce}_5\text{Si}_4$ . In addition, the temperature and magnetic field dependence of the dc magnetization were measured for the magnetic field  $H//[001]$  and  $H//[100]$ . The temperature dependence of the magnetization shows a peak corresponding magnetic phase transition for  $H//[100]$  at 2.7 K. On the other hand, a kink corresponding magnetic phase transition has been observed for  $H//[001]$  at 2.7 K. A clear magnetic anisotropy has been observed between  $H//[001]$  and  $H//[100]$ ; while [001] is the magnetization-easy axis, [100] is the magnetization-hard axis. Our thermodynamic as well as transport results consistently indicate that the antiferromagnetic transition occurs at  $T_N \approx 2.7$  K in the present single crystalline sample. Here, the obtained value of Néel temperature contrasts starkly with precisely reported values ( $T_N = 5.6$  K [2], and  $T_N = 3.8$  K [3]), implying that there is a remarkable difference between the sample quality of single crystals and that of polycrystalline samples. In our presentation, we will discuss the transport and magnetic properties of  $\text{Ce}_5\text{Si}_4$ , showing the obtained new experimental results.

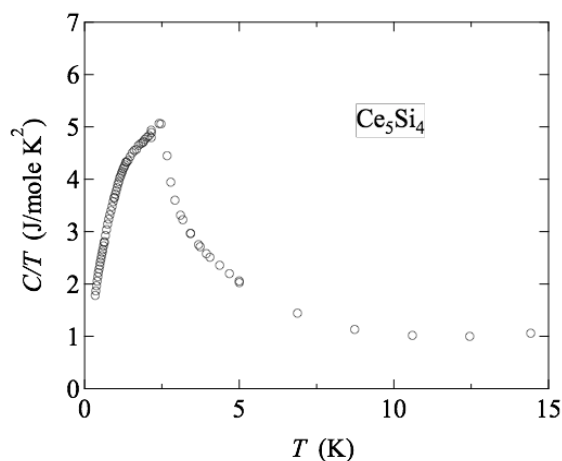


Figure.1 Temperature dependence of the heat capacity of  $\text{Ce}_5\text{Si}_4$  ( $C/T$  vs  $T$ ).

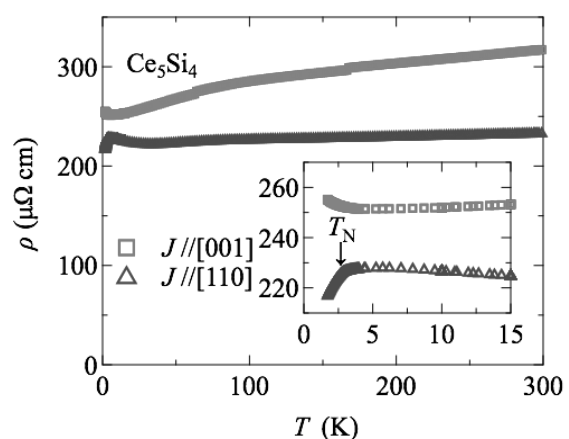


Figure.2 Temperature dependence of the resistivity for  $J//[001]$  (open square) and  $J//[110]$  (open triangle). The inset shows the enlarged figure below 15 K.

- [1] S. Mühlbauer, B. Binz, F. Jonietz, C. Pfleiderer, A. Rosch, A. Neubauer, R. Georgii, P. Böni, *Science*, **323**, 915 (2009).  
 [2] J. Vejpravová, J. Prokleška, S. Daniš, V. Sechovský, *Physica B*, **378-380**, 784-785 (2006).  
 [3] H. Zhang, Y. Mudryk, Q. Cao, V. K. Pecharský, K. A. Gschneidner Jr., Y. Long, *J. Appl. Phys.*, **107**, 013909 (2010).

## P-21

Theoretical study on magnetoelectric response in the honeycomb antiferromagnet  $\text{Co}_4\text{Nb}_2\text{O}_9$ Y. Yanagi<sup>1</sup>, S. Hayami<sup>2</sup>, and H. Kusunose<sup>1</sup><sup>1</sup>Meiji University, Kawasaki 214-8571, Japan<sup>2</sup>Hokkaido University, Sapporo 060-0810, Japan

A honeycomb antiferromagnet  $\text{Co}_4\text{Nb}_2\text{O}_9$  shows linear magnetoelectric (ME) effects below the Néel temperature [1]. Recent experiments for single crystalline samples have revealed the magnetic structures and details of a ME response [2,3]. According to the neutron diffraction measurements [3], the magnetic structure is collinear with the ordering vector  $\mathbf{q}=\mathbf{0}$ , where the antiferromagnetic (AFM) moment is almost lying in the  $ab$ -plane. Due to the weak magnetic anisotropy in the  $ab$ -plane, the external magnetic field in the easy plane directs the AFM moment perpendicular to the applied magnetic field. As a result, when the magnetic field is rotated anticlockwise in the  $ab$ -plane, the AFM moment is also rotated anticlockwise so as to keep its direction orthogonal to the magnetic field. Remarkably, the electric polarization is rotated clockwise with a period half of that of the AFM moment rotation under the anticlockwise rotating magnetic field in the  $ab$ -plane (see, Fig. 1)[3]. In the present study, we elucidate the origin of the novel ME effects observed in  $\text{Co}_4\text{Nb}_2\text{O}_9$ .

To this end, we calculate the ME tensor of the realistic effective model, which is derived from the density functional calculation. The obtained magnetic field angle dependence of the electric polarization qualitatively reproduces the experimental result. In order to gain clear insight into the emergence of such ME effects, we also derive a simpler model and unveil the minimal condition for the novel ME response in  $\text{Co}_4\text{Nb}_2\text{O}_9$ .

This work has been supported by JSPS KAKENHI Grant Number 15H05885 (J-Physics) and 15K05176.

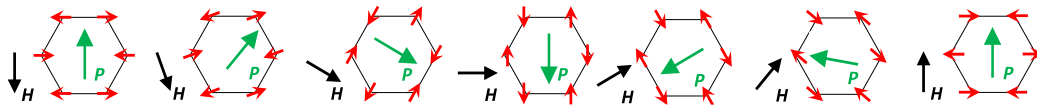


Figure 1. Electric polarization under the in-plane rotating magnetic field.

[1] E. Fischer et al., *Solid State Commun.* **10**, 1127 (1972).

[2] I. V. Solovyev and T. V. Kolodiazny, *Phys. Rev. B* **93**, 094427 (2016).

[3] N. D. Khanh et al., *Phys. Rev. B* **93**, 075117 (2016); N. D. Khanh, Ph. D thesis (Tohoku Univ., 2015).

## P-22

Atomic imaging around Pr atoms in  $\text{Ca}_{1-x}\text{Pr}_x\text{Fe}_2\text{As}_2$  by x-ray fluorescence holography

K. Kudo<sup>1</sup>, S. Ioka<sup>1</sup>, N. Happo<sup>2</sup>, H. Ota<sup>1</sup>, Y. Ebisu<sup>3</sup>, K. Kimura<sup>4</sup>, T. Hada<sup>2</sup>, T. Kimura<sup>1</sup>, H. Tajiri<sup>5</sup>, S. Hosokawa<sup>6</sup>,  
K. Hayashi<sup>4</sup>, and M. Nohara<sup>1</sup>

<sup>1</sup>Okayama University, Okayama, Japan

<sup>2</sup>Hiroshima City University, Hiroshima, Japan

<sup>3</sup>Hiroshima Institute of Technology, Hiroshima, Japan

<sup>4</sup>Nagoya Institute of Technology, Nagoya, Japan

<sup>5</sup>Japan Synchrotron Radiation Research Institute, Hyogo, Japan

<sup>6</sup>Kumamoto University, Kumamoto, Japan

$\text{Ca}_{1-x}\text{Pr}_x\text{Fe}_2\text{As}_2$  has been reported to exhibit local superconductivity at  $T_c = 49$  K around the doped Pr atoms [1,2,3]. We performed the state-of-the-art technique, x-ray fluorescence holography experiment [4] in order to visualize the local 3D atomic configurations [5] around Ca and Pr atoms. The atomic images of As revealed that As positions fluctuated significantly even in the parent  $\text{CaFe}_2\text{As}_2$  compound. For  $\text{Ca}_{0.9}\text{Pr}_{0.1}\text{Fe}_2\text{As}_2$ , we found that the positional fluctuations of As were almost unchanged around Pr atoms compared with the parent  $\text{CaFe}_2\text{As}_2$ , but the positional fluctuations were significantly increased around Ca atoms. These observations were consistent with the local superconductivity around the Pr.

[1] B. Lv *et al.*, PNAS **108**, 15705 (2011).

[2] S. R. Saha *et al.*, Phys. Rev. B **85**, 024525 (2012).

[3] K. Gofryk *et al.*, Phys. Rev. Lett. **112**, 047005 (2014).

[4] K. Hayashi *et al.*, J. Phys.: Condens. Matter **24**, 093201 (2012).

[5] J. J. Barton, Phys. Rev. Lett. **67**, 3106 (1991).

Hall Resistivity of Non-Kramers System  $\text{PrT}_2\text{Zn}_{20}$  ( $T = \text{Ir, Rh}$ )J. Ogawa<sup>1</sup>, Y. Machida<sup>1</sup>, K. Izawa<sup>1</sup>, N. Nagasawa<sup>2</sup>, T. Onimaru<sup>2</sup>, and T. Takabatake<sup>2</sup><sup>1</sup>Dept. of Phys. Tokyo Tech., Japan<sup>2</sup>Dept. of Quantum matter, Hiroshima Univ., Japan

In strongly correlated  $f$ -electron systems such as Ce and Yb compounds, localized  $f$ -electrons often acquire itinerant character via hybridization with conduction electrons, and consequently give rise to a rich variety of phenomena, such as magnetic order, heavy-Fermion, and quantum criticality. Most of these phenomena are governed by spin degrees of freedom of the  $f$ -electrons, and their electronic states have been understood based on the Doniach picture. On the other hand, electronic states inherent to orbital degrees of freedom remain to be clarified experimentally owing to the lack of suitable systems. Pr compounds  $\text{PrT}_2\text{Zn}_{20}$  ( $T = \text{Ir, Rh}$ ) have attracted attention because they have a  $\Gamma_3$  non-Kramers doublet ground state without dipole degrees of freedom. The diagonal transport coefficients and thermodynamic properties reveal four intriguing states in these compounds at low temperatures as well as (i) a long range antiferro quadrupole ordered state, (ii) a non-Fermi liquid (NFL) state, (iii) a novel heavy-fermion state in the vicinity of critical magnetic field of the quadrupole ordered state, and (iv) a field-induced singlet state above  $B_h$  [1, 2]. However, the off-diagonal components of transport coefficients, especially the Hall coefficient, have been less understood both experimentally and theoretically while they are powerful tools to probe the electronic properties.

In this work, we studied the Hall effect of  $\text{PrT}_2\text{Zn}_{20}$  ( $T = \text{Ir, Rh}$ ) to understand the electronic state in non-Kramers system. Figure 1 shows magnetic field dependence of Hall coefficient  $R_H$ . In both compounds, being different from Hall coefficient expected in simple metals,  $R_H$  shows strong magnetic field dependence and the absolute value increases as the field increases in the NFL state, but it shows weak field dependence above  $B_h$ . Interestingly, as shown in the inset of Figure 1, the magnetic field dependence of  $R_H$  is scaled by  $B_h$  regardless the temperature suggesting that NFL-FL crossover connects to the quadrupolar Kondo effect [3], though the scaling functions are different between the compounds. In the presentation, we will discuss these results in terms of non-Kramers doublet and quadrupolar Kondo effect.

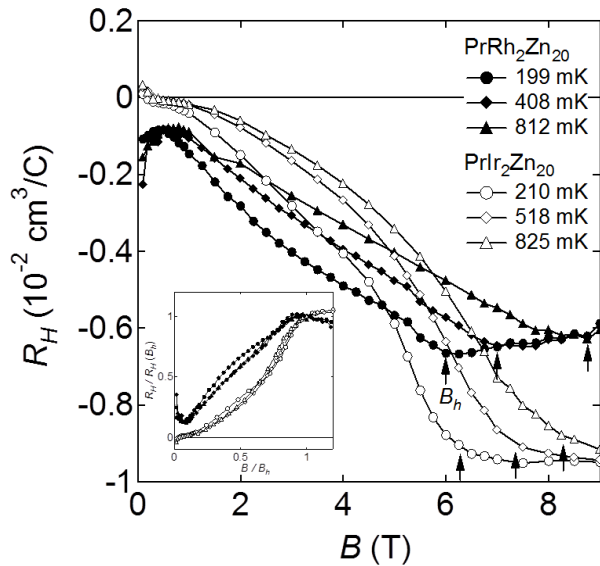


Figure 1: Magnetic field dependence of Hall coefficient  $R_H$  of  $\text{PrIr}_2\text{Zn}_{20}$  and  $\text{PrRh}_2\text{Zn}_{20}$ . The arrows indicate crossover field  $B_h$  between the NFL state and FIS state. The inset shows the scaling plot of  $R_H$  with respect to  $B/B_h$ .

- [1] T. Onimaru *et al.*, Phys. Rev. B **86**, 184426 (2012).
- [2] T. Yoshida *et al.*, J. Phys. Soc. Jpn. **86**, 044711 (2017).
- [3] S. Yotsuhashi *et al.*, J. Phys. Soc. Jpn. **71**, 1705 (2002).

Resonant x-ray scattering study on hybridized orbital states in  $f$ -electron systemH. Nakao<sup>1</sup>, C. Tabata<sup>1</sup>, K. Iwasa<sup>2</sup> and H. Amitsuka<sup>3</sup><sup>1</sup> Condensed Matter Research Center and Photon Factory, Institute of Materials Structure Science, High Energy Accelerator Research Organization, Tsukuba 305-0801, Japan<sup>2</sup> Frontier Research Center for Applied Atomic Sciences & Institute of Quantum Beam Science, Ibaraki University, Tokai, Naka, Ibaraki 319-1106, Japan<sup>3</sup> Graduate School of Science, Hokkaido University, Sapporo 060-0810, Japan

In the  $f$ -electron system, orbital hybridization between the conduction electron and the localized  $f$ -electron, so called  $c$  hybridization ( $d$  hybridization), is crucial in the physical properties. Hence the study of hybridized orbital state is an important issue. Resonant X-ray scattering (RXS) technique is a powerful tool for observing the multipole orderings in the  $f$ -electron system [1]. The resonant signal at particular absorption energy reveals element- and orbital-selective information of electronic states relevant to unconventional phenomena. Hence the electronic-state modifications due to the hybridized orbital state can be identified from the RXS signals at the absorption energies of the hybridized ions. Here, we present the RXS investigations on the skutterudite  $\text{PrRu}_4\text{P}_{12}$  and the uranium compound.

Filled skutterudite  $\text{PrRu}_4\text{P}_{12}$  exhibits a metal-insulator (MI) transition at  $T = 63$  K [2, 3], and has attracted much attention to an origin of the transition, i.e. charge density wave [4], antiferro-hexadecapole order [5, 6], and so on. Neutron scattering study elucidated the presence of strong orbital hybridization between Pr and P ( $d$  hybridization), which causes the formation of staggered  $f$ -electron order below  $T$  [7]. Hence the hybridization is expected to be essential for the MI transition. In order to clarify the hybridized orbital state in the unconventional ordered phase, resonant x-ray scattering has been performed at the Pr  $f$ -edge ( $f \rightarrow d$  transition) and at the P  $p$ -edge ( $p \rightarrow d$  transition). Resonating energy spectra were found at the Pr  $f$ -edge and at the P  $p$ -edge, and the signal at the P  $p$ -edge reflecting the P  $p$  state is much stronger than that at the Pr  $f$ -edge. This result is expected to be related with the strong  $d$  hybridization effect on the staggered order phase.

Uranium-based compound shows a rich variety of the physical properties. The  $f$ -electron duality feature of localized and itinerant states is a key to understand such properties. The  $d$  orbital is also important for the itinerant character in the uranium compounds, because the wave function of the U  $d$  orbital, which forms the conduction band, extends more than that of U  $f$  orbital. Moreover, the U  $d$  orbital can directly hybridize with the U  $f$  orbital in a crystal without inversion symmetry. Hence the observation of the respective RXS signals reflecting U  $f$  and  $d$  orbital is expected to give a microscopic view of parity-mixing electronic states. We started a feasibility study to observe the RXS at the U  $f$ -edge ( $f \rightarrow d$  transition) and at the U  $d$ -edge ( $d \rightarrow f$  transition), where the U  $f$  and  $d$  electronic states can be detected respectively.

This research was supported by JSPS KAKENHI Grant Number JP15H05885 (J-Physics).

[1] T. Matsumura et al., J. Phys. Soc. Jpn. **82**, 021007 (2013), and references therein.

[2] C. Sekine et al., Phys. Rev. Lett. **9**, 3218 (1997).

[3] C. H. Lee et al., Phys. Rev. B **0**, 153105 (2004).

[4] H. Harima et al., Physica B **312** **313**, 843 (2002).

[5] T. Takimoto, J. Phys. Soc. Jpn. **5**, 034714 (2006).

[6] Y. Kuramoto, Prog. Theo. Phys. Suppl. **1** **6**, 77 (2008).

[7] K. Iwasa et al., Phys. Rev. B **2** (2005) 024414, J. Phys. Soc. Jpn. **34**, 1930 (2005).

Field-induced topological phase in the s-wave superconductor on a mono-layered checkerboard triangular lattice

S.Sakuraba, Y.Tobita, and J.Goryo  
 Hirosaki University, Hirosaki, 036-8561, Japan

Sato and Fujimoto considered s-wave superfluid in a two-dimensional square lattice with Rashba spin-orbit coupling (SOC). Due to the enhancement of the Pauli paramagnetic limit by the Rashba SOC, the superfluid is robust against the magnetic field along z-axis, and they found a topological phase transition below the enhanced Pauli limit by increasing the field [1]. The topological phase possesses the chiral edge states. The orbital depairing limit is, however, a serious obstacle when we apply their scenario to a superconductor.

We consider the s-wave superconductor in a mono-layered checkerboard triangular lattice such as MoS<sub>2</sub> [2]. The system possesses the anti-symmetric SOC compatible to the lack of inversion symmetry in the lattice, and in this case the Pauli limit for the in-plane field is enhanced. This mono-layer superconductor is thus quite robust against the in-plane field due to the absence of the orbital limit for the in-plane field. We may also introduce the Rashba SOC by an electric field along z-axis.

We then consider the ribbon with straight edges (Fig. 1). We solve the Bogoliubov-de-Gennes equation using certain tight-binding parameters, and obtained the quasiparticle energy spectrum. We find the topological phase transition indicated by the typical band touching, i.e., the gap closing and reopening at a certain value of k in the Brillouin zone (k=0 in our case). In Fig. 2, purple and green dots indicate Pauli limit and the gap closing, and blue line is the orbital limit. We see the topological phase below both Pauli and orbital depairing limits. The Fig. 3 shows the energy spectrum at the black star in Fig.2, and we see the zero energy state at k=0. The spatial dependence of the probability density reveals that the zero energy state is indeed the boundary state at edges (Fig. 4).

In addition, we also consider the ribbon with zigzag edges and also find the topological phase transition. Detail will be given in our presentation.

This work was supported by JSPS KAKENHI Grant Number JP 15H05885 (J-Physics).

- [1] M. Sato and S. Fujimoto, PRB79 094504(2009).
- [2] Y. Saito et al, Nature Phys. 12 (2016) p144-150.

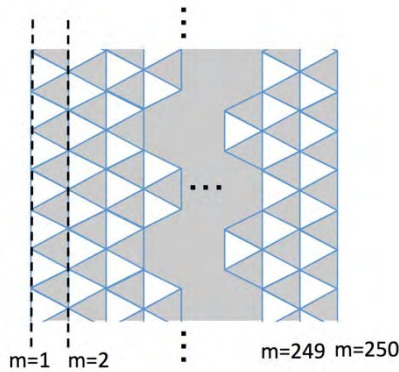


Fig. 1: The straight ribbon.

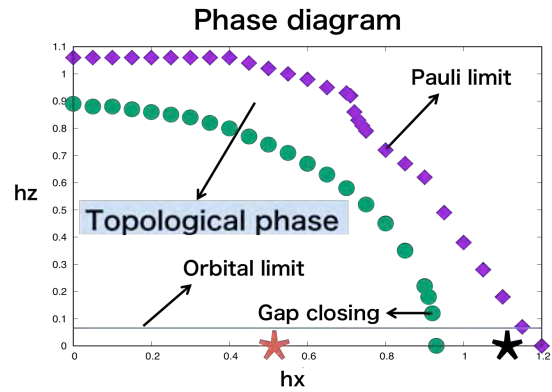


Fig. 2: Phase diagram for the straight ribbon. Horizontal and vertical axis show the non-dimensional field components  $hx$  and  $hz$ .

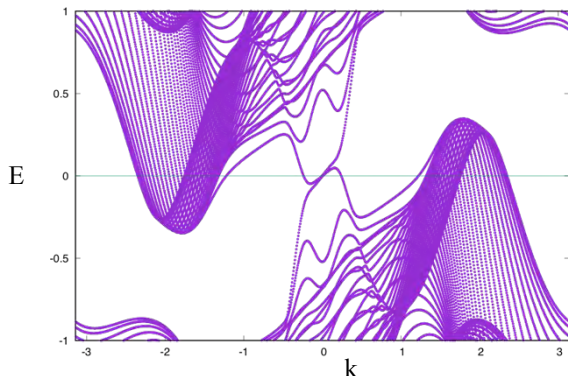


Fig.3: Energy spectrum at the black star in Fig.2.

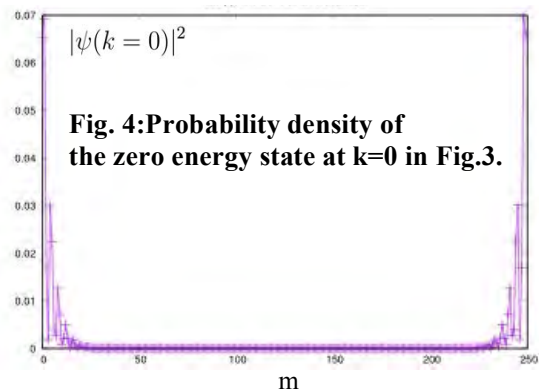


Fig. 4: Probability density of the zero energy state at  $k=0$  in Fig.3.

## Topological feedback on superconductor

Y. Tobita and J. Goryo

Hirosaki University, Hirosaki 036-8561, Japan

The spin fluctuation feedback was known to be involved in stabilizing the chiral  $p$ -wave superconducting state [1, 2]. In addition, another one owing to the chirality of the state, the chiral feedback, is proposed [3, 4]. This chiral feedback mechanism has an origin in the Chern-Simons (CS) term induced in low-energy effective action [5, 6, 7] of the system with broken time reversal symmetry. From the CS term, a charge-density–charge-current correlation also contributes to the pairing interaction. The feedback mechanism by this additional contribution can be understood in the following intuitive picture; due to the CS term, the magnetic flux is attached to the charges and an electron forming Cooper pair with chirality receives the Lorentz force from the other. This effect strengthens a rotation of the pair and gives a positive feedback to the chiral  $p$ -wave state. Although the magnitude of the chiral feedback correction to the GL free energy is smaller than that of the spin-fluctuation feedback because of higher order correction, it should be noted that this feedback originating in the topological term is a universal mechanism of stabilization of the system with electric charge and chirality.

In this talk, we will show the extension of the chiral feedback to a multi-band superconducting state such as the chiral  $p$ -wave superconductivity of  $\text{Sr}_2\text{RuO}_4$ . For multi-band superconducting states, a charge-current–charge-current correlation could also contribute to the stabilization of the state that vanishes in single-band one. In order to analyze the contribution from this additional interaction, we use a simple  $d_{xz} - d_{yz}$  interorbital pairing model for the chiral  $p$ -wave state of  $\text{Sr}_2\text{RuO}_4$ . In this model, off-diagonal parts of current operator exist and an antisymmetric part of the charge-current–charge-current correlation does not vanish [8]. We will discuss about the topological feedback correction to the 4th order term in the GL free energy and the contribution to the stabilization of chiral  $p$ -wave superconductivity of  $\text{Sr}_2\text{RuO}_4$ .

This work was supported by JSPS KAKENHI Grant Number JP15H05885 (J-Physics).

## References

- [1] P. W. Anderson and W. F. Brinkman. *Phys. Rev. Lett.*, 30:1108, 1973.
- [2] Y. Kuroda. *Prog. Theor. Phys.*, 51:1269, 1974.
- [3] J. Goryo and M. Sigrist. *J. Phys. C*, 12:L599, 2000.
- [4] J. Goryo and M. Sigrist. *Europhys. Lett.*, 57:578, 2002.
- [5] G. E. Volovik. *JETP*, 67:1804, 1988.
- [6] J. Goryo and K. Ishikawa. *Phys. Lett. A*, 246:549, 1998.
- [7] J. Goryo and K. Ishikawa. *Phys. Lett. A*, 260:294, 1999.
- [8] E. Talyor and C. Kallin. *Phys. Rev. Lett*, 108:157001, 2012.

## P-27

de Hass-van Alphen effect of the itinerant weak ferromagnetic filled skutterudite  $\text{LaFe}_4\text{As}_{12}$ 

N. Nakamura<sup>1</sup>, T. Namiki<sup>2</sup>, T. D. Matsuda<sup>1</sup>, R. Higashinaka<sup>1</sup>, Y. Aoki<sup>1</sup>, R. Settai<sup>3</sup>, Y. Onuki<sup>4</sup>,  
H. Sato<sup>1</sup> and H. Harima<sup>5</sup>

<sup>1</sup>Department of Physics, Tokyo Metropolitan University, Hachioji 192-0397, Japan

<sup>2</sup>Department of Materials Science and Engineering, University of Toyama, Toyama 930-8555, Japan

<sup>3</sup>Department of Physics, Niigata University, Niigata, 950-2181, Japan

<sup>4</sup>Department of Physics, Ryukyu University, Nakagami 903-0213, Japan

<sup>5</sup>Graduate School of Science, Kobe University, Kobe 657-8501, Japan

The filled-skutterudite compounds  $\text{LaFe}_4\text{P}_{12}$  ( $\text{LaFe}_4\text{As}_{12}$  and  $\text{LaFe}_4\text{Sb}_{12}$ ;  $T$  = rare earth;  $T = \text{Fe, Ru and Os}$ ; and  $X = \text{P, As and Sb}$ ) crystallizing in the cubic  $\text{LaFe}_4\text{P}_{12}$ -type structure (space group #203,  $\bar{3}$ ) have attracted much attention because of their novel physical properties. Among  $\text{LaFe}_4\text{P}_{12}$  compounds, while  $\text{LaFe}_4\text{P}_{12}$  is a Pauli paramagnet with the electronic specific heat coefficient  $\gamma = 57 \text{ mJ/K}^2\text{mol}$ ,<sup>1</sup>  $\text{LaFe}_4\text{As}_{12}$  and  $\text{LaFe}_4\text{Sb}_{12}$  show Curie-Weiss behaviors and enhanced  $\gamma$  values, i.e., 135 and 200  $\text{mJ/K}^2\text{mol}$ , respectively.<sup>2,3</sup> In order to understand these unusual electronic states, we have measured, for the first time, the de Hass-van Alphen (dHvA) effect of  $\text{LaFe}_4\text{As}_{12}$  using high quality single crystals to determine the Fermi surface.

High-quality single crystals of  $\text{LaFe}_4\text{As}_{12}$  with the residual resistivity ratio of 280 have been synthesized under high pressure of 4 GPa at 1000 °C. The dHvA measurements have been performed by two different methods, i.e., modulation coil method and cantilever method using a top loading dilution refrigerator down to 60 mK with a 17 T superconducting magnet. The angular dependence of the dHvA frequency was measured every 4.5 degrees between the principal field directions. The angular dependences of the dHvA frequencies indicate that the Fermi surface consists of at least one spherical sheet and multiply connected sheet. It has been also revealed that the cyclotron effective mass  $m^* = (0.9-1.0)m_0$  is roughly two times larger than those obtained from a band calculation.

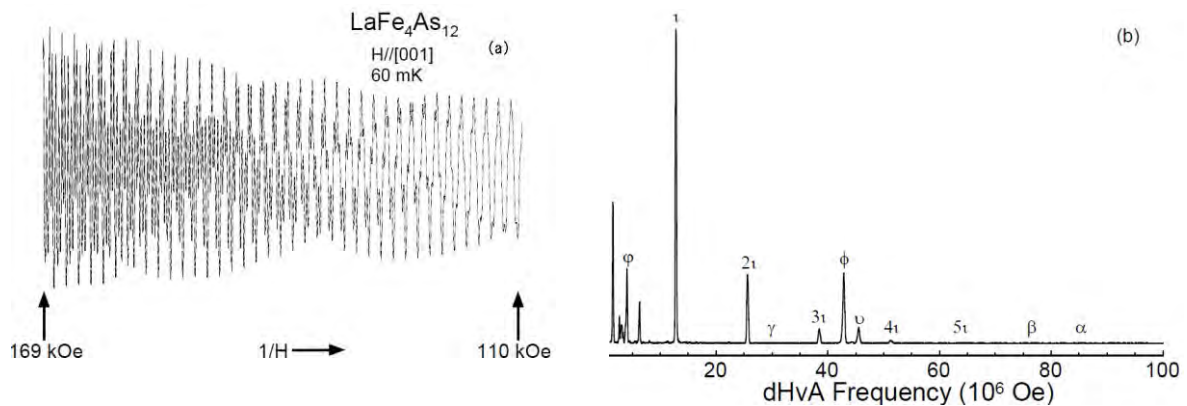


Fig. 1. (a) Typical dHvA oscillations and (b) its fast Fourier transformation spectrum for the field near the [001] direction in  $\text{LaFe}_4\text{As}_{12}$ .

[1] G. P. Meisner, G. R. Stewart, M. S. Torikachvili, and M. B. Maple:Proc. LT-17, p. 711, (1984).

[2] T. Namiki et.al: J. Phys. Soc. Jpn. 9 074714 (2010) .

[3] K. Tanaka et.al: J. Phys. Soc. Jpn. 6 103704 (2007).

# P-28

## Field tuned ferromagnetic instabilities in the ferromagnetic superconductor URhGe and related materials

D. Aoki<sup>1,2</sup>

<sup>1</sup>IMR, Tohoku University, Oarai, 311-1313, Japan

<sup>2</sup>INAC/PHELIQS, CEA-Grenoble, 38054 Grenoble, France

The coexistence of ferromagnetism and superconductivity is one of the most interesting topics in the correlated electron systems[1]. The microscopic coexistence is established in three uranium ferromagnets, UGe<sub>2</sub>, URhGe and UCoGe. The spin-triplet state is believed to be realized, because the spin-singlet state is not compatible with the large internal field due to the ferromagnetism. Surprisingly the field-reentrant (reinforced) superconductivity is observed with the extremely large upper critical field. The unusual superconducting behavior is due to the ferromagnetic fluctuations and Fermi surface instabilities under magnetic field. The microscopic evidence for the ferromagnetic fluctuations is given by the NMR experiments. The Fermi surface instabilities at high fields are clearly observed in the quantum oscillations and thermopower measurements. We review our recent studies on URhGe and UCoGe with fine tuning field angle and pressure, focusing on the Fermi surface instabilities and field induced phenomena[2,3,4]. Furthermore we present our new results on the reentrant superconductivity tuned by the uniaxial stress[5]. This work was done in collaboration with G. Knebel, G. Bastien, A. Gourgout, B. Wu, A. Pourret, J. P. Brison, D. Braithwaite, J. Flouquet, A. Nakamura, Y. Tokunaga, S. Kambe, A. Nikitin, A. de Visser, A. Miyake.

This work was supported by J-Physics and KAKENHI.

[1] D. Aoki and J. Flouquet: J. Phys. Soc. Jpn. 81, 011003 (2012)

[2] B. Wu, et al. Nature Com. 8, 14480 (2017).

[3] G. Bastien, et al.: Phys. Rev. Lett. 117, 206401 (2016).

[4] A. Gourgout, et al.: Phys. Rev. Lett. 117, 046401 (2016).

[5] D. Braithwaite et al.: to be published

## Development of Scanning Hall Probe Microscopy toward Observation of Novel Magnetic Domains

Kazutoshi Emi, Takuya Aoyama, Yoshinori Imai, and Kenya Ohgushi  
Tohoku University, Sendai 980-8578, Japan

### [Introduction]

Electric and magnetic multipoles appear in a material depending on what kind of symmetry are broken. If a spatial inversion symmetry is broken, electric dipoles become finite. A ferroic order of electric dipole is known to be ferroelectrics, in which the electric polarization is ordered. If a time reversal is broken, magnetic dipoles become finite. A ferroic order of magnetic dipole is known to be ferromagnets, in which the magnetic moment (spin) is ordered. If both spatial inversion and time reversal symmetry are broken, magnetic quadrupole moments, which are rank-2 odd-parity magnetic moments, could be finite. A material with ferroic order of magnetic quadrupole can be called as quadrupole magnet. This novel class of materials include a classical magnetoelectric material  $\text{Cr}_2\text{O}_3$ .

We here focus on  $\text{BaMn}_2\text{As}_2$  as a candidate material of quadrupole magnets.  $\text{BaMn}_2\text{As}_2$  has  $\text{ThCr}_2\text{Si}_2$ -type structure classified to tetragonal space group  $4/mmm$ . Neutron diffraction experiments revealed that magnetic moments of  $\text{Mn}^{2+}$  ions show  $d$ -type antiferromagnetism below  $T_N \sim 625$  K (FIG. 1(a)) [1]. The magnetic space group in the antiferromagnetic phase is  $4/m'm'$ , in which both spatial inversion and time reversal symmetry are broken. The magnetic point group  $4/m'm'$  is nothing but the symmetry held by  $d$ - $d$ -type magnetic quadrupole, so that one can recognize  $\text{BaMn}_2\text{As}_2$  as a quadrupole magnet (FIG. 1(b)). As in ferromagnets, there are domain structures in a quadrupole magnet  $\text{BaMn}_2\text{As}_2$ ; there are two types of ferroic order of magnetic quadrupoles with distinct sign, which are connected with each other by spatial inversion or time reversal symmetry. Such kind of domain structures are expected to be visualized by detecting weak magnetic fields generated by magnetic quadrupoles. Therefore, we developed a scanning Hall probe microscope to detect local magnetic fields.

### [Methods]

We constructed a scanning Hall probe microscopy by using Hall elements HG-166A-2U and HW-101A-E manufactured by Asahi Kasei Electronics Corporation. The Hall elements were attached to a probe made of a brass rod. The sample surface were scanned with this probe by moving the stage on which the sample is placed. At each point on the surface, Hall voltage is acquired and it is converted to magnetic field by using Hall coefficient of each element. The measurement system is controlled by using LabVIEW software (National Instruments). The samples used for the measurement are a magnetized Fe, a single crystal of  $\text{Cr}_2\text{O}_3$ , and a single crystal of  $\text{BaMn}_2\text{As}_2$ .  $\text{BaMn}_2\text{As}_2$  single crystals were synthesized by the self-flux method.

### [Results]

Our scanning Hall probe microscope can detect weak magnetic field of the order of  $100 \mu\text{T}$  for a restricted area of  $0.070 \text{ mm}^2$ . By using this apparatus, we succeeded in visualizing the domain structure of ferromagnetic Fe. However, we could not detect any meaningful signal from possible quadrupole magnets,  $\text{Cr}_2\text{O}_3$  and  $\text{BaMn}_2\text{As}_2$ . This is probably because the magnetic fields generated by magnetic quadrupoles is less than  $10 \mu\text{T}$ . To overcome this difficulty, we are intending to improve Hall elements which have high spatial resolution and magnetic field detection capability.

[1] Y. Singh, *et al.*, Phys. Rev. B **80**, 100403 (2009).

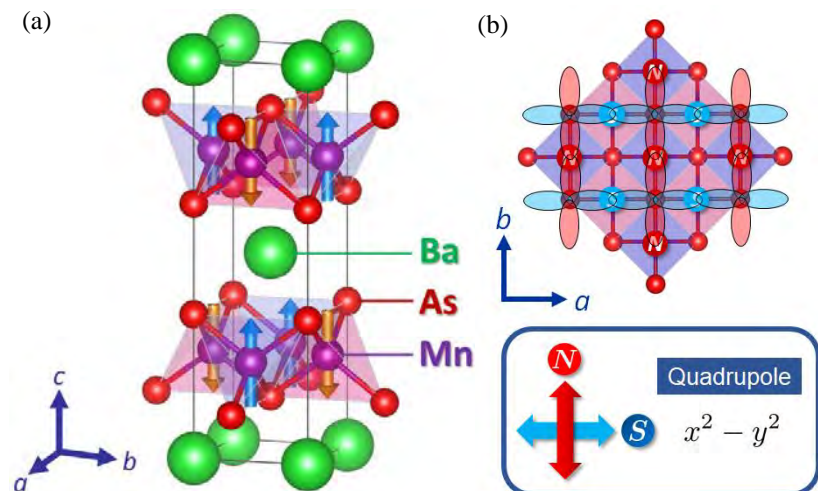


FIG. 1(a) Crystal and magnetic structure of  $\text{BaMn}_2\text{As}_2$ .  
(b) Magnetic quadrupole order on the square lattice of Mn and As.

## Systematic Study of the 4<sup>th</sup> Electronic State and Low-Energy Phonon in the Light-Rare-Earth RBe<sub>13</sub>

H. Hidaka<sup>1</sup>, S. Yamazaki<sup>1</sup>, R. Nagata<sup>1</sup>, K. Mizuuchi<sup>1</sup>, N. Miura<sup>1</sup>, S. Mombetsu<sup>1</sup>, C. Tabata<sup>2</sup>, Y. Shimizu<sup>3</sup>,  
T. Yanagisawa<sup>1</sup>, and H. Amitsuka<sup>1</sup>

<sup>1</sup> Graduate School of Science, Hokkaido University, Japan

<sup>2</sup> KEK, IMSS, CMRC, Japan

<sup>3</sup> IMR, Tohoku University, Japan

The intermetallic compounds RBe<sub>13</sub> (R = rare earths and actinides) crystallize in the NaZn<sub>13</sub>-type cubic structure (space group  $Fm\bar{3}c$ ,  $Oh^6$ , No. 226), whose unit cell contains R atoms in 8a site, Be<sup>I</sup> atoms in 8c site, and Be<sup>II</sup> atoms in 96h site [1]. It is characteristic that the unit cell has two cage-like structures: the R atom is surrounded by 24 Be<sup>II</sup> atoms, nearly forming a snub cube, and the Be<sup>I</sup> atom is surrounded by 12 Be<sup>II</sup> atoms, forming an icosahedron cage. Among them, UBe<sub>13</sub> is well known as the second heavy-fermion superconductor discovered by Ott *et al.* in 1983 [2]. Despite extensive studies over 30 years, the exact nature of the superconductivity for UBe<sub>13</sub> still remains unresolved. This puzzle may mainly stem from the difficulty in understanding the 5<sup>th</sup> electronic state of this system, such as a valence state, *c* hybridization effect, and crystalline-electric-field effect. In addition, it has been reported that UBe<sub>13</sub> possesses a phonon mode associated with the presence of a low-energy Einstein phonon [3], so that it is necessary to reveal a role of the low-energy phonon in the electronic state via an electron-phonon coupling. Recently, we have performed a systematic study on the light-rare-earth RBe<sub>13</sub> compounds [4-6], since it is expected that the understanding of 4<sup>th</sup> electronic state will bring important insights for understanding the 5<sup>th</sup> electronic state in UBe<sub>13</sub>. In this presentation, we summarize results of electrical resistivity, specific heat, magnetization, and X-ray diffraction measurements using single-crystalline samples of LaBe<sub>13</sub>, PrBe<sub>13</sub>, NdBe<sub>13</sub>, SmBe<sub>13</sub>, EuBe<sub>13</sub>, and GdBe<sub>13</sub>. The main obtained summaries, including the results reported previously [3,7,8], are as follows: (i) the *c* hybridization effect is weak, and the 4<sup>th</sup> electronic state can be explained by a localized picture for R<sup>3+</sup> even at low temperatures, (ii) magnetic RBe<sub>13</sub> compounds prefer a helical magnetic ordered state, and (iii) the low-energy phonon mode should be commonly present in the present systems.

The present work was supported by JSPS KAKENHI Grant Number JP15H05882, JP15H05885 and JP15K21732 (J-Physics), and the Strategic Young Researcher Overseas Visits Program for Accelerating Brain Circulation from the Japan Society for the Promotion of Science.

- [1] M. W. McElfresh *et al.*, *Acta Cryst. C* **6**, 1579 (1990).
- [2] H. R. Ott *et al.*, *Phys. Rev. Lett.* **50** (1983) 1595.
- [3] B. Renker *et al.*, *Phys. Rev. B* **32**, 1859 (1985).
- [4] H. Hidaka *et al.*, *J. Phys. Sci. Jpn.* **86**, 023704 (2017).
- [5] H. Hidaka *et al.*, *J. Phys. Sci. Jpn.* **86**, 076703 (2017).
- [6] R. Nagata *et al.*, 71th JPS Annual Meeting (Tohoku Gakuin Univ.) 19aBL-7.
- [7] E. Bucher *et al.* *Phys. Rev. B* **11**, 440 (1975).
- [8] F. Bourée-Vignerot, *Phys. Scr.* **27** (1991).

## P-31

Study of angle resolved photoemission spectroscopy in Dirac fermion system NiTe<sub>2</sub>S. Miyasaka<sup>1</sup>, M. Nishino<sup>1</sup>, Z. H. Tin<sup>1</sup>, T. Adachi<sup>1</sup>, S. Ideta<sup>2,3</sup>, K. Tanaka<sup>2,3</sup>, H. Usui<sup>1</sup>, K. Kuroki<sup>1</sup>, and S. Tajima<sup>1</sup><sup>1</sup>Department of Physics, Graduate School of Science, Osaka University, Osaka 560-0043, Japan<sup>2</sup>UVSOR Facility, Institute for Molecular Science, Okazaki 444-8585, Japan<sup>3</sup>School of Physical Sciences, The Graduate University for Advanced Studies (SOKENDAI), Okazaki 444-8585, Japan

Transition metal dichalcogenides with layered structures show a variety of physical phenomena such as the charge density wave, superconductivity and so on [1]. Recent experimental studies on Pd and Pt dichalcogenides with CdI<sub>2</sub>-type structure have indicated that these systems have new exotic electronic state, type II Dirac fermion state [2-3]. The results of angle resolved photoemission spectroscopy (ARPES) have revealed that the Dirac point exists at (0,0,k<sub>z</sub>) and the Dirac cone is strongly tilted along  $\Gamma$ -A direction (k<sub>z</sub>-direction) in the Pd and Pt dichalcogenides.

In the present work, we have performed the measurements of ARPES in NiTe<sub>2</sub> to clarify the electronic structure and confirm the existence of Dirac fermions in this system. NiTe<sub>2</sub> also has the CdI<sub>2</sub>-type structure and is a related system of the Pd and Pt dichalcogenides [1]. The single crystal of NiTe<sub>2</sub> was grown by Bridgeman technique. The ARPES experimental was carried out at BL-7U in UVSOR Facility, Institute for Molecular Science.

The band calculation in consideration of spin-orbit interaction has indicated that as well as Pd and Pt systems, NiTe<sub>2</sub> is the type II Dirac fermion system with the Dirac point at (0,0,k<sub>z</sub>). The results of ARPES also suggested the existence of Dirac point at (0,0,k<sub>z</sub>). We measured the band dispersion along k<sub>||</sub> (k<sub>||</sub>⊥k<sub>z</sub>) at different k<sub>z</sub>. At k<sub>z</sub>=0, there are several hole- and electron-like bands around  $\Gamma$  and K points, respectively. With increasing k<sub>z</sub>, the energy level of the hole-like band around  $\Gamma$  point decreases, and the top of this band touches Fermi level at k<sub>z</sub>~0.2c\*. At this k<sub>z</sub>, the band dispersion around  $\Gamma$  point shows a linear k<sub>||</sub>-dependence. This result has suggested that Dirac point exists very near Fermi level at (0,0,~0.2c\*) in NiTe<sub>2</sub>.

This work was supported by KAKENHI Grant Number JP16H01075.

[1] J. A. Wilson and A. D. Yoffe, *Adv. Phys.* **18**, 193 (1969).

[2] Han-Jin Noh, Jinwon Jeong, En-Jin Cho, Kyo Kim, B. I. Min, *Phys. Rev. Lett.* **119**, 016401 (2017).

[3] Kenan Zhang, Mingzhe Yan, Haoxiong Zhang, Huaqing Huang, Masashi Arita, Zhe Sun, Wenhui Duan, Yang Wu, and Shuyun Zhou, arXiv:1703.04242.

# P-32

## Multi-orbital aspects of heavy fermion behavior in LiV<sub>2</sub>O<sub>4</sub>

H. Shinaoka<sup>1</sup>, Y. Nomura<sup>2</sup>, S. Biermann<sup>3</sup>, M. Harland<sup>4</sup>, A. I. Lichtenstein<sup>4</sup>

<sup>1</sup>Department of Physics, Saitama University, Saitama, Japan

<sup>2</sup>Department of Applied Physics, University of Tokyo, 7-3-1 Hongo, Bunkyo-ku, Tokyo, 113-8656, Japan

<sup>3</sup>Centre de Physique Theorique, École polytechnique, CNRS, Université Paris-Saclay, F-91128 Palaiseau, France

<sup>4</sup>Institut für Theoretische Physik, Universität Hamburg, Jungiusstraße 9, 20355, Hamburg, Germany

Pyrochlore-type oxides are model systems for studying the effects of spin-orbital interplay and geometrical frustration. LiV<sub>2</sub>O<sub>4</sub> is a 3d spinel compound. The first reported heavy fermion system without f electrons in this system 20 years ago. Despite of extensive studies in the last two decades, the origin is still under debate. By means of LDA+DMFT (dynamical mean-field theory) method, we reveal the connection between the heavy fermion behavior and the multi-orbital aspects of the compound from first-principles calculations. We show that the eg' orbitals act as a reservoir which keeps the filling of the a1g orbital close to half filling, e.g.,  $n \sim 0.8$ . A single-orbital model would not show a heavy fermion behavior at  $n \sim 0.8$ . In LiV<sub>2</sub>O<sub>4</sub>, the Hund's coupling plays an important role in stabilizing the heavy fermion behaviour in this substantially doped region. .

H.S. was supported by JSPS KAKENHI Grants No. 16H01064 (J-Physics) and No. 16K17735. J.O. was supported by JSPS KAKENHI Grants No. 26800172 and No. 16H01059 (J-Physics).

## DFT+DMFT approach to multipolar ordering in f-electron materials

J. Otsuki<sup>1</sup>, K. Yoshimi<sup>2</sup>, and H. Shinaoka<sup>3</sup><sup>1</sup>Department of Physics, Tohoku University, Sendai 980-8578, Japan<sup>2</sup>Institute for Solid State Physics, University of Tokyo, Chiba 277-8581, Japan<sup>3</sup>Department of Physics, Saitama University, Saitama 338-8570, Japan

A number of rare-earth materials exhibit long-range order of localized moment of 4f electrons. The order parameters of low-temperature phases are classified by means of the multipolar expansion of the charge-density and spin-density distributions. Because of strong spin-orbit coupling, the total angular momentum  $J$  is a good quantum number and high-rank multipoles may exist. Extensive investigations in the last two decades have established that high-rank multipoles often play dominant role in some rare-earth and actinide compounds, leading to rich phase diagrams including, e.g., the electronic quadrupole and the magnetic octupole [1].

The microscopic origin of multipolar ordering is explained by the RKKY interactions. For practical calculations of order parameters and transition temperatures of the individual material, one needs to take realistic energy-band structure into account. Complexity of rare-earth materials, however, lies in those electronic structure. In particular, strong correlations, which is not considered in ordinary density-functional-theory (DFT) calculations, give rise to damping of quasiparticle excitations and spectral-weight transfer between low and high energies. Recent advances in electronic structure calculations using dynamical mean-field theory (DMFT) combined with DFT enable first-principles calculations for strongly correlated materials [2]. The next important step of the DFT+DMFT method is to compute the two-particle correlations toward prediction of phase transition including multipolar ordering [3].

We compute momentum-dependent susceptibilities in DFT+DMFT approach and investigate multipolar ordering in rare-earth and actinide materials. We present details of the computational scheme together with demonstrative results for multipolar susceptibilities in CeB<sub>6</sub>.

J.O. was supported by JSPS KAKENHI Grant Nos. 26800172, 16H01059 (J-Physics). K.Y. was supported by Building of Consortia for the Development of Human Resources in Science and Technology, MEXT, Japan. H.S. was supported by JSPS KAKENHI Grant Nos. 15H05885 (J-Physics), 16K17735.

[1] See for example, Y. Kuramoto, H. Kusunose, A. Kiss, *J. Phys. Soc. Jpn.* **78**, 103704 (2006).

[2] G. Kotliar, S. Y. Savrasov, K. Haule, V. S. Oudovenko, O. Parcollet, and C. A. Marianetti, *Rev. Mod. Phys.* **78**, 865 (2006)

[3] J. Kuneš, I. Leonov, P. Augustinsky, V. Krapek, M. Kollar and D. Vollhardt, *Euro. Phys. J.* **226**, 2641 (2017)

Spectral Change in  $3d$ - $4f$  Resonant Inelastic X-ray Scattering of Ce intermetallics

N. Sasabe and T. Uozumi

Graduate School of Engineering, Osaka Prefecture University, Sakai, Osaka 599-8531, Japan

Ce intermetallics show a lot of macroscopic phenomena, such as heavy fermion behavior, magnetical/multipole ordering, Kondo effects, and super conductivity, and they have been paid attention to so far. The variety of these phenomena is attributed to the ground-state property of Ce in compounds, which is characterized by competition between Ruderman-Kittel-Kasuya-Yosida (RKKY) interaction and Kondo interaction: The former leads to a long-range magnetically ordered state, while the latter to the so-called Kondo singlet (KS) state. The relationship of the competition for Ce intermetallics is basically classified in Doniach phase diagram. For example,  $\text{CeB}_6$  is categorized in the RKKY regime, and shows antiquadrupole (AFQ) and antiferromagnetic (AFM) ordering below 3.2 K and 2.3 K, respectively. However,  $\text{CeB}_6$  also shows Kondo behaviour, corresponding to Kondo temperature  $T_K \simeq 2$  K [1,2]. This means that the RKKY interaction can compete with the Kondo interaction in  $\text{CeB}_6$ . Thus, in order to clarify the ground-state character of Ce intermetallics, the comprehensive understanding for the competition between Kondo interaction and RKKY interaction is required.

X-ray core-level spectroscopy is an efficient technique to investigate the electronic states of strongly correlated systems. Recent years, experimental techniques have been rapidly developing and, especially, the progress in experimental resolution has enabled us to observe fine spectral features, which were not previously observed. These advantages will enable us to observe spectral fine features related to the difference in the ground-state character of Ce intermetallics.

In this study, we report the spectral change due to the Kondo effect for  $\text{CeB}_6$ ; for the Kondo effect, the different electronic states for the KS and the localized-spin (LS) are compared [3]. Moreover, we show the AFQ ordering effects in resonant inelastic X-ray scattering (RIXS). In order to simulate the electronic state of  $\text{CeB}_6$  with AFQ ordering, we use an impurity Anderson model including realistic valence structure and a simplified RKKY interaction [4].

[1] N. Sato, A. Sumiyama, S. Kunii, H. Nagano, and T. Kasuya, J. Phys. Soc. Jpn. **54**, 1923 (1985).

[2] Y. Ōnuki, T. Komatsubara, P. H. P. Reinders, and M. Springford, J. Phys. Soc. Jpn. **58**, 3698 (1989).

[3] N. Sasabe, H. Tonai, and T. Uozumi, J. Phys. Soc. Jpn. **86**, 093701 (2017).

[4] F. J. Ohkawa, J. Phys. Soc. Jpn. **52**, 3897 (1983).

## Ground-state phase diagram of the $S = 1$ one-dimensional lattice model with a uniaxial anisotropy under transverse field

Kohei Suzuki and Kazumasa Hattori

Tokyo Metropolitan University, Hachioji 192-0397, Japan

Some of Uranium compounds have been paid attention for their coexistence of ferromagnetism (FM) and superconductivity (SC) [1]. URhGe is one of such ferromagnetic superconductors and the SC disappears when a magnetic field  $H \sim 2$  T parallel to the hard magnetization axis, but reappears for  $H = 9 \sim 13$  T. The superconducting transition temperature  $T_{SC}$  is strongly enhanced around  $H \sim 12$  T. This enhancement is expected to be caused by the FM fluctuations when the Curie temperature is suppressed under the transverse magnetic fields. Taking into account such fluctuations, several theoretical proposals have been done [2-4].

We focus on the one-dimensional chain of URhGe and analyzed the  $S = 1$  one-dimensional lattice model with a uniaxial anisotropy  $D$  under a transverse field  $h$  by means of density matrix renormalization group [5]. The Hamiltonian in this study is

$$H = -t \sum_{i=1}^{N-1} \sum_{\sigma} \left( c_{i,\sigma}^{\dagger} c_{i+1,\sigma} + \text{h.c.} \right) + J \sum_{i=1}^N \mathbf{s}_i \cdot \mathbf{S}_i - h \sum_{i=1}^N (s_i^x + S_i^x) - D \sum_{i=1}^N (S_i^z)^2$$

Here,  $\mathbf{s}_i$  is the  $S = 1/2$  spin operator for the conduction electron  $c_{i,\sigma}$  ( $\sigma = \uparrow, \downarrow$ ) and  $\mathbf{S}_i$  is the  $S = 1$  spin operator of the localized spin, and the others are in a standard notation.

We find various phase such as FM, antiferromagnetism (AFM), Tomonaga-Luttinger liquid (TLL), and Kondo plateau (KP) phases in  $h$ - $J$  ground state phase diagram as shown in Fig. 1. The ordered states (FM, AFM) are both Ising like, while their mechanisms are different; the gain in the kinetic energy favors the FM and the " $2k_F$ " Ruderman-Kittel-Kasuya-Yosida interaction [6] does the AFM. In the KP phase, local singlets formed by the conduction electrons and the localized spins are very strong, which leads to the pseudo plateau in  $K = 1/N \sum_{i=1}^N \langle s_i \cdot S_i \rangle$  as shown in Fig. 2. The TLL occupies a large part of the phase diagram and the spin correlations are long range in this phase. For sufficiently high fields, a fully polarized state appears.

On the basis of the results within the one-dimensional model, we discuss the mechanism for the SC in URhGe. Of interest is the meta-magnetic behavior observed around 12 T [1], and we consider it a key to understanding the shape of the superconducting dome. In our model, such behavior is, indeed, found between the FM and the KP and we discuss these results and relations between the SC and FM.

This work is supported by a Grant-in-Aid for Scientific Research [Grant No. 16H0107900] from the Japan Society for the Promotion of Science.

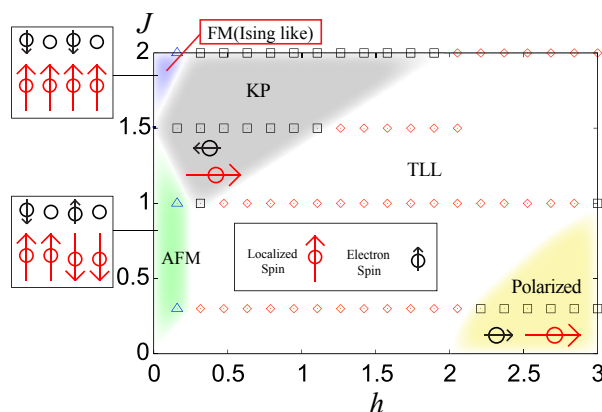


Fig. 1: The  $h$ - $J$  phase diagram of the ground state for the conduction electron number  $n = 0.5$  per site.

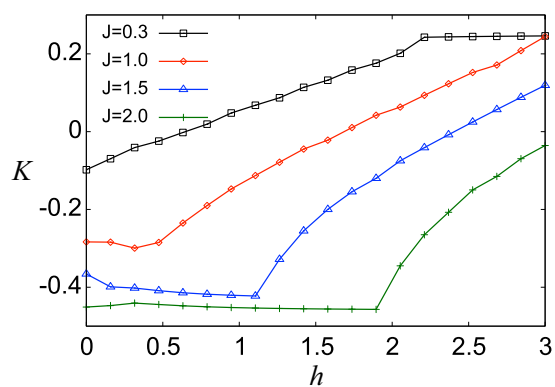


Fig. 2: The  $h$  dependence of  $K = 1/N \sum_{i=1}^N \langle s_i \cdot S_i \rangle$

- [1] D. Aoki and J. Flouquet, J. Phys. Soc. Jpn. **81**, 011003 (2012).  
 [2] V. P. Mineev, Phys. Rev. B **66**, 134504 (2002); Phys. Rev. B **83**, 064515 (2011).  
 [3] K. Hattori and H. Tsunetsugu, Phys. Rev. B **87**, 064501 (2013).  
 [4] Y. Tada et al., Phys. Rev. B **93**, 174512 (2016).  
 [5] S. R. White, Phys. Rev. Lett. **69**, 2863 (1992); Phys. Rev. B **48**, 10345 (1993).  
 [6] M.A. Ruderman and C. Kittel, Phys. Rev. **96**, 99 (1954). T. Kasuya, Prog. Theor. Phys. **16**, 45 (1956). K. Yosida, Phys. Rev. **106**, 893 (1957).

<sup>73</sup>Ge-NQR studies on ferromagnetic superconductor UGe<sub>2</sub> under pressure

Y. Noma<sup>1</sup>, T. Kubo<sup>1</sup>, H. Kotegawa<sup>1</sup>, H. Tou<sup>1</sup>, H. Harima<sup>1</sup>, Y. Haga<sup>2</sup>, E. Yamamoto<sup>2</sup>,  
Y. Ōnuki<sup>3</sup>, K. M. Itoh<sup>4</sup>, E. E. Haller<sup>5</sup>, A. Nakamura<sup>6</sup>, Y. Homma<sup>6</sup>, F. Honda<sup>6</sup>, and D. Aoki<sup>6</sup>

<sup>1</sup>Department of Physics, Kobe University, Kobe 657-8501, Japan

<sup>2</sup>Advanced Science Research center, Japan Atomic Energy Agency, Tokai, Ibaragi 319-1195, Japan

<sup>3</sup>Faculty of Science, University of the Ryukyus, Nishihara, Okinawa 903-0213, Japan

<sup>4</sup>School of Fundamental Science and Technology, Keio University, Yokohama 223-8522, Kanazawa, Japan

<sup>5</sup>Lawrence Berkeley Laboratory, University of California, Berkeley, California 94720, U.S.A.

<sup>6</sup>Institute for Materials Research, Tohoku University, Oarai 311-1313, Ibaraki, Japan.

UGe<sub>2</sub> is a ferromagnet with the ferromagnetic (FM) Curie temperature  $T_{\text{Curie}} = 52$  K at ambient pressure and the  $T_{\text{Curie}}$  is suppressed to 0 K with increasing the pressure. The superconducting (SC) transition was observed in the pressure range of  $P = 1$  to 1.5 GPa.[1] The magnetization shows the enhancement at  $T_X$  in the FM phase.[2] The transition between FM1 with smaller ordered moment and FM2 with larger one is a broad crossover at ambient pressure. However, the crossover region terminates by applying the pressure. The terminal point is called a critical point (CP), above which the FM1-FM2 transition is of a first order. The CP in UGe<sub>2</sub> is reported as  $T_{\text{CP}} = 7$  K and  $P_{\text{CP}} = 1.16$  GPa. The FM1-FM2 transition disappears above  $P = 1.2$  GPa where the superconducting transition temperature is highest. This suggests the SC is involved in the FM1-FM2 transition in UGe<sub>2</sub>.

The NMR measurements were performed in UCoGe which is one of the ferromagnetic superconductors. The measurements of the spin-lattice relaxation rate  $1/T_1$  in UCoGe indicated that UCoGe possesses the Ising type magnetic fluctuation along the magnetic easy axis ( $c$ -axis).[3] In addition, it was reported that the anisotropic fluctuation correlates closely with the SC.[4] On the other hand, the details of the magnetic fluctuations in UGe<sub>2</sub> have not been reported. In order to clarify the anisotropy of the magnetic fluctuations in UGe<sub>2</sub>, we carried out the <sup>73</sup>Ge-NQR measurement under pressure.

Figure 1(a) shows the NQR spectra for the paramagnetic (PM) phase at  $T = 70$  K and  $P = 0$  GPa. The three inequivalent Ge sites exist in one unit cell and the four resonance lines are expected as dominant transition for one <sup>73</sup>Ge site with  $\gamma = 9/2$ . The spectra consist of four peaks in each Ge site and are reproduced well by a simulation using the respective NQR parameters. In the FM phase, the NQR spectra are drastically changed (Fig.1(b)) because of the presence of the internal field which induces the Zeeman splitting. Since the satellite peaks in Ge2 site are equally separated above 11 MHz, the spectra in Ge2 site are reproduced accurately by assuming  $H_{\text{int}} = 5.6$  T.

We measured  $T_1$  and the spin-spin relaxation time  $T_2$  to clarify the anisotropy of the magnetic fluctuations at  $T_X$ . Fig.2 shows the temperature dependences of  $1/T_1T$  and  $1/T_2$  at  $P = 0$  and 0.98 GPa. Below  $T_X$ , the suppression of  $1/T_1T$  is observed at 0 and 0.98 GPa. On the other hand,  $1/T_2$  is enhanced near  $T_X$ . The behaviour of  $1/T_2$  shows the large divergence at 0.98 GPa, where is close to  $T_{\text{CP}}$ . These results suggest that the magnetic fluctuations along  $a$  axis is enhanced toward the CP.

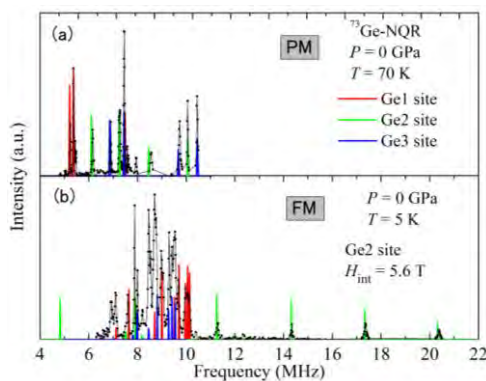


Fig.1. NQR spectra in (a) PM phase and (b) FM phase

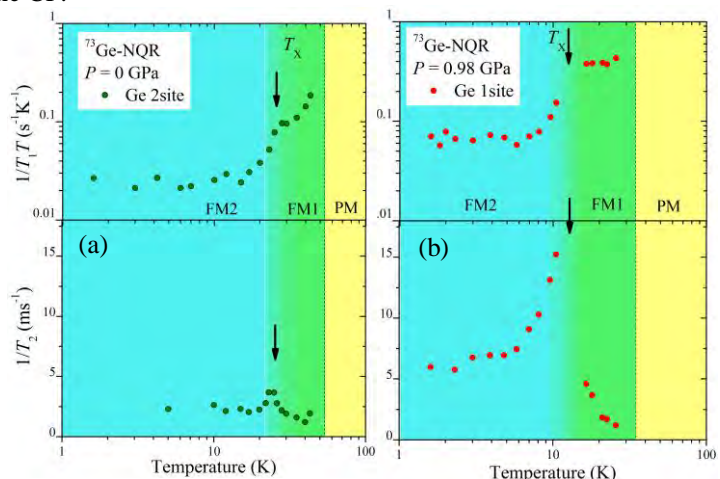


Fig.2.  $T$  dependence of  $1/T_1T$  and  $1/T_2$  at (a)  $P = 0$  and (b) 0.98 GPa

- [1] S. Saxena *et al.*, Nature **06**, 587 (2000).  
 [2] N. Tateiwa *et al.*, J. phys. Soc. Jpn. **0**, 2876(2001).  
 [3] Y. Ihara *et al.*, Phys. Rev. Lett. **105**, 206403(2010).  
 [4] T. Hattori *et al.*, Phys. Rev. Lett. **108**, 066403(2012).

Magnetic-field induced interactions in  $\text{PrTi}_2\text{Al}_{20}$ K. Hattori

Tokyo Metropolitan University, Minami-osawa, Hachioji, 192-0397, Japan

Orbital orders in spin-orbital coupled systems have been attracted much attention due to their novel properties distinct from magnetic counter parts in recent years [1]. Pr-based 1-2-20 compounds are such systems with non-Kramers doublet ground state in the two f-electron ground state. Among several compounds in the Pr-1-2-20 family,  $\text{PrTi}_2\text{Al}_{20}$  is believed to be a ferro-quadrupole metal at low temperature [2]. A naïve expectation about the effects of magnetic fields on the ferro-quadrupole order based on a simple interacting quadrupole model [3,4] is that the order smears out under magnetic fields and it is trivial and is not of interest. However, experiments show a clear phase transition survives even under magnetic fields along [001] direction [5].

In order to explain the temperature-magnetic field phase diagram for  $\text{PrTi}_2\text{Al}_{20}$ , we point out in this poster that there exists field-induced interaction between quadrupole moments that can modify the order parameter configuration under magnetic fields. If this type of interaction is sufficiently large competing with the effective magnetic fields on the quadrupole moments, the first-order ferro-quadrupole order remains even under finite magnetic fields, aligning along the direction *not* parallel to the effective magnetic field. The analysis is based on the symmetry argument and we discuss the nature of possible phase transitions within the Landau theory. As a possible physical origin for this, the interaction mediated by conduction electrons is investigated in details.

This work is supported by a Grant-in-Aid for Scientific Research [Grant No. 16H01079] from the Japan Society for the Promotion of Science.

- [1] T. Onimaru and H. Kusunose, J. Phys. Soc. Jpn. **85**, 082002 (2016).
- [2] A. Sakai, K. Kuga, and S. Nakatsuji, J. Phys. Soc. Jpn. **81**, 083702 (2012).
- [3] K. Hattori and H. Tsunetsugu, J. Phys. Soc. Jpn. **83**, 034709 (2014).
- [4] K. Hattori and H. Tsunetsugu, J. Phys. Soc. Jpn. **85**, 094001 (2016).
- [5] T. Taniguchi et al., unpublished.

Theoretical study of the antiferro quadrupole and superconducting ordered state  
in Pr 1-2-20 systems.

A. Tsuruta<sup>1</sup> and K. Miyake<sup>2</sup>

<sup>1</sup>Department of Materials Engineering Science, Osaka University, Osaka, Japan

<sup>2</sup>Center for Advanced High Magnetic Field Science, Osaka University, Osaka, Japan

Non-Fermi liquid behaviors in the resistivity have been reported in PrV<sub>2</sub>Al<sub>20</sub> [1] and PrIr<sub>2</sub>Zn<sub>20</sub> [2]. Namely, the electrical resistivity is in proportion to  $T^{0.5}$  in rather wide low  $T$  region above the quadrupolar transition temperature  $T_Q$ . The Specific heat increases like  $C_0 - C_1 T^{0.5}$  as  $T$  decreases at  $T > T_Q$ . The ground state of the crystalline-electric field (CEF) of the local f-electron was identified to be the  $\Gamma_3$  non-Kramers doublet in 4f<sup>2</sup> configuration [2]. Such a system in f<sup>2</sup> configuration is expected to exhibit an anomalous behaviors associated with the two-channel Kondo effect.

Tsuruta *et al.* investigated electronic states in the  $M$ -channel Anderson lattice model using the expansion from the limit of large spin-orbital degeneracy  $N$  ( $1/N$ -expansion) [3], and showed that the inclusion of the self-energy of  $O((1/N)^0)$  leads to heavy electrons with degeneracy of channel and spin-orbit. In the single channel case, the imaginary part of the self-energy of conduction electrons (ISE) exhibits the Fermi liquid behavior: i.e. ISE is given by a form proportional to  $T^2$  owing to the inter-site correlation effects in higher order terms in power of  $1/N$ .

In the two-channel case, however, a  $T$ -linear term in ISE at the Fermi level, in contrast to a  $T^2$ -term in the Fermi liquid is found in the limit of  $T \rightarrow 0$ . However, a  $T^{0.5}$  dependence appears in a rather wide low  $T$  region, which explains quite well the non-Fermi liquid behavior observed experimentally.

Because of the anomalous  $T$  dependence of ISE, the chemical potential is given by  $\mu_0 - \mu_1 T^{0.5}$ , and the specific heat is given by  $C_0 - C_1 T^{0.5}$ . We also obtain the scaling behavior  $f(T/T_0)$ ,  $T_0$  is defined as the crossover temperature at which the  $T$  dependence of ISE starts to deviate from the  $\sqrt{T}$  dependence to that with a much lower exponent as  $T$  increases, in electrical resistivity, chemical potential, specific heat and magnetic susceptibility, explaining non-Fermi liquid properties observed in Pr 1-2-20 compounds.[4]

We will present the results of the theoretical study of the antiferro quadrupole and superconducting ordered state in Pr 1-2-20 systems.

[1] A. Sakai and Nakatsuji, J. Phys. Soc. Jpn. **80**, 063701 (2011).

[2] T. Onimaru *et al.*, Phys. Rev. Lett. **106**, 177001 (2011).

[3] A. Tsuruta *et al.*, J. Phys. Soc. Jpn. **68**, 1067 (1999).

[4] A. Tsuruta and K. Miyake, J. Phys. Soc. Jpn. **84**, 114714 (2015).

## Structural stability and electronic state of Rhombohedral As, Sb and Bi

Y. Totoki, H. Funashima and H. Harima

Department of Physics, Kobe University, Kobe 657-0013, Japan

Some of the group 15 elements are semimetal. One can claim this is because that they have both covalent and metallic bonding properties. Among them, As, Sb and Bi are slightly distorted from cubic structure and crystalize in a rhombohedral lattice. It has been reported that the classification of the group 15 elements by using  $p^2 - sp$  hybrids, but the effect of the spin-orbit coupling (SOC) was not considered[1]. For their space group  $R\bar{3}m$ (#166,  $D_{3d}^5$ ), structural parameters are an angle of primitive translation vector  $\alpha_{\text{trg}}$  and a  $z$  parameter for 6c-site with a lattice constant. The distortion is classified into two changes, distortion of unit cell and breaking the local spatial centrosymmetry, where a dimer is formed. Structural parameters of experiments and corresponding to cubic structure are given in Table 1. The change from the simple cubic structure is shown in Figure 1.

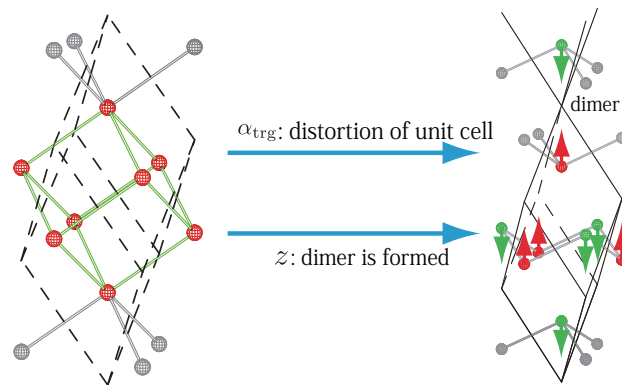


Figure 1: Conceptual diagram of distortion from the cubic structure. Arrows represent the movement of atoms.

Table 1. Structural parameter of rhombohedral group 15 elements and simple cubic structure.

element	experiment			optimized	
	$\alpha_{\text{trg}}$ [deg]	$z$	reference	$\alpha_{\text{trg}}$ [deg]	$z$
$^{33}\text{As}$	54.1	0.227	[2]	54.5	0.230
$^{51}\text{Sb}$	57.2	0.227	[3]	56.5	0.236
$^{83}\text{Bi}$	57.32	0.234	[4]	57.5	0.237
Simple Cubic	60	0.25			

The total energy of unit cell as a function of structural parameters are calculated under the condition that the volume of the unit cell is constant,  $V_{\text{exp}}$ . Calculation method is the full potential linearized augmented plane wave (FLAPW) method based on density functional theory. We explore optimized structure using this calculation and compare the results with experiment. The optimized parameters are also shown in Table 1. SOC is acting on valence  $p$  electrons. As a result, the effect of SOC is the strongest for Bi, against others. To understand structural stability qualitatively, we investigate the band structures from two points, such as the distortion and breaking the local spatial centrosymmetry. We will also discuss the effect of the SOC.

- [1] P. B. Littlewood: J. Phys. C: Solid St. Phys., **13**, 4855 (1980).
- [2] T. Kitagawa and H. Iwasaki: J. Phys. Soc. Jpn **56**, 3417 (1987).
- [3] W-S. Kim: J. Alloys Compd. **252**, 266 (1997).
- [4] S. Golin: Phys. Rev. **166**, 643 (1968).

## Magnetic structure analysis of valence ordering compound YbPd

K. Oyama<sup>1</sup>, A. Mitsuda<sup>1</sup>, K. Ohoyama<sup>2</sup>, T. Matsukawa<sup>3</sup>, Y. Yoshida<sup>3</sup>,  
A. Hoshikawa<sup>3</sup>, T. Ishigaki<sup>3</sup>, K. Iwasa<sup>3</sup>, H. Wada<sup>1</sup>

<sup>1</sup>Department of Physics, Kyushu University, Fukuoka 819-0395, Japan

<sup>2</sup>Graduate School of Science and Engineering, Ibaraki University, Hitachi 316-8511, Japan

<sup>3</sup>Frontier Research Center for Applied Atomic Sciences, Ibaraki University, Tokai 319-1106, Japan

YbPd is a valence fluctuating compound, which crystallizes in the cubic CsCl type structure at room temperature. It shows four phase transitions at  $T_1=125$  K,  $T_2=105$  K,  $T_3=1.9$  K and  $T_4=0.5$  K [1]. With decreasing temperature, the structure is transformed into a tetragonal symmetry ( ) at  $T_1$ . Below  $T_2$ , magnetic  $\text{Yb}^{3+}$  ions and non-magnetic  $\text{Yb}^{2.6+}$  ions are arranged alternately along the  $c$  axis, which means valence order [2, 3]. Valence order is usually observed in materials with worse electrical conductivity. Since YbPd shows metallic electrical conductivity in all temperature region, the valence order in YbPd is intriguing. Below  $T_3$ , the  $\text{Yb}^{3+}$  ions exhibit antiferromagnetism. This magnetic structure should be strongly related to the valence order. Previously, we examined neutron diffraction of powdered and single crystalline samples to determine the magnetic structure. These experiments suggested that the magnetic structure is long-periodic incommensurate structure with  $\mathbf{k}$ -vector of  $(\frac{1}{2}, \frac{1}{2}, 0)$  in terms of cubic structure [4]. However, we could not determine the magnetic structure for the following two reasons. (1) In powder diffraction, we obtained only one magnetic peak possibly due to bad quality of the powdered sample with strains introduced to the lattice in pulverizing the bulk sample. (2) In the single crystal diffraction, a domain structure is formed at the structural transition into the tetragonal symmetry at  $T_1$ . As a result, magnetic diffraction intensities were affected by the domain structure, which prevented us from determining the magnetic structure. Recently, we succeeded in synthesizing strain-less powdered samples and carried out powder neutron diffraction at  $T=0.6$  K and 3 K at BL-20 (iMATERIA) of J-PARC. We observed a few magnetic diffraction peaks whose intensities are not influenced by the domain structure. On the basis of these results, we analyse the magnetic structure.

According to the lattice symmetry, we focused on possible directions of the magnetic moment: along the  $a$ -axis and within the  $ac$ -plane [5]. The  $\mathbf{k}$ -vector of  $(\frac{1}{2}, \frac{1}{2}, 0)$  in terms of the cubic structure corresponds to three possible  $\mathbf{k}$ -vectors of  $(\frac{1}{2}, \frac{1}{2}, 0)$ ,  $(\frac{1}{2}, 0, \frac{1}{2})$  and  $(0, \frac{1}{2}, \frac{1}{2})$  in terms of the tetragonal structure. We refine the diffraction intensities for these three  $\mathbf{k}$ -vectors using the Rietveld method and conclude that  $\mathbf{k} = (\frac{1}{2}, 0, \frac{1}{2})$  explains the measured magnetic diffraction profiles better than the others. The most probable magnetic structure is a sinusoidal structure characterized by the  $\text{Yb}^{3+}$  moments parallel to the  $a$ -axis, amplitude of  $0.3\mu_B$  and  $\mathbf{k}=(0.080,0,0.32)$  in terms of tetragonal symmetry. The magnetic moments in this structure are still thermally fluctuating and should stop fluctuating at lower temperatures. This implies that the magnetic structure transforms into a commensurate one from the incommensurate one below  $T_4$ .

- [1] R.Pott *et al.*, Phys. Rev. Lett. **5**, 481 (1985).
- [2] R.Takahashi *et al.*, Phys. Rev. B **88**, 054109 (2013).
- [3] A.Mitsuda *et al.*, J. Phys. Soc. Jpn. **82**, 084712 (2013).
- [4] M.Sugishima private communication.
- [5] A.S.Wills, Physica B **26**, 680 (2000).

## P-41

Transport property of  $\text{EuT}_2\text{P}_2$  (T=Ni, Co) in magnetic fields

K. Tanabe, I. Yamamoto, A. Mitsuda and H. Wada  
Department of Physics, Kyushu University, Fukuoka 819-0385, Japan

We take notice of two Eu-based ternary phosphides,  $\text{EuNi}_2\text{P}_2$  and  $\text{EuCo}_2\text{P}_2$ , which crystallize in the tetragonal  $\text{ThCr}_2\text{Si}_2$ -type structure. We report the resistance and the Hall effect of these compounds and discuss the behavior associated with the Eu valence instability in terms of the electrical conductivity.

$\text{EuNi}_2\text{P}_2$  exhibits an intermediate valence even at the lowest temperatures and a large electrical specific heat coefficient  $\gamma$  of  $\sim 100 \text{ mJ/mol K}^2$  [1,2]. Recently, this compound is pointed out to be a rare heavy fermion system in Eu-based compound [3]. We attempt to compare the behavior of  $\text{EuNi}_2\text{P}_2$  with that of Ce-based heavy fermion systems. We obtain the following three results.

- 1) Kondo like behavior appears in the temperature dependence of a magnetic contribution to the electrical resistivity by subtracting the resistivity of  $\text{SrNi}_2\text{P}_2$  from that of  $\text{EuNi}_2\text{P}_2$ .
- 2) The behavior of the magnetoresistance in  $\text{EuNi}_2\text{P}_2$  is similar to that observed in Ce-based heavy electron systems.
- 3) The temperature dependence of the Hall resistance shows a change in sign at around 50K and has a downward peak at around 30K. This behavior is very different from that of ordinary metals. We will discuss this behavior by using  $\text{SrNi}_2\text{P}_2$  as a reference material.

As a result of analysis, the temperature dependence of the resistivity, the magnetoresistance, and the Hall effect of  $\text{EuNi}_2\text{P}_2$  is similar to that of the Ce-based heavy electron system, but its characteristic temperature is one order of magnitude larger.

In  $\text{EuCo}_2\text{P}_2$ , an antiferromagnetic order is caused at  $T_N=66.5\text{K}$  by the magnetic moments of  $\text{Eu}^{2+}$  ions under ambient pressure. This compound undergoes a pressure-induced structural transition from an uncollapsed phase to a collapsed phase at around  $P=2.5 \text{ GPa}$  [4,5]. This transition is accompanied by the valence transition of Eu from  $2+$  to  $3+$  and the magnetic transition of Co. At  $P>2.5 \text{ GPa}$ , a magnetic order is caused at  $T=260\text{K}$  by the Co moments. To clarify this intriguing phenomenon, we measured the temperature dependence of the Hall resistivity of a single-crystalline sample under hydrostatic pressure. It is found that  $\text{EuCo}_2\text{P}_2$  exhibits a smaller Hall resistance at  $P<2.5 \text{ GPa}$  and a larger one at  $P>2.5 \text{ GPa}$ .

- [1] B. Perscheid et al., J. Magn. Magn. Matter 47&48 (1985) 410  
 [2] R. A. Fisher et al., Phys. Rev. B 52 (1995) 13519  
 [3] S. Danzenbacher et al., Phys. Rev. Lett. 102 (2009) 026403  
 [4] M. Chefki et al., Phys. Rev. Lett. 80 (1998) 802  
 [5] D. Nakamura et al., JPS Conf. Proc 3 (2014) 011036

## Electronic and spin structures in ullmanite-type PdBiSe and NiSbS

H. Funashima, R. Komiya, and H. Harima

Department of Physics, Kobe University, 1-1 Rokkodai-cho, Nada-ku, Kobe 675-0013, Japan

In the band structure for non-centrosymmetric compounds, even if nonmagnetic case, the spin-degeneracy is lifted in general, which is called parity violation splitting. In this study, we performed the band calculation to ullmanite-type PdBiSe and NiSbS. This structure belongs to the space group  $T^4$  ( $P2_13$ , #198) and contains only 4 three fold rotational axes and 3 two fold screw axes without space inversion symmetry, so it may be called as a non-symmorphic cubic chiral structure.

In the band structure for non-centrosymmetric compounds, even if nonmagnetic case, the spin-degeneracy is lifted in general, which is called parity violation splitting. In this study, we performed the band calculation to ullmanite-type PdBiSe and NiSbS. This structure belongs to the space group  $T^4$  ( $P2_13$ , #198) and contains only 4 three fold rotational axes and 3 two fold screw axes without space inversion symmetry, so it may be called as a non-symmorphic cubic chiral structure. Such the spin structures might cause the physical properties under magnetic fields, e.g. anomalous magnetic break down in de Haas-van Alphen effect [1].

Recently, good single crystals of ullmannite-type structure, PdBiSe and NiSbS are synthesized and the Fermi surface properties was investigated by de Haas-van Alphen (dHvA) effect by Y. Onuki et al [2, 3] and band structure and Fermi surface calculation was performed by H. Harima [4]. Harima indicated that the topology of the Fermi surfaces of both compounds is very similar, but the magnitudes of the splitting, caused by the parity violation, of the Fermi surfaces are quite different. We will compare and discuss about electronic structure, spin structure and chiral spin-texture for these compounds.

In this work, we calculate the spin structure for PdBiSe and NiSbS. Band structure calculations are performed based on an FLAPW (full potential linear augmented plane wave) method with a local density approximation(LDA). The relativistic effect is considered by using the technique proposed by Koelling and Harmon [5] including relativistic electron mass collection, which Harima pointed out important role for spin-splitting in ullmannite-type structure [4]. We draw the spin texture for 149th and 150th band for PdBiSe[Fig.1]. In our result, the orientations of the spins are basically opposite between the 149th band and the 150th band as they are a pair split by spin degree of freedom[Fig.2]. As a result, in Fig.1, there is the vortex of spin texture.

The spin orientations are more opposite in NiSbS than in PdBiSe, because the smaller splitting due to the small spin-orbit coupling causes small effect by other bands.

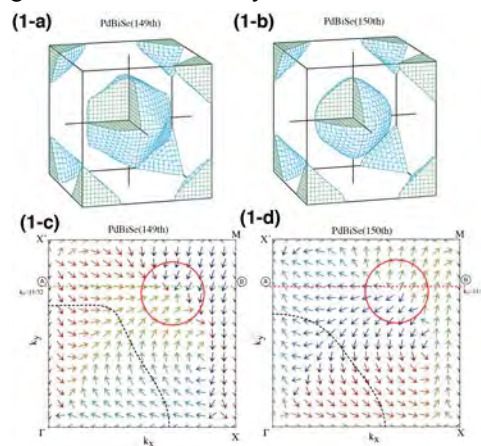


Fig.1 (1-a) Fermi surface of 149<sup>th</sup> and (1-b) that of 150<sup>th</sup> of PdBiSe, (1-c) Spin structure of the 149th band for PdBiSe and that of 150th in the first quadrant. Blue Arrows represents the orientation of the spin, and the black dot line are cross sections of the Fermi surface. The spins are sucked inside a red circle. (right) The energy dispersions parallel to  $\Delta(\Gamma-X)$  axis with  $k_y=0$  and  $11/32$ .

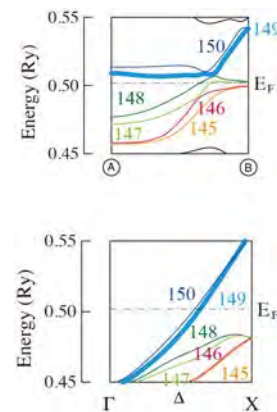


Fig.2 The energy dispersions parallel to  $\Delta(\Gamma-X)$  axis with  $k_y=0$  and  $11/32$ .

- [1] A. Nakamura, et al., J. Phys. Soc. Jpn., **82**, 113705 (2013).
- [2] M. Kakihana, A. Nakamura, A. Teruya, H. Harima, Y. Haga, M. Hedo, T. Nakama, and Y. Onuki, J. Phys. Soc. Jpn. **84** (2015) 033701.
- [3] M. Kakihana, A. Teruya, K. Nishimura, A. Nakamura, T. Takeuchi, Y. Haga, H. Harima, M. Hedo, T. Nakama, Y. Onuki, J. Phys. Soc. Jpn. **84** (2015) 094711
- [4] H. Harima, Physics Procedia. **84** (2015) 094711
- [5] D. D. Koelling and B. N. Harmon: J. Phys. C: Solid State Phys. **10** (1977) 3107.

Unusual Normal and Superconducting States in  $U_{1-x}Th_xBe_{13}$ 

## Probed by Thermal Transport Coefficients

K. Fukuchi<sup>1</sup>, Y. Machida<sup>1</sup>, T. Imai<sup>1</sup>, K. Izawa<sup>1</sup>, Y. Shimizu<sup>2</sup>, Y. Homma<sup>2</sup>, D. Aoki<sup>2</sup><sup>1</sup>Tokyo Institute of Technology, Tokyo 152-8551, Japan<sup>2</sup>Tohoku University, Sendai 950-8578, Japan

$UBe_{13}$  is a heavy fermion superconductor that exhibits Non-Fermi Liquid (NFL) behaviors in the normal state. We have studied the NFL behavior of  $UBe_{13}$  under pressure by means of the transport coefficients and found that an energy scale characterizing the NFL behavior is suppressed with decreasing pressure. On the other hand, it has been reported that by substituting Th for U in  $U_{1-x}Th_xBe_{13}$  the NFL behaviors become much more conspicuous in the vicinity of  $x \sim 0.03$  [1]. Furthermore, it has been reported that the superconducting (SC) state also shows a unique response to Th substitution; the SC transition temperature is monotonously suppressed by Th substitution for  $x < 0.02$  but it turns to increase above  $x \sim 0.02$  and shows maximum around  $x = 0.03$ . In addition,  $U_{1-x}Th_xBe_{13}$  exhibits a double transition in the SC states for  $0.02 < x < 0.04$ . Since both NFL behaviors and SC transition are most pronounced around  $x = 0.03$ , it is expected that there is a close relationship between them.

In this study, low-temperature transport properties were measured for a single crystal of  $U_{0.96}Th_{0.04}Be_{13}$  in order to clarify the nature of NFL behavior in the normal states and the SC states including the gap structure.

In the SC states, thermal conductivity shows weak field dependence at low fields, suggesting absence of quasiparticle excitation induced by magnetic field. On the other hand, it was found that a large residual thermal conductivity exists in the low temperature limit, the absolute value of the residual term is comparable to the one of superconductors with line nodes, indicating that there is a residual density of states near the Fermi level. These results suggest that  $U_{0.96}Th_{0.04}Be_{13}$  has anisotropic full gap or nodes along the direction where the Fermi surface is absent.

In the normal states, we found that Seebeck coefficient divided by temperature  $|S/T|$  exhibits a striking enhancement and it reaches about  $18 \mu V/K^2$ , which is about 100 times larger than that of normal metals. The divergent behavior of  $|S/T|$  is highly contrast with  $T$ -independent  $|S/T|$  for Fermi liquid. Furthermore, we found that the divergent behaviors are most pronounced in magnetic field around the upper critical field  $H_{c2}(0)$ . This behavior is clearly different from the divergent behavior of  $|S/T|$  in  $UBe_{13}$  that is monotonously suppressed by the magnetic field.

In the presentation, based on these results, we will discuss the connection between the NFL behaviors and the enhancement of SC transition temperature in  $U_{1-x}Th_xBe_{13}$ .

[1] E. A. Knetsch *et al.*, *Physica B* **186 - 188**, 251 (1993).[2] R. H. Heffner *et al.*, *Phys. Rev. Lett.* **65**, 2816 (1990).

Effect of Sn substitution on the structural and magnetic properties of PrRu<sub>2</sub>Zn<sub>20</sub>

K. Wakiya<sup>1</sup>, Y. Sugiyama<sup>1</sup>, J. Gouchi<sup>2</sup>, Y. Uwatoko<sup>2</sup>, M. Kishimoto<sup>3</sup>, T. D. Matsuda<sup>3</sup>,  
M. Uehara<sup>1</sup>, and I. Umehara<sup>1</sup>

<sup>1</sup>Department of Physics, Yokohama National University, Yokohama 240-8501, Japan

<sup>2</sup>Institute for Solid State Physics, University of Tokyo, Kashiwa 277-8581, Japan

<sup>3</sup>Department of Physics, Tokyo Metropolitan University, Hachioji, 192-0397, Japan

Caged compounds PrT<sub>2</sub>X<sub>20</sub> (T: transition metal, X = Al, Zn) have attracted much attention because they show various phenomena arising from the quadrupolar degrees of freedom of the 4*f* electrons. For example, PrT<sub>2</sub>Zn<sub>20</sub> (T = Rh, and Ir) and PrT<sub>2</sub>Al<sub>20</sub> (T = Ti and V) undergo the superconducting transition in the presence of quadrupole ordering [1-5]. In these compounds, the crystalline electric field (CEF) ground state of Pr<sup>3+</sup> ion is the nonmagnetic  $\Gamma_3$  doublet that has no magnetic dipole but electric quadrupoles. On the other hand, isostructural PrRu<sub>2</sub>Zn<sub>20</sub> shows a structural transition at  $T_s = 138$  K [6]. Thereby, the CEF ground state doublet is split into two singlets, and thus multipole ordering is avoided. First-principles calculation and inelastic x-ray scattering measurements suggested that the structural transition is attributed to the low-energy vibration of the Zn atom at 16c site (Zn(16c)) encapsulated in an oversized cage [7, 8]. Recently, it is reported that Zn(16c) can be replaced by Sn for the compound with T = Fe and Co [9]. Because the lattice parameter of NdCo<sub>2</sub>Zn<sub>20</sub> is increased by the Sn substitution [9], atomic radius of Sn is larger than that of Zn in this compound. Therefore, it is expected that the structural transition in PrRu<sub>2</sub>Zn<sub>20</sub> is suppressed by the Sn substitution due to the reduction of the cage space.

In this study, we have synthesized the single crystalline samples of Sn substituted PrRu<sub>2</sub>Zn<sub>20</sub> by the Sn-flux method. The samples were characterized by the powder x-ray diffraction and electron probe microanalysis. These characterizations of the obtained samples confirmed that the main phase is of the cubic CeCr<sub>2</sub>Al<sub>20</sub> type. The atomic composition determined by electron-probe microanalysis is PrRu<sub>2.03</sub>Zn<sub>17.35</sub>Sn<sub>2.32</sub>, where it is assumed that the Pr ion is fully occupied. Measurements of the electrical resistivity, specific heat, and magnetization were performed in the temperature range from 2 to 300 K. We found that the electrical resistivity and specific heat show no anomaly down to 2 K, implying the disappearance of the structural transition. The magnetic susceptibility follows the Curie-Weiss law above 50 K with the effective magnetic moment 3.47  $\mu_B$ /Pr. Van-Vleck paramagnetic like-behavior is observed below 10 K, suggesting that the CEF ground state is nonmagnetic.

- [1] T. Onimaru *et al.*, Phys. Rev. Lett. **106**, 177001 (2011).
- [2] T. Onimaru *et al.*, Phys. Rev. B **86**, 184426 (2012).
- [3] A. Sakai *et al.*, J. Phys. Soc. Jpn. **81**, 083702 (2011).
- [4] K. Matsubayashi *et al.*, Phys. Rev. Lett. **109**, 187004 (2012).
- [5] M. Tsujimoto *et al.*, Phys. Rev. Lett. **113**, 267001 (2014).
- [6] T. Onimaru *et al.*, J. Phys. Soc. Jpn. **79**, 033704 (2010).
- [7] T. Hasegawa *et al.*, J. Phys. Conf. Ser. **391**, 012016 (2012).
- [8] K. Wakiya *et al.*, Phys. Rev. B **93**, 064105 (2016).
- [9] Y. Isikawa *et al.*, J. Phys. Soc. Jpn. **84**, 074707 (2015).

Magnetotransport of  $\text{CaMn}_2\text{Bi}_2$  in pulsed high magnetic fieldYoshiaki Koike<sup>1</sup>, N. Abe<sup>1</sup>, Y. Tokunaga<sup>1</sup>, K. Akiba<sup>2</sup>, M. Tokunaga<sup>2</sup>, and T. Arima<sup>1</sup><sup>1</sup>Department of Advanced Materials Science, University of Tokyo, Kashiwa, 277-8561, Japan<sup>2</sup>International MegaGauss Science Laboratory, Institute for Solid State Physics, University of Tokyo, Kashiwa, 277-8581, Japan

Novel quantum transport has been investigated in so-called Dirac/Weyl semimetal, such as  $\text{Cd}_3\text{As}_2$  [1], TaAs [2]. In contrast, quantum transport phenomena associated with the lack of both time reversal and space inversion symmetries remain experimentally elusive.

In this study, we infer that  $\text{CaMn}_2\text{Bi}_2$  is a candidate material which shows novel quantum transport phenomena induced by Mn moments on a buckled honeycomb lattice.  $\text{CaMn}_2\text{Bi}_2$  belongs to space group  $P\bar{3}m1$ . Mn spin moments are arranged antiferromagnetically below  $T_N=154$  K. While the basic electronic structure was recently reported in single crystal of  $\text{CaMn}_2\text{Bi}_2$  [3], there is no report on magnetotransport properties in high magnetic fields.

Here we report unusual magnetotransport properties of a single crystal of  $\text{CaMn}_2\text{Bi}_2$  in pulsed high magnetic field. Upon increasing magnetic field below 30 K, the in-plane resistivity first increased with having a maximum at around 4 T, and then started to decrease. Hall resistivity was proportional to magnetic field above 70 K. Nonlinear Hall resistivity was observed below 40 K. In order to reveal the origin of the novel quantum transport phenomena, we compared magnetotransport properties with magnetization. Unusual behavior observed in magnetoresistance and Hall resistivity did not correspond to that in magnetization. Observed unusual behavior is possibly caused by conduction electrons in  $\text{Bi } 6p_{x,y}$  bands, but not by localized magnetic moments on Mn atoms.

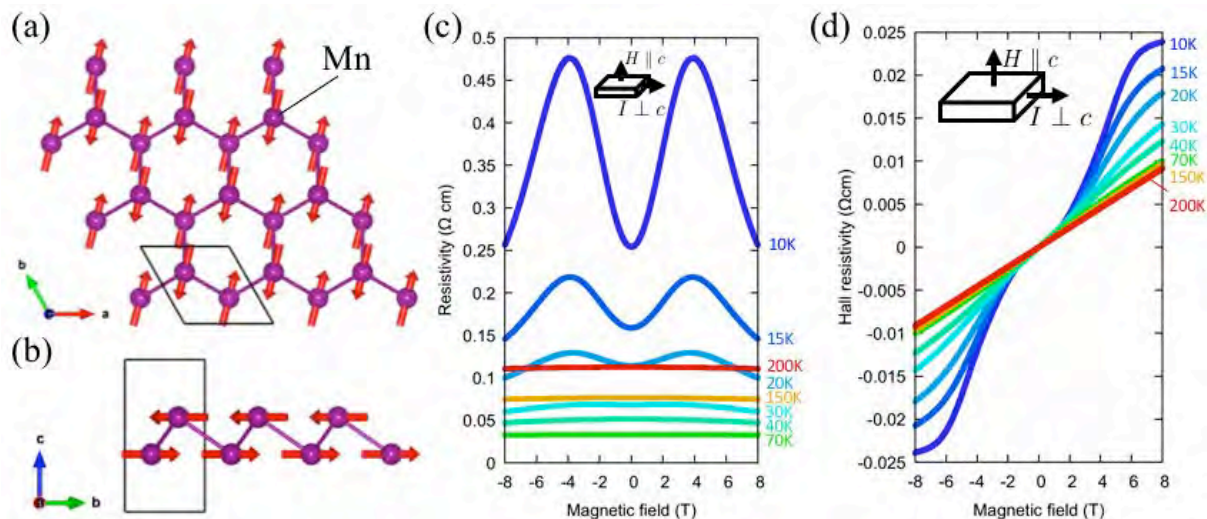


Fig. 1 : Magnetic structure of  $\text{CaMn}_2\text{Bi}_2$  and magnetotransport properties in magnetic field applied in [001] direction. (a) Top view of Mn atoms. (b) Side view of Mn atoms. (c) In-plane resistivity between  $\pm 8$  T [4]. Inset shows a schematic sample configuration for the resistivity measurement. (d) Hall resistivity between  $\pm 8$  T [4].

[1] T. Liang *et al.*, Nat. Mater. **14**, 280284 (2015).[2] X. Huang *et al.*, Phys. Rev. X **5**, 031023 (2015).[3] Q. D. Gibson *et al.*, Phys. Rev. B **91**, 085128 (2015).[4] Y. Koike *et al.*, 2017 JPS annual meeting, 18pL22-9 (2017).

## Magnetic ordering in the d-p model with spin-orbit couplings on a zigzag chain

M. Yatsushiro<sup>1</sup>, S. Hayami<sup>2</sup>  
<sup>1,2</sup>Hokkaido University, Sapporo 060-0810, Japan

The antisymmetric spin-orbit coupling (ASOC), which originates from the atomic spin-orbit coupling in noncentrosymmetric systems, has attracted interest, since it becomes a source of various fascinating phenomena, such as the Dirac electrons at the surface of topological insulator and noncentrosymmetric superconductivity. Meanwhile, such an ASOC appears even in centrosymmetric systems where there is no inversion center at each lattice site, e.g. zigzag chain, honeycomb structure, and diamond structure [1,2]. The ASOC on these lattice structures is induced in a staggered way, reflecting the absence of inversion center at each lattice site. This is in contrast to the ASOC in noncentrosymmetric systems where the uniform component of ASOC is activated. Nevertheless, the ASOC on centrosymmetric systems can acquire a net component, once the inversion symmetry is broken by spontaneous electronic orderings. Especially, staggered magnetic orderings lead to intriguing phenomena including magnetoelectric effects, since the spatial inversion and the time-reversal symmetries are broken simultaneously. Furthermore, the staggered magnetic orderings on the systems with the staggered ASOC activate odd-parity multipoles. For instance, as shown in Fig. 1, the staggered magnetic ordering on the zigzag chain induces magnetic quadrupole and toroidal dipole [3]. However, it is still open questions when and how such magnetic orderings with odd-parity multipoles can be realized from the microscopic point of view.

In the present study, we focus on the effect of the staggered ASOC on the magnetic orderings in the multi-orbital system. We consider a multi-orbital system consisting of the d-p model, which incorporates the staggered ASOC on a one-dimensional zigzag chain. We obtain the ground-state phase diagram in the wide range of parameters, such as the ASOC, Coulomb interaction, and the energy splitting between the atomic d-p levels, within the mean-field calculations. We discuss what situation is appropriate to realize the magnetic orderings with odd-parity multipoles, such as magnetic quadrupole and toroidal dipole.

This work has been supported by JSPS KAKENHI Grant Number 16H06590.

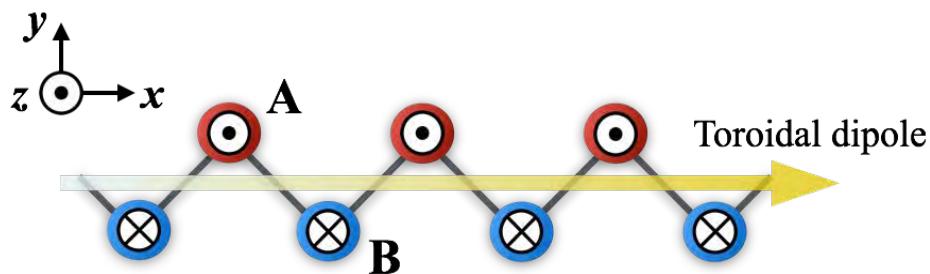


FIG. 1. The staggered magnetic ordering with aligning the magnetic moments along  $z$  axis. This ordering is accompanied by the toroidal dipole.

[1] Y. Yanase: J. Phys. Soc. Jpn. **83** (2014) 014703.

[2] S. Hayami, H. Kusunose, and Y. Motome: Phys. Rev. B **90** (2014) 024432.

[3] S. Hayami, H. Kusunose, and Y. Motome: J. Phys.: Condens. Matter **28** (2016) 395601.

Single crystal growth and peculiar magnetic properties of UIrSi<sub>3</sub>

F. Honda<sup>1</sup>, A. Nakamura<sup>1</sup>, J. Valenta<sup>2</sup>, M. Valiska<sup>2</sup>, B. Vondrackova<sup>2</sup>, P. Opletal<sup>2</sup>, J. Kastil<sup>3</sup>, J. Prchal<sup>2</sup>,  
D. X. Li<sup>1</sup>, Y. Homma<sup>1</sup>, V. Sechovsky<sup>2</sup>, and Dai Aoki<sup>1</sup>

<sup>1</sup> Inst. for Materials Res., Tohoku Univ., Oarai, Ibaraki, 311-1313, Japan

<sup>2</sup> Fac. of Math and Physics, Charles Univ., Prague Czech Republic

<sup>3</sup> Inst. Phys, Acad. Sci. CR, Cukrovanicka, Prague, Czech Republic

The wide variety of electronic properties in *f*-electron compounds provides ample opportunity for systematic studies from both the fundamental interest and application points of view. This variety originates from the hybridization effect of *f*-electrons with surrounded ligands of *d*- and/or *p*-electrons. For a systematic understanding of the nature of *f*-electrons, we focused on the compounds having non-centrosymmetric crystal structure and started investigation of their electronic properties. The compounds without inversion symmetry in the crystal structure has been receiving increasing attention in these days, since the lack of inversion symmetry yields unique physical properties, such as skyrmion [1], superconductivity with parity mixing [2], etc. One of the typical examples studied recently is a RTX<sub>3</sub> (R: rare-earth, T: transition metal, X: metalloid) system with having the BaNiSn<sub>3</sub> type-tetragonal structure. We have tried to grow single crystals of UIrSi<sub>3</sub> with various techniques in order to clarify basic physical properties of actinide 1-1-3 compounds.

Although many kinds of 1-1-3 compounds are known to exist in rare-earth compounds, there are only few compounds reported in actinides, which are ThTSi<sub>3</sub> (T = Rh, Ir), UNiGa<sub>3</sub>, and UIrSi<sub>3</sub>. Among them, ThTSi<sub>3</sub> are superconductors with the superconducting transition temperature ( $T_{sc}$ ) of about 1.8 K, and UNiGa<sub>3</sub> and UIrSi<sub>3</sub> are antiferromagnets with the Néel temperature of 39 and 42 K, respectively. So far, no detailed investigations were done in these compounds. After several attempt, we succeeded to grow single crystals of UIrSi<sub>3</sub> for the first time with floating zone method installed at Charles University Prague.

The results give evidence of an antiferromagnetic ordering at  $T_N = 41.7$  K. Under applied magnetic field the antiferromagnetic ordering is destroyed by a metamagnetic transition (MT) in the critical magnetic field  $H_C$  if the field is applied along *c*-axis ( $\mu_0 H_C = 7.3$  T at  $T = 2$  K). Temperature evolution of the value of  $H_C$  is decreasing with increasing temperature. The MT exhibits an unusual hysteresis as shown in Fig. 1, which becomes reduced with increasing temperature up to 30 K. The magnetoresistance curves reveal the same temperature evolution of MT with asymmetric hysteresis up to 30 K.  $H_C$  manifests as a sharp drop in magnetoresistance curves up to 30 K and above this temperature  $H_C$  is recognized as a maximum in magnetoresistance curves. The scenario of important point at 30 K in the phase diagram is in corroboration with results of specific heat under applied magnetic field. In low magnetic fields below 5.6 T (above 30 K) the magnetic transition is second order-type and above 5.6 T (below 30 K) it is first order-type transition. These results are similar to properties of UNiAl with the tri-critical point [3] which lead us to estimation of presence of tri-critical point in UIrSi<sub>3</sub> at  $T_{cr} \sim 30$  K.

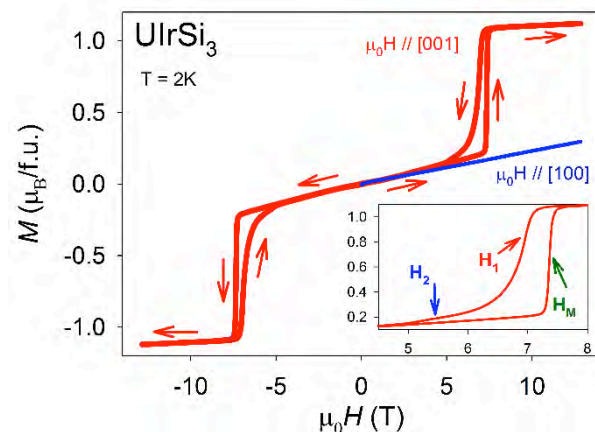


Fig.1 Magnetization curve of UIrSi<sub>3</sub> single crystal at 2 K.

This research is supported by Grant Agency of Charles University (GAUK) by project no. 188115 and the Czech Science Foundation, grant No. P204/15-03777S. This work was also supported by the Japan Society for the Promotion of Science (JSPS) KAKENHI with the grant nos. 15K05156 and 15KK0149.

- [1] X. Z. Yu, Y. Onose, N. Kanazawa, J. H. Park, J. H. Han, Y. Matsui, N. Nagaosa, and Y. Tokura, *Nature* **465**, 901 (2010).
- [2] E. Bauer and M. Sigrist, *Non-Centrosymmetric Superconductors: Introduction and Overview* (Springer, Heidelberg, 2012) Lecture Notes in Physics.
- [3] V. Sechovsky et al., *Phys. Rev. B*, **49** (1994) 13.

Ferromagnetic quantum criticality on  $\text{YbNi}_4\text{P}_2$  probed by  $^{31}\text{P}$ -NMR

Y. Kishimoto<sup>1,2</sup>, T. Kubo<sup>1,2</sup>, H. Yasuoka<sup>2</sup>, K. Kliemt<sup>3</sup>, C. Krellner<sup>3</sup>,  
H. Kotegawa<sup>1</sup>, H. Tou<sup>1</sup>, C. Geibel<sup>2</sup> and M. Baenitz<sup>2</sup>

<sup>1</sup>Kobe University, 1-1 Rokkodai-cho, Nada-ku Kobe, Japan

<sup>2</sup>Max Planck Institute for Chemical Physics of Solids, 01187 Dresden, Germany

<sup>3</sup>Goethe University Frankfurt, 60438 Frankfurt am Main, Germany

Ytterbium based compound  $\text{YbNi}_4\text{P}_2$  crystallizes in the tetragonal  $\text{ZrFe}_4\text{Si}_2$  structure and belongs to the space group  $P4_2/mnm$  (No. 136). (Figure. 1) P-Yb-P trio along  $[110]$  direction in the basal  $c$ -plane rotates by 90 degree in the next  $\pm c/2$  plane, where the P-Yb-P trios lie along  $[110]$  direction in this compound. This compound is expected to show an anisotropic magnetic behavior because the Yb site possesses a local symmetry of orthorhombic. Indeed,  $\text{YbNi}_4\text{P}_2$  shows the anisotropic behavior between the  $c$ -axis and the  $ab$ -plane in the magnetic susceptibility and the electric resistivity.<sup>1,2)</sup> Furthermore, this material shows non-Fermi-liquid (NFL) behavior,  $C/T \propto T^{-0.41}$  and  $\rho \propto T$ , in a low temperature region and a ferro-magnetic ordering at  $T_c = 170$  mK. [3] Thus,  $\text{YbNi}_4\text{P}_2$  is attracted as a candidate of the ferro-magnetic quantum criticality compound. In order to investigate the magnetic anisotropy from a microscopic view, we have carried out  $^{31}\text{P}$ -NMR measurements using a single crystal. Figure 2 illustrates the temperature dependence of the Knight shift for each direction. The slope of the Knight shift clearly changes at around 40 K, implying the CEF effect. This result is consistent with the macroscopic measurements. The temperature dependence of  $1/T_1T$  under the magnetic field  $\mu_0H \sim 2$  T show the anisotropic behavior as well as the Knight shift.  $1/T_1T$  can probe hyperfine-field fluctuations perpendicular to the applied field. Figure 3 shows the  $T$ -dependence of magnetic fluctuation  $S_i(q, \omega)$  ( $i=P1, P2$  and  $c$ ). Above  $T=10$  K, we found the uniaxial anisotropy as  $S_c \approx S_{P1} \gg S_{P2}$ . On the other hand,  $S_c$  progressively increases toward low temperatures below  $T=10$  K, whereas  $S_{P1}$  stays almost constant. This result indicates that an Ising-like magnetic fluctuation develops below 10 K. Such the anisotropy of magnetic fluctuation may lead to non-Fermi liquid behavior in  $\text{YbNi}_4\text{P}_2$ . We will discuss the magnetic anisotropy in the dilution refrigerator temperature range.

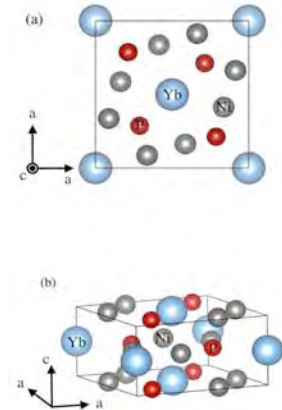


Fig. 1 The view of crystal structure of the tetragonal  $\text{YbNi}_4\text{P}_2$  (space group  $P4_2/mnm$ ;  $Z = 2$ ) from (a)  $c$ -axis and (b) in-plane.

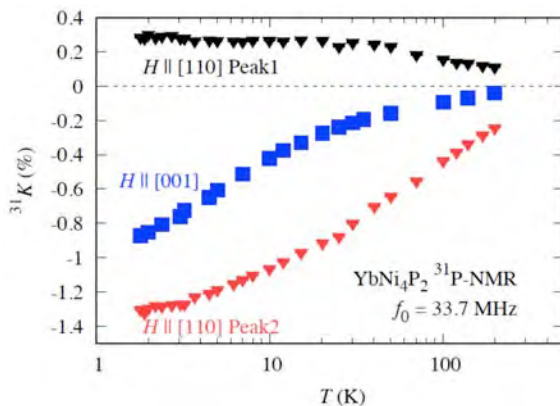


Fig. 2 The  $T$ -dependence of Knight shift for  $^{31}\text{P}$ . The anisotropic behavior clearly appears in all temperature range (1.8-200 K).

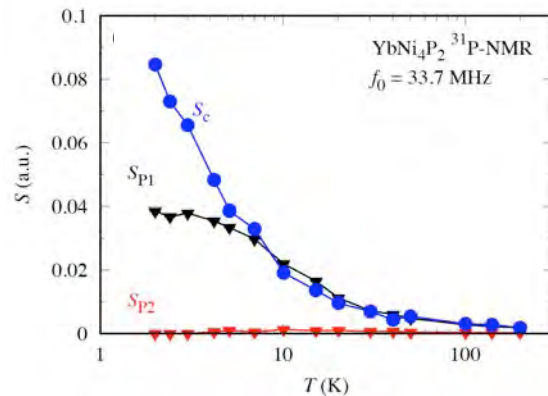


Fig. 3  $T$ -dependences of the magnetic fluctuation component  $S_i$  evaluated by using a relationship between  $1/T_1T$  and the hyperfine field.

- [1] C. Krellner, S. Lausberg, A. Steppke, M. Brando, L. Pedrero, H. Pfau, S. Tencé, H. Rosner, F. Steglich and C. Geibel., *New Journal of Physics* **13** (2011) 103014  
[2] C. Krellner and C. Geibel., *J. Phys. Conf. Ser.* **39** (2012) 012032

## Magnetic fluctuations at the interface region in the artificially engineered heavy-fermion superlattices

Genki Nakamine<sup>1</sup>, Takayoshi Yamanaka<sup>2</sup>, Shunsaku Kitagawa<sup>1</sup>, Kenji Ishida<sup>1</sup>, Masahiro Naritsuka<sup>1</sup>, Tomohiro Ishii<sup>1</sup>, Masaaki Shimozawa<sup>3</sup>, Hiroaki Shishido<sup>4</sup>, Takasada Shibauchi<sup>5</sup>, Takahito Terashima<sup>1</sup>, Yuji Matsuda<sup>1</sup>

<sup>1</sup>Department of Physics, Kyoto University, Kyoto 606-8502, Japan

<sup>2</sup>Department of Physics, Tokyo University of Science, Chiba 278-0022, Japan

<sup>3</sup>Institute for Solid State Physics, the University of Tokyo, Kashiwa 277-8581, Japan

<sup>4</sup>Department of Physics and Electronics, The School of Engineering, Osaka Prefecture University, Sakai 599-8531, Japan

<sup>5</sup>Department of Advanced Materials Science, Graduate School of Frontier Sciences, The University of Tokyo, Kashiwa 277-8561, Japan

Magnetic fluctuations in strongly correlated electron systems have been intensively studied from experimental and theoretical aspects, since most of unconventional superconductors have been discovered in the verge of the magnetic phase, and possess mainly strong antiferromagnetic (AFM) fluctuations[1]. The heavy-fermion(HF) superconductor CeCoIn<sub>5</sub> is one of such unconventional superconductors. The superconducting (SC) transition temperature  $T_c$  of CeCoIn<sub>5</sub> is 2.3 K, which is the highest  $T_c$  among Ce-based HF superconductors. In addition, it has been considered that the superconductivity is mediated by AFM spin fluctuations with quantum critical character.

Recently, progress in the epitaxial-growth technique enabled to synthesize artificial Kondo superlattices (SLs) of alternating layers of HF CeCoIn<sub>5</sub>/conventional-metal YbCoIn<sub>5</sub>, and CeCoIn<sub>5</sub>/spin-density-wave (SDW)-metal CeRhIn<sub>5</sub> with a few atomic layer thickness[2]. The superlattices provide new platform to study the two-dimensional electronic properties of the HF superconductors, interaction between two different block layers (BLs), and magnetic properties at the interfaces.

To study magnetic properties of the SL compounds, nuclear magnetic resonance (NMR) and nuclear quadrupole resonance (NQR) are one of the best experimental probes, since they can provide spatially resolved microscopic information about the target BLs. We performed <sup>59</sup>Co-nuclear magnetic resonance (NMR) measurement on the both SLs focused on spin-fluctuation properties in the CeCoIn<sub>5</sub> BLs. From the result of NMR spin-lattice relaxation rate  $1/T_1$  measurement, we found that compared with bulk data the antiferromagnetic(AFM) spin fluctuation of the CeCoIn<sub>5</sub> BL in the CeCoIn<sub>5</sub>/YbCoIn<sub>5</sub> is suppressed[Fig.]. The suppression is consistent with the result of <sup>115</sup>In-NMR study[3]. We also measured the  $1/T_1$  of CeCoIn<sub>5</sub>/CeRhIn<sub>5</sub> and found that in the CeCoIn<sub>5</sub> BL, there is no suppression of AFM spin fluctuation which is observed in the case of CeCoIn<sub>5</sub>/YbCoIn<sub>5</sub>. Moreover, there is short- $T_1$  component which indicates enhancement of AFM spin fluctuation[Fig.].

The origin of difference of the behavior of  $1/T_1$  is considered as the difference of dominant interaction at the interface and it is indicated that there is possibility that spin fluctuation in BLs of the SLs controllable by changing the combination of compounds of the adjacent BLs or thickness of BLs.

In this poster presentation, I will show details of the experiments and discuss the dominant interactions at the interface.

[1]N. D. Mathur *et al.*, Nature **394**, 39 (1998).

[2] Y. Mizukami, *et al.*, Nat. Phys. **7**, 849 (2011).

[3] T. Yamanaka, *et al.*, Phys. Rev. B **92**, 241105 (2015).

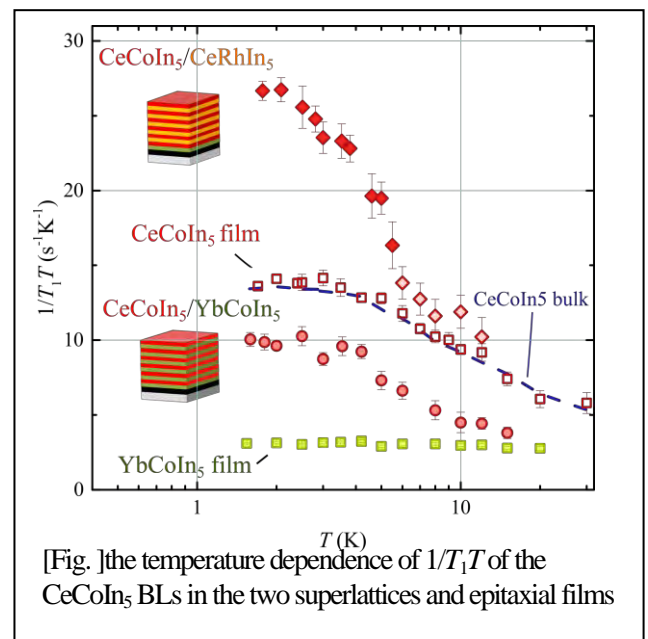


[Fig.] the temperature dependence of  $1/T_1T$  of the CeCoIn<sub>5</sub> BLs in the two superlattices and epitaxial films

## Thermal Hall effect and multipole

Michiyasu Mori

Japan Atomic Energy Agency, Tokai 319-1195, Japan

In a paramagnetic insulator, heat flow is carried by lattice vibrations, which have neither charge nor spin. Heat diffuses from hotter to colder regions and a temperature drop perpendicular to the heat flow could not occur. Nevertheless, it is reported that the paramagnetic insulator,  $\text{Tb}_3\text{Ga}_5\text{O}_{12}$  (TGG), shows a transverse heat conduction under a magnetic field at low temperatures around 5 K [1,2]. This is one kind of thermal Hall effect and is called phonon Hall effect (PHE), since the transverse conduction of phonons is induced by a magnetic field.

In the former half of this presentation, we will discuss that this phenomenon originates from a resonant scattering of phonons at Tb ions [3]. A key is a coupling between the quadrupole moment of Tb ions and the lattice strain. The transverse component of heat flow must be induced by this interaction with a quasi-doublet state of Tb ions, which is split by an applied magnetic field and results in an asymmetric scattering of phonons. The obtained magnitude of the effect is in agreement with experiments and furthermore we predict that the magnitude of the effect grows significantly with temperature.

In the latter half, we will discuss another materials showing the PHE particularly focusing on  $\text{Ba}_2\text{CuSb}_2\text{O}_9$  (BCSO) [4]. In the former case of TGG, Tb ions have a large angular momentum  $J=6$ . Spins and phonons can couple to each another through the crystal field of Tb ions and strain. On the other hand, in the latter case of BCSO, only  $\text{Cu}^{2+}$  has spin  $S=1/2$  which comprises a triangular lattice. There is a big difference between  $J$  and  $S$ , i.e.  $J$  can have multipoles but  $S$  cannot. Then, what is the origin of the PHE in BCSO? This insulator does not show any magnetic long-ranged order. Since the spin gap appears below 50 K, the thermal conductivity in low temperatures is dominated by phonons. It should be noted that a mean free path of phonons in BCSO is quite short such as 'phonon glass'. This must be caused by defects in the triangular lattice. In fact, 5~16% of spins are moved from the triangular lattice into another layer in the crystal. Those depleted spins are observed as orphan spins. We will propose that this defect can induce a magnetic quadrupole by a magnetic field. The quadrupole can couple to the strain, i.e., phonons, and such a coupling can induce the skew scattering of phonons.

The phonon engineering is one of hot subjects in condensed matter physics. If a heat current can be controlled by spins, energy efficiency will be improved by magnetism.

This work is supported by Grant-in-Aid for Scientific Research (Grant No.16H01082) from MEXT, and by the inter-university cooperative research program of IMR Tohoku University.

[1] C. Strohm, G. L. J. A. Rikken, and P. Wyder, Phys. Rev. Lett. **95**, 155901 (2005).

[2] A. V. Inyushkin and A. N. Taldenkov, JETP Lett. **86**, 379 (2007).

[3] M. Mori, A. Spencer-Smith, O.P. Sushkov, S. Maekawa, Phys. Rev. Lett. **113**, 265901 (2014).

[4] K. Sugii, M. Shimosawa, D. Watanabe, Y. Suzuki, M. Halim, M. Kimata, Y. Matsumoto, S. Nakatsuji, M. Yamashita, Phys. Rev. Lett. **118**, 145902 (2017).

[5] H. Kusunose, J. Phys. Soc. Jpn. **77**, 064710 (2008).

[6] M.-T. Suzuki, T. Koretsune, M. Ochi, and R. Arita, Phys. Rev. B **95**, 094406 (2017).

## Observation of the linear dichroism in core-level photoemission reflecting 4f ground-state symmetry of strongly correlated cubic Ce compounds

Yuina KANAI<sup>1,2</sup>, Kohei YAMAGAMI<sup>1,2</sup>, Shuhei FUJIOKA<sup>1,2</sup>, Hidenori FUJIWARA<sup>1,2</sup>,  
Atsushi HIGASHIYA<sup>2,3</sup>, Toshiharu KADONO<sup>2,4</sup>, Shin IMADA<sup>2,4</sup>, Takayuki KISS<sup>1,2</sup>,  
Arata TANAKA<sup>5</sup>, Kenji TAMASAKU<sup>2</sup>, Makina YABASHI<sup>2</sup>, Tetsuya ISHIKAWA<sup>2</sup>,  
Fumitoshi IGA<sup>6</sup>, Takao EBIHARA<sup>7</sup>, and Akira SEKIYAMA<sup>1,2</sup>

<sup>1</sup>*Division of Materials Physics, Graduate School of Engineering Science, Osaka University, Toyonaka, Osaka, Japan*

<sup>2</sup>*RIKEN SPring-8 Center, Sayo, Hyogo, Japan*

<sup>3</sup>*Faculty of Science and Engineering, Setsunan University, Neyagawa, Osaka, Japan*

<sup>4</sup>*Department of Physical Science, Ritsumeikan University, Kusatsu, Shiga, Japan*

<sup>5</sup>*Department of Quantum Matter, ADSM, Hiroshima University, Higashihiroshima, Hiroshima, Japan*

<sup>6</sup>*College of Science, Ibaraki University, Mito, Ibaraki, Japan*

<sup>7</sup>*Department of Physics, Shizuoka University, Shizuoka, Japan*

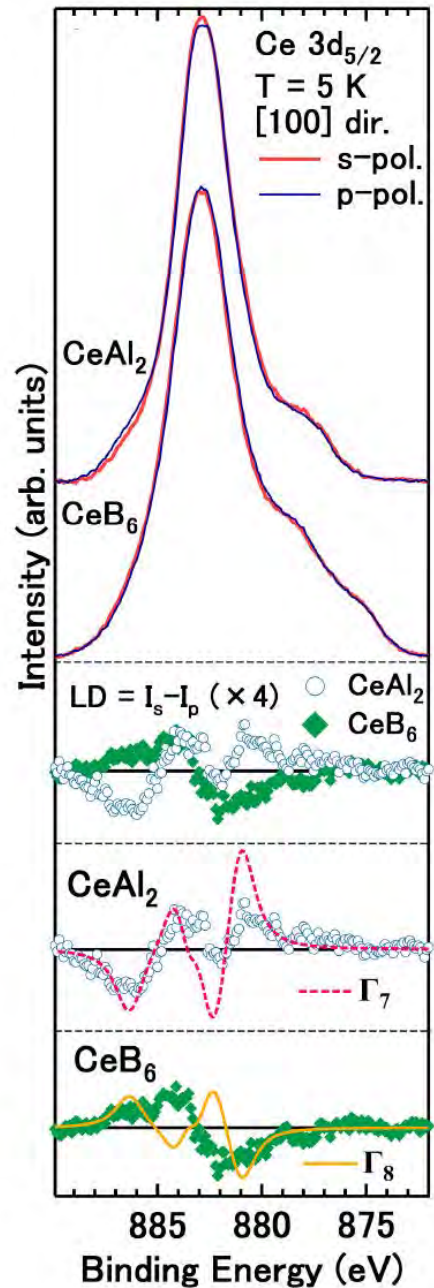
Rare earth-based strongly correlated electron systems show various interesting behavior, for example, formation of heavy fermion, superconductivity, and magnetic/multipolar ordering. Since such phenomena are seen at low temperatures, the information of rare-earth 4f ground-state symmetry is important to clarify mechanisms for these interesting phenomena.

To determine such a local electronic structure, linear dichroism in X-ray absorption spectroscopy (LD-XAS) is powerful [1, 2]. However, LD-XAS cannot be observed for materials in cubic symmetry. On the other hand, rare-earth 3d core-level photoemission process is similar to that for the X-ray absorption except for the final-state energy, linear dichroism in the *angle-resolved* 3d core-level photoemission (LD-PES) also reflects 4f charge spacial distributions. Since there is another controllable measurement parameter in photoemission called as the “photoelectron detection direction” relative to the single-crystalline axis in addition to the excitation-light polarization direction, LD-PES can be applicable for the compounds even in the cubic symmetry. Indeed, we have successfully determined the 4f ground states of tetragonal and cubic Yb compounds by LD in Yb<sup>3+</sup> 3d<sub>5/2</sub> core-level PES spectra [3, 4]. Since LDs are seen in the atomic-like multiplet-split structure in the core-level photoemission final states, they are expected to be observed for Ce compounds with nearly localized Ce<sup>3+</sup> ions. Due to the core-hole potential worked on electrons in outer shell, the Yb<sup>3+</sup> state (3d<sup>9</sup>4f<sup>13</sup> configurations) is well separated from the Yb<sup>2+</sup> state (3d<sup>9</sup>4f<sup>14</sup> configurations) in the 3d PES spectra. On the other hand, since there are the 3d<sup>9</sup>4f<sup>0</sup> and 3d<sup>9</sup>4f<sup>2</sup> states nearby the 3d<sup>9</sup>4f<sup>1</sup> states in Ce 3d core-level PES spectra, the multiplet-split structures might be modified caused by the final-state hybridization effects. Therefore, we have verified whether the LD in the core-level PES for the Ce compounds can be reproduced by the ionic calculations taking the full multiplet and local crystalline electric field (CEF) theories.

We have observed the LD in the Ce 3d<sub>5/2</sub> core-level PES spectra for CeB<sub>6</sub>, CeAl<sub>2</sub> and CeIn<sub>3</sub>. The LD for CeB<sub>6</sub> and that for CeAl<sub>2</sub> have different features where the former indicates the  $\Gamma_8$  ground-state symmetry and the latter is well explained by the simulation for the  $\Gamma_7$  ground state, as shown in the right figure. We have also measured temperature dependence of the LD in the Ce 3d core-level PES for CeB<sub>6</sub>.

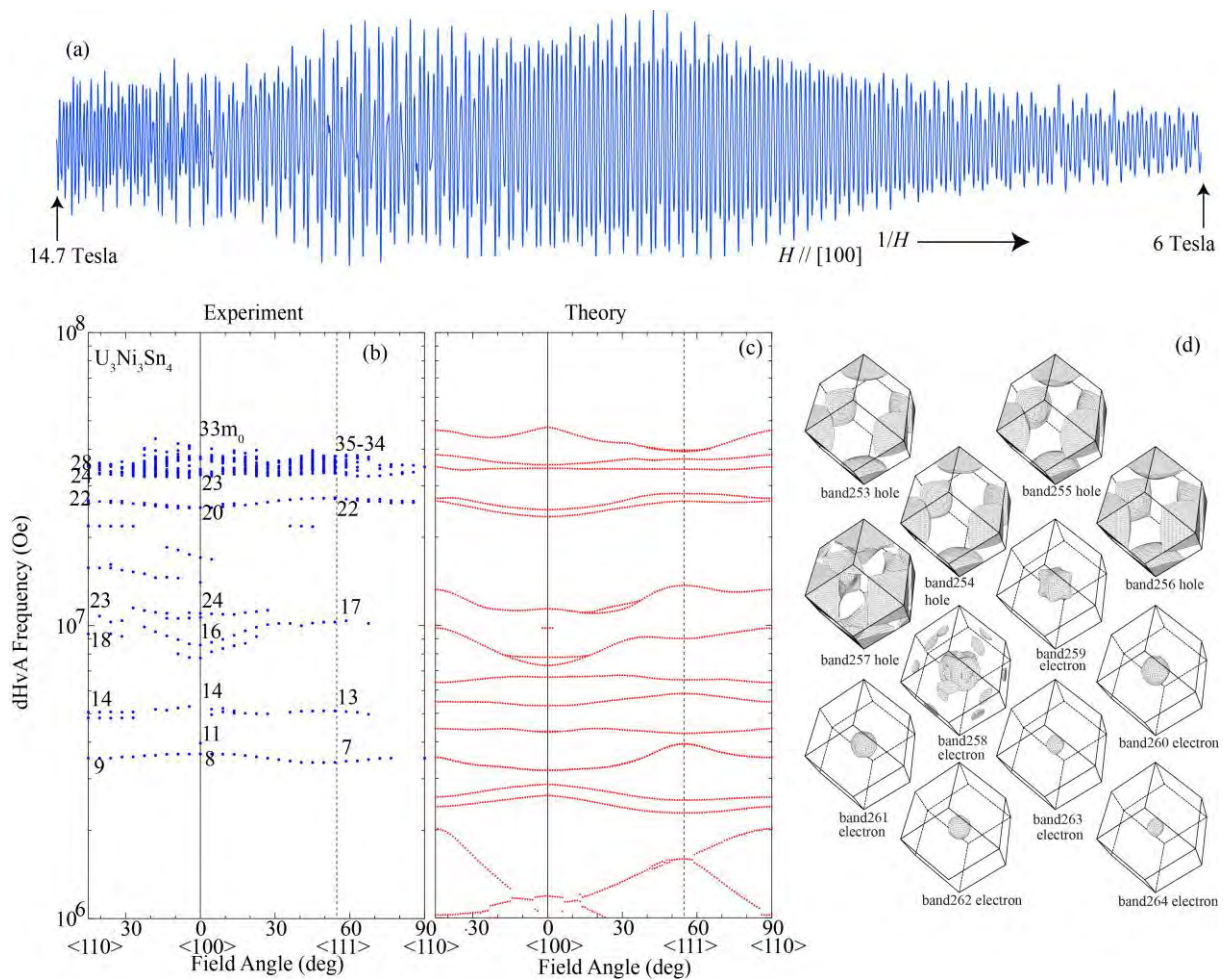
This work was supported by the JSPS KAKENHI Grant Number JP16H01074 (J-Physics), and the JSPS Research Fellowships for Young Scientists.

[1] P. Hansmann *et al.*, Phys. Rev. Lett. **100**, 066405 (2008). [2] T. Willers *et al.*, Phys. Rev. B **80**, 115106 (2009). [3] T. Mori *et al.*, J. Phys. Soc. Jpn. **83**, 123702 (2014). [4] Y. Kanai *et al.*, J. Phys. Soc. Jpn. **84**, 073705 (2015).



Crystal growth and dHvA effect studies of  $U_3Ni_3Sn_4$ A. Maurya<sup>1</sup>, A. Nakamura<sup>1</sup>, Y. Homma<sup>1</sup>, Y. Shimizu<sup>1</sup>, D. X. Li<sup>1</sup>, F. Honda<sup>1</sup>, H. Harima<sup>2</sup>, and D. Aoki<sup>1</sup><sup>1</sup>Institute for Materials Research, Tohoku University, Japan<sup>2</sup>Graduate School of Science, Kobe University, Japan

$U_3Ni_3Sn_4$  is a non-centrosymmetric moderate heavy fermion paramagnetic compound, which crystallizes in  $Y_3Au_3Sb_4$ -type cubic structure in the space group  $I-43d$  (#220) and has lattice parameter,  $a = 9.3575(4)$  Å. A single crystal of  $U_3Ni_3Sn_4$ , grown by high temperature Bridgeman method have exceptionally high residual resistivity ratio ( $RRR$ ), of a value up to 480. Sharp spots in the single crystal x-ray diffraction further attest the well-ordered feature of the grown crystal. This makes it one of the favorable material to be explored by de Haas-van Alphen effect (dHvA). Magnetization, electrical resistivity, and heat capacity measurements are consistent with moderate heavy fermion behavior reported on polycrystalline samples. The dHvA signal obtained in field modulation technique at temperature  $\sim 35$  mK contains several frequencies with a marginal orientation dependence, corresponding to nearly spherical Fermi surfaces. The LDA band structure calculation predicts many Fermi surfaces with nearly spherical shape, and 12 bands crossing the Fermi energy in  $U_3Ni_3Sn_4$ .



The existence of multiple Fermi surfaces and antisymmetric spin orbit coupling in  $U_3Ni_3Sn_4$  lead to partial breaking of the spin degeneracy of the cyclotron orbits. This is marked by multiple splitting of the dHvA frequencies. Some of the splitting dHvA frequencies are due to the magnetic breakdown. From the temperature dependence of the dHvA frequencies we could detect heavy Fermi surfaces with cyclotron effective mass,  $m^*$ , of value as large as  $35 m_0$ .

We acknowledge support from the J-Physics project.

[1] T. Takabatake et al., *J. Phys. Soc. Jpn.* **59**, 12 (1990).

[2] E. Bauer and M. Sigrist: *Non-Centrosymmetric superconductors* (Springer, Heidelberg, 2012) Lecture Notes in Physics, Vol. 847.

[3] D. Shoenberg, *Magnetic oscillations in metals* (Cambridge University Press, 1984).

## Field-insensitive Kondo behavior in $\text{SmT}_2\text{Al}_{20}$ and Superconducting properties in cage-structure compound $\text{LaT}_2\text{X}_{20}$

Akira Yamada, Ryuji Higashinaka, Tatsuma D. Matsuda, and Yuji Aoki  
Tokyo Metropolitan University, Tokyo 192-0397, Japan

$RT_2X_{20}$  family compounds ( $R$ : rare earth,  $T$ : transition metal,  $X$ : Al, Zn, and Cd) crystallizing in the cubic  $\text{CeCr}_2\text{Al}_{20}$ -type structure with the space group #227, have attracted much attention due to the heavy-fermion states with large Sommerfeld coefficient in Yb compounds and the possible quadrupolar-mediated superconductivity in Pr compounds [1]. In  $\text{SmT}_2\text{Al}_{20}$  family, unusually field-insensitive Kondo behavior, such as  $-\log T$  dependent resistivity and large mass enhancement, was found [2].

In recent years, we have studied La-substitution effect on the Kondo behavior in  $\text{SmT}_2\text{Al}_{20}$  and obtained following experimental results from the resistivity and X-ray absorption spectroscopy measurements [3,4].

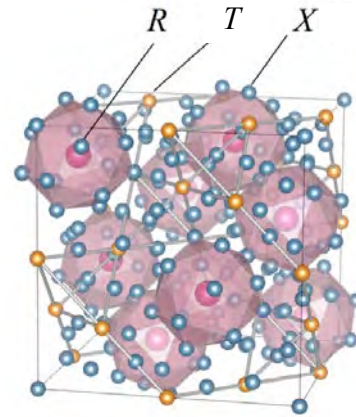


Fig.1 Crystal structure of  $RT_2X_{20}$

- (1) Unusually field-insensitive  $-\log T$  dependences were observed in Sm-diluted compounds with Sm concentration down to 1 %. This finding indicates that the  $-\log T$  dependence is caused by a local single-ion Kondo effect.
- (2) Sm ions are in a mixed valence state with the average valence of +2.87, which is independent on temperature and the Sm concentration.

In some of no-4f reference compounds  $\text{LaT}_2\text{Al}_{20}$ , we have found the emergence of superconductivity. It might be caused by the anharmonic large-amplitude oscillations at the rare-earth  $8a$  site or  $X$ -ion  $16c$  site. We present the superconducting properties in  $\text{LaT}_2\text{Al}_{20}$  comparing with other  $RT_2X_{20}$  superconductors.

- [1] A. Sakai *et al.*, J. Phys. Soc. Jpn **81**, 083702 (2012).
- [2] R. Higashinaka *et al.*, J. Phys. Soc. Jpn. **80**, 093703 (2011).
- [3] A. Yamada *et al.*, Phys. Procedia **75**, 522 (2015).
- [4] A. Yamada *et al.*, J. Phys. Conf. Ser. **683**, 012020 (2016).

Exotic phase transitions in zig-zag structure:  
superconductivity in CrAs and metal-insulator transition in RuAs

H. Kotegawa<sup>1</sup>, K. Matsushima<sup>1</sup>, Y. Kuwata<sup>1</sup>, S. Nakahara<sup>1</sup>, H. Tou<sup>1</sup>,  
K. Takeda<sup>2</sup>, E. Matsuoka<sup>1</sup>, H. Sugawara<sup>1</sup>, T. Sakurai<sup>1</sup>, H. Ohta<sup>1</sup>, and H. Harima<sup>1</sup>  
<sup>1</sup>Kobe University, Kobe 658-8530, Japan

<sup>2</sup>Muroran Institute of Technology, Muroran, Hokkaido 050-8585, Japan

We report several experimental results and band calculations on isostructural CrAs and RuAs, which crystalize in the same orthorhombic structure with non-symmorphic  $a$  space group. Figure 1 shows the crystal structure of CrAs. The Cr atoms form a zig-zag chain along the  $a$  axis, and the inversion symmetry is missing locally at the Cr and As sites. For CrAs, the magnetic transition of a first order into a double-helical state occurs at  $T_N \sim 265$  K. The application of pressure drastically suppresses  $T_N$ , and the HM phase disappears above a critical pressure of  $p_c \sim 0.7$  GPa. Superconductivity appears together with the suppression of the HM phase, showing a maximum superconducting transition temperature of  $T_c = 2.2$  K at  $\sim 1.0$  GPa, after which  $T_c$  decreases gradually with increasing pressure [1,2]. We have observed a clear indication of magnetic fluctuations in the paramagnetic state near  $p_c$  in NQR measurement [3], even though the magnetic transition is of strong first order. The close relationship between the magnetic fluctuations and superconductivity has been also confirmed. We will show the results of Knight shift in the normal state and discuss the anisotropy of the magnetic correlations.

On the other hand, isostructural RuAs shows successive metal-insulator transitions at  $T_{MI1} = 250$  K and  $T_{MI2} = 190$  K [4]. We successfully obtained single crystal by Bi-flux method. It shows clear two metal-insulator transitions as shown by resistivity measurement in Fig. 2. The X-ray diffraction revealed a formation of superlattice below  $T_{MI2}$  through a change of the unit cell from orthorhombic to monoclinic. The multiple As sites observed in the NQR spectrum also demonstrate the formation of the superlattice in the ground state, which is nonmagnetic. The divergence in  $1/T_1$  at  $T_{MI1}$  reveals that the metal-insulator transition is accompanied by a strong critical fluctuation of possible electric origin. Using the structural parameters in the insulating state, the first principle calculation reproduces successfully the reasonable size of nuclear quadrupole frequency,  $\nu_Q$  for multiple inequivalent As sites, ensuring the validity of the structural parameters and the calculation. We will show the calculated electronic state above and below the metal-insulator transition, and discuss the origin of the metal-insulator transition of RuAs with paying attention to the feature of the non-symmorphic space group.

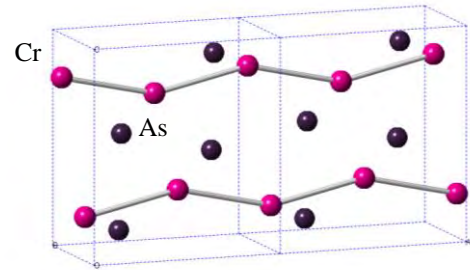


Fig. 1: The crystal structure of CrAs.

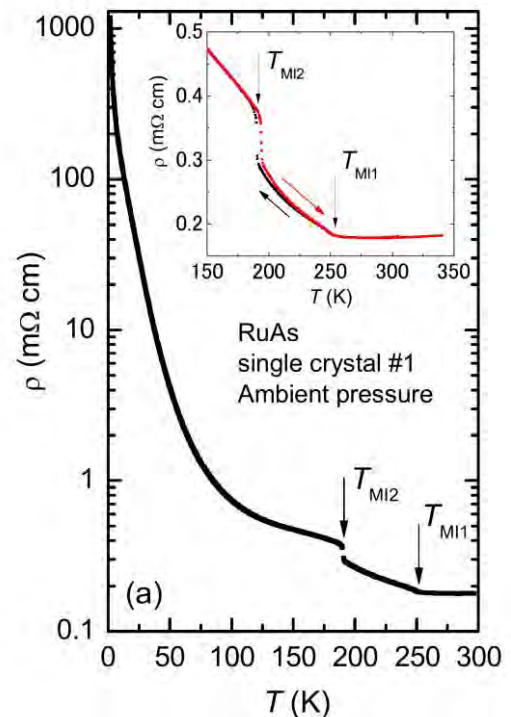


Fig. 2:  $T$  dependence of resistivity of RuAs.

- [1] W. Wu *et al*, Nature Commun. **5**, 5508 (2014).
- [2] H. Kotegawa *et al*, J. Phys. Soc. Jpn. **83**, 093702 (2014).
- [3] H. Kotegawa *et al*, Phys. Rev. Lett. **111**, 117002 (2015).
- [4] D. Hirai *et al*, Phys. Rev. B **85**, 140509(R) (2012).

## P-55

Observation of superlattice reflections in BiS<sub>2</sub> layered superconductor LaO<sub>0.5</sub>F<sub>0.5</sub>BiS<sub>2</sub>

Joe Kajitani<sup>1</sup>, Ryoko Sagayama<sup>2</sup>, Hajime Sagayama<sup>2‡</sup>, Reiji Kumai<sup>2</sup>, Youichi Murakami<sup>2</sup>, Keisuke Matsuura<sup>3</sup>, Masaaki Mita<sup>1</sup>, Takuya Asano<sup>1</sup>, Ryuji Higashinaka<sup>1</sup>, Tatsuma D. Matsuda<sup>1</sup>, and Yuji Aoki<sup>1</sup>

<sup>1</sup> Tokyo Metropolitan Univ., Minami-Osawa 1-1, Hachioji, 192-0397, Tokyo, Japan,

<sup>2</sup> Institute of Materials Structure Science, High Energy Accelerator Research Organization, Tsukuba, Ibaraki 305-0801 Japan

<sup>3</sup> Department of Advanced Materials Science, the University of Tokyo, Kashiwa 277-8561, Japan

Recently, new layered superconducting material was discovered in a quasi-two-dimensional bismuth chalcogenide REO<sub>1-x</sub>F<sub>x</sub>BiS<sub>2</sub> (RE: rare earth) and these have been intensively investigated to clarify a mechanism of superconductivity. The mother material REOBiS<sub>2</sub> is a band insulator or a semimetal. By partial substitution of divalent oxygen ions with univalent fluorine ions, it becomes metallic, resulting in superconductivity. Typical material LaO<sub>0.5</sub>F<sub>0.5</sub>BiS<sub>2</sub> exhibits the superconductivity with  $T_{SC} = 2.7$  K. In this material, superconducting transition temperature further increases by applying hydrostatic pressure with  $T_{SC} = 10.6$  K [1], [2]. A charge density wave (CDW) state is theoretically expected owing to the strong nesting condition of its rectangle Fermi surface. The existence of the CDW state is implied by anomalies in the transport measurements of EuFBiS<sub>2</sub> [3], LaO<sub>0.5</sub>F<sub>0.5</sub>BiS<sub>2</sub> [4]. So far, a long range lattice modulation which indicate a bulk CDW states does not reported by experimental studies.

In this study, we precisely investigated the lattice structure of LaO<sub>0.5</sub>F<sub>0.5</sub>BiS<sub>2</sub> with a single-crystal sample using the synchrotron radiation X-ray diffraction technique using a beam line of BL-8A/B and NE-1A of PF in KEK above 10K. We discover the existence of long-periodic lattice modulation for the first time. Super-lattice structure reflections with the propagation vector  $\mathbf{q} = (\zeta \zeta 0.5)$  appeared at low temperatures (50 K) under ambient pressure with  $\zeta$  of approximately 0.207 as shown in Figure 1. The  $L$  of Miller indices of the vector was 0.5, which is the first experimental evidence indicating the importance of interlayer interaction. The super-lattice reflections disappeared upon the application of pressure along with a significant enhancement of  $T_C$ , which suggests a competitive relationship between the super-lattice structure and the superconductivity.

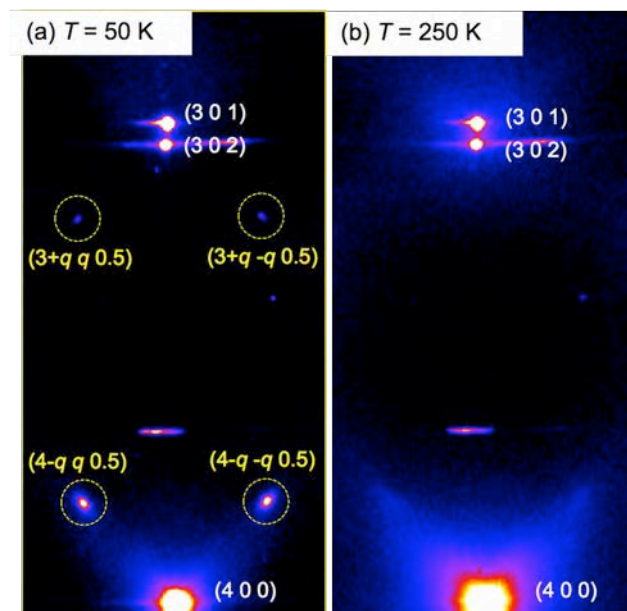


Figure 1. X-ray oscillation photographs observed at 50 K (a) and 250 K (b).

[1] Y. Mizuguchi *et al.*, J. Phys. Soc. Jpn. **81**, 114725 (2012).

[2] H. Kotegawa *et al.*, J. Phys. Soc. Jpn. **81**, 103702 (2012).

[3] H.-F. Zhai *et al.*, Cao, Phys. Rev. B **90**, 064518 (2014).

[4] A. Omachi *et al.*, J. Appl. Phys. **115**, 083909 (2014).

## Mean-field phase diagram for multipole ordering in $f^2$ -electron systems on the basis of a $j$ - $j$ coupling scheme

Ryosuke Yamamura and Takashi Hotta

Tokyo Metropolitan University, Hachioji, Tokyo 192-0397, Japan

In recent decades, multipole ordering in  $f$ -electron systems has been one of important research topics in the field of condensed matter physics [1]. In most cases, theoretical studies on multipole ordering have been phenomenologically performed on the basis of an  $s$ - $d$  coupling scheme from a localized picture. In fact, these studies have succeeded in explaining experimental results concerning multipole ordering, especially in Ce compounds, since  $f$  electrons are considered to be almost localized [2].

However, when localized  $f$  electrons gain itinerant nature due to the hybridization with conduction electrons in rare-earth and actinide compounds with plural numbers of  $f$  electrons, the phenomenological theories sometimes face difficulties to include such itinerant nature and explain the multipole ordering. For instance, in  $\text{PrPb}_3$  with the  $\text{AuCu}_3$ -type simple cubic structure, peculiar modulated anti-ferro (AF) non-Kramers quadrupole ordering has been reported [3], but the mechanism has not been clarified yet. In order to explain such multipole ordering concerning plural numbers of  $f$  electrons, it seems to be important to consider alternative theoretical research complementary to the previous one. Thus, we consider that it is meaningful to develop a microscopic theory for multipole ordering from an itinerant picture.

In this study, as the first step of our research, we consider the two-orbital Hubbard Hamiltonian composed of  $\Gamma_8$  quartet on the basis of a  $j$ - $j$  coupling scheme [4]. This Hamiltonian is considered to be the minimal model to discuss the multipole ordering in  $f$ -electron systems. The Hamiltonian is given by

$$H = \sum_{i\mathbf{a}\tau\tau'\sigma} t_{\tau\tau'}^{\mathbf{a}} f_{i\tau\sigma}^\dagger f_{i+\mathbf{a}\tau'\sigma} + U \sum_{i\tau} n_{i\tau\uparrow} n_{i\tau\downarrow} + U' \sum_i n_{ia} n_{ib} + J \sum_{i\sigma\sigma'} f_{ia\sigma}^\dagger f_{ib\sigma'}^\dagger f_{ia\sigma'} f_{ib\sigma} + J' \sum_{i\tau\neq\tau'} f_{i\tau\uparrow}^\dagger f_{i\tau\downarrow}^\dagger f_{i\tau\downarrow} f_{i\tau\uparrow},$$

where  $f_{i\tau\sigma}$  is the annihilation operator for an electron with spin  $\sigma$  ( $= \uparrow, \downarrow$ ) in the  $\tau$  ( $= a, b$ ) orbital at site  $i$ ,  $\mathbf{a}$  is the vector connecting nearest neighbor sites,  $t_{\tau\tau'}^{\mathbf{a}}$  denotes the nearest-neighbor hopping amplitude between adjacent  $\tau$  and  $\tau'$  orbitals along  $\mathbf{a}$  directions,  $n_{i\tau\sigma} = f_{i\tau\sigma}^\dagger f_{i\tau\sigma}$ , and  $n_{i\tau} = \sum_{\sigma} n_{i\tau\sigma}$ . The coupling constants  $U$ ,  $U'$ ,  $J$ , and  $J'$  indicate the intra-orbital, inter-orbital, Hund's rule, and pair-hopping interactions, respectively. Note that  $J$  and/or  $J'$  are allowed to be negative so as to reproduce the local  $\Gamma_3$  non-Kramers doublet state under the constraint of  $U = U' + J + J'$ , since they are considered to be effective interactions among  $f$  electrons in the  $\Gamma_8$  quartet.

In order to determine the type of multipole order, we define the multipole operator as spin-charge density in the form of one-body operator and construct the mean-field procedure with respect to the multipole operators. When we derive the eigenstate of the mean-field Hamiltonian  $|\psi_{\text{MF}}\rangle$  from a stationary condition for the variational principle with respect to the one-body wave function, we find that  $|\psi_{\text{MF}}\rangle$  satisfies the relation  $\langle\psi_{\text{MF}}|H|\psi_{\text{MF}}\rangle = E_{\text{MF}}$ , where  $E_{\text{MF}}$  is the corresponding eigenvalue. Thus, in our mean-field approximation, we perform the decoupling of two-body interaction terms in  $H$  so as to satisfy the relation  $\langle\psi_{\text{MF}}|H|\psi_{\text{MF}}\rangle = E_{\text{MF}}$ .

As a typical example of our theory, we perform the self-consistent calculations on a simple cubic lattice with the  $2 \times 2 \times 2$  unit cell for the case of  $\nu = 2$ , corresponding to  $\text{Pr}^{3+}$  and  $\text{U}^{4+}$  ions, where  $\nu$  denotes the average  $f$ -electron number per site. The first Brillouin zone is divided into  $8 \times 8 \times 8$  meshes. In Fig. 1, we show the ground-state phase diagram for multipole ordering on the  $(J, J')$  plane for  $U' = 5$ , in which  $O_2^0$  and  $O_2^z$  denote non-Kramers  $\Gamma_3$  quadrupoles, whereas  $J^{4u1}$ ,  $T_{xyz}^{2u}$ , and  $O_{xy}$  denote  $\Gamma_{4u}$  dipole and octupole,  $\Gamma_{2u}$  octupole, and  $\Gamma_{5g}$  quadrupole, respectively. We find four multipole ordered states and the stability of each phase can be explained by the competition among the interaction energies. In particular, we find the AF ordering of  $O_2^0$  and  $O_2^z$ , but their ordering vectors are different from each other. Namely, the order of  $O_2^0$  and  $O_2^z$  are expressed as G-AF and C-AF, respectively.

In the presentation, we will also report the results for the larger unit cell such as  $4 \times 4 \times 4$  lattice and discuss the stability of the multipole phases.

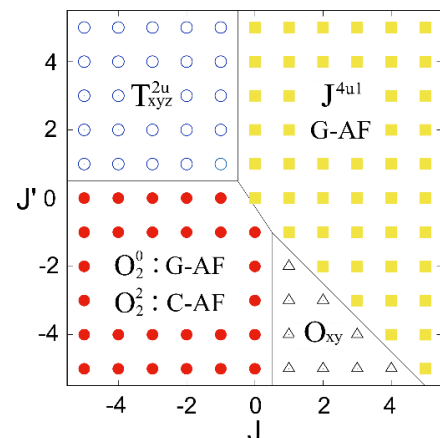


Fig. 1: Ground-state phase diagram for multipole ordering in the simple cubic lattice on the  $(J, J')$  plane for  $U' = 5$ .

[1] P. Santini, S. Carretta, G. Amoretti, R. Caciuffo, N. Magnani, and G. H. Lander: Rev. Mod. Phys. **81** (2009) 807.

[2] O. Sakai, R. Shiina, H. Shiba, and P. Thalmeier: J. Phys. Soc. Jpn. **66** (1997) 3005.

[3] T. Onimaru, T. Sakakibara, N. Aso, H. Yoshizawa, H. S. Suzuki, and T. Takeuchi: Phys. Rev. Lett. **9** (2005) 197201.

[4] T. Hotta and K. Ueda: Phys. Rev. B **6** (2003) 104518.

## NQR study on Ullmannite-type compounds

M. Yogi<sup>1</sup>, M. Morishima<sup>2</sup>, N. Higa<sup>2</sup>, H. Uehara<sup>2</sup>, F. Kubota<sup>2</sup>, M. Kakihana<sup>2</sup>, K. Nishimura<sup>2</sup>, Y. Ashitomi<sup>2</sup>, M. Hedo<sup>1</sup>, T. Nakama<sup>1</sup>, and Y. Ōnuki<sup>1</sup>

<sup>1</sup>Faculty of Science, University of the Ryukyus, Nishihara 903-0213, Japan

<sup>2</sup>Graduate School of Engineering and Science, University of the Ryukyus, Nishihara 903-0213, Japan

The equiatomic ternary compounds of NiSbS and PdBiSe crystallize in the Ullmannite-type cubic chiral crystal structure ( $P_{213}$ ,  $T_4$ , No. 198) [1]. In this crystal structure, the inversion symmetry is broken along [100], [010] and [001] axes, but three-fold symmetry holds in the [111] direction, and each atom in the compound lies on the straight line directed the [111] axis. In order to clarify the electronic states of the cubic chiral crystal structure compounds from the microscopic view point, we carried out the nuclear quadrupole resonance (NQR) measurement. The measurements of  $^{121,123}\text{Sb}$ -NQR and  $^{209}\text{Bi}$ -NQR were performed by using the powder samples, which crushed coarsely the single crystals of NiSbS and PdBiSe grown by the Bridgman method [2]. We obtained the resonance spectra and the nuclear spin-lattice relaxation time  $T_1$ .

In NiSbS, five resonance lines of Sb-NQR corresponding to two isotopes  $^{121}\text{Sb}$  ( $I = 5/2$ ) and  $^{123}\text{Sb}$  ( $I = 7/2$ ) were observed. The nuclear quadrupole frequencies of  $^{121}\text{Sb}$  and  $^{123}\text{Sb}$  are obtained as  $^{121}\nu_Q = 62.076$  MHz and  $^{123}\nu_Q = 38.044$  MHz, respectively. The asymmetry parameter becomes zero ( $\eta = 0$ ) because of the axially symmetric electric field gradient at Sb site.

In PdBiSe, four NQR spectra corresponding to the nuclear spin  $I = 9/2$  of  $^{209}\text{Bi}$  were observed. The nuclear quadrupole frequency  $^{209}\nu_Q = 26.09$  MHz was estimated. The peak splittings were observed in three spectra sited low frequency side among four spectra. The peak shape can be explained by taking into account not only the nuclear quadrupole interaction but also the indirect interaction between Bi nucleus and the surrounding nuclei. This result shows that the nuclear spin indirect interaction is effective on the shape of Bi-NQR spectra in PdBiSe, because of large atomic weight of Pd and Bi compared with Ni and Sb in NiSbS.

The values of  $1/T_1T$  in both compounds of NiSbS and PdBiSe are temperature independent, i.e.,  $1/T_1T = \text{const.}$ , which is the Pauli paramagnetic behaviour as that in normal metal. The ratio between the values of  $1/T_1$  for  $^{121}\text{Sb}$  and  $^{123}\text{Sb}$ ,  $^{121}(1/T_1)/^{123}(1/T_1) = 3.62$ , and that of the values of square of nuclear gyromagnetic ratio  $\gamma$ ,  $(^{121}\gamma)^2/(^{123}\gamma)^2 = 3.41$ , are almost the same, which reveals that the magnetic relaxation process is dominant in NiSbS.

[1] A. J. Foecker and W. Jeischko, J. Solid State Chem. **162**, 69 (2001).

[2] M. Kakihana, *et al.*, J. Phys. Soc. Jpn. **84**, 033701 (2015).

## Magnetic order and coupled charge-density waves in noncentrosymmetric intermetallic TbNiC<sub>2</sub>

C. Tabata<sup>1</sup>, H. Nakao<sup>1</sup>, S. Shimomura<sup>2</sup>, and H. Onodera<sup>3</sup>

<sup>1</sup>Condensed Matter Research Center and Photon Factory, Institute of Materials Structure Science,  
High Energy Accelerator Research Organization, Tsukuba 305-0801, Japan

<sup>2</sup>Kyoto Sangyo University, Kyoto 603-8555, Japan

<sup>3</sup>Tohoku University, Sendai 980-8577, Japan

NiC<sub>2</sub> (= rare earth) compounds have attracted a lot of interests recently as novel systems showing strong couplings between charge density waves (CDW) and magnetism. In NiC<sub>2</sub> compounds, diverse order such as superconductivity, ferromagnetic and antiferromagnetic order appear, coexisting and/or competing with CDW. A recent synchrotron X-ray diffraction experiment revealed that TbNiC<sub>2</sub> exhibits CDW states with two different propagation vectors of  $\mathbf{q}_1 = (0.5, \sim 0.5, 0)$  and  $\mathbf{q}_2 = (0.5, 0.5, 0.5)$ . The former coexists with antiferromagnetic order ( $T_N = 26$  K) while the latter vanishes when the magnetic order sets in [1]. This means that both coexistence and competition between magnetic order and CDW take place simultaneously.

Magnetic field effect on TbNiC<sub>2</sub> gives essential information to unravel the interplay between the CDW and magnetism. Actually, an isostructural GdNiC<sub>2</sub> has a very complicated and interesting magnetic phase diagram with many magnetic phases which correlate with CDW [2]. In order to elucidate magnetic field effect on CDW in TbNiC<sub>2</sub>, we performed a non-resonant X-ray diffraction experiment in magnetic field up to 7.5 T at a synchrotron radiation facility, Photon Factory. Our measurements using a single crystalline sample revealed that the only CDW with  $\mathbf{q}_2$  survives in field-induced phases, in contrast to the case in zero magnetic field. This indicates that the system chooses either of the CDW states with  $\mathbf{q}_1$  or  $\mathbf{q}_2$ , in reference to the magnetic order in each phase (see Fig. 1).

We also carried out resonant X-ray diffraction experiments at the  $\bar{c}$ -edge of Tb for further information from a viewpoint of magnetism. A strong resonant signal at  $\mathbf{q}_1$  was found to develop as decreasing temperature below  $T_N$ , which is a direct evidence of magnetic order of 4f electrons of Tb. We also report magnetization and specific heat measurements, for a discussion of interplay between CDW and magnetism in TbNiC<sub>2</sub>.

[1] S. Shimomura *et al.*, Phys. Rev. B **93**, 165108 (2016).

[2] N. Hanasaki *et al.*, Phys. Rev. B **95**, 085103 (2017).

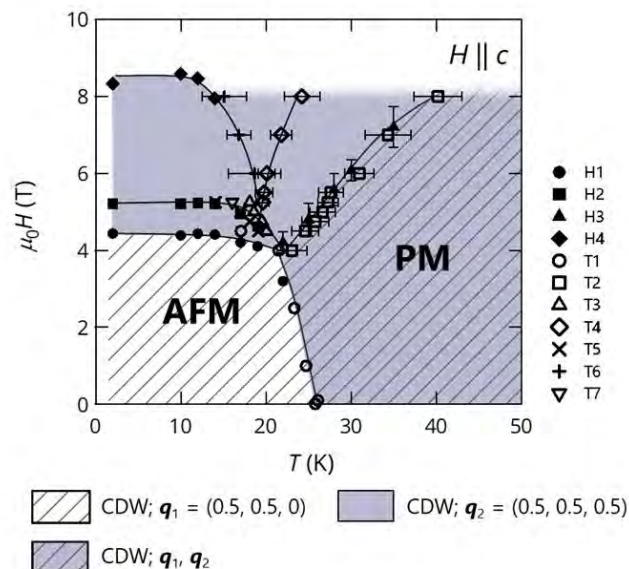


FIG 1. Magnetic-field-temperature phase diagram in TbNiC<sub>2</sub> in magnetic field applied along the  $c$  axis. The phase diagram was obtained from measurements of magnetization and specific heat.

# P-59

## The magnetic field angular dependence of flux-flow resistance in $\text{FeSe}_{1-x}\text{Te}_x$

S. Ayukawa<sup>1</sup>, K. Hirata<sup>2</sup>, D. Kakehi<sup>3</sup>, S. Ooi<sup>2</sup>, T. Noji<sup>4</sup>, Y. Koike<sup>4</sup>, and H. Kitano<sup>3</sup>

<sup>1</sup>Okayama University, Okayama 700-8530, Japan

<sup>2</sup>National Institute for Materials Science (NIMS), Tsukuba 305-0047, Japan

<sup>3</sup>Aoyama Gakuin University, Sagami-hara 252-5258, Japan

<sup>4</sup>Tohoku University, Sendai 980-8579, Japan

Intrinsic Josephson effects and mixed Abrikosov vortices with Josephson cores were reported in 1111 and 24622 iron-based superconductors [1,2]. We fabricated small junctions of  $\text{FeSe}_{1-x}\text{Te}_x$  single crystals, and studied the magnetic field angular dependence of the interlayer resistance at various temperatures. If the magnetic field is parallel to layers, the interlayer resistance has a peak, and vortex flow occurred. With decreasing temperatures, the peak height is also decreased down to  $T^*$  but is increased below  $T^*$ . Moreover, the peak widths are found to be decreased with decreasing temperature. These results suggest that vortex core changes from Abrikosov to Josephson core.

This work was supported by JSPS KAKENHI Grant Number JP17K14343.

[1] P. J. W. Moll *et al.*, Nat. Mater. **12**, 134 (2013).

[2] P. J. W. Moll *et al.*, Nat. Phys. **10**, 644 (2014)

## NMR studies of the incommensurate helical antiferromagnet Eu compounds.

N. Higa<sup>1,2</sup>, Q-P. Ding<sup>2</sup>, H. Uehara<sup>1</sup>, F. Kubota<sup>1</sup>, M. Yogi<sup>3</sup>, Y. Furukawa<sup>2</sup>,N. S. Sangeetha<sup>2</sup>, D. C. Johnston<sup>2</sup>, A. Nakamura<sup>4</sup>, M. Hedo<sup>3</sup>, T. Nakama<sup>3</sup>, Y. Ōnuki<sup>3</sup><sup>1</sup>Graduate School of Engineering and Science, University of the Ryukyus, Nishihara, Okinawa 903-0213, Japan<sup>2</sup>The Ames Laboratory and Department of Physics and Astronomy, Iowa State University, Ames, Iowa 50011, USA<sup>3</sup>Department of Physics, Faculty of Science, University of Ryukyus, Nishihara, Okinawa 903-0213, Japan<sup>4</sup>Institute for Materials Research, Tohoku University, Oarai, Ibaraki 319-1195, Japan

Eu is a rare-earth element known to have two kinds of valence state. The divalent Eu state  $\text{Eu}^{2+}$  ( $4f^6$ ) is magnetic ( $J = S = 7/2$ ,  $L = 0$ ), where  $J$  is the total angular momentum,  $S$  is the spin angular momentum, and  $L$  is the orbital angular momentum. Therefore, the compounds with divalent Eu ions tend to order magnetically, following the Ruderman-Kittel-Kasuya-Yosida (RKKY) interaction. In contrast, the trivalent Eu state  $\text{Eu}^{3+}$  ( $4f^7$ ) is nonmagnetic ( $J = 0$ ,  $S = L = 3$ ).

The Eu-based intermetallic compound  $\text{EuCo}_2\text{X}_2$  ( $\text{X} = \text{As}, \text{P}$ ) crystallizes in the  $\text{ThCr}_2\text{Si}_2$ -type structure (Space group: No. 139,  $I4/mmm$ ,  $D^{17}_{4h}$ ) as shown in Fig. 1. The Eu ion has the divalent state, and orders antiferromagnetically below the Néel temperature  $T_N = 47$  K for  $\text{EuCo}_2\text{As}_2$  [1, 2] and  $T_N = 66.5$  K for  $\text{EuCo}_2\text{P}_2$  [3-6], respectively. The antiferromagnetic (AFM) structure below  $T_N$  was reported to be helical from the neutron diffraction (ND) study [2, 3]. The Eu ordered moments are aligned ferromagnetically in the  $ab$ -plane with the helix axis along the  $c$ -axis [2, 3]. The magnetic structure is usually determined by using ND measurements. The AFM propagation vector  $\mathbf{k}$  of the incommensurate helical state in  $\text{EuCo}_2\text{X}_2$  ( $\text{X} = \text{As}, \text{P}$ ) was successfully determined by using nuclear magnetic resonance (NMR) [7, 8].

In this study, we investigate magnetic properties of  $\text{EuCo}_2\text{X}_2$  ( $\text{X} = \text{As}, \text{P}$ ) from microscopic point of view by using NMR technique. In the AFM state below  $T_N$ , we succeeded in observing  $^{153}\text{Eu}$ ,  $^{59}\text{Co}$ ,  $^{75}\text{As}$  and  $^{31}\text{P}$  NMR signal. The external magnetic field dependence of  $^{153}\text{Eu}$ ,  $^{75}\text{As}$ ,  $^{31}\text{P}$  NMR spectra for single-crystalline  $\text{EuCo}_2\text{As}_2$  and  $\text{EuCo}_2\text{P}_2$  clearly evidenced the incommensurate helical AFM structure. We determined the AFM propagation vector characterizing the incommensurate helical AFM state by  $^{59}\text{Co}$  NMR at zero magnetic field for each compound.

The research was supported by the U.S. Department of Energy, Office of Basic Energy Sciences, Division of Materials Sciences and Engineering. Ames Laboratory is operated for the U.S. Department of Energy by Iowa State University under Contract No. DE-AC02-07CH11358. Part of the work was supported by the Japan Society for the Promotion of Science KAKENHI: J-Physics (Grant Nos. JP15K21732, JP15H05885, and JP16H01078). N. H. also thanks the KAKENHI: J-Physics for financial support to be a visiting scholar at the Ames laboratory.

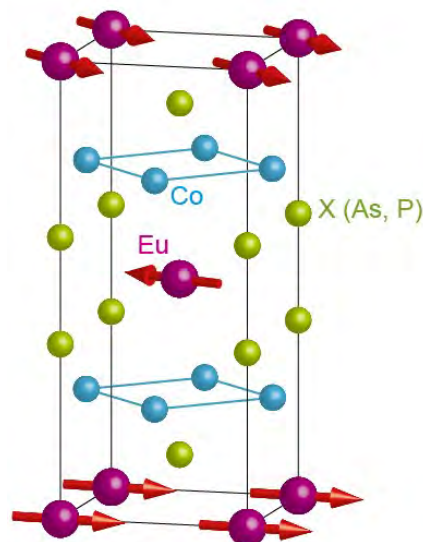


Fig. 1. The crystal and magnetic structures  $\text{EuCo}_2\text{X}_2$  ( $\text{X} = \text{As}, \text{P}$ )

[1] H. Raffius et al.: J. Phys. Chem. Solids **54**, 135 (1993)

[2] X. Tan et al.: J. Am. Chem. Soc. **138**, 2724 (2016).

[3] M. Reehuis et al. J. Phys. Chem. Solids **53**, 687 (1992).

[4] R. Marchand and W. Jeitschko, J. Solid State Chem. **24**, 351 (1978).

[5] T. Nakama et al. J. Phys. Conf. Ser. **200**, 032050 (2010).

[6] N. S. Sangeetha et al. Phys. Rev. B **94**, 014422 (2016).

[7] Q-P. Ding et al. Phys. Rev. B **95**, 184404 (2017).

[8] N. Higa et al.: Phys. Rev. B **96**, 024405 (2017).

## P-61

Spectral function and density of states in the superconducting state of high- $T_c$  cuprates incorporating strong correlation effects

H. Morita, T. Kita

Hokkaido University, Sapporo 060-0810, Japan

Many theoretical studies have been performed to describe basic properties of high- $T_c$  superconductors. Noteworthy among them is the fluctuation exchange (FLEX) approximation [1]. This formulation, which is based on the Fermi liquid theory, incorporates higher-order terms in the perturbation expansion that are responsible for the density fluctuations, longitudinal magnetic fluctuations, transverse magnetic fluctuations, and singlet two-particle fluctuations. This FLEX approximation have been successful in reproducing various in normal-state properties of high- $T_c$  superconductors, especially transport phenomena.

However, the standard FLEX approximation cannot describe properties of the superconducting state. Moreover, some approaches for the superconducting state don't satisfy the conservation laws, so we can't describe the transport phenomena appropriately.

Recently, a concise extension of FLEX approximation to the superconducting state was developed, called FLEX-S approximation [2]. This extension was performed by incorporating all the pair process by symmetrizing the vertex of each Feynman diagram considered in the original FLEX approximation. Using this formulation, we can perform a closed self-consistent perturbation expansion in terms of one particle normal Green's function, self-energy, and pair potential. This approach is expected to describe the properties of the superconducting state in such a way as to extend the FLEX approximation for the normal state.

Note in this context that these two formulations are based on the “ $\Phi$ -derivable approximation” formulated by Baym and Kadanoff. Therefore they satisfy various conservation laws naturally.

In this presentation, we report calculations of the spectral function and the density of state in superconducting state based on the FLEX-S approximation. In this calculation, we apply this formulation to the Hubbard model on a 2D square lattice assuming a spin-singlet pairing. We set the parameters in the Hubbard model so as to reproduce the observed band structure of cuprate superconductors [3]. We show the band structure, the formation of the Fermi surface and the relaxation time of the quasiparticle from the spectral function, and the energy scale of pair potential from density of state.

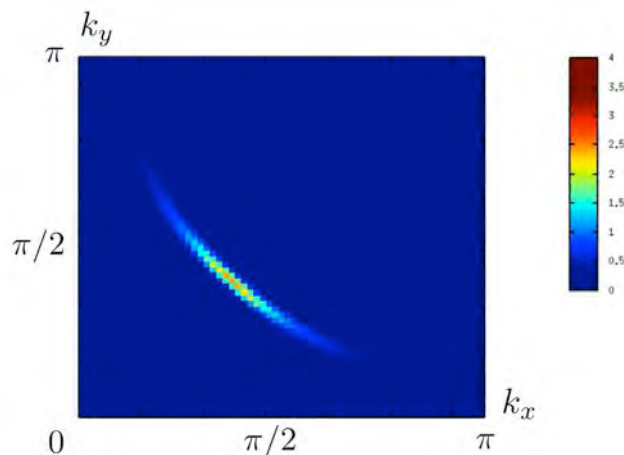


Fig.1 The Fermi surface of the YBCO model. We can see Fermi arc near  $k_x \sim k_y$

[1] N. E. Bickers and D.J.Scalapino Ann. Phys. (N.Y.) **193** (1989) 206.

[2] T. Kita, J. Phys. Soc. Jpn. **80** (2011) 124704.

[3] H. Kontani, K.Kanki and K.Ueda, Phys. Rev. B. **59** (1999) 14273.

Heavy fermion superconductivity and non-Fermi liquid  
in the quadrupole Kondo lattice  $\text{PrTr}_2\text{Al}_{20}$  ( $Tr = \text{Ti}, \text{V}$ )

A. Sakai<sup>1</sup>, M. Tsujimoto<sup>1</sup>, Y. Matsumoto<sup>2</sup>, Y. Shimura<sup>1</sup>, T. Tomita<sup>1</sup> and S. Nakatsuji<sup>1</sup>  
<sup>1</sup>Institute for Solid State Physics, University of Tokyo, Kashiwa, Chiba 277-8581, Japan  
<sup>2</sup>Max Planck Institute for Solid State Research, 70569 Stuttgart, Germany

New quantum states of matter have been discovered in the strongly correlated  $f$  electron systems. Especially, unconventional superconductivity is found near quantum critical points (QCPs), where the magnetic order is suppressed due to the two competing interactions between  $4f$  and conduction ( $c$ -) electrons, Kondo effect and Ruderman-Kittel-Kasuya-Yosida (RKKY) interaction. By replacing  $4f$  spins with electrical quadrupole (orbital), exotic states can be found similarly. In particular, non-Fermi liquid is theoretically predicted for the ground state of  $c$ - $f$  hybridized quadrupole system, so called quadrupole Kondo effect [1]. To study such quadrupole physics, nonmagnetic  $\Gamma_3$  state, which can be realized in the cubic crystalline electric field (CEF) for non-Kramers  $f^2$  systems such as Pr-based compounds, is suitable due to the absence of the magnetic dipole moment.

The cubic  $\text{PrTr}_2\text{Al}_{20}$  ( $Tr = \text{Ti}, \text{V}$ ) is the first example of quadrupolar Kondo lattice system, in which both strong  $c$ - $f$  hybridization and nonmagnetic cubic  $\Gamma_3$  CEF ground state are realized simultaneously [2]. CEF ground state is determined to nonmagnetic cubic  $\Gamma_3$  state initially from the specific heat  $C_P$  and magnetic susceptibility  $\chi$  and later from various experiments such as neutron inelastic experiment [2, 3, 4]. Ferro- and antiferro- quadrupole ordering at  $T_Q = 2.0$  K (Ti), 0.6 K (V) is observed due to the degeneracy of the  $\Gamma_3$  quadrupole.  $c$ - $f$  hybridization is particularly strong, as revealed from logarithmic increase of the resistivity  $\rho$  and the observation of the Kondo resonance peak at the Fermi energy [2, 5]. Moreover, anomalous metallic behaviors are observed in  $\text{PrV}_2\text{Al}_{20}$  above  $T_Q$ , indicating the quadrupole Kondo effect [2].

Significantly, superconductivity is found at  $T_c = 0.2$  K and 0.05 K in the quadrupole ordered state of  $\text{PrTi}_2\text{Al}_{20}$  and  $\text{PrV}_2\text{Al}_{20}$ , respectively [6, 7]. Effective mass estimated from the Sommerfeld coefficient and upper critical field is enhanced to  $m^*/m_0 \sim 20$  and 140 for  $\text{PrTi}_2\text{Al}_{20}$  and  $\text{PrV}_2\text{Al}_{20}$ , respectively. Surprisingly,  $T_c$  and  $m^*$  for  $\text{PrTi}_2\text{Al}_{20}$  are highly enhanced by applying the pressure of  $P \sim 8$  GPa up to  $T_c \sim 1.1$  K and  $m^*/m_0 \sim 110$  [8]. Around this pressure,  $T_Q$  starts to be suppressed, suggesting the proximity to the QCP of the quadrupolar ordering.

In this presentation, we will review the basic properties of the  $\text{PrTr}_2\text{Al}_{20}$  ( $Tr = \text{Ti}, \text{V}$ ) and discuss the unconventional superconductivity and anomalous metallic state including recent experiments.

- [1] D. L. Cox, Phys. Rev. Lett., **59**, 1240 (1987).
- [2] A. Sakai and S. Nakatsuji, J. Phys. Soc. Jpn., **80**, 063701 (2011).
- [3] M. Koseki, Y. Nakanishi, K. Deto, G. Koseki, R. Kashiwazaki, F. Shichinomiya, M. Nakamura, M. Yoshizawa, A. Sakai, and S. Nakatsuji, J. Phys. Soc. Jpn., **80**, SA049, (2011).
- [4] T. J. Sato, S. Ibuka, Y. Nambu, T. Yamazaki, T. Hong, A. Sakai, and S. Nakatsuji, Phys. Rev. B, **86**, 184419 (2012).
- [5] M. Matsunami, M. Taguchi, A. Chainani, R. Eguchi, M. Oura, A. Sakai, S. Nakatsuji, and S. Shin, Phys. Rev. B, **84**, 193101 (2011).
- [6] A. Sakai, K. Kuga, and S. Nakatsuji, J. Phys. Soc. Jpn., **81**, 083702 (2012).
- [7] M. Tsujimoto, Y. Matsumoto, T. Tomita, A. Sakai, and S. Nakatsuji, Phys. Rev. Lett. **113**, 267001 (2014).
- [8] K. Matsubayashi, T. Tanaka, A. Sakai, S. Nakatsuji, Y. Kubo, and Y. Uwatoko, Phys. Rev. Lett., **109**, 187004 (2012).

Single-site non-Fermi liquid state in a dilute Pr system  $Y_{1-x}Pr_xIr_2Zn_{20}$ 

Yu Yamane<sup>1</sup>, Takahiro Onimaru<sup>1</sup>, Kazuto Uenishi<sup>1</sup>, Kazuhei Wakiya<sup>1</sup>, Keisuke T. Matsumoto<sup>1</sup>, Kazunori Umeo<sup>2</sup>, and Toshiro Takabatake<sup>1</sup>

<sup>1</sup>AdSM, <sup>2</sup>N-BARD, Hiroshima University, Higashi-Hiroshima 739-8530, Japan

A variety of exotic phenomena arising from active quadrupoles in non-Kramers doublets of  $4f^2$  systems have attracted much attention. In diluted  $U^{4+}$  or  $Pr^{3+}$  systems with  $4f^2$  configuration, non-Fermi liquid (NFL) behaviors could manifest themselves due to interaction between conduction electrons and electric quadrupole moments of localized  $4f^2$  electrons, as predicted for an impurity quadrupole Kondo effect in the cubic  $\Gamma_3$  doublet system [1]. In this model, NFL behaviors involve three ingredients,  $-\ln T$  divergence of magnetic specific heat divided by temperature  $C_m/T$ ,  $\sqrt{T}$  dependence of electrical resistivity  $\rho$ , and residual entropy of  $(1/2) \ln 2$ . In spite of much experimental efforts to address the issue, no clear evidence of the impurity quadrupole Kondo effect has been obtained yet. Recently, in  $PrIr_2Zn_{20}$  with the  $\Gamma_3$  doublet ground state, NFL behaviors were observed in the specific heat and  $\rho$ , suggesting formation of the quadrupole Kondo lattice [2,3]. Therefore, dilution of the Pr ions in this system may realize the single-site NFL state due to the  $4f^2$  electrons. Bearing this in mind, we have measured  $C_m$  and  $\rho$  of the Pr diluted alloy  $Y_{1-x}Pr_xIr_2Zn_{20}$  for  $x \leq 0.05$ .

We have found that  $C_m$  exhibits a Schottky-type maximum at around 12 K which can be reproduced by the doublet-triplet two-level model. It assures that the crystalline electric field (CEF) ground state of  $Pr^{3+}$  in  $Y_{1-x}Pr_xIr_2Zn_{20}$  maintains the  $\Gamma_3$  doublet [4].

Figure shows  $C_m/T$  for  $x = 0.044$  in magnetic fields up to 12 T applied along the [100] direction. The data of  $C_m/T$  for  $B = 4$  T exhibits a broad maximum at 0.3 K, which shifts to higher temperatures with increasing  $B$  and reaches 2.3 K at  $B = 12$  T. Values of  $C_m/T$  calculated by considering the CEF and Zeeman effects are shown with the colored solid lines in the figure. The inset depicts the magnetic field variations of the energy of the  $\Gamma_3$  doublet and the first excited  $\Gamma_4$  triplet. For  $B \geq 4$  T, the broad maxima can be moderately reproduced by the calculations. On the other hand, the data for  $B = 2$  T deviates from the calculation, suggesting an additional contribution of the degenerate quadrupolar degrees of freedom in the  $\Gamma_3$  doublet at the low magnetic fields of  $B \leq 2$  T.

The temperature variations of the electrical resistivity for  $x = 0.024$  and 0.044 display upward curvatures on cooling below 1 K (not shown). Furthermore, the differential electrical resistivity,  $\Delta\rho(T) = \rho(T) - \rho(T = 3 \text{ K})$ , is well scaled by the Pr composition  $x$ , and it follows  $\sqrt{T}$  for 0.07–0.4 K. The results indicate the manifestation of the impurity quadrupole Kondo effect inherent in the  $4f^2$  state of  $Y_{1-x}Pr_xIr_2Zn_{20}$ .

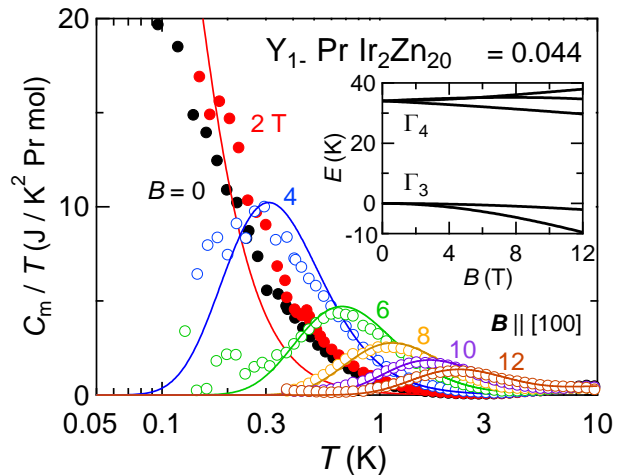


Figure: Temperature dependence of the magnetic specific heat divided by temperature  $C_m/T$  in magnetic field applied along the [100] direction. The inset shows the magnetic field variations of the energy of the  $\Gamma_3$  and  $\Gamma_4$  multiplets.

[1] D. L. Cox and Z. Zawadowski, *Adv. Phys.* **47**, 599 (1998).

[2] T. Onimaru *et al.*, *Phys. Rev. B* **94**, 075134 (2016).

[3] T. Onimaru and H. Kusunose, *J. Phys. Soc. Jpn.* **85**, 082002 (2016).

[4] Y. Yamane *et al.*, *Physica B*, in press.

NMR study of tetrahedrite  $\text{Cu}_{12}\text{Sb}_4\text{S}_{13}$ T. Matsui<sup>1</sup>, H. Matsuno<sup>1</sup>, H. Kotegawa<sup>1</sup>, H. Tou<sup>1</sup>, K. Suekuni<sup>2</sup>, H. I. Tanaka<sup>3</sup>, and T. Takabatake<sup>3</sup><sup>1</sup>Department of Physics, Graduate School of Science, Kobe University, Kobe 657-8501, Japan<sup>2</sup>Department of Applied Science for Electronics and Materials, Interdisciplinary Graduate School of Engineering Sciences, Kyushu University, Kasuga, Fukuoka, 816-8580, Japan<sup>3</sup>Department of Quantum Matter, Graduate School of AdSM, Hiroshima University, Higashi-Hiroshima, 739-8530, Japan

Tetrahedrite has attracted much attention because it is high-performance thermoelectric material with environmental-friendliness and earth-abundance.<sup>[1]</sup> The crystal structure of  $\text{Cu}_{12}\text{Sb}_4\text{S}_{13}$  is a body-centered-cubic (bcc) with space group  $I-432$  (No. 217,  $Z = 2$ ) at a room temperature, as shown in Fig. 1.  $\text{Cu}_{12}\text{Sb}_4\text{S}_{13}$  has inequivalent two Cu sites, where their Wyckoff positions are  $12c$  and  $12e$ . Particularly, it is reported that  $\text{Cu}12e$  site has large and anharmonic vibration mode, which is so-called “rattling” mode. It has been argued that the rattling suppresses the thermal conductivity in tetrahedrites.<sup>[2]</sup> However, details of dynamical properties of rattling in tetrahedrites have not been experimentally confirmed.

Furthermore,  $\text{Cu}_{12}\text{Sb}_4\text{S}_{13}$  exhibits metal-semiconductor transition (MST) at  $T_{\text{MST}} = 85$  K and its mechanism is still unclear. It has been discussed that the MST is caused by the lattice instability.

Firstly, we studied on the MST of tetrahedrite using nuclear magnetic resonance (NMR). We observed two kinds of Cu-NMR lines above  $T_{\text{MST}}$ . From spectrum simulations, the narrow lines correspond to the Cu atom at the  $12c$  site, whereas the broad lines correspond to the  $12e$  site as shown in the Fig. 2. We observed that Cu-NMR line shape at  $\text{Cu}12e$  site drastically changes below  $T_{\text{MST}}$ . From spectrum simulations, the asymmetry of electric field gradient at  $\text{Cu}12e$  site increased markedly below  $T_{\text{MST}}$ . This fact strongly suggests that the MST involves a distortion of the local structure around  $\text{Cu}12e$  site. We will report the details of the simulation.

Secondly, we also studied on dynamical property of tetrahedrite using NMR. In the high temperature region above  $T_{\text{MST}}$ , we found that the nuclear spin-spin relaxation rate  $1/T_2$  of  $\text{Cu}12c$  site drastically increases with increasing temperature ( $T > 170$  K) and we cannot observe NMR signal above 220 K. This fact indicates the slow fluctuation at  $\text{Cu}12c$  site, which may originate from rattling motion of  $\text{Cu}12e$  atoms. We will report further study on dynamical properties such as  $1/T_2$  of  $\text{Cu}12e$  site or spin-lattice relaxation rate  $1/T_1$ .

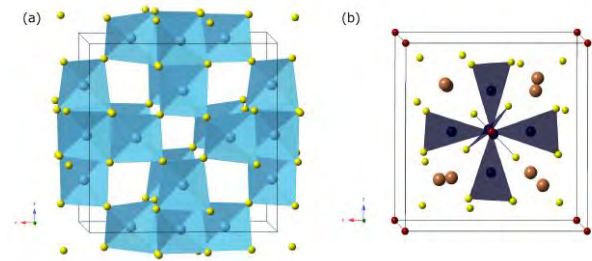


Fig. 1. Crystal structure of  $\text{Cu}_{12}\text{Sb}_4\text{S}_{13}$ . (a) shows  $\text{Cu}12c$  in  $\text{S}_4$  tetrahedron, and (b) shows  $\text{Cu}12e$  in  $\text{S}_3$  triangle plane.

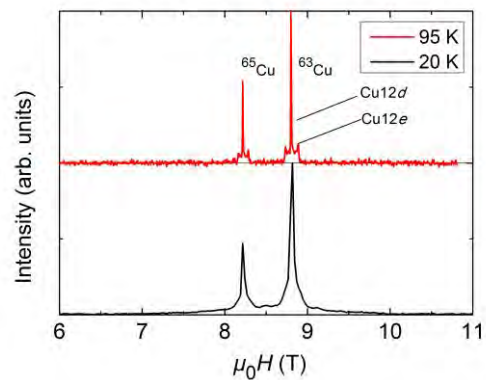


Fig. 2. NMR spectra above  $T_{\text{MST}}$  (upper) and below  $T_{\text{MST}}$  (lower). Both are measured with NMR frequency = 99.363 MHz.

[1] K. Suekuni, K. Tsuruta, T. Ariga, and M. Koyano, Appl. Phys. Express **5**, 051201 (2012).

[2] K. Suekuni and T. Takabatake, APL Mater. **4**, 104503 (2016).

## Investigation of symmetry change through the hidden order transition in URu<sub>2</sub>Si<sub>2</sub> by Ru-NMR and thermal expansion measurements

T. Mito<sup>1</sup>, T. Miki<sup>1</sup>, G. Motoyama<sup>2</sup>, N. Emi<sup>1</sup>, K. Ueda<sup>1</sup>, M. Yokoyama<sup>3</sup>, and H. Amitsuka<sup>4</sup>

<sup>1</sup>Graduate School of Material Science, University of Hyogo, Hyogo 678-1297, Japan

<sup>2</sup>Department of Materials Science, Shimane University, Shimane 690-8504, Japan

<sup>3</sup>Faculty of Science, Ibaraki University, Mito 310-8512, Japan

<sup>4</sup>Graduate School of Science, Hokkaido University, Sapporo 060-0810, Japan

The phase transition called “hidden order” that the uranium compound URu<sub>2</sub>Si<sub>2</sub> undergoes at  $T_{HO} = 17.5$  K has attracted much interest, since the nature of this transition is still a mystery despite a large jump of the specific heat at  $T_{HO}$ . One of the points in controversy is how the symmetry of the system changes through the transition. Recently symmetry breaking from the fourfold tetragonal symmetry to twofold symmetry in the basal plane was reported by the measurement of magnetic susceptibility using torque method [1]. Then it is followed by other experimental reports, such as high precision x-ray diffraction [2,3] and NMR using a <sup>29</sup>Si-enriched single crystalline sample [4]. The recent <sup>29</sup>Si-NMR study [4] found the peculiar  $|\cos(2\theta)|$  angular dependence of the line width, where  $\theta$  is measured relative to the [110] axis in the basal plane, and a few scenarios have been proposed: One is based on the assumption that there exist twofold ordered domain states [4], and an alternative explanation is based on the susceptibility of the magnetic-broadening centers and a Ruderman-Kittel-Kasuya-Yosida coupling [5].

In this study, we have approached the problem of the angular dependent NMR linewidth from different aspect: <sup>99</sup>Ru-NMR (nuclear spin  $I=5/2$ ) and thermal expansion measurements. Quite analogous phenomenon was found even in the measurement of <sup>99</sup>Ru-NMR spectrum. However a remarkable point is that such an angular dependence of linewidth is observed only for quadrupole split lines and not for a central line. Note that the former line is sensitive to changes in local charge distribution through electronic interactions, therefore this observation may indicate that the symmetry of the crystal structure at the Ru site is locally incompatible with the fourfold tetragonal symmetry. However, we also found that this  $\theta$  dependence of the linewidth is observed even above  $T_{HO}$ , suggesting that it may not be related to the hidden order transition. Moreover we are interested in the magnetic field dependence of this anomalous behaviour. Since it is actually difficult to scan <sup>99</sup>Ru-NMR spectra in a wide range of field, we have performed the measurement of the thermal expansion which is sensitive to lattice anomaly. In the session, we will present the results as well as the details of the NMR study.

- [1] R. Okazaki *et al.*, Science **331** (2011) 439.
- [2] S. Tonegawa *et al.*, Nat. Commun. **5** (2014) 4188.
- [3] C. Tabata *et al.*, Philosophical magazine **9**, (2014) 3691.
- [4] S. Kambe *et al.*, Phys. Rev. Lett. **110**, (2013) 246406.
- [5] R.E. Walstedt *et al.*, Phys. Rev. B **93**, (2016) 045122.

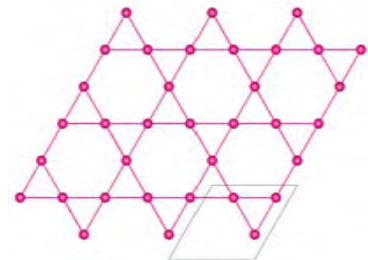
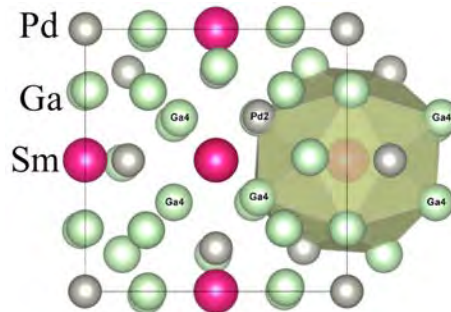
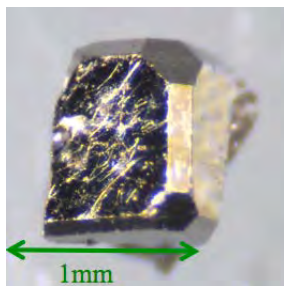
Magnetic properties of a new compounds with kagome lattice  $RPd_3Ga_8$ 

T. D. Matsuda, K. Hara, A. Yamada, R. Higashinaka, and Y. Aoki

*Department of Physics, Tokyo Metropolitan University, Hachioji 192-0397, Japan*

Over the past decade, there has been increasing interest in the strongly correlated electron behaviors appearing in Sm-based intermetallic compounds. Typical such examples are unusual magnetic-field-insensitive heavy-fermion behavior in  $SmOs_4Sb_{12}$ [1,2], magnetic-field-insensitive phase transition and largely-enhanced Sommerfeld coefficients in  $SmT_2Al_{20}$  ( $T$ : transition metal) [3, 4, 5], metal-insulator(MI) transition and magnetic-field-induced charge ordering in  $SmRu_4P_{12}$ [6, 7], and MI transition under pressure in  $SmX$  ( $X$ : S, Se, and Te)[9, 10, 11]. Since Sm ions in all of these compounds have cubic site symmetries, the crystalline-electric-field ground state tend to be highly degenerate with active multipole degrees of freedom. In order to investigate the role of such CEF degeneracy on the strongly correlated electron behaviors, it may be useful to study systems with lower site symmetry and compare them with the cubic ones.

Recently, we have developed a new compounds of  $RPd_3Ga_8$  ( $R$ :rare earth), and succeeded in growing single crystals. Figure 1 shows a typical shape of single crystal. We performed a single crystal x-ray diffraction and tried to determine a detail of the atomic coordination of crystal structure. Although the shape of unit cell is very close to a cubic structure, this system has a rhombohedral structure as shown in Figure 2. The atomic coordinates are also very close to a cubic system of  $RCd_{11}$ . The structure of  $RPd_3Ga_8$  corresponds to a structure in which a Cd site in  $RCd_{11}$  is split into two different lower symmetry sites. From another viewpoint of this structure, it is a stacking of rare earth kagome lattice along [111] direction. We also performed the magnetic and specific heat measurements on  $SmPd_3Ga_8$ . Although, the both of temperature dependence of magnetic susceptibility and specific heat indicate the antiferromagnetic ordering at  $T_a = 3.1$  K, it shows that the  $\chi(T)$  increases with decreasing temperature below  $T_a$  and  $C(T)$  shows an anomalous hump structure in the ordered state. These behaviors are very similar to those in  $SmPt_2Si_2$  in which the magnetic frustration might play an important role[12]. In this presentation, we would like to present systematic investigations of the physical properties on this system.

Fig. 1: Single crystal of  $SmPd_3Ga_8$ .Fig. 2: Crystal structure of  $RPd_3Ga_8$ .Fig. 3: kagome lattice of  $R$  in the (111) plane

- [1] S. Sanada *et al.*, J. Phys. Soc. Jpn. 74, 246 (2005).
- [2] W. M. Yuhasz *et al.*, Phys. Rev. B 71, 104402 (2005).
- [3] R. Higashinaka *et al.* J. Phys. Soc. Jpn. 80, 093703 (2011).
- [4] A. Sakai, and S. Nakatsuji, Phys. Rev. B 84, 201106(R) (2011).
- [5] A. Yamada *et al.*, J. Phys. Soc. Jpn. 82, 123710 (2013).
- [6] C. Sekine *et al.*, in Science and Technology of High Pressure, *ed.* M. H. Manghnani, W. J. Nellis, and M. F. Nicol (Universities Press, Hyderabad, 2000) p. 826.
- [7] K. Matsuhira *et al.*, J. Phys. Soc. Jpn. 71 [Suppl.], 237 (2002). 5
- [8] T. Matsumura *et al.*, Phys. Rev. B 89, 161116(R) (2014).
- [9] F. Lapierre *et al.*, Solid State Commun. 40, 347 (1981).
- [10] M. W. Elmiger and P. Wachter, J. Magn. Magn. Mater. 63-64, 612 (1987).
- [11] A. Jayaraman *et al.*, Phys. Rev. Lett. 25, 368 (1970).
- [12] K. Fushiya *et al.*, J. Phys. Soc. Jpn. 83, 113708 (2014).

## Elastic properties of Eu-based compounds $\text{EuX}_4$ (X: Ge, Al) probed by ultrasonic measurements

Y. Nakanishi<sup>1</sup>, Y. Ohyama<sup>1</sup>, M. Taniguchi<sup>1</sup>, M. Nakamura<sup>1</sup>, J. Hasegawa<sup>1</sup>,  
M. T. Nakamura<sup>1</sup>, M. Yoshizawa<sup>1</sup>, A. Nakamura<sup>2</sup>, M. Hedo<sup>2</sup>, and Y. Ônuki<sup>2</sup>

<sup>1</sup>Iwate University, Morioka 020-8551, Japan

<sup>2</sup>University of Ryukyus, Nishihara 903-0213, Japan

The coexistence of magnetism and charge-density-wave (CDW) phase has received sustained interest in the correlated electron systems as a result of nested Fermi surfaces and  $4f$ -electron valence instability [1-3]. Recently, the coexistence and a strong interplay of a CDW and a magnetic order were reported in Eu-based compounds such as  $\text{EuX}_4$  (X: Ge, Al) [4,5]. The family crystallizes in the  $\text{BaAl}_4$ -type tetragonal structure (space group :  $I4/m$ ). The divalent Eu compound  $\text{EuAl}_4$  has a CDW transition and an AFM transition at  $T_{\text{CDW}} = 140$  K and  $T_{\text{N}} = 6$  K, respectively. However, the recent detailed experiments regarding the AFM transition revealed that the Néel temperature of  $\text{EuAl}_4$  is not 6 K but  $T_{\text{N}1} = 15.4$  K, with three successive AFM transitions at  $T_{\text{N}2} = 13.2$  K,  $T_{\text{N}3} = 12.2$  K, and  $T_{\text{N}4} = 10.0$  K. The latter two transitions are of the first-order. On the other hand,  $\text{EuGa}_4$  has only an AFM transition at  $T_{\text{N}} = 15$  K at ambient pressure. However, the transport experiments indicate strongly that a plausible CDW phenomenon would show up under pressure in  $\text{EuGa}_4$ , being quite similar to those observed in  $\text{EuAl}_4$  at ambient pressure. The transition occurs at around 150 K under a pressure of 2 GPa [5]. Regarding the crystal structure, it should be noted that the well-known  $\text{ThCr}_2\text{Si}_2$ -type tetragonal structure is derived from that of  $\text{BaAl}_4$ -type, e.g. where the atomic sites of Cr and Si in  $\text{ThCr}_2\text{Si}_2$  are replaced by Al.

In order to elucidate the  $4f$  electronic state of Eu anions and unveil a new kind of Fermi-surface instability in  $\text{EuX}_4$ , being possibly associated with a one-dimensional the zigzag chain of Si sites in the  $\text{ThCr}_2\text{Si}_2$ -type crystal structure, we have investigated elastic properties of Eu-based compounds  $\text{EuX}_4$  (X: Ge, Al) probed by ultrasonic measurements. The isostructural reference material  $\text{SrAl}_4$  was also studied for comparison. Ultrasonic measurement is a powerful experimental probe for investigating a strain-quadrupole interaction and symmetry of order parameter of a phase transition, and its dynamical fluctuation due to precursor phenomena as well.

We found a pronounced elastic softening toward the  $T_{\text{CDW}}$  in the temperature dependence of all the principal elastic constants  $C_{11}$ ,  $C_{33}$ ,  $C_{44}$ , and  $C_{66}$  of  $\text{EuAl}_4$ . However, no elastic anomaly due to the AFM transitions were somewhat invisible, probably due to small coupling between elastic strains associated with sound waves and relevant magnetic moments. Similarly, a pronounced elastic softening was observed in the temperature dependence of all the principal elastic constants  $C_{11}$ ,  $C_{33}$ ,  $C_{44}$ , and  $C_{66}$  of  $\text{EuGa}_4$ . However, the softening directs toward  $T_{\text{N}} = 15$  K, in which a CDW transition does not take place at ambient pressure in contrast to the  $\text{EuAl}_4$  system. From the detailed analysis of the elastic anomalies, in particular precursor softening of principal elastic constants large Jahn-Teller energies  $E_{\text{JT}}$  are deduced in  $\text{EuX}_4$  systems. These values  $E_{\text{JT}}$  exceed those of Fe-based superconductors of 122 family, in which strong lattice instability give rise to in the vicinity of the critical temperature, previously reported by our group [6]. The compound of the 122 family crystallizes in a  $\text{ThCr}_2\text{Si}_2$ -type structure with a tetragonal. In view of such a striking resemblance between  $\text{EuX}_4$  and Fe-based 122 superconductor systems, it might be expected that the crystal structure would play a key role in emergence of the lattice instability as well as Fermi surface one.

We discuss in detail the ground state properties and origin of the pronounced elastic anomalies of the  $\text{EuX}_4$  systems based on the experimental data from the viewpoint of their elastic properties. The pronounced precursor elastic anomalies can be explained by a deformation potential coupling on elastic constants, e.g., the experimental data can be fit well by the so-called band Jahn-Teller formula.

This work was supported by the Japan Society for the Promotion of Science through Grants-in- Aid for Scientific Research (KAKENHI Grant Numbers 15H05883).

- [1] S. Shimomura, C. Hayashi, G. Asaka, N. Wakabayashi, M. Mizumaki, and H. Onodera, *Phys. Rev. Lett.* **102**, 076404 (2009).
- [2] T. Sato, S. Souma, K. Nakayama, T. Takahashi, S. Shimomura, and H. Onodera, *J. Phys.Soc. Jpn.* **79**, 044707 (2010).
- [3] F. Galli, S. Ramakrishnan, T. Taniguchi, G. J. Nieuwenhuys, J. A. Mydosh, S. Geupel, J. Lüdecke, and S. van Smaalen, *Phys. Rev. Lett.* **85**, 158 (2000).
- [4] A. Nakamura, T. Uejo, F. Honda, T. Takeuchi, H. Harima, E. Yamamoto, Y. Haga, K. Matsubayashi, Y. Uwatoko, M. Hedo, T. Nakama, and Y. Ônuki, *J. Phys.Soc. Jpn.* **84**, 124711 (2015).
- [5] A. Nakamura, Y. Hiranaka, M. Hedo, T. Nakama, Y. Miura, H. Tsutsumi, A. Mori, K. Ishida, K. Mitamura, Y. Hirose, K. Sugiyama, F. Honda, R. Settai, T. Takeuchi, M. Hagiwara, T. D. Matsuda, E. Yamamoto, Y. Haga, K. Matsubayashi, Y. Uwatoko, H. Harima, and Y. Ônuki, *J. Phys.Soc. Jpn.* **82**, 104703 (2013).
- [6] M. Yoshizawa, D. Kimura, T. Chiba, S. Simayi, Y. Nakanishi, K. Kihou, C. H. Lee, A. Iyo, H. Eisaki, M. Nakajima, and S. Uchida, *J. Phys.Soc. Jpn.* **81**, 024604 (2012).

Single crystal growth and thermal expansion measurement  
of quadrupole Kondo lattice PrV<sub>2</sub>Al<sub>20</sub>

Y. Nagaoka, A. Sakai, H. Suzuki, M. Tsujimoto, Y. Shimura and S. Nakatsuji

Institute for Solid State Physics, University of Tokyo, Kashiwa, Chiba 277-8581, Japan

Recently, interesting phenomena, such as unconventional type of anomalous Hall effect and spin liquid like behaviour, have been observed in the Pr-based compounds [1, 2]. Among these compounds, PrT<sub>2</sub>Al<sub>20</sub> (T = transition metal) have attracted much interest, because of the unique physical properties driven by the hybridization between conduction electrons and orbital (quadrupole) moments in the non-magnetic  $\Gamma_3$  ground doublet [3]. Such a hybridization is called quadrupole Kondo effect, and can induce non-Fermi liquid due to the overscreening.

PrV<sub>2</sub>Al<sub>20</sub> shows quadrupole ordering at  $T_Q = 0.6$  K and heavy fermion superconductor with  $T_C = 50$  mK at ambient pressure [3,4]. Above  $T_Q$ , non-Fermi liquid behaviour is observed, indicating the quadrupole Kondo effect. Moreover,  $T_Q$  is suppressed to zero by the magnetic field  $\mu_0 H \sim 11$  T parallel to [111], and non-Fermi liquid behaviour in electrical resistivity is observed at  $\mu_0 H_c$ , suggesting the possible field induced quantum critical point (QCP) [5].

To study the quantum criticality, Grüneisen coefficient  $\Gamma \sim \frac{\beta}{C} = -\frac{1}{VT} \frac{(\partial S/\partial p)_T}{(\partial S/\partial T)_p}$ , where  $\beta$  and  $C$  are the volume thermal expansion coefficient and specific heat, is one of the most powerful probe because it diverges at any QCPs and shows universal critical scaling reflecting the type of QCP [6,7]. In this presentation, I will report the results of my thermal expansion and magnetostriction measurements of PrV<sub>2</sub>Al<sub>20</sub> at low temperature and discuss the possible quantum criticality in quadrupole system. We have also performed the new single crystal growth to obtain enough large crystals for neutron scattering so it will also be presented.

- [1] S. Nakatsuji, Y. Machida, Y. Maeno, T. Tayama, T. Sakakibara, J. van Duijn, L. Balicas, J. N. Millican, R. T. Macaluso, and Julia Y. Chan, Phys. Rev. Lett. **96**, 087204 (2006).
- [2] Y. Machida, S. Nakatsuji, S. Onoda, T. Tayama and T. Sakakibara, Nature **463**, 210 (2010).
- [3] A. Sakai and S. Nakatsuji, J. Phys. Soc. Jpn. **80**, 063701 (2011).
- [4] M. Tsujimoto, Y. Matsumoto, T. Tomita, A. Sakai, and S. Nakatsuji, Phys. Rev. Lett. **113**, 267001 (2014).
- [5] Y. Shimura, M. Tsujimoto, B. Zeng, L. Balicas, A. Sakai, and S. Nakatsuji, Phys. Rev. B, **91**, 241102(R) (2015).
- [6] L. Zhu et al., Phys. Rev. Lett. **91**, 066404 (2003).
- [7] M. Garst and A. Rosch, Phys. Rev. B **72**, 205129 (2005).

## P-69

Magnetism and superconductivity in the  $Ce_nPd_mIn_{3n+2m}$  and  $Ce_nPt_mIn_{3n+2m}$  homologous series

K. Uhlířová<sup>1</sup>, J. Volný<sup>1</sup>, J. Prokleška<sup>1</sup>, M. Kratochvílová<sup>1</sup>, B. Vondráčková<sup>1</sup>, M. Dušek<sup>2</sup>, J. Custers<sup>1</sup>, V. Sechovský<sup>1</sup>

<sup>1</sup>Charles University in Prague, Faculty of Mathematics and Physics, Ke Karlovu 3, 121 16 Praha 2, Czech Republic

<sup>2</sup>Institute of Physics ASCR, v.v.i., Na Slovance 2, 182 21 Prague, Czech Republic

The family of  $Ce T In_{3+2m}$  ( $m = 1, 2$ ;  $T =$  transition metal) heavy fermion compounds has been intensively studied owing to variety of magnetic ordering and superconductivity. All the compounds crystallize in tetragonal type structure with  $CeIn_3$ - and  $TIn_2$ - layers alternating along the  $c$ -axis. Besides the well-known  $CeTIn_5$  and  $Ce_2TIn_8$  ( $T = Co, Rh, Ir$ ) compounds, new materials  $CePtIn_7$ ,  $Ce_2PtIn_8$ ,  $Ce_3PtIn_{11}$ ,  $Ce_2PdIn_8$ ,  $Ce_3Pd_2In_{19}$  and  $Ce_3PdIn_{11}$  have been discovered [1-4].

The  $Ce T In_{3+2m}$  compounds containing Pd or Pt cover the wider composition range compared to the other known series. Such existence of a system of compounds with various layer-stacking opens a possibility to study a scenario of evolution of magnetism and superconductivity with the dimensionality of the Fermi surface.  $Ce_2PdIn_8$  shows no magnetic ordering but becomes superconducting below  $T_c = 0.7$  K. In  $Ce_3PdIn_{11}$ , we have observed magnetic order below  $T_N = 1.7$  K and subsequent transition to superconducting state below  $T_c = 0.4$  K [3]. Similarly  $Ce_3PtIn_{11}$  order magnetically below  $T_N = 2.2$  K and becomes superconducting below 0,35 K [4], while  $CePt_2In_7$  exhibits pressure-induced superconductivity at  $T_c \approx 2.1$  K [5].

A specific feature of the  $Ce Pd In_{3+2m}$  and  $Ce Pt In_{3+2m}$  compounds is the lattice parameter  $a$  of their tetragonal structure being almost identical with the lattice parameter of the cubic  $CeIn_3$ . This may play an important role in the stability of various compounds with different combinations of  $CeIn_3$ - and  $PdIn_2$ - ( $PtIn_2$ -) layer stacking; however, it also seems to result in difficulties with sample preparation. Multilayer inclusions of neighboring phases are hardly avoidable in growing single crystals from metallic flux. While tuning the growth conditions of  $Ce_3PdIn_{11}$  and  $Ce_2PdIn_8$ , thin layers of  $CePdIn_5$  have been found in several samples. Further attempts to obtain larger samples of  $CePdIn_5$  were not successful.

In order to isolate the  $CePdIn_5$  single crystals and verify the results obtained on  $Ce_3PdIn_{11}$  and  $Ce_2PdIn_8$  single crystals, microfabrication of samples by focused ion beam (FIB) microscope has been implemented. By this method, few tens of micrometers long bars can be cut from desired area of sample (inspected by elemental mapping) and transferred on a substrate and further structured. In combination with electron beam lithography, the sample can be subject to electric transport measurement or simply transferred on a Hall probes for indirect measurements of magnetization.

We will present current overview about the synthesis and physical properties of the  $Ce Pd In_{3+2m}$  and  $Ce Pt In_{3+2m}$  including our most recent studies.

#### Acknowledgement

The work was supported by the Czech Science Foundation via Grant No. GP14-17102P. Experiments were performed in the research infrastructure MGML ([www.mgml.eu](http://www.mgml.eu))

- [1] Z. M. Kurenbaeva et al., *Intermetallics* **16**, 979 (2008)
- [2] A. Tursina et al., *J. Sol. State Chem.* **200**, 7 (2013)
- [3] M. Kratochvílová et al., *Scientific Reports* **5**, 15904 (2015)
- [4] J. Prokleška *Phys. et al.*, *Rev. B* **92**, 161114(R) (2015)
- [5] M. M. Altarawneh et al., *Phys. Rev. B* **83**, 081103 (2011)

## P-70

## Low Temperature Thermal Expansion and Magnetostriction Measurements of Quantum Spin Ice

N. Tang<sup>1</sup>, A. Sakai<sup>1</sup>, K. Kimura<sup>2</sup>, Y. Matsumoto<sup>3</sup>, S. Nakatsuji<sup>1</sup>

<sup>1</sup>ISSP, University of Tokyo, Japan

<sup>2</sup>Osaka University, Japan

<sup>3</sup>Max Planck Institute, Germany

Geometrical frustration suppresses a long-range order and gives rise to macroscopically degenerate ground states. Pyrochlore oxides, for example,  $\text{Dy}_2\text{Ti}_2\text{O}_7$ , are typical frustrated magnets and known to be so called (classical) spin ice that has 2-in 2-out configuration [1]. On the other hand, if the magnetic element is replaced with the one with a smaller spin such as Pr, quantum fluctuation, which lifts the macroscopic degeneracy of the spin ice, can be important.  $\text{Pr}_2\text{Zr}_2\text{O}_7$  and  $\text{Pr}_2\text{Ir}_2\text{O}_7$  are the candidates of such *at* spin ice materials.  $\text{Pr}_2\text{Ir}_2\text{O}_7$  is metallic and exhibits anomalous hall effect without magnetic field or magnetization, indicating the possible chiral spin liquid [2]. Besides, recent Angle-resolved photoemission spectroscopy (ARPES) measurement reveals that the Ir conduction band touches quadratically to the Fermi surface only at the  $\Gamma$  point [3]. This quadratic band touching can be the origin of the various topological phases such as Weyl semimetals, which can also give rise to the intrinsic anomalous hall effect.

Compared to  $\text{Pr}_2\text{Ir}_2\text{O}_7$ , *lat*  $\text{Pr}_2\text{Zr}_2\text{O}_7$  allows us to study much simpler quantum spin ice physics due to the absence of the conduction electrons. Pinch points, which are indications of spin-ice correlation and magnetic monopoles, are observed in  $\text{Pr}_2\text{Zr}_2\text{O}_7$  by the neutron scattering experiment [4]. In addition, an anomaly is reported from the recent thermal conductivity measurement [5]. Thermal conductivity increases under 200mK, and shows a peak around 80mK. Since there are no thermal carriers at such low temperatures, the theoretically proposed new quasiparticle "photon" must be the carriers [6].

$\text{Pr}^{3+}$  is a non-Kramers ion, and sensitively reacts to the lattice strain hence thermal expansion and magnetostriction becomes crucial. In this poster session, I will report the result of thermal expansion/magnetostriction at low temperature, using high quality single crystal of  $\text{Pr}_2\text{Zr}_2\text{O}_7$ .

[1] A. P. Ramirez, A. Hayashi, R. J. Cava, R. *et al.*, Nature **399**, 333-335 (1999).

[2] Y. Machida, S. Nakatsuji, S. Onoda, *et al.*, Nature **63**, 210 (2010).

[3] T. Kondo, M. Nakayama, *et al.*, Nature Communications **6**, 10042 (2015).

[4] K. Kimura, S. Nakatsuji, J-J. Wen, C. Broholm, M. B. Stone, E. Nishibori & H. Sawa, Nature Communications **1934** (2013).

[5] Y. Tokiwa, *et al.*, APS March Meeting 2016.

[6] O. Benton, O. Sikora, N. Shannon, Phys. Rev. B **86**, 075154 (2012).

## Successive phase transition in $\text{PrV}_2\text{Al}_{20}$ probed by ultrasound measurements ( II )

M. Taniguchi<sup>1</sup>, M. Nakamura<sup>1</sup>, J. Hasegawa<sup>1</sup>, Y. Ohyama<sup>1</sup>, Y. Nakanishi<sup>1</sup>,  
M. Nakamura<sup>1</sup>, M. Yoshizawa<sup>1</sup>, M. Tsujimoto<sup>2</sup>, S. Nakatsuji<sup>2</sup>

<sup>1</sup>Graduate School of Engineering Univ. Iwate

<sup>2</sup>ISSP, Univ. Tokyo

Strongly correlated electron systems (SCES), e.g. materials in which the electrons strongly interact with each other, exhibit emergent collective behavior giving rise to exotic quantum phases and quantum phase transitions. To elucidate the mechanism for the quantum phases is one of the central issues to be solved in condensed matter physics. Exploring elastic properties of SCES, we can obtain their ground state properties and microscopic information on a quadrupole moment. We have investigated elastic properties of the Pr based cage compound  $\text{PrTr}_2\text{Al}_{20}$  (Tr : Ti, V) by means of ultrasonic measurement.  $\text{PrV}_2\text{Al}_{20}$  has the cubic  $\text{CeCr}_2\text{Zn}_{20}$ -type structure with the space group  $\text{Fd}\bar{3}\text{m}$ , e.g. belongs to so-called Frank-Kasper (FK) compounds. Pr and V atoms form a diamond structure and a  $\beta$ -pyrochlore type partial sub lattices, respectively. On the other hand, Al atoms forms a FK cage suitable for encapsulation of guest ions including Pr atom. This unique crystal structure is expected to induce unanticipated quantum phenomena due to characteristic effects such as anharmonic vibration of the rare earth ions formed in the cage and significant strong hybridization. It was believed that  $\text{PrV}_2\text{Al}_{20}$  exhibits a quadrupole transition due to its non-Kramers doublet  $\Gamma_3$  ground state at the initial state, evidenced by the specific heat and magnetic susceptibility measurements [1-3]. However, another clear anomaly was observed in its specific heat

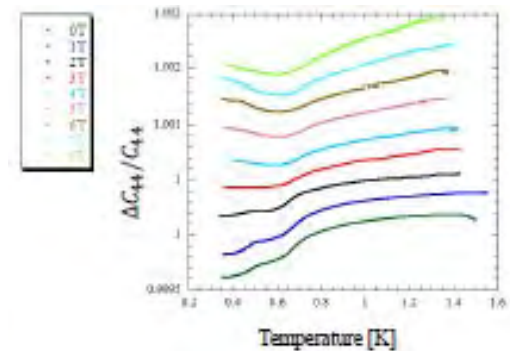


Fig.1

measurement using the larger-size and higher quality single crystal.

Fig.1 shows the temperature dependence of a relative change of the transverse elastic constant  $C_{44}$  under a selected magnetic field. Two clear elastic anomalies are recognized at around 0.6 K and 0.5 K, being in consistent with the specific heat measurement. Based on the phase diagram constructed by the present data, we discuss the updated magnetic phase diagram in detail.

- [1] K. Araki, Y. Shimura, N. Kase, T. Sakakibara, A. Sakai, S. Nakatsuji, : J. Phys. Soc. Jpn. Conf. Proc. **3** (2014) 011093
- [2] M. Tsujimoto, Y. Matsumoto, T. Tomita, A. Sakai, and S. Nakathuji, : Phys. Rev. Lett. **113** (2014) 267001
- [3] Y. Shimura, M. Tsujimoto, B. Zeng, L. Balicas, A. Sakai, and S. Nakatsuji, : J. Phys. Rev. B. **91** (2015) 241102

Ultrasonic investigation of the Nd-based cage compound  $\text{NdV}_2\text{Al}_{20}$ 

M. Nakamura<sup>1</sup>, M. Taniguchi<sup>1</sup>, Y. Nakanishi<sup>1</sup>, M. T. Nakamura<sup>1</sup>, M. Yoshizawa<sup>1</sup>,  
T. Namiki<sup>2</sup>, and K. Nishimura<sup>2</sup>

<sup>1</sup>Iwate University, Morioka 020-8551, Japan

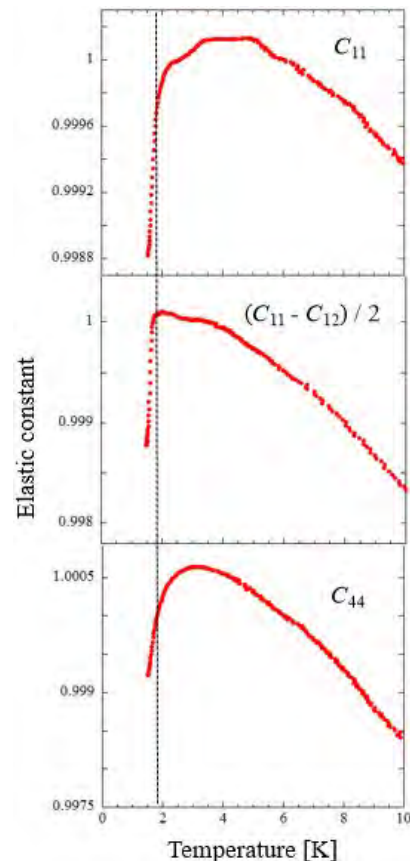
<sup>2</sup>University of Toyama, Toyama 930-8555, Japan

Strongly correlated electron systems (SCES) with a plural number of  $4f$  electrons are one of the most intriguing topics to be studied, in particular if they exhibit typical heavy fermion behavior. Pr-based systems with  $4f^2$  electric configuration is one of the candidates. To extend further, we investigated Nd-based systems with  $4f^3$  electric configuration such as  $\text{NdV}_2\text{Al}_{20}$ .

$\text{NdV}_2\text{Al}_{20}$  crystallizes in the  $\text{CeCr}_2\text{Zn}_{20}$ -type cubic structure with space group  $\text{Fd}\bar{3}\text{m}$ . The Nd atom forms the diamond structure and is encapsulated in a Frank-Kasper cage formed by 16 Al atoms, while the V atom has the icosahedral Al coordination, forming caged structures.  $\text{NdV}_2\text{Al}_{20}$  exhibits a ferromagnetic phase transition at 1.8 K, previously reported by the specific heat and magnetic susceptibility measurements [1]. It should be noted that  $\text{NdV}_2\text{Al}_{20}$  exhibits a resistivity minimum at around 20 K in the temperature  $T$  dependence of the electrical resistivity  $\rho$ , then the  $\rho$  increases logarithmically with decreasing  $T$ . This implies that  $\text{NdV}_2\text{Al}_{20}$  demonstrates typical Kondo behavior at low temperatures. Furthermore, the specific heat  $C$  measurement indicates that the  $C/T$  in zero field remains extremely large at about  $4 \text{ J}/(\text{K}^2 \text{ mol})$  at 0.5 K. In these experiments,  $\text{NdV}_2\text{Al}_{20}$  is considered to be a heavy fermion compound.

In order to elucidate the  $4f$  electronic state of Nd anions and obtain the deeper understanding of SCES with a plural number of  $4f$  electrons, we have investigated elastic properties of Nd-based cage-compound  $\text{NdV}_2\text{Al}_{20}$  probed by ultrasonic measurements. Ultrasonic measurement is a powerful experimental probe for investigating a strain-quadrupole interaction and symmetry of order parameter of a phase transition, and its dynamical fluctuation caused by precursor phenomena as well.

We found a pronounced elastic softening toward the  $T_c = 1.8 \text{ K}$  in the temperature dependence of all the principal elastic constants  $C_{11}$ ,  $(C_{11} - C_{12})/2$  and  $C_{44}$  of  $\text{NdV}_2\text{Al}_{20}$ . The elastic softening was suppressed gradually with increasing a magnetic field. From the detailed analysis of the elastic anomalies, in particular precursor softening of principal elastic constants, we determine microscopic important parameters such as a quadrupole - strain interaction and a quadrupole - quadrupole interaction. We discuss in detail the ground state properties and origin of the pronounced elastic anomalies of the  $\text{NdV}_2\text{Al}_{20}$  based on the experimental data from the viewpoint of their elastic properties as well.



This work was supported by the Japan Society for the Promotion of Science through Grants-in- Aid for Scientific Research (KAKENHI Grant Numbers 15H05883).

[1] T. Namiki, Q. Lei, Y. Ishikawa, and K. Nishimura, J. Phys. Soc. Jpn. **85**, 073706(2016).

## MnSi-nanostructures obtained from thin films: magnetotransport and Hall effect

D. Schroeter<sup>1</sup>, N. Steinki<sup>1</sup>, A. Fernández Scarioni<sup>2</sup>, H. W. Schumacher<sup>2</sup>, S. Süllow<sup>1</sup>, and D. Menzel<sup>1</sup>

<sup>1</sup>Technische Universität Braunschweig, Institut für Physik der Kondensierten Materie, Germany

<sup>2</sup>Physikalisch-Technische Bundesanstalt, 2.52 Nanomagnetism, Germany

In recent years, the field of “Skyrmionics”, which is devoted to the principles and possible applications of complex spin structures, has emerged as a major topic in modern condensed matter physics. In this context, bulk material MnSi has been established as a prime material to study the physics of such skyrmionic phases [1]. Skyrmions are nano-scale spin vortices with interesting physical properties, in particular the enhanced stability due to their non-zero topological winding number resulting in a topologically protected state. Together with their efficient coupling to the conduction electrons skyrmions have a high potential for future data storage techniques.

The cubic B20 material MnSi undergoes a magnetic transition into a helical phase below  $T_N = 29$  K in zero magnetic field which switches into a conical state upon increase of the field to 0.1 T. Furthermore the existence of the so-called A-phase in the phase diagram of MnSi has been established in the temperature range  $\sim 28$ -29 K and fields between 0.1 and 0.2 T [1]. It has been the first observed formation of skyrmions in the solid state, which afterwards resulted in the discovery of a multitude of skyrmionic materials (for an overview see Ref. [2]).

For MnSi bulk material, a comprehensive study of the properties regarding the skyrmion objects has been done. This brings up the question if in thin film MnSi there is a skyrmionic phase as in bulk material. Experimental studies on thin films have as yet been inconclusive – implicitly, it is assumed that signatures in the magnetotransport and magnetization imply skyrmionic phases, although a topological Hall effect as unique signature of the A-phase in bulk MnSi has never been observed [3]. On behalf of theory it was argued that for thin films the skyrmionic phase should be stabilized, but this notion has not been proven experimentally so far [4].

In this situation, we have set out to reinvestigate the (magneto)resistivity and Hall effect in MnSi thin films. Samples of different thicknesses were grown by molecular beam epitaxy and characterized regarding their physical properties. Afterwards Hall geometry nanostructures of various sizes were produced to determine the intrinsic transport properties with means of Hall and resistivity experiments. We compare bulk, thin film and nanostructure data and discuss our results in consideration of electronic correlations and structural as well as morphologic characterization of the samples.

We gratefully acknowledge support by the Braunschweig International Graduate School of Metrology B-IGSM and the DFG Research Training Group GrK1952/1 "Metrology for Complex Nanosystems".

- [1] S. Mühlbauer, B. Binz, F. Jonietz, C. Pfleiderer, A. Rosch, A. Neubauer, R. Georgii, P. Böni, Science 323, 915 (2009).
- [2] N. Nagaosa, Y. Tokura, Nature Nanotechnology 8, 899 (2013).
- [3] A. Neubauer, et al., Phys. Rev. Lett. 102, 186602 (2009).
- [4] A. B. Butenko, A. A. Leonov, U. K. Rößler, A. N. Bogdanov, Phys. Rev. B 82, 052403 (2010).

Uranium ferromagnet with negligible magnetocrystalline anisotropy –  $\text{U}_4\text{Ru}_7\text{Ge}_6$ 

M. Vališka<sup>1</sup>, M. Diviš<sup>1</sup>, V. Sechovský<sup>1</sup>

<sup>1</sup> Faculty of Mathematics and Physics, Charles University, DCMP, Ke Karlovu 5, CZ-12116 Praha 2, Czech Republic

Strong magnetocrystalline anisotropy (MA) is a well-known property of uranium compounds. The almost isotropic ferromagnetism in  $\text{U}_4\text{Ru}_7\text{Ge}_6$  is a striking exception. We present results for magnetization, AC susceptibility, thermal expansion, specific heat and electrical resistivity measurements performed on a  $\text{U}_4\text{Ru}_7\text{Ge}_6$  single crystal at various temperatures and magnetic fields. These results will be discussed in relation to first-principles electronic-structure calculations.  $\text{U}_4\text{Ru}_7\text{Ge}_6$  behaves as an itinerant  $5f$ -electron ferromagnet  $T_C = 10.7$  K,  $\mu_S = 0.85 \mu_B/\text{f.u.}$  at 1.9 K [1]. The ground-state easy-magnetization direction is along the [111] axis of the cubic lattice of the  $Im\bar{3}m$  space group. The anisotropy field  $\mu_0 H_a$  along the [001] direction is only about 0.3 T, which is at least three orders of magnitude smaller than for other U ferromagnets. At  $T_r = 5.9$  K the easy magnetization direction changes to [001], and remains [001] up to  $T_C$ . This transition is due to a change in magnetic symmetry, and is quite apparent in the low-field magnetization, AC susceptibility and thermal expansion data, whereas only weak anomalies are observed at  $T_r$  in the temperature dependence of the specific heat and electrical resistivity. The magnetoelastic interaction induces a rhombohedral (tetragonal) distortion of the paramagnetic cubic crystal lattice in case of the [111]([001]) easy-magnetization direction. The rhombohedral distortion is connected with two crystallographically inequivalent U sites. Our density functional theory (DFT) calculations, including spin-orbit interaction (SOI) of the U  $5f$ -electrons, also produces two inequivalent U sites, because SOI leads to a reduction of the symmetry of the former cubic structure. The calculated ground state is in agreement with the experimentally observed [111] easy-magnetization direction. The first excited state has moments along the [001] direction, which agrees with the moment orientation for  $T > T_r$ . The energy of the first excited state is 0.9 meV above the ground state, which is comparable to the value of 0.51 meV, corresponding to  $k_B T_r$ . We propose that weak MA of the  $\text{U}_4\text{Ru}_7\text{Ge}_6$  compound is due to the lack of direct overlap of the  $5f$  orbitals of the nearest U ions, which is screened out by the closed Ru and Ge cuboctahedra coordinating each U ion.

[1] Michal Vališka, Martin Diviš, and Vladimír Sechovský, Phys. Rev. B, **95**, 085142 (2017).

Electronic and magnetotransport properties of pyrochlore  $\text{Pr}_2\text{Ir}_2\text{O}_7$  epitaxial thin films

T. Ohtsuki<sup>1</sup>, Z. Tian<sup>1</sup>, A. Endo<sup>1</sup>, M. Halim<sup>1</sup>, S. Katsumoto<sup>1</sup>,  
Y. Kohama<sup>1</sup>, K. Kindo<sup>1</sup>, S. Nakatsuji<sup>1,2</sup>, and M. Lippmaa<sup>1</sup>

<sup>1</sup>Institute for Solid State Physics, The University of Tokyo, Kashiwa, Chiba 277-8581, Japan

<sup>2</sup>CREST, Japan Science and Technology Agency (JST), Kawaguchi, Saitama 332-0012 Japan

In 5d electron system represented by iridates, spin-orbit and Coulomb interactions are of approximately the same order of magnitude. As a result, novel topological phases such as Weyl semimetal and strongly correlated topological insulator are predicted to emerge [1]. Here, one of pyrochlore iridates,  $\text{Pr}_2\text{Ir}_2\text{O}_7$  is focused.  $\text{Pr}_2\text{Ir}_2\text{O}_7$  shows interesting physical properties: it is metallic down to the lowest temperature [2]; it behaves as spin liquid and magnetic long range order is not confirmed down to 0.3 K [2,3]; it exhibits spontaneous Hall effect generated by spin chirality [4]; it has a Fermi node formed by quadratic band touching of the doubly degenerate valence and conduction bands at the  $\Gamma$  point at the Fermi level [5]. Moreover, it shows anisotropic magnetotransport, that is, spontaneous Hall resistivity is maximized when magnetic field is applied along [111] direction [6]. For the  $\text{Pr}_2\text{Ir}_2\text{O}_7$ , the studies have preceded using bulk samples, but recently, we successfully fabricated (111)-oriented pyrochlore  $\text{Pr}_2\text{Ir}_2\text{O}_7$  epitaxial thin films [7]. In this study, the electronic and magnetotransport properties of pyrochlore  $\text{Pr}_2\text{Ir}_2\text{O}_7$  epitaxial thin films are investigated.

$\text{Pr}_2\text{Ir}_2\text{O}_7$  thin films are deposited on yttria-stabilized zirconia (111) substrate by pulsed laser deposition at room temperature, and then, the as-grown films are crystallized by post-annealing.

When the sample is cooled from room temperature, the longitudinal resistivity of  $\text{Pr}_2\text{Ir}_2\text{O}_7$  thin films monotonically decreases at first, indicating metallic conductivity. Then, the resistivity minimum is observed at 47 K, followed by a nondivergent upturn towards 0 K. The results of Hall measurement are noteworthy. The magnetic field dependence of the Hall resistivity shows a hysteresis loop around zero field below 50 K. Bulk samples are also known to exhibit the non-zero remanent Hall resistivity, but the onset temperature of 1.5 K for the bulk samples is much lower than that for our thin film case. When magnetization curve of  $\text{Pr}_2\text{Ir}_2\text{O}_7$  thin film is measured, hysteresis loop is not found. Therefore,  $\text{Pr}_2\text{Ir}_2\text{O}_7$  thin film shows a spontaneous Hall effect without magnetic field nor spontaneous magnetization. The spontaneous Hall effect is not caused by the conventional mechanism for anomalous Hall effect related to ferromagnetism, but by the unconventional one originating from a non-coplanar or non-collinear spin texture.

This work was supported by CREST (Grant No. JPMJCR15Q5), Japan Science and Technology Agency, Grants-in-Aid for Scientific Research (Grant Nos. 16H02209, 25707030, and 26105002), by Grants-in-Aid for Scientific Research on Innovative Areas “J-Physics” (Grant Nos. 15H05882 and 15H05883), Program for Advancing Strategic International Network to Accelerate the Circulation of Talented Researchers (Grant No. R2604) from the Japanese Society for the Promotion of Science, and the support of ICAM Branches Cost Sharing Fund.

- [1] W. Witczak-Krempa *et al.*, *Annu. Rev. Condens. Matter Phys.* **5**, 57 (2013).
- [2] S. Nakatsuji *et al.*, *Phys. Rev. Lett.* **96**, 087204 (2006).
- [3] Y. Tokiwa *et al.*, *Nat. Mater.* **13**, 356 (2014).
- [4] Y. Machida *et al.*, *Nature* **463**, 210 (2010).
- [5] T. Kondo *et al.*, *Nat. Commun.* **6**, 10042 (2015).
- [6] L. Balicas *et al.*, *Phys. Rev. Lett.* **106**, 217204 (2011).
- [7] T. Ohtsuki *et al.*, preprint.

## Synthesis, structure and magnetism in honeycomb magnets of $R\text{Ni}_3\text{Al}_9$ , $R\text{Ni}_3\text{Ga}_9$ , $R_2\text{Pt}_6\text{Ga}_{15}$ and $R_2\text{Rh}_3\text{Ga}_9$ ( $R$ : rare-earth elements)

S. Ohara<sup>1,2</sup>, T. Kano<sup>2</sup>, K. Hyodo<sup>2</sup>, K. Kishimoto<sup>2</sup>, T. Ueda<sup>1</sup>, and H. Ninomiya<sup>1</sup>

<sup>1</sup>Department of Engineering Physics, Electronics and Mechanics, Graduate School of Engineering, Nagoya Institute of Technology, Nagoya 466-8555, Japan

<sup>2</sup>Department of Physical Science and Engineering, Graduate School of Engineering, Nagoya Institute of Technology, Nagoya 466-8555, Japan

We have synthesized single crystals of  $R\text{Ni}_3\text{Al}_9$ ,  $R\text{Ni}_3\text{Ga}_9$ ,  $R_2\text{Pt}_6\text{Ga}_{15}$ , and  $R_2\text{Rh}_3\text{Ga}_9$ , here  $R$  are rare-earth elements [1-4]. These compounds belong to the ternary rare-earth intermetallic system of  $R_2T_{3n}M_3(2n+m)$  ( $R$ =rare-earth,  $T$ =transition metal,  $M$ =Al, Ga, and  $m, n=1, 2$ ), and have a similar layered structure [5]. The crystal structure is characterized by the presence of  $R_2M_3$ -layer. In this layer,  $R$ -atoms and the centers of small  $M$ -atom triangles also form a triangular mesh. As a result,  $R$ -atoms form a honeycomb-structure. Thus, we can study the properties of the honeycomb magnet using these compounds. Recently, new current-induced magnetoelectric effect was predicted theoretically for the locally non-centrosymmetric material [6]. Since the inversion symmetry is broken locally at the site on the honeycomb structure, this material system is also well suited to study the physics for the locally non-centrosymmetric material.

To study the physical properties of  $R\text{Ni}_3\text{Al}_9$ ,  $R\text{Ni}_3\text{Ga}_9$ ,  $R_2\text{Pt}_6\text{Ga}_{15}$ , and  $R_2\text{Rh}_3\text{Ga}_9$ , we grew the single crystal by flux-method [1]. We measured the X-ray diffraction and determined the crystal structure. Specific heat, magnetic susceptibility, magnetization, and electrical resistivity were measured from 2 to 300 K. We have also attempted to detect the current-induced magnetization.

We found that  $R\text{Ni}_3M_9$ ,  $R_2\text{Pt}_6\text{Ga}_{15}$ , and  $R_2\text{Rh}_3\text{Ga}_9$  crystallize in the trigonal  $\text{ErNi}_3\text{Al}_9$ -type structure of space group  $R32$ , hexagonal  $\text{Sc}_{0.67}\text{Fe}_2\text{Si}_5$ -type structure of  $P6_3/mmc$ , and orthorhombic  $\text{Y}_2\text{Co}_3\text{Ga}_9$ -type structure of  $\text{Cmcm}$ , respectively. It is noted that trigonal  $R\text{Ni}_3M_9$  has chiral crystal structure. In orthorhombic  $R_2\text{Rh}_3\text{Ga}_9$ , the honeycomb structure is slightly elongated along  $a$ -axis.

For these honeycomb magnets, we found various magnetic states and transitions, such as chiral helix with chiral-soliton-lattice, canted antiferromagnetic structure, magnetic plateaus with metamagnetic transition, and multipole order. For one example,  $\text{DyNi}_3\text{Ga}_9$  shows ferroquadrupolar order at 10 K and has the canted antiferromagnetic structure below 9 K [6, 7]. Magnetization curves of  $\text{DyNi}_3\text{Ga}_9$ , for three distinct crystal axes at 2K, are shown in Fig. 1. Below 2 K, magnetic plateaus with metamagnetic transitions are clearly observed, when the magnetic field is in the honeycomb plane.

We will present the details of crystal structures and some of the highlights of the magnetic properties for  $R\text{Ni}_3\text{Al}_9$ ,  $R\text{Ni}_3\text{Ga}_9$ ,  $R_2\text{Pt}_6\text{Ga}_{15}$ , and  $R_2\text{Rh}_3\text{Ga}_9$ . The recent result of current-induced magnetization for chiral helical magnet  $\text{YbNi}_3\text{Al}_9$  will also be given.

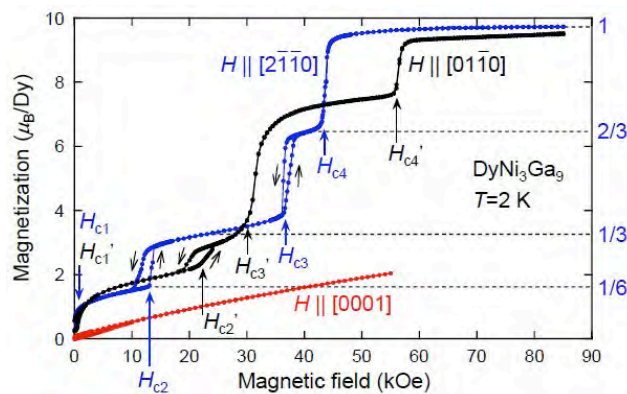


Fig. 1 Magnetization curves of  $\text{DyNi}_3\text{Ga}_9$ , for three distinct crystal axes at 2K

This work was supported by Grant-in-Aid for Scientific Research (Grant number JP26400333), Grant-in-Aid for Scientific Research on Innovative Areas “J-Physics” (Grant number JP16H01073), and Core-to-Core Program “A Consortium to Exploit Spin Chirality in Advanced Materials” from the Ministry of Education, Culture, Sports, Science and Technology, Japan.

- [1] T. Yamashita, R. Miyazaki, Y. Aoki and S. Ohara, J. Phys. Soc. Jpn. **81**, 034705 (2012).  
 [2] T. Yamashita, S. Ohara, and I. Sakamoto, J. Phys. Soc. Jpn. **80**, S49 (2011).  
 [3] S. Ohara, T. Fukuta, K. Ohta, H. Kono, T. Yamashita, Y. Matsumoto, and J. Yamaura, JPS Conf. Proc. **3**, 017016 (2014).

- [4] Y. Matsumoto, T. Ueda, and S. Ohara, J. Phys. Conf. Series. **683**, 012035 (2016).  
 [5] Y. Lutsyshyn, Y. Tokaychuk, V. Davydov, and R. Gladyshevskii, Chem. Met. Alloys **1**, 303 (2008).  
 [6] S. Hayami, H. Kusunose, and Y. Motome, Phys. Rev. B **90**, 024432 (2014)  
 [7] H. Ninomiya, Y. Matsumoto, S. Nakamura, Y. Kono, S. Kittaka, T. Sakakibara, K. Inoue, and S. Ohara, (to be submitted)  
 [8] I. Ishii, K. Takezawa, T. Mizuno, S. Kamikawa, H. Ninomiya, Y. Matsumoto, S. Ohara, and T. Suzuki, (to be submitted)

# P-77

## Dynamical Multiferroicity

Dominik M. Juraschek  
ETH Zurich, Switzerland

An appealing mechanism for inducing multiferroicity in materials is the generation of electric polarization by a spatially varying magnetization that is coupled to the lattice through the spin-orbit interaction. Here we describe the reciprocal effect, in which a time-dependent electric polarization induces magnetization even in materials with no existing spin structure. We develop a formalism for this dynamical multiferroic effect in the case for which the polarization derives from optical phonons, and compute the strength of the phonon Zeeman effect, which is the solid-state equivalent of the well-established vibrational Zeeman effect in molecules, using density functional theory. We further show that a recently observed behavior—the resonant excitation of a magnon by optically driven phonons—is described by the formalism. Finally, we discuss examples of scenarios that are not driven by lattice dynamics and interpret the excitation of Dzyaloshinskii-Moriya-type electromagnons and the inverse Faraday effect from the viewpoint of dynamical multiferroicity.

Magnetic phase diagram in  $\text{Sr}_{2-x}\text{La}_x\text{IrO}_4$  synthesized by mechanical alloying method

K. Horigane<sup>1</sup>, M. Fujii<sup>2</sup>, H. Okabe<sup>3</sup>, K. Kobayashi<sup>1,2</sup>, R. Horie<sup>1</sup>, H. Ishii<sup>4</sup>, Y. Kubozono<sup>1</sup>  
A. Koda<sup>3</sup>, R. Kadono<sup>3</sup> and J. Akimitsu<sup>1</sup>

<sup>1</sup>Research Institute for Interdisciplinary Science, Okayama University, Okayama, Japan  
<sup>2</sup>Graduate School of natural science and technology, Okayama University, Okayama, Japan  
<sup>3</sup>Institute of Materials Structure Science/J-PARC Center, KEK, Ibaraki, Japan  
<sup>4</sup>National Synchrotron Radiation Research Center, Hsinchu 30076, Taiwan.

Layered perovskite *5d* transition metal oxides  $\text{Sr}_2\text{IrO}_4$  has attracted much attention because several experiments have revealed a novel spin-orbit-induced  $J_{\text{eff}}=1/2$  Mott insulating behavior at low temperature. In this insulator with effectively one hole per Ir ion, this pseudospin remains a good quantum number and orders antiferromagnetically ( $T_N \sim 240\text{K}$ ). From the Monte Carlo study, Watanabe et al. point out that the superconducting state is found stable only by electron doping [1]. These results suggest that  $\text{Sr}_2\text{IrO}_4$  is good candidate for unconventional superconductivity by carrier doping.

Experimentally, physical properties in electron doped  $\text{Sr}_2\text{IrO}_4$  systems were extensively studied by several groups. Castaneda et al. reported the structure and magnetic properties of polycrystalline samples of  $\text{Sr}_{2-x}\text{La}_x\text{IrO}_4$ . They found that electrical resistivity increases with increasing La concentration and magnetic susceptibility results show the canted antiferromagnetism below 240K in both  $\text{Sr}_2\text{IrO}_4$  and electron doped  $\text{Sr}_{1.85}\text{La}_{0.15}\text{IrO}_4$  [2]. However, Neutron scattering and magnetic susceptibility measurements using single crystalline samples of  $\text{Sr}_{2-x}\text{La}_x\text{IrO}_4$  revealed that long-range AF order was suppressed up to  $x = 0.04$  and short-range AF order persisted up to  $x=0.12$  by La doping [3]. T. F. Qi et al. reported oxygen vacancies into single crystal  $\text{Sr}_2\text{IrO}_{4-\delta}$  ( $0 < \delta < 0.04$ ) lead to significant reduction of resistivity and  $\text{Sr}_2\text{IrO}_{4-\delta}$  ( $\delta=0.04$ ) shows metal-insulator transition at 105K [4]. Thus, the physical property differences between poly crystal and single crystal are still unsolved issue.

In this study, thus, we performed mechanical alloying (MA) synthesis because MA is well known to improve chemical reaction. We report the crystal structure and physical properties of  $\text{Sr}_{2-x}\text{La}_x\text{IrO}_4$  using synchrotron powder x-ray diffraction, magnetic susceptibility, electrical resistivity and muon spin relaxation ( $\mu\text{SR}$ ) measurements.

The result of magnetic susceptibility in  $\text{Sr}_{2-x}\text{La}_x\text{IrO}_4$  is shown in Fig. 1-(a). The observed values of magnetic susceptibility tend to decrease with La concentration. The La doping leads to significant straightening of the I-O-Ir bond angles, so the reduction of magnetic susceptibility is caused by not only the carrier doping but also the Ir-O-Ir bond angles. As for the  $T_N$ , a clear reduction of  $T_N$  is observed by La doping and  $T_N$  is changed from 240K ( $x=0$ ) to 114K ( $x=0.13$ ). These resistivity and magnetic susceptibility results are consistent with the previous results using single crystalline samples [3].

As for the zero field  $\mu\text{SR}$  study, we found that short-range AF order is realized in  $\text{Sr}_{1.9}\text{La}_{0.1}\text{IrO}_4$  and spin glass state is stabilized in low temperature region. The Ir moment estimated by the LF  $\mu\text{SR}$  result is  $0.045 \mu_B$ , 9 times smaller than that of  $\text{Sr}_2\text{IrO}_4$  ( $\sim 0.4 \mu_B$ ). Furthermore, we found the relation between  $T_N$  and tetragonal distortion ( $c/a$ ) in this system. This result suggests that magnetism of Sr214 system is strongly correlated with the crystal structure.

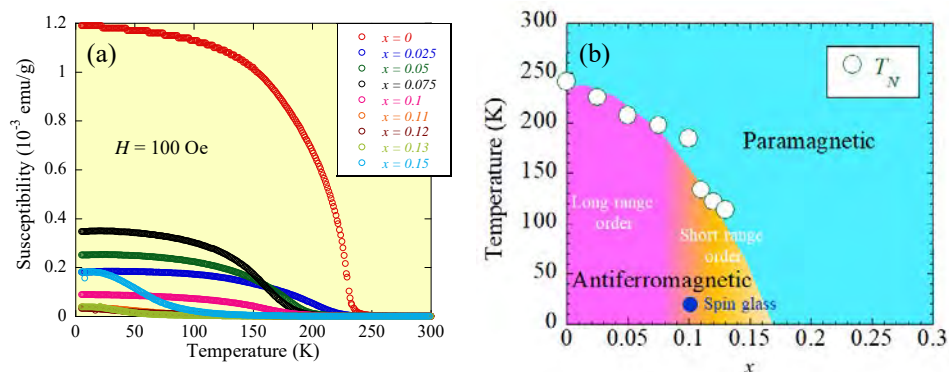


Figure 1 (a) Temperature dependence of magnetic susceptibility of  $\text{Sr}_{2-x}\text{La}_x\text{IrO}_4$ . (b) Magnetic phase diagram of  $\text{Sr}_{2-x}\text{La}_x\text{IrO}_4$  determined by magnetic susceptibility and  $\mu\text{SR}$  measurements.

- [1] H. Watanabe, T. Shirakawa and S. Yunoki, Phys. Rev. Lett. **110**, 027002 (2013)  
[2] C. C. Castaneda et al., J. Phys.:Condens. Matter 19 446210 (2007).  
[3] X. Chen et al., Phys. Rev. B 92 075125 (2015)  
[4] T. F. Qi et al., Journal of Applied Physics 109 07D906 (2011)

## Intercalated Bismuth Selenide superconductor: Resilient superconductivity over structural transition

K. Kobayashi<sup>1,2</sup>, T. Ueno<sup>2</sup>, H. Fujiwara<sup>2</sup>, T. Yokoya<sup>1,2</sup> and J. Akimitsu<sup>1</sup>

<sup>1</sup>Research Institute for Interdisciplinary Science, Okayama University, Okayama 700-8530, Japan

<sup>2</sup>Department of Physics, Okayama University, Okayama 700-8530, Japan

Superconductors with topologically protected gapless surface states are called topological superconductors (TSC) and discussed for their exotic properties [1]. The downside of the uprising field enjoying the daily update of new knowledge is less experimental studies compared to the theoretical proposals. To provide more stages to the field, we synthesized various intercalated bismuth selenide ( $\text{Bi}_2\text{Se}_3$ ) in pursuit of new topological superconductor and obtained superconducting Nb intercalated between the quintuple layers ( $\text{Nb}_x\text{Bi}_2\text{Se}_3$  in composition).

The compound ( $\text{Nb}_x\text{Bi}_2\text{Se}_3$ ) is reported to have ferromagnetic order coexistence with superconductivity [2], as well as the even-function structure within the conducting layer [3] and many other interesting properties [4,5]. Unlike the sister compound  $\text{Cu}_x\text{Bi}_2\text{Se}_3$ , it is stable in air and Nb is also stable in air, making it the easiest-to-handle candidate of topological superconductor in bismuth selenide family. This benefits the compound to be the stage to study the superconductivity in the series, which is strongly expected to be TSC. Thus it is interesting to see how superconducting state is obtained in the system and how it disappears to understand the mechanism of superconductivity.

To study how superconductivity changes in  $\text{Nb}_x\text{Bi}_2\text{Se}_3$ , we synthesized for  $x=0$  to 1. The superconductivity appears in all compound except  $x=0$ . This implies that the superconductivity is stable in various Nb-doping. This contrasts the behaviour of  $\text{Sr}_x\text{Bi}_2\text{Se}_3$  of which superconductivity appears in very little amount of Sr intercalation. The powder X-ray diffraction pattern of  $\text{Nb}_{0.05}\text{Bi}_2\text{Se}_3$  is shown in Fig. 1(a). In increasing Nb( $x$ ), the structure gradually changes from  $\text{Bi}_2\text{Se}_3$  to BiSe. BiSe structure is one of the infinite layer structures in Bi-Se compounds discussed for their structural stability in various Bi-Se ratio [6], shown in lower panel of Fig.1(b). We observed BiSe structure to be stable beyond  $x=0.3$  indicating that the superconductivity is stable in BiSe and the possibility of new doping mechanism in the material family.

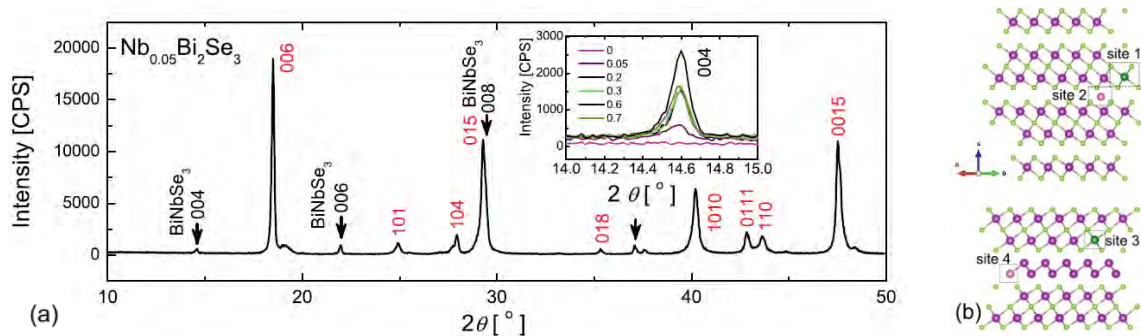


Fig. 1(a) Powder X-ray diffraction pattern of  $\text{Nb}_{0.05}\text{Bi}_2\text{Se}_3$ . Main peaks are indexed with  $\text{Bi}_2\text{Se}_3$  structure in addition to the impurity  $\text{BiNbSe}_3$  peaks indicated with arrows. Inset: (004) peak of  $\text{BiNbSe}_3$  does not change the position by increasing Nb from 0.05 to 0.7. (b) upper panel:  $\text{Bi}_2\text{Se}_3$  structure with 2 possible Nb positions (site 1, 2). Lower panel: BiSe structure with 2 possible Nb positions (site 3, 4).

This work is supported by Grant-in-Aid from Ministry of Education, Culture, Sports, Science and Technology (MEXT) under No. 25000003, 15K13524, 15H03691, and 26247057, by JSPS KAKENHI Grant Number 15H05886 and partially by the Program for Advancing Strategic International Networks to Accelerate the Circulation of Talented Researchers from Japan Society for the Promotion of Science.

- [1] L. Fu and E. Berg, Phys. Rev. Lett., **105**, 097001 (2010).
- [2] Y. Qiu, K. N. Sanders, J. Dai, J. E. Medvedeva, W. Wu, P. Ghaemi, T. Vojta, Y. S. Hor, arXiv:1512.03519 (2015).
- [3] T. Asaba, B. J. Lawson, C. Tinsman, L. Chen, P. Corbae, G. Li, Y. Qiu, Y. S. Hor, L. Fu, and L. Li, Phys. Rev. X **7**, 011009 (2017).
- [4] M. P. Smylie, H. Claus, U. Welp, W.-K. Kwok, Y. Qiu, Y. S. Hor, and A. Snezhko, Phys. Rev. B **94**, 180510(R) (2016).
- [5] K. Kobayashi, T. Ueno, H. Fujiwara, T. Yokoya, and J. Akimitsu, Phys. Rev. B **95**, 180503(R) (2017).
- [6] H. Lind, S. Lidin, and U. Häussermann, Phys. Rev. B **72**, 184101 (2005).

Doping Dependence of the Anomalous Transport Properties of  $\text{Mn}_3\text{Sn}$ 

M. Ikhlas<sup>1,2</sup>, T. Tomita<sup>1,2</sup>, T. Koretsune<sup>3,4</sup>, M.-T. Suzuki<sup>2,4</sup>, D. Nishio-Hamane<sup>1</sup>, R. Arita<sup>2,4</sup>, Y. Otani<sup>1,2,4</sup>, and S. Nakatsuji<sup>1,2</sup>

*Institute for Solid State Physics (ISSP), The University of Tokyo<sup>1</sup>, JST CREST<sup>2</sup>, JST PRESTO<sup>3</sup>, RIKEN-CEMS<sup>4</sup>*

The non-collinear triangular antiferromagnet  $\text{Mn}_3\text{Sn}$  has been experimentally shown to exhibit large anomalous Hall conductivity of  $\sim 100 \text{ } \Omega^{-1} \text{ cm}^{-1}$ , in spite of carrying a vanishing in-plane magnetization of only  $\sim 3 \text{ m}\mu_{\text{B}}/\text{Mn}$ [1]. Theoretically, it has been proposed that the large anomalous Hall conductivity in  $\text{Mn}_3\text{Sn}$  is driven by the Berry curvature of Weyl points in the vicinity of the Fermi energy. Thus,  $\text{Mn}_3\text{Sn}$  could be the first case of the elusive magnetic Weyl metallic state[2]. It has been known that  $\text{Mn}_3\text{Sn}$  single crystal is stable only in the presence of excess Mn, which occupies the Sn site in the hexagonal lattice. Hence, it is important to clarify how this dopant modifies the transport properties of  $\text{Mn}_3\text{Sn}$ . Here we will report our measurements of both the transport and magnetic properties of  $\text{Mn}_3(\text{Sn}_{1-x}\text{Mn}_x)$  single crystals grown by the Bridgman method. We have found that the excess Mn effectively dopes electron into the system. In addition, we will compare the trend in the change of Hall conductivity and transverse thermoelectric conductivity as a function of Mn doping with our first-principle calculation which points to the existence of Weyl points above the Fermi energy in the undoped  $\text{Mn}_3\text{Sn}$  [3].

[1] S. Nakatsuji, N. Kiyohara, and T. Higo, *Nature* **527**, 212 (2015).

[2] H. Yang, Y. Sun, Y. Zhang, W.-J. Shi, S. Parkin, and B. Yan, *New J. Phys.* **19**, 015008 (2017).

[3] M. Ikhlas, T. Tomita, T. Koretsune, M.-T. Suzuki, R. Arita, Y. Otani, and S. Nakatsuji, *Nat. Phys.* (2017)

# P-81

## Relation of quasiparticle mass enhancement to antiferroquadrupolar order in PrOs<sub>4</sub>Sb<sub>12</sub>.

A. McCollam<sup>1</sup>, N. Hesp<sup>1</sup>, I. Broeders<sup>1</sup>, L.M.K. Tang<sup>1</sup>, J.A.N. Bruin<sup>1</sup>, S.R. Julian<sup>2</sup>, and B. Andraka<sup>3</sup>

<sup>1</sup>High Field Magnet Laboratory (HFML-EMFL), Radboud University, Nijmegen, The Netherlands.

<sup>2</sup>Department of Physics, University of Toronto, Toronto, Canada.

<sup>3</sup>Department of Physics, University of Florida, Gainesville, USA.

PrOs<sub>4</sub>Sb<sub>12</sub> was reported as the first Pr-based heavy fermion superconductor [1], with  $T_C \sim 1.85$  K. Soon afterwards, a region of long range antiferroquadrupolar order was identified at magnetic fields above 4 T [2-4], slightly higher than the superconducting upper critical field of  $\sim 2$  T. Measurements of the de Haas-van Alphen effect showed that the quasiparticle masses are moderately enhanced in this material, at  $\sim 2 m_e$  to  $8 m_e$  [5], and indicate involvement of the Pr  $f$ -electrons, but the mechanism of mass enhancement is not yet established. One appealing suggestion is that antiferroquadrupole fluctuations, interacting with conduction electrons via crystalline electric field excitations, may be responsible for the quasiparticle mass enhancement [6], and may also be involved with the superconductivity, but a detailed study of the magnetic field dependence of the mass enhancement has not, so far, been available. We have recently measured de Haas-van Alphen oscillations across the extended magnetic field vs. temperature phase diagram of PrOs<sub>4</sub>Sb<sub>12</sub>, between 3 T and 33 T and from 2 K to 50 mK, and have extracted the quasiparticle effective masses over this whole region. I will present our results, which reveal significant magnetic field dependence of the quasiparticle masses, and will discuss evolution of the mass with respect to the antiferroquadrupolar and crystal field excitations in the system.

- [1] E. Bauer *et al.*, Physical Review B, **65**, 100506(R) (2002).
- [2] Y. Aoki *et al.*, Journal of the Physical Society of Japan, **71**, 2098 (2002).
- [3] M. Kohgi *et al.*, Journal of the Physical Society of Japan, **72**, 1002 (2003).
- [4] K. Kaneko *et al.*, Physical Review B, **75**, 094408 (2007).
- [5] H. Sugawara *et al.*, Physical Review B, **66**, 220504(R) (2002).
- [6] H. Tou *et al.*, Journal of the Physical Society of Japan, **80**, 074703 (2011).

## Homo-chiral crystal growth and mono-chiral helimagnetism in inorganic chiral magnetic compounds

Y. Kousaka<sup>1,2</sup>, K. Ohishi<sup>3</sup>, H. Ninomiya<sup>4</sup>, Y. Matsumoto<sup>5</sup>, S. Ohara<sup>4</sup>, K. Kakurai<sup>3</sup>, V. Hutanu<sup>6</sup>, J. Suzuki<sup>3</sup>, J. Campo<sup>7</sup>, K. Inoue<sup>2,8</sup>, and J. Akimitsu<sup>1,2</sup>

<sup>1</sup>Research Institute for Interdisciplinary Science, Okayama University, Okayama, Okayama 700-8530, Japan

<sup>2</sup>Center for Chiral Science, Hiroshima University, Higashi-hiroshima, Hiroshima 739-8526, Japan

<sup>3</sup>Neutron Science and Technology Center, Comprehensive Research Organization for Science and Society (CROSS), Tokai, Ibaraki 319-1106, Japan

<sup>4</sup>Graduate School of Engineering, Nagoya Institute and Technology, Nagoya 466-8555, Japan

<sup>5</sup>Graduate School of Science and Engineering, University of Toyama, Toyama 930-8555, Japan

<sup>6</sup>Institute of Crystallography, RWTH Aachen University and Julich Centre for Neutron Science (JCNS) at Heinz Maier-Leibnitz Zentrum (MLZ), 85747 Garching, Germany

<sup>7</sup>Aragon Materials Science Institute (CSIC-University of Zaragoza), 50009 Zaragoza, Spain

<sup>8</sup>Graduate School of Science, Hiroshima University, Higashi-hirosima, Hiroshima 739-8526, Japan

The concept of chirality, meaning left- or right-handedness, plays an essential role in symmetry properties of nature at all length scales from elementary particles to cosmic science. In material sciences, it is very important to understand the chirality in molecules, crystals and magnetic structures both from theoretical and experimental viewpoints. Chiral helimagnetic structure, forming only one-handed chiral domain, has attracted attention due to emergence of unique magnetic textures such as skyrmion lattice and chiral magnetic soliton lattice. Therefore, it is very important to investigate interplay between crystallographic and helimagnetic chirality because the helicity of a screw magnetic structure strongly depends on the chiral crystal structure as requested by the anti-symmetric Dzyaloshinskii-Moriya (DM) interaction. However, there have been only few experimental results on studying the interplay between crystallographic chirality and that of magnetic structure because of difficulty in controlling the crystallographic chirality

Firstly, we will present our crystallization technique to make a single crystallographic chirality in inorganic compounds. For an example, by adopting spontaneous crystallization with stirring, we succeeded in obtaining the cm-sized homo-chiral single crystals of CsCuCl<sub>3</sub>. Secondly, we will present polarized neutron diffraction works of CsCuCl<sub>3</sub> and YbNi<sub>3</sub>Al<sub>9</sub>, performed at BL15 (TAIKAN) in the Materials and Life Science Experimental Facility (MLF) of J-PARC and instrument POLI at Maier-Leibnitz Zentrum (MLZ) in Germany. We observed a strong relationship between crystal and magnetic chiralities, which governs the nature of anti-symmetric Dzyaloshinskii-Moriya interaction. Figure 1 shows omega-scan profiles of the (1/3, 1/3, 6-q) in homo-chiral crystals of CsCuCl<sub>3</sub>. The difference in intensity between different spin-flip cross sections in neutron scattering indicates mono-chiral helimagnetic structure.

This work was supported by JSPS KAKENHI Grant Number 25220803, 25390139, 26108719, 15H03680, 15H05885, 15H05886, 16KK0102, 17H02912, 17H02767, and 17H02815. JC acknowledges the Grant Number MAT2015-68200-C2-2-P from the Spanish Ministry of Economy and Competitiveness.

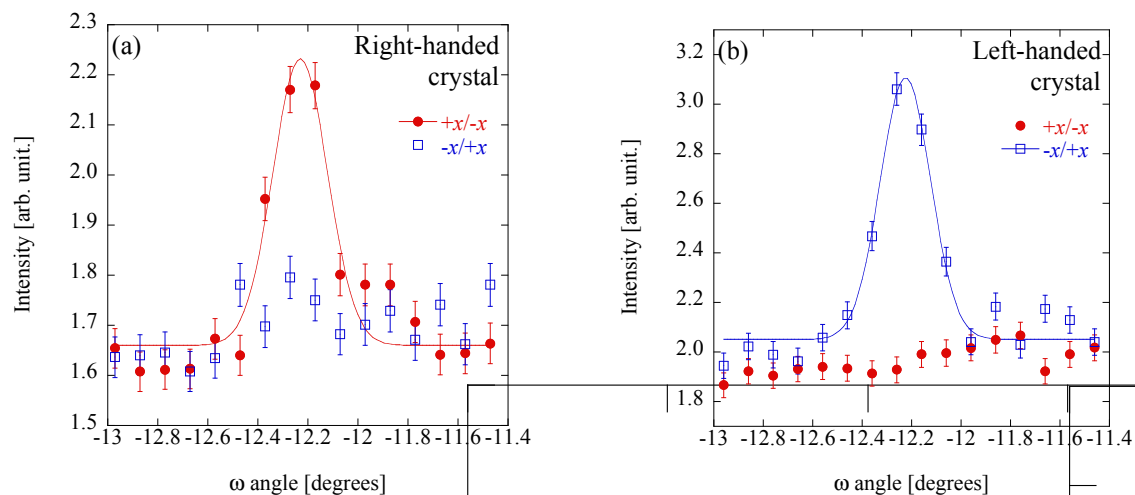


Fig. 1 Omega-scan profiles of the (1/3, 1/3, 6-q) magnetic Bragg reflections for (a) right-handed and (b) left-handed homo-chiral crystals of CsCuCl<sub>3</sub>

Single crystal study for a ferromagnetic Kondo compound  $\alpha$ -CeNiSb<sub>3</sub>Y. Muro<sup>1</sup>, Y. Kamiya<sup>1</sup>, T. Fukuhara<sup>1</sup>, T. Kuwai<sup>2</sup>, and S. Masubuchi<sup>3</sup><sup>1</sup>Dept. Intelligent Systems Design Engineering, Toyama Prefectural University, Imizu 939-0398, Japan<sup>2</sup>Graduate school of Science and Engineering, University of Toyama, Toyama 930-8555, Japan<sup>3</sup>Dept. Physics, Tokyo Medical University, Tokyo 160-8402, Japan

A ternary Ce compound  $\alpha$ -CeNiSb<sub>3</sub>, crystallizing in the orthorhombic space group Pbcm, shows a layered structure composed of two-dimensional Ce and Sb nets and TSb<sub>6</sub> octahedra [1]. The results of magnetic susceptibility, which is not shown as a figure, electrical resistivity on the  $bc$ -plane and specific heat indicate  $\alpha$ -CeNiSb<sub>3</sub> is a ferromagnetic Kondo compound with the transition temperature  $T_C = 6$  K [2]. The pressure study suggests a change of electronic structure above 35 kbar [3]. In order to investigate the ferromagnetic nature and magnetic anisotropy of  $\alpha$ -CeNiSb<sub>3</sub> at ambient pressure, we measured the magnetic susceptibility, magnetization, and electrical resistivity by using a high quality single crystal.

Single crystals were grown by the Sb self-flux method. The structure parameters obtained by Rietveld refinements agreed well with those reported in ref. [1]. The magnetic susceptibility  $\chi(T)$  is highly anisotropic with  $\chi_c > \chi_b > \chi_a$ . At low temperatures, a sudden increase of  $\chi$  due to the ferromagnetic transition are observed in  $\chi_c$  and  $\chi_a$ , while a sharp cusp is observed in  $\chi_b$  at  $T_C = 6$  K. In the magnetization  $M(B)$  at 2 K, a metamagnetic-like anomaly is shown at 2 T in  $B \parallel a$  and  $B \parallel b$ . In addition, the anomaly in  $B \parallel a$  accompanies a hysteretic behaviour. These features in  $\chi_b$ ,  $M(B \parallel a)$ , and  $M(B \parallel b)$  suggest that the magnetic order of  $\alpha$ -CeNiSb<sub>3</sub> is not a simple ferromagnetic one. The electrical resistivity  $\rho(T)$  shows a nearly two-dimensional anisotropy: the value of  $\rho(T)$  for the  $a$ -axis is 10 times larger than those for the  $b$ - and  $c$ -axes. This feature is similar to  $\rho(T)$  for another ferromagnetic Kondo compound CeAgSb<sub>2</sub> [4]. Therefore, the nearly two-dimensional electronic structure and the distorted square structure of Ce layer may result in the complex magnetic structure below  $T_C$ .

- [1] R. T. Macaluso, D. M. Wells, R. E. Sykora, T. E. Albrecht-Schmitt, A. Mar, S. Nakatsuji, H. Lee, Z. Fisk, and J. Y. Chan, *J. Solid State Chemistry* **177**, 293 (2004).
- [2] E. L. Thomas, D. P. Gautreaux, H. Lee, Z. Fisk, and J. Y. Chan, *Inorg. Chem.* **46**, 3010 (2007).
- [3] V. A. Sidorov, E. D. Bauer, H. Lee, S. Nakatsuji, J. D. Thompson, and Z. Fisk, *Phys. Rev. B* **71**, 094422 (2005).
- [4] Y. Inada, A. Thamizhavel, H. Yamagami, T. Takeuchi, Y. Sawai, S. Ikeda, H. Shishido, T. Okubo, M. Yamada, K. Sugiyama, N. Nakamura, T. Yamamoto, K. Kindo, T. Ebihara, A. Galatanu, E. Yamamoto, R. Settai, and Y. Ōnuki, *Phil. Mag. B* **82**, 1867 (2002).

Linear dichroism in *angle-resolved* core-level photoemission spectra  
reflecting anisotropic strongly correlated outer-orbital charge distributions

A. Sekiyama<sup>1,2</sup>, Y. Kanai<sup>1,2</sup>, S. Hamamoto<sup>1,2</sup>, S. Fujioka<sup>1,2</sup>, T. Mori<sup>1</sup>, H. Aratani<sup>1,2</sup>, Y. Nakatani<sup>1,2</sup>,  
K. Yamagami<sup>1,2</sup>, M. Kawada<sup>1,2</sup>, H. Fujiwara<sup>1,2</sup>, K. Kuga<sup>2</sup>, T. Kiss<sup>1,2</sup>, A. Higashiya<sup>2,3</sup>, T. Kadono<sup>2,4</sup>, S. Imada<sup>2,4</sup>,  
A. Tanaka<sup>5</sup>, K. Tamasaku<sup>2</sup>, M. Yabashi<sup>2</sup>, T. Ishikawa<sup>2</sup>, Y. Onuki<sup>6</sup>, and T. Ebihara<sup>7</sup>

<sup>1</sup>Division of Materials Physics, Graduate School of Engineering Science, Osaka University, Toyonaka, Osaka  
560-8531, Japan

<sup>2</sup>RIKEN SPring-8 Center, Sayo, Hyogo 679-5148, Japan

<sup>3</sup>Faculty of Science and Engineering, Setsunan University, Neyagawa, Osaka 572-8508, Japan

<sup>4</sup>Department of Physical Sciences, Ritsumeikan University, Kusatsu, Shiga 525-8577, Japan

<sup>5</sup>Department of Quantum Matter, Graduate School of Advanced Sciences of Matter, Hiroshima University,  
Higashihiroshima, Hiroshima 739-8530, Japan

<sup>6</sup>Faculty of Science, University of the Ryukyus, Nishihara, Okinawa 903-0213, Japan

<sup>7</sup>Department of Physics, Graduate School of Science, Shizuoka University, Shizuoka 422-8529, Japan

Ground- and excited-states orbital symmetry or orbital polarization in strongly correlated electron systems has crucial roles in their functional properties. Recently, it has been reported that the ground-state 4f-orbital symmetry can be uniquely determined by linear polarization-dependent angle-resolved core-level photoemission of Yb compounds [1,2]. This technique has an advantage in the applicability to the systems in cubic symmetry and in perfectly determining the charge distribution including the directions (signs in the coefficients for components of the wavefunction, in other words), which can be understood by considering the photoemission process [3] as discussed below.

In the core-level photoemission process, one inner-core electron with the quantum numbers  $\lambda_c \equiv (n_c l_c m_c s_c)$  is removed from the strongly correlated sites in the final states, where  $n_c$ ,  $l_c$ ,  $m_c$ , and  $s_c$  denotes the principal, orbital, magnetic, and spin quantum numbers. The  $n_c l_c$  core-level photoemission spectra of the strongly correlated electron systems have so far been expressed using an angle-integrated form as a function of energy  $\omega \equiv E_K^* - h\nu$ , as

$$\rho(\omega) = \sum_{n, m_c, s_c} |(E_f^{(n)}(\underline{\lambda}_c) | a_{\lambda_c} | E_i \rangle|^2 \delta(\omega + E_f^{(n)}(\underline{\lambda}_c) - E_i),$$

where  $E_i$  and  $E_f^{(n)}(\underline{\lambda}_c)$  stand for the initial-state energy and the eigenenergy of one of the final states ( $n$ ) with the core hole  $\underline{\lambda}_c$ , and  $E_K^*$  denotes the photoelectron kinetic energy in a solid. For obtaining the above formula, it is assumed that the matrix elements mainly describing a photoexcitation process have negligible emission angle and polarization dependence within the  $n_c l_c$  core-level excitations. In order to understand LD in the angle-resolved core-level photoemission spectra of a single crystal, however, we need to start from the form in which the matrix elements are explicitly taken into account. After the discussions of the photoemission process from a single ion under the crystalline electric fields, the angle-resolved  $n_c l_c$  core-level photoemission spectra can be expressed as

$$\rho(\omega, \vec{e}, \theta_k, \varphi_k) \simeq \sum_{n, m_c, s_c} \left| \sum_{m'} Y_{l_c+1}^{m'}(\theta_k, \varphi_k) A_{\lambda_c}^{k(l_c+1)m'}(\vec{e}) \langle E_f^{(n)}(\underline{\lambda}_c) | a_{\lambda_c} | E_i \rangle \right|^2 \delta(\omega + E_f^{(n)}(\underline{\lambda}_c) - E_i),$$

$$A_{\lambda_c}^{kl'm'}(\vec{e}) = 4\pi \iiint R_{k'l'}^*(r) Y_{l'}^{m'*}(\theta, \varphi) (\vec{e} \cdot \vec{p}) R_{n_c l_c}(r) Y_{l_c}^{m_c}(\theta, \varphi) dV,$$

where  $\vec{e}$ ,  $\theta_k$ , and  $\varphi_k$  stand for the polarization vector of the excitation light, polar and azimuthal angles to the quantum axis  $z$ , and  $m' = m_c (m_c \pm 1)$  for  $\vec{e} \parallel z$  ( $\vec{e} \perp z$ ) derived from the selection rules [3].

Actually, we have successfully detected LD in the core-level photomission for Ce, Pr, Sm, and Yb compounds, in which the ground-state 4f charge distributions have uniquely been determined. For the tetragonal compounds with ThCr<sub>2</sub>Si<sub>2</sub>-type crystal structure CeCu<sub>2</sub>Ge<sub>2</sub>, CeNi<sub>2</sub>Ge<sub>2</sub>, and SmCu<sub>2</sub>Si<sub>2</sub>, their 4f ground states have been identified as the “Σ-type”  $\Gamma_7$  symmetry from the LD in the core-level photoemission, which charge distributions is elongated to the Ge or Si sites as seen for YbCu<sub>2</sub>Si<sub>2</sub> [1].

This work was supported by the JSPS KAKENHI Grant Numbers JP16H01074 (J-Physics) and JP16H04014, and the JSPS Research Fellowships for Young Scientists.

- [1] T. Mori *et al.*, J. Phys. Soc. Jpn. **83**, 123702 (2014).
- [2] Y. Kanai *et al.*, J. Phys. Soc. Jpn. **84**, 073705 (2015).
- [3] A. Sekiyama, Y. Kanai, A. Tanaka, and S. Imada, arXiv:1611.01981.

## Phase transitions in vanadium chalcogenides with a two dimensional triangular lattice

N. Katayama<sup>1</sup>, S.-H. Lee<sup>2</sup><sup>1</sup>Dept. Appl. Phys., Nagoya University, Nagoya 464-8603, Japan<sup>2</sup>Dept. Phys., University of Virginia, Charlottesville 22904, U.S.

Transition metal compounds with a geometrically frustrated lattice, such as a triangular or a pyrochlore lattice, have been intensively studied. When the  $t_{2g}$  orbitals are partially occupied, utilizing the multiple degrees of freedom, such as spin, orbital and charge degrees of freedom, various magnetic ground states appear in low temperatures. We have been interested in vanadium chalcogenides with two dimensional triangular lattices, where the various exotic states appear due to the entanglement among multiple degrees of freedom: successive orbital ordering transitions in  $\text{NaVO}_2$ [1], complex “trimer molecular” cluster formations in a spin singlet state in  $\text{LiVS}_2$  ( : O, S)[2] and the emergence of various electric phases in  $\text{LiVS}_2$  ( $0 \leq \leq 1$ )[3].

Here, we report the phase transitions in  $\text{NaVS}_2$  and  $\text{NaVSe}_2$  with spin and orbital degrees of freedom, which are isostructural with  $\text{LiVS}_2$  and  $\text{LiVSe}_2$ .  $\text{LiVS}_2$  shows metal to nonmagnetic insulator transition with trimer  $V_3$  cluster formation at around 314 K. The transition is suppressed by substituting S by Se, resulting in paramagnetic metal in all temperature regions in  $\text{LiVSe}_2$ . On contrast, both  $\text{NaVS}_2$  and  $\text{NaVSe}_2$  exhibit antiferromagnetic transition at around 55 K (Fig.1) with keeping their metallic conductivity down to the lowest temperatures. Although the low temperature ground states are different between Li and Na derivatives, both systems show some anomalous features in high temperature paramagnetic metallic phases. Our synchrotron x-ray diffraction studies have been clarifying the enhancement of factors for vanadium ions just above the phase transition in  $\text{LiVS}_2$ , indicating the emergence of short range ordering of vanadium trimer in high temperature metallic phase. On contrast in  $\text{NaVS}_2$  and  $\text{NaVSe}_2$ , strong excitation appears in inelastic regions just above the antiferromagnetic transitions (Fig.2), indicating the magnetic short range orderings. In the presentation, we discuss the origin of the various magnetic phase transitions in vanadium chalcogenides by focusing on the local structures around  $V_6$  ( : S, Se) octahedra.

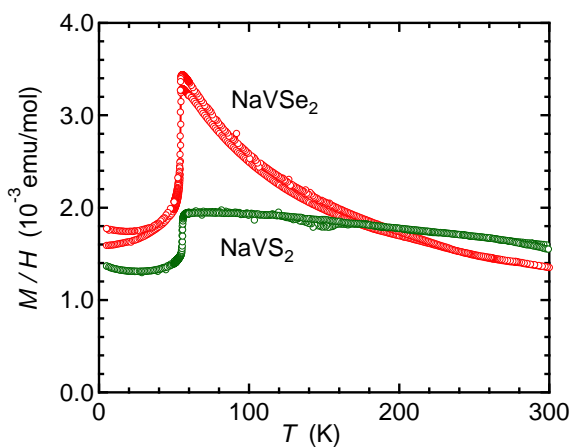


Fig. 1 Temperature dependences on magnetic susceptibility in  $\text{NaVS}_2$  and  $\text{NaVSe}_2$ .

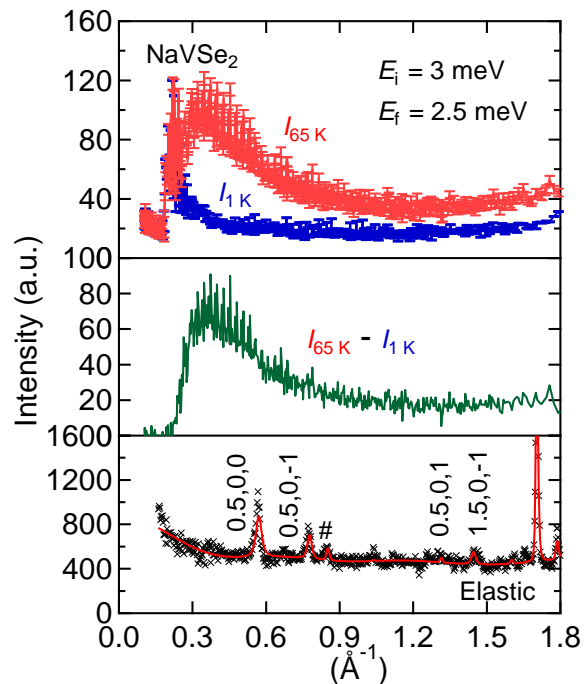


Fig. 2 Magnetic fluctuations in  $\text{NaVSe}_2$ . Magnetic fluctuation does not originate from the magnetic Bragg peak positions.

[1] T.M. McQueen *et al.*, Phys. Rev. Lett. **101** (2008) 166402.

[2] N. Katayama *et al.*, Phys. Rev. Lett. **103** (2009) 146405.

[3] D.W. Murphy *et al.*, Inorg. Chem. **16** (1977) 3027.

Linear dichroism in angle-resolved core level photoemission  
reflecting 4 ground state symmetry of strongly correlated cubic Pr compounds

S. Hamamoto<sup>1,2</sup>, S. Fujioka<sup>1,2</sup>, Y. Kanai<sup>1,2</sup>, Y. Nakatani<sup>1,2</sup>, K. Yamagami<sup>1,2</sup>, H. Fujiwara<sup>1,2</sup>, T. Kiss<sup>1,2</sup>,  
A. Higashiya<sup>2,3</sup>, A. Yamasaki<sup>2,3</sup>, S. Imada<sup>2,5</sup>, A. Tanaka<sup>6</sup>, K. Tamasaku<sup>2</sup>, M. Yabashi<sup>2</sup>, T. Ishikawa<sup>2</sup>,  
K. T. Matsumoto<sup>6</sup>, T. Onimaru<sup>6</sup>, T. Takabatake<sup>6</sup>, and A. Sekiyama<sup>1,2</sup>

<sup>1</sup>Graduate School of Engineering Science, Osaka University, Toyonaka, 560-8531, Japan

<sup>2</sup>RIKEN SPring-8 Center, Sayo, 679-5148, Japan

<sup>3</sup>Faculty of Science and Engineering, Setsunan University, Neyagawa, 572-8508, Japan

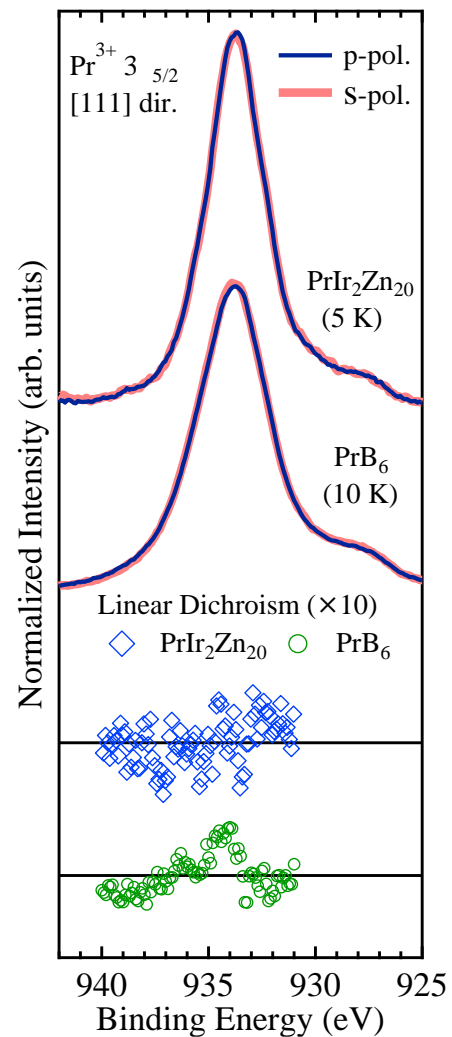
<sup>4</sup>Faculty of Science and Engineering, Konan University, Kobe, 658-8501, Japan

<sup>5</sup>Department of Physical Sciences, Ritsumeikan University, Kusatsu, 525-8577, Japan

<sup>6</sup>Graduate School of Advanced Sciences of Matter, Hiroshima University, Higashihiroshima, 739-8511, Japan

<sup>7</sup>Institute for Advanced Materials Research, Hiroshima University, Higashihiroshima, 739-8511, Japan

Rare-earth-based strongly correlated electron systems show various interesting phenomena such as competition between magnetism and unconventional superconductivity, charge and/or multipole ordering, and the formation of a narrow ( $\sim$ meV) gap at low temperatures. For clarifying origins of the phenomena, it is important to determine the 4 ground-state symmetry.  $\text{PrIr}_2\text{Zn}_{20}$  undergoes an antiferroquadrupolar (AFQ) ordering at  $T_Q = 0.11$  K and a superconducting transition at  $T_c = 0.05$  K [1]. Below 10 K, the increase in magnetic susceptibility for this compound tends to saturate, indicating the van Vleck susceptibility with nonmagnetic crystalline electric field (CEF) ground states of the  $\Gamma_3$  doublet [2]. On the other hand,  $\text{PrB}_6$  with a cubic crystal structure shows an incommensurate antiferromagnetic transition at 7 K and a commensurate antiferromagnetic ordering at 4.2 K [3]. These phenomena suggest the  $\Gamma_5$  ground state for  $\text{PrB}_6$ . Recently, the linear dichroism (LD) in angle resolved Yb 3 core level photoemission spectra reflecting the anisotropy of the 4 charge distribution has been reported, by which the 4 ground-state symmetry of the surveyed compounds has been clarified [4,5]. We have applied this technique to  $\text{PrIr}_2\text{Zn}_{20}$  and  $\text{PrB}_6$  in cubic symmetry, and successfully observed the LD in the Pr 3 core level photoemission spectra reflecting the anisotropy in the 4 charge distributions, which leads to the determination of the 4 ground-state symmetry by the comparison with the experimental results and the simulations. Actually, we have performed ionic calculations including the full multiplet theory and the local CEF splitting using the XTLS 9.0 program [6]. A comparison of the polarization dependent background-subtracted  $\text{Pr}^{3+} 3d_{5/2}$  hard X-ray photoemission (HAXPES) spectra of  $\text{PrIr}_2\text{Zn}_{20}$  and  $\text{PrB}_6$ , and their LD along the [111] photoelectron directions are shown in Fig. 1. The observed LD and spectra for  $\text{PrIr}_2\text{Zn}_{20}$  and  $\text{PrB}_6$  are reproduced by the simulations for the  $\Gamma_3$  and  $\Gamma_5$  ground state, respectively. Furthermore, we have also observed the LD in the Pr 4 core level photoemission spectra reflecting the anisotropy of the 4 charge distribution for  $\text{PrB}_6$ . The observed Pr 4 spectra and LD are well reproduced by the simulations for the  $\Gamma_5$  ground state [7].



1 Polarization-dependent  $\text{Pr}^{3+} 3d_{5/2}$  core-level HAXPES spectra and LD of  $\text{PrIr}_2\text{Zn}_{20}$  and  $\text{PrB}_6$  along the [111] direction.

- [1] T. Onimaru *et al*, Phys. Rev. Lett. **106**, 177001 (2011).  
 [2] T. Onimaru *et al.*, J. Phys.: Condens. Matter **2**, 294207 (2012).  
 [3] S. Kobayashi *et al*, J. Phys. Soc. Jpn. **0**, 1721 (2001).  
 [4] T. Mori *et al*, J. Phys. Soc. Jpn. **83**, 123702 (2014).  
 [5] Y. Kanai *et al*, J. Phys. Soc. Jpn. **8**, 073705 (2015).  
 [6] A. Tanaka and T. Jo, J. Phys. Soc. Jpn. **63**, 2788 (1994).  
 [7] S. Hamamoto *et al*, arXiv:1705.04295.

## P-87

**Electronic and magnetic properties of CePt<sub>2</sub>In<sub>7</sub>**

M. Raba<sup>1,2,3</sup>, E. Ressouche<sup>4</sup>, N. Qureshi<sup>5</sup>, C. V. Colin<sup>2,3</sup>, V. Nassif<sup>2,3</sup>,  
S. Ota<sup>6</sup>, Y. Hirose<sup>7</sup>, R. Settai<sup>7</sup>, D. Aoki<sup>8</sup>, P. Rodière<sup>2,3</sup> and I. Sheikin<sup>1</sup>

<sup>1</sup>*Laboratoire National des Champs Magnétiques Intenses (LNCMI-EMFL), CNRS, UGA, 38042 Grenoble, France*

<sup>2</sup>*Université Grenoble Alpes, Institut Néel, F-38000 Grenoble, France*

<sup>3</sup>*CNRS, Institut Néel, F-38000 Grenoble, France*

<sup>4</sup>*INAC, CEA and Univ. Grenoble Alpes, CEA Grenoble, F-38054 Grenoble, France*

<sup>5</sup>*Institut Laue Langevin, 71 rue des Martyrs, BP156, 38042 Grenoble Cedex 9, France*

<sup>6</sup>*Graduate School of Science and Technology, Niigata University, Niigata 950-2181, Japan*

<sup>7</sup>*Department of Physics, Niigata University, Niigata 950-2181, Japan*

<sup>8</sup>*IMR, Tohoku University, Ibaraki, Japan*

CePt<sub>2</sub>In<sub>7</sub> is a recently discovered heavy fermion material belonging to the same family as the well-studied isotropic CeIn<sub>3</sub> and quasi-two-dimensional CeRhIn<sub>5</sub> compounds. The spacing between Ce-In planes in CePt<sub>2</sub>In<sub>7</sub> is drastically increased [1] as compared to CeRhIn<sub>5</sub>, implying a more two-dimensional crystal structure.

Along with the other compounds of its family, CePt<sub>2</sub>In<sub>7</sub> temperature-pressure phase diagram exhibits an antiferromagnetic phase below 5.5 K at ambient pressure. The Neel temperature is suppressed by increasing pressure. A superconducting dome emerges around a quantum critical point at  $P_c = 3.2$  GPa [2] associated with this magnetic phase, whose magnetic structure was unknown until very recently.

I will present the results of a single-crystal neutron diffraction experiment on CePt<sub>2</sub>In<sub>7</sub>, which allowed us to determine its antiferromagnetic structure [3]. I will then show some recent preliminary results of quantum oscillation measurements using a tunnel-diode-oscillator circuit and high pressure cells.

[1] T. Klimczuk et al., J. Phys.: Condens. Matter **26** (2014) 402201 (5pp)

[2] V. A. Sidorov et al., Phys. Rev. B **88**, 020503(R) (2013)

[3] M. Raba et al., Phys. Rev. B **95**, 161102(R) (2017)

## Magnetic structure and magnetoelectric effect in buckled honeycomb lattice antiferromagnet $\text{Co}_4\text{Ta}_2\text{O}_9$

N. Abe<sup>1</sup>, N. D. Khanh<sup>2,3</sup>, T. Omi<sup>1</sup>, T. Moyoshi, A. Nakao<sup>4</sup>, Y. Tokunaga<sup>1</sup>, T. Arima<sup>1</sup>

<sup>1</sup>Department of Advanced Materials Science, the University of Tokyo, Kashiwa 277-8561, Japan

<sup>2</sup>Department of physics, Tohoku University, Sendai 980-8577, Japan

<sup>3</sup>Center for Emergent Matter Science, RIKEN, Wako 351-0198, Japan

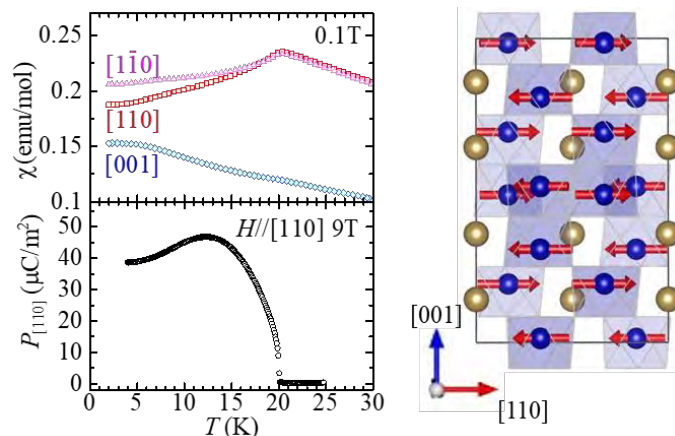
<sup>4</sup>Neutron Science and Technology Center, CROSS, Tokai 319-1106, Japan

Odd-parity magnetic multipole ordering in a matter causes a linear magnetoelectric effect [1,2]. The diagonal terms of the magnetoelectric effect tensor are coupled with the magnetic monopole, and the off-diagonal terms are related to the magnetic quadrupole and toroidal moments. For example,  $\text{Cr}_2\text{O}_3$  shows diagonal magnetoelectric effects which are caused by the magnetic monopole like antiferromagnetic ordering of  $\text{Cr}^{3+}$  magnetic moment [3]. A structure in which the local inversion symmetry is broken like zigzag chain and honeycomb structure with spin-orbit coupling are the key factor of realization of odd-parity magnetic multipole ordering.

$\text{A}_4\text{B}_2\text{O}_9$  ( $\text{A} = \text{Mn, Co, B} = \text{Nb, Ta}$ ) belongs to the corundum-related structure with space group  $\bar{3}c1$ ,  $2^+$  layers of buckled honeycomb structure stack along the  $c$ -axis [4]. Because the honeycomb structure breaks the local inversion symmetry, these compound candidates for odd-parity magnetic multipole ordering and magnetoelectric multiferroics. In fact,  $\text{Co}_4\text{Nb}_2\text{O}_9$  shows a large linear magnetoelectric effect [5,6].  $\text{Co}^{2+}$  spin moments are ordered in an antiferromagnetically below  $T_N = 27$  K, and simultaneously the linear magnetoelectric effect emerges. Recently, we reported its magnetic structure and magnetoelectric effect by using single crystal [7]. In the antiferromagnetic ordered phase,  $\text{Co}^{2+}$  spin moments are antiferromagnetically align in  $a$  plane. Moreover, both diagonal and off-diagonal terms of magnetoelectric effect are observed.

In this study, we investigate magnetic structure and magnetoelectric properties of  $\text{Co}_4\text{Ta}_2\text{O}_9$  by using single crystal. This compound shows similar magnetic ordering and magnetoelectric effect with  $\text{Co}_4\text{Nb}_2\text{O}_9$  as shown in figure. Below  $T_N = 20$  K,  $\text{Co}^{2+}$  moments are aligned in  $a$  plane and magnetoelectric effect is observed. However, nonlinear magnetoelectric effect is observed, which is clearly different from  $\text{Co}_4\text{Nb}_2\text{O}_9$ . To reveal the origin of the nonlinear magnetoelectric effect, we investigated the magnetic structure in a magnetic fields.

This work was partly supported by a Grant-In-Aid for Scientific Research (Grant No. 16H01065). The neutron experiments were performed at the Materials and Life Science Experimental Facility of the J-PARC under User Programs No. 2017A0220.



(Left) Magnetic susceptibility, electric polarization and (right) magnetic structure of  $\text{Co}_4\text{Ta}_2\text{O}_9$ .

- [1] D. I Khomskii, *et al* *Phys. Rev. Lett.* **5**, 4793 (2014).  
 [2] N. A. Spaldin *et al* *Nature* **88**, 094429 (2013).  
 [3] G. T. Rado and V. J. Folen, *Phys. Rev.* **1**, 310 (1961).  
 [4] E.F. Bertaut *et al* *Phys. Rev.* **21**, 234(1961).  
 [5] E. Fishcher *et al* *Phys. Rev. Lett.* **10**, 1127 (1972).  
 [6] Y. Fang *et al* *Phys. Rev. Lett.* **113**, 3860 (2014).  
 [7] N.D.Khanh *et al* *Phys. Rev. Lett.* **93**, 075117 (2016).

## P-89

Magnetic and structural properties of BiS<sub>2</sub>-based layered superconductors LnO<sub>1-x</sub>F<sub>x</sub>BiS<sub>2</sub>

R. Higashinaka<sup>1</sup>, J. Kajitani<sup>1</sup>, M. Mita<sup>1</sup>, N. Yamamoto<sup>1</sup>, H. Endo<sup>1</sup>, T. D. Matsuda<sup>1</sup> and Y. Aoki<sup>1</sup>  
<sup>1</sup>Department of Physics, Tokyo Metropolitan University, Hachioji 192-0397, Japan

BiS<sub>2</sub>-based layered superconductors LnO<sub>1-x</sub>F<sub>x</sub>BiS<sub>2</sub> (Ln: rare earth) have been attracting much attention[1]. Similar to iron pnictides superconductors, these compounds consist of alternative stacking of two conductive BiS<sub>2</sub> layers and insulating Ln<sub>2</sub>O<sub>2</sub> block layers. These compounds become superconducting (SC) when charge carriers are introduced via electron doping by partial substitution of O for F. Although there are many investigations for their SC properties, there is little investigation for their magnetisms. We have investigated the magnetism of 4f electrons on block layers in LnO<sub>1-x</sub>F<sub>x</sub>BiS<sub>2</sub> (Ln: rare earth) compounds using high-quality single crystals and discovered the presence of quantum critical fluctuations of 4f magnetic moments in CeOBiS<sub>2</sub>[2] and the heavy-fermion-like low energy excitation in NdO<sub>0.5</sub>F<sub>0.5</sub>BiS<sub>2</sub>[3].

Recently, we have succeeded in growing single crystals of Pr and Eu compounds and measured physical properties using these single crystals. In PrO<sub>1-x</sub>F<sub>x</sub>BiS<sub>2</sub>, there are a metamagnetic anomaly and a clear magnetic anisotropy in PrOBiS<sub>2</sub> (Fig.1). The metamagnetic anomaly vanishes and the magnetic anisotropy becomes weaker with increasing the F doping. In EuFBiS<sub>2</sub>, although the polycrystalline sample shows SC at 0.3 K[4], the resistivity using single crystal shows semiconductive behavior without SC transition down to 0.1 K and an anomalous large negative magnetoresistance appears at low temperatures (Fig.2). These results indicate that the interaction between block and conductive layer would play an important role for the magnetic and transport properties. In this presentation, we would like to present systematic investigations of physical properties for these compounds.

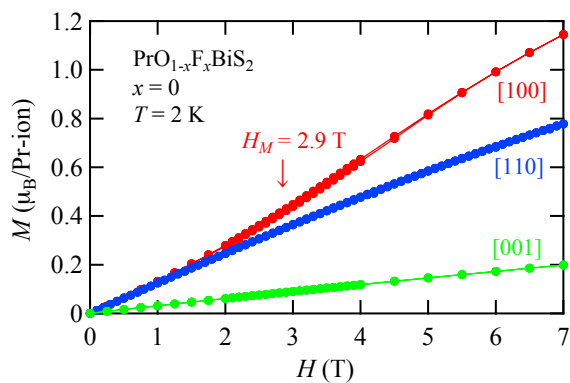


Fig. 1:  $H$  dependence of magnetization of PrOBiS<sub>2</sub>

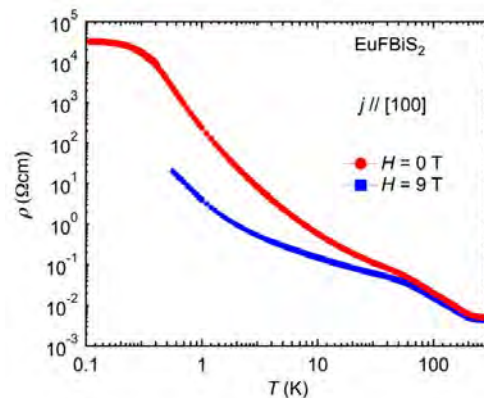


Fig. 2:  $T$  dependence of resistivity of EuFBiS<sub>2</sub>

[1] Y. Mizuguchi: J. Phys. Chem. Solids, **84** 34-48 (2015)

[2] R. Higashinaka, T. Asano, T. Nakashima, K. Fushiya, Y. Mizuguchi, O. Miura, T. D. Matsuda, and Y. Aoki: J. Phys. Soc. Jpn. **84** 023702 (2015)

[3] M. Mita, R. Higashinaka *et al.*: JPS autumn meeting 15aPS-82 (2016).

[4] Hui-Fei Zhai *et al.*: Phys. Rev. B **90** 064518 (2014).

Observation of a nonreciprocal signal in ferromagnetic resonance in multiferroic GaFeO<sub>3</sub>

T. Omi<sup>1</sup>, M. Akaki<sup>2</sup>, N. Abe<sup>1</sup>, Y. Tokunaga<sup>1</sup>, S. Kimura<sup>3</sup>, M. Hagiwara<sup>2</sup> and T. Arima<sup>1</sup>

<sup>1</sup> e a t e t a c e a t e a l c e c e  
 T e e t T a a a a  
 e t e a c e H a e t c e l c e c e a a t e c l c e c e  
 a a e t T a a a a  
<sup>3</sup> t t t e a t e a l e e a c T e t e a a a

If the time reversal symmetry and space inversion symmetry are simultaneously broken in a matter, the linear magnetoelectric (ME) effect may appear. The linear ME materials also show nonreciprocal directional dichroism (NDD) to an electromagnetic wave. The linear ME effect and NDD are explained by odd-parity magnetic multipoles like toroidal moment [1]. A polar magnet, which has ferrotoroidic order, is expected to show linear ME effect and NDD. In polar magnets, NDD could be observed in the Voigt configuration  $k \parallel (P \times M)$ . Here,  $k$  is the wave vector of incident wave,  $P$  and  $M$  describe the polarization and the magnetization[2], respectively. Not only the reversal of  $k$  but also that of  $M$  give sign changes of NDD. There have been the experimental reports on NDD of polar magnets to electromagnetic waves at various frequency regions so far[3].

For electromagnetic waves in the frequency range from GHz to THz, NDD coupled with the excitation of a quasi-particle will emerge. Particularly, NDD coupled with a magnon excitation has been much attractive. Some polar magnets show NDD for THz region[4],[5], but there are few reports on NDD for GHz region in polar magnets.

We successfully observed NDD to microwaves of frequencies 80 GHz to 300 GHz either by the reversal of  $k$  or by that of  $M$  in a ferrotoroidic material GaFeO<sub>3</sub>. The crystal and magnetic structures of GaFeO<sub>3</sub> are shown in Fig.1. This substance belongs to the orthorhombic crystal system, and magnetic space group is  $c'2'_1$  [6]. Magnetic easy axis is  $c$  axis and the ferrimagnetic transition temperature is about 210 K. The spontaneous polarization  $P$  exists along the  $a$  axis. NDD is expected in  $k \parallel (P \times M) \parallel a$  configuration.

To investigate the response to microwave for GaFeO<sub>3</sub>, a ferromagnetic resonance (FMR) was measured. FMR measurement was performed in AHMF, Osaka University. Unpolarized microwave of frequencies in the range of 80 GHz to 300 GHz was used for measurements. The microwave absorption of GaFeO<sub>3</sub> was measured for each frequency at 100 K.

Fig.2 shows FMR spectra of 160 GHz at 100 K. The vertical axis is the absorption strength of microwave, and the horizontal axis is the absolute value of the external magnetic field. Red (blue) line shows the data in positive (negative) magnetic fields  $H \parallel c$ , respectively. Large absorption peak was found around 2.5 T. This peak was characterized as the absorption by the uniform mode magnon by investigating the relation between the resonant frequency and the resonant magnetic field. The difference in the absorption of the microwave for this peak by the uniform mode magnon between  $H > 0$  and  $H < 0$  was observed. Furthermore, the sign of difference was reversed by the inversion of  $k$ . Such differences in absorption were also observed at every frequency from 100 GHz to 300 GHz. In conclusion, the difference in the microwave absorption results from the dynamical magnetoelectric property of GaFeO<sub>3</sub>.

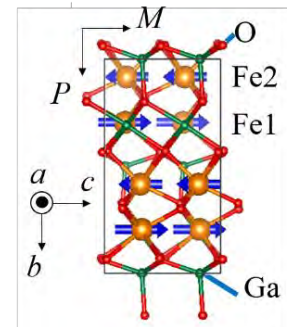


FIG. 1 Crystal structure of GaFeO<sub>3</sub> projected along the  $a$  axis. Blue arrows show the magnetic moments of Fe ions.

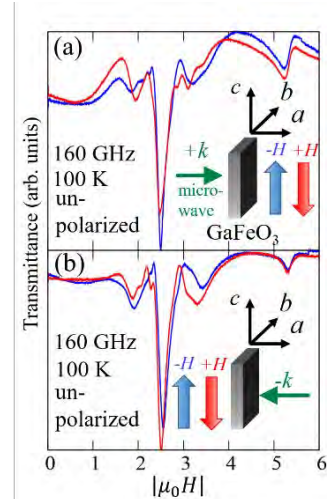


FIG.2  $H$ - and  $k$ - direction dependence of FMR spectra measured at a frequency of 160 GHz using an unpolarized microwave. Incident microwave wavevector  $k$  shown by green arrow is (a) parallel and (b) antiparallel to the  $a$  axis.

[1] N. A. Spaldin *et al.*, Phys. Rev. B **88**, 094429 (2013).  
 [2] Y. Tokura, *et al.*, Rep. Prog. Phys. **77**, 076501 (2014).  
 [3] M. Kubota, *et al.*, Phys. Rev. Lett. **92**, 137401 (2004).  
 [4] S. Bordács, *et al.*, Phys. Rev. B **92**, 214441 (2015).  
 [5] Y. Takahashi *et al.*, Phys. Rev. Lett. **111**, 037204 (2013)  
 [6] T. Arima, *et al.*, Phys. Rev. B **70**, 064426 (2004).

Current-induced magnetization on UNi<sub>4</sub>B and CeRh<sub>2</sub>Si<sub>2</sub>H. Saito<sup>1</sup>, Y. Suzuki<sup>1</sup>, N. Shikanai<sup>1</sup>, N. Miura<sup>1</sup>, H. Hidaka<sup>1</sup>, T. Yanagisawa<sup>1</sup>, H. Amitsuka<sup>1</sup>, and C. Tabata<sup>2</sup><sup>1</sup>Grad. School of Science, Hokkaido Univ., Sapporo 060-0810, Japan<sup>2</sup>KEK IMSS CMRC, Tsukuba, Japan

Toroidal moment  $\mathbf{t}$  is one of the parameters that describe a strength of the magnetoelectric coupling. It is defined as a vector product of position  $\mathbf{r}$  and spin  $\mathbf{S}$ . In the last several years, the toroidal order, which is the ordered periodic array of the toroidal moments, has attracted much interest in connection with multiferroic insulating materials. Recently, S. Hayami *et al* theoretically predicted that such an exotic order can occur also in metallic systems, and exotic phenomena such as magnetization induced by electric current can occur in the toroidal ordered metal [1].

In order to test this theory, we have performed magnetization measurements under electric current on an antiferromagnetic metal, UNi<sub>4</sub>B. It is suggested that this compound orders antiferromagnetically in a magnetic structure, where the magnetic moments carried by the 2/3 of U ions make the vortices in each triangular lattice plane of U below  $T_N = 20.4$  K [2]. Since this magnetic structure is the same as that assumed in the above theory, the system is considered to be a candidate for the above theory. We observed that magnetization is induced by constant electric current in the ordered state of UNi<sub>4</sub>B [3]. Therefore, the validity of the theory is confirmed in part by the experiments. However, the fact that the magnetic structure of UNi<sub>4</sub>B is not fully confirmed makes it difficult to compare the experimental results with the theory, hindering further understanding of the observed phenomenon.

We have recently started searching for another candidate metal for the theory. In this presentation, we report another system which shows a current-induced change of magnetization, CeRh<sub>2</sub>Si<sub>2</sub>. The system crystallizes into ThCr<sub>2</sub>Si<sub>2</sub>-type hexagonal structure (symmetry: I4/mmm, D<sub>4h</sub><sup>17</sup>, No.139). It shows successive antiferromagnetic transitions at  $T_{N1} = 36$  K and  $T_{N2} = 25$  K. The former possesses the wave vector  $\mathbf{q} = [1/2, 1/2, 0]$ . The latter possesses  $\mathbf{q} = [1/2, 1/2, 1/2]$  in addition to  $\mathbf{q} = [1/2, 1/2, 0]$ . Magnetic moments oriented along the [001] direction in both phases [4]. Single-crystalline sample is prepared by Czochralski pulling method in our group. Constant current magnetization measurement for each settings of  $\parallel a, c$ -axes and  $\parallel a, c$ -axes have been performed. We observed that electric current applied parallel to the  $a$ -axis causes the change in magnetization along to the  $c$ -axis only between  $T_{N1}$  and  $T_{N2}$ . The results with other geometries as well as a comparative review of our results and the theory will be presented.

In addition, magnetization change in the antiferromagnetic ordered state of UNi<sub>4</sub>B caused by a pulsed square-wave current will also be presented.

This work was supported by JSPS KAKENHI Grant Number JP15H05885 and JP15K21732 (J-Physics).

[1] S. Hayami, H. Kusunose, and Y. Motome, Phys. Rev. B **90**, 024432 (2014).

[2] S. A. M. Mentink, A. Drost, G. J. Nieuwenhuys, E. Frikkee, A. A. Menovsky, and J. A. Mydosh, Phys. Rev. Lett. **3**, 1031 (1994).

[3] H. Saito, K. Uenishi, N. Miura, C. Tabata, H. Hidaka, T. Yanagisawa, and H. Amitsuka, 20th International Conference on Magnetism (Barcelona), TU.A-P67 (2015).

[4] S. Kawarazaki, M. Sato, Y. Miyako, N. Chigusa, K. Watanabe, N. Metoki, Y. Koike and M. Nishi, Phys. Rev. B **61**, 4167 (2000).

Ultrasonic measurement of Fe-based superconducting  $\text{SrFe}_2(\text{As}_{1-x}\text{P}_x)_2$ 

Jo IMAI, Keita HORIKOSHI, Yoshiki NAKANISHI, Mitsuteru NAKAMURA,  
Tatsuya KOBAYASHI<sup>A</sup>, Toru ADACHI<sup>A</sup>,  
Shigeki MIYASAKA<sup>A</sup>, Setsuko TAJIMA<sup>A</sup>, Masahito YOSHIZAWA  
Iwate University, Graduate School of Engineering, Morioka, Japan  
Osaka University, Department of Physics, Toyonaka, Japan<sup>A</sup>

Interplay between orbital degrees of freedom and spin ones plays an important role in determining a variety of novel phases in quantum materials including exotic superconductors. We have investigated elastic properties of the prototypical compound of the 122 class of Fe-based superconductors,  $\text{SrFe}_2(\text{As}_{1-x}\text{P}_x)_2$  probed by ultrasonic measurement to gain insight into the mechanism underlying the formation of electron pairs. Ultrasonic measurement is a powerful probe for investigating orbital properties since it is markedly sensitive to a strain-quadrupole interaction and symmetry of order parameter of phase transitions including structural one. We measured temperature  $T$  dependences of elastic constants of  $\text{SrFe}_2(\text{As}_{1-x}\text{P}_x)_2$ . Furthermore, the experimental data were compared with those for other 122 class of Fe-based superconductors,  $\text{BaFe}_2(\text{As}_{1-x}\text{P}_x)_2$ , reported previously by our group.

The  $T$  dependences of the transverse elastic constants  $C_{66}$  and  $C_{44}$  in  $\text{SrFe}_2(\text{As}_{1-x}\text{P}_x)_2$  for  $x = 0.2$  are shown in Figs. 1 and 2, respectively[1]. The black and red curves denote experimental data and the theoretical results, respectively. The blue ones denote a background parameter for fitting. A noticeable elastic anomaly, softening toward around  $T = 140$  K was observed in the  $T$  dependence of  $C_{66}$ . The relative change of  $C_{66}$ ,  $\Delta C_{66}$  associated with the phase transition is about 10 %. However, no remarkable elastic anomaly is invisible at  $T_{\text{SC}}$  for  $x = 0.2$ . Similarly, a noticeable elastic anomaly, softening toward around  $T = 60$  K was observed in the  $T$  dependence of  $C_{44}$  for  $x = 0.28$ . From the analysis of the elastic anomalies, e.g. precursor softening of the elastic constants, one can estimate Jahn-Teller energy, which is one of the key physical parameters in Fe-based superconductors. In this experiment, even for the optimized case of Sr-122 for  $x=0.28$ , the  $E_{\text{JT}}$  is estimated to be 3.4 K.

Hence we obtained the Jahn-Teller energies  $E_{\text{JT}} = 0.34$  K and 3.4 K for  $x = 0.2$  of  $C_{66}$  and  $x = 0.28$  of  $C_{44}$ , respectively. It should be noted that these values are significantly smaller than those of Ba-122 series with  $E_{\text{JT}} = 50$  K. The experimental data suggest that the origin of the mechanism underlying the formation of electron pairs would be largely different between Sr-122 and Ba-122 systems.

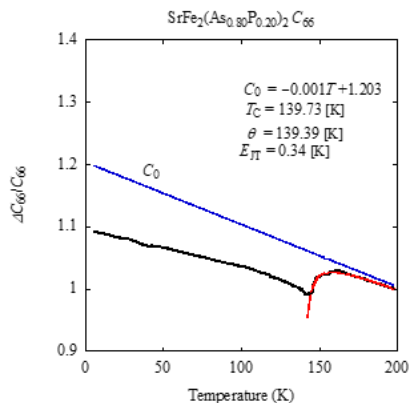


Fig.1

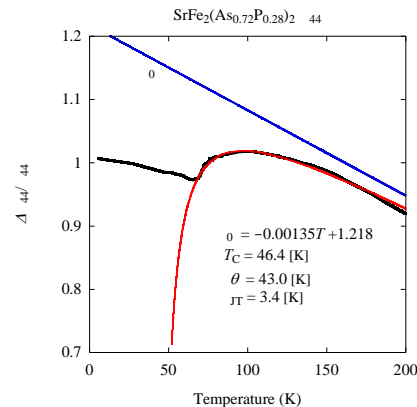


Fig.2

[1] M. Yoshizawa, D. Kimura, T. Chiba, S. Simayi, Y. Nakanishi, K. Kihou, C. H. Lee, A. Iyo, H. Eisaki, M. Nakajima, and S. Uchida, J. Phys.Soc. Jpn. **81**, 024604 (2012).